LONG-WAVE WIND EFFECTS ON CLOSED LAKES,
WITH SPECIAL APPLICATION TO
THE MURRAY MOUTH LAKES, SOUTH AUSTRALIA.

by

Patrick Joseph Walsh

B.Sc.(Hons), University of Adelaide.

Thesis submitted for the degree of

Doctor of Philosophy

in the

University of Adelaide

Department of Applied Mathematics

May 1974

TABLE OF CONTENTS

SUMMARY

This thesis reports a theoretical investigation into long-wave effects on a closed body of water resulting from wind stress at the surface. Results from both analytical and numerical models are compared with data collected from the lakes of the Murray Mouth, a series of shallow, interconnected lakes situated roughly 100km south-east of Adelaide, South Australia.

The linearized long-wave equations are considered. Hence, a closed lake responding to the action of surface wind stress may be viewed as a linear system, and the concept of the response function, a convenient means of characterizing a linear system, becomes immediately relevant. The response function, in this context, is defined as the time invariant part of the steady state lake response (either water level or velocity response) measured at a given station on the lake, to a wind stress of sinusoidal time variation and constant strength and direction over the surface.

Analytical response functions for the single-layered rectangular lake (neglecting Coriolis force) and single-layered circular lake (including Coriolis force), both lakes being constant in depth, are derived. Finite difference methods for calculating response functions for basins of arbitrary contour and depth are considered. Several different numerical models of the Murray Mouth lakes have been constructed.

Additional problems treated include the response of a two-layered (stratified) lake of constant depth, and the coupling effects between connected lake systems.

Results indicate that damping forces play a dominant role in wind induced motions of the Murray Mouth lakes. Generally, satisfactory comparisons between predicted and measured lake responses have been achieved.

SIGNED STATEMENT

I hereby declare that this thesis contains no material which has been accepted for the award of any other degree of diploma in any University and, to the best of my knowledge and belief, it contains no material previously published by any other person, except where due reference is made in the text of the thesis.

P. J. Walsh

ACKNOWLEDGEMENTS

INTRODUCTION

The major cause of movements of waters within most lakes is the direct action of surface wind stress. Both free and forced water level oscillations as well as circulation of short and long term duration may be induced by varying types of wind. The effects are felt within all basins, regardless of size. Generally, they are complicated by the earth's rotation and, possibly, by stratification within the fluid.

Strong winds often result in flooding of areas adjacent to a lake. Regardless of strength, wind action largely determines the mixing process within a lake, and hence the quality of its waters if it is subject to pollution discharges.

The Murray Mouth lakes of South Australia - Lake Alexandrina, Lake Albert and the Coorong lagoons - are typical of most Australian lakes in being shallow, highly saline and well-mixed. They are coastal lagoons, connected to the Southern Ocean through the narrow Murray Mouth, and are thus strongly influenced by prevailing winds.

Chapter 1 touches briefly on the physics of the various types of effects within a closed lake that result from the action of surface wind stress. Chapter 2 discusses the mathematical equations used to analyse the effects and the various simplifying assumptions needed to make them solvable. The simplified equations are linearized, so that the concept of <u>the response function</u> - a natural means of characterizing a linear system - may be used to describe the response of a closed lake to a wind stress input. Relatively simple and readily interpretable solutions to a variety of wind effect

problems may be obtained in this manner.

Wind effects on a rectangular, non-rotating basin of constant depth - the so-called "narrow lake' - are examined in Chapter 3, using the response function method. The results are applicable to the elongated Coorong lagoons. Theoretical response functions for the North Coorong are derived. Comparison with an experimentally determined function (Chapter 8) enables estimates to be made of the values of different types of damping parameters used to specify the system. It is shown that the North Coorong wind-water level system is heavily damped, so that the fundamental longitudinal free oscillation is unlikely to occur.

Chapter 4 presents a generalized theory for wind effects in constant depth basins of arbitrary contour, with Coriolis and damping influences included. Such a theory has applications to the "non-narrow" Lakes Alexandrina and Albert. In particular, from certain analytical solutions, we infer that the earth's rotation has little effect on wind induced motions within these lakes.

Direct numerical calculation of response functions for realistic, finite difference models (both one- and two-dimensional) of the Murray Mouth lakes is achieved in Chapter 5. Here the Coriolis forces are neglected. A series of numerical experiments on a model which incorporates both Lakes Alexandrina and Albert and their connecting link, the Narrung channel, indicates that remarkably strong currents are induced within the channel by wind action on the separate lakes. These currents are well known to local inhabitants of the area, and considerably influence wind induced motions in the separate lakes.

Chapter 6 examines wind effects on a stably stratified, simple two-layered lake of constant depth. Though not applicable to the Murray Mouth lakes, this model represents the behaviour in many lakes in colder regions of the northern hemisphere, e.g. the Great Lakes of North America. Use of response functions enables easy observation and interpretation of barotropic and baroclinic modes in the basin response.

In Chapter 7 the problem of coupling effects in the wind induced motion of a connected lake system is considered. A simple analytical model indicates the importance of damping processes in determining the extent of interaction between the separate lakes.

The concluding chapter presents the results of analyses of wind and water level data from the Murray Mouth lakes using methods of analysis largely developed by Noye (1970). For the Coorong lagoons, experimental response functions may be determined by cross-spectral analysis of such data at a given station. In addition, techniques of Fourier analysis enable predictions to be made of water levels due to measured wind velocities for both the Coorong lagoons and the "non-narrow" Lake Alexandrina, provided values of the response function for the wind-water level system are known over a wide frequency range. Some satisfactory comparisons with measured water levels have been achieved.

Among several Appendices is one which describes the Murray Mouth lakes and details the present and future impact of man on the system. The decision of the South Australian Government to site a new city, Monarto, in the vicinity of the lakes, is certain to diversify the uses of the lake waters. Thus, they have great recreational potential; at the same time,

they may serve as a useful outlet for effluent disposal. The work reported in this thesis was undertaken to assist in the more satisfactory assessment of man's impact on the environment of the Murray Mouth lakes.

CHAPTER 1

A PHYSICAL INTRODUCTION TO WIND EFFECTS

1.1 Wind Effects - Short Waves and Viscous Shear

The mechanism of wind-induced momentum transfer at an air-water interface is a most complex phenomenon which, at present, defies complete description. There are essentially two effects that occur, as stated by Phillips (1969), p.145:-

"...it appears that the transfer of momentum from the wind is

shared largely between direct viscous shear and the momentum

flux from the inner viscous layer to short waves..."

The two phenomena - formation of localized short waves and action of direct viscous shear or stress - are coupled in a way that is largely unknown. Decaying short waves possibly act as an energy source for the surface currents that result from the viscous shear.

It is common to consider the two effects quite independently of each other, and that practice is adhered to in this thesis. Our attention is directed to the second of the two effects, viz. the action of direct viscous shear on the water surface. Hereafter, unless otherwise stated, the term "wind effects" will refer to such action.

It is assumed that the wind stress, denoted by τ_s, is equivalent to the stress exerted on a rigid surface with an aerodynamic roughness that clearly must vary with the velocity of the wind. The stress is related to the mean wind velocity, u_s, measured at some point above the turbulent

portion of the air flow (normally a height of 10m), i.e. at the edge of
the surface boundary layer, by the drag law

$$\tau_s = C_s \rho_a u_s^2 \qquad (1.1.1)$$

where C_s is a dimensionless drag coefficient and ρ_a is the density of air.

There have been many empirical formulations suggested for the drag
coefficient; for a summary of these refer, for example, Wilson (1960),
Welander (1961) and Smith (1973). It is generally agreed that above a
certain transition wind velocity, possibly a transition from an aero-
dynamically smooth surface to an aerodynamically rough surface, C_s
increases with increasing velocity. For example Heaps and Ramsbottom
(1966) suggest that

$$C_s = \begin{cases} 5.65 \times 10^{-4}, & u_s \leq 5 \text{ m.sec}^{-1} \\ (-1.2 + 1.37 u_s) \times 10^{-4}, & 5 \text{ m.sec}^{-1} \leq u_s < 20 \text{ m.sec}^{-1}. \end{cases}$$

$$(1.1.2)$$

The resultant stress-velocity relationship is shown graphically in
Fig. 1.1.

In reality, of course, considerable scatter from the form (1.1.2) is
observed, due partly to small scale turbulent fluctuations in the air flow
above the interface. Deacon and Webb (1962) report that the drag coef-
ficient is strongly affected by thermal atmospheric stability. It has
not yet been shown, however, how such effects may be properly incorpor-
ated into the drag law.

1.2 A Description of Wind Effects in Shallow, Closed Lakes

The primary effect of direct wind shear on a surface of water is to induce upper-level drift currents in the direction of the wind stress.

In a non-stratified shallow lake, the drift currents produced by a steady wind result in a "piling-up" of water along the leeward side of the lake (Fig. 1.2). This elevation in turn produces gravity currents directed vertically downwards and hence lower level currents return water to the windward side of the lake.

Circulation in the vertical plane is thus set up with a velocity profile across a section near the centre of the lake of the form shown. Eventually the water surface reaches an equilibrium position at which the hydrostatic force due to the tilting of the surface balances the sum of the aerodynamic stress, τ_s, of the wind on the upper surface and the friction stress, τ_b, that the lake bottom exerts on return currents. Such a displacement of the water level from its mean position is often referred to as wind tide or wind set-up. At equilibrium the total fluid transport across a given vertical section is zero, provided the wind stress is homogeneous (spatially uniform) across the lake surface.

For laminar flow of a lake of uniform depth, H, it may be shown (Hellstrom (1941), Keulegan (1951)) that the fluid velocity profile at equilibrium is parabolic. The velocity is zero at depth $\frac{1}{3}H$ and the maximum return velocity magnitude, equal to a third of the surface velocity magnitude, occurs at depth $\frac{2}{3}H$. Experimentally, Francis (1954) showed that the profile under realistic (turbulent) conditions is considerably flatter near the bottom than the theoretical profile. These

results are shown in Fig. 1.3a.

The mechanism of wind tide formation in a stably stratified lake is considerably more complicated (Hutchinson (1957), Heaps and Ramsbottom (1966)). For example, in a lake separated into two layers of densities ρ_1 (upper) and ρ_2 (lower), the interface separating the two layers is tilted in a direction opposite to that of the surface. This is because surface currents in the lower layer flow in the opposite direction to the wind (Fig. 1.3b) and return currents in the lower layer thus move in the same direction as the wind.

A simple physical argument suggests that the interface slope will be much greater in magnitude than the surface slope. Consider the interface between two fluids of densities ρ (upper) and ρ' (lower). The potential energy of a volume of one fluid displaced a vertical distance ζ from its undisturbed position is directly proportional to the product $(\rho'-\rho)\zeta$. For the surface layer in Fig. 1.3b, $\rho = \rho_a$ and $\rho' = \rho_1$ so $(\rho' - \rho) \sim \rho_1$; for the lower layer of Fig. 1.3b, $(\rho' - \rho) = (\rho_2 - \rho_1) \ll \rho_1$ since the density difference between the two layers is extremely small, of $O(10^{-3} gm.cm^{-3})$. Hence, if the same amount of energy is available to both layers, the distance ζ will be much greater for the lower layer than for the upper layer. Clearly this argument is an over-simplification, but such behaviour in stratified fluids is well known, both for the open ocean (Charney (1955)) and for closed lakes (Csanady (1972)).

If the wind stress is unsteady, i.e. its strength or direction changes in time, then the induced currents and the lake surface will likewise change their pattern.

For example, if the steady wind suddenly ceases, then free surface oscillations (seiches) will occur as the surface, returning from its equilibrium set-up position to its mean-level, moves in pendulum-like fashion about that level. Damping forces within the fluid determine the rate at which the _free_ oscillations decay. A great deal of the literature on the motions of lake fluids is devoted to a description of seiches; refer, for example, Proudman (1953), Defant (1961) and Wilson (1972).

Time-varying wind stresses also give rise to _forced_ motions within a lake. The equilibrium wind tide may be regarded as a limiting or trivial case of forced motion. Forced surface oscillations are well documented in many lakes, though they may often be difficult to distinguish from free oscillations.

Generally, free and forced wind-induced motions both play important roles in the dynamical behaviour of a given lake system. In extremely shallow lakes, however, forced motions are normally of greater significance, since free motions are heavily damped.

1.3 Some Examples of Wind Effects on Closed Lakes

As stated previously, wind action on a closed lake results in a mass transport of fluid within the lake and an associated displacement of the lake surface from its mean level.

The slope of the displaced lake level is determined by the _strength_ of the wind, and also by the _depth_ of the lake. Typically its magnitude is of $0(10^{-5})$. The wind-induced surface slope increases as the depth decreases since the return flow is more heavily restricted and so there

is greater accumulation of fluid along the leeward shore. Clearly too, for a given surface slope, wind _fetch_ (the amount of lake surface over which the wind acts) is important in determining the amount of displacement of the surface from its mean level.

Thus a wind of high velocity acting over a large, shallow lake would produce large wind tides.

Perhaps the best known examples of this effect are provided by the North American Great Lakes, the surface movements of which are strongly influenced by winds.

Lake Erie is of longitudinal shape, the length being about 250km. It is, further, much shallower than the other lakes, particularly towards its western end where the depth is generally less than 20m. During a period of high winds in November 1972, Lake Survey Center water level gauges at opposite ends of the lake - at Buffalo and Toledo - recorded a simultaneous difference of about 2.5m. Harris (1954) has reported how a storm on September 25, 1941, raised the level at Buffalo by 2m and lowered the level at Toledo by nearly the same amount.

Even in periods of low winds, the effects are still noticeable. Platzman (1966), in an analysis of six months of hourly data of the Lake Erie water level, found a diurnal (24 hr) constituent of the longitudinal oscillation of the Lake and concluded that this was caused almost entirely by wind stress.

A knowledge of wind tides and associated currents is clearly of importance for the lessening of erosion and property damage and for

the protection of harbour installations and shipping. Newspaper reports of the wind-tidal flooding of the Great Lakes shores in March, 1973, spoke of millions of dollars damage being inflicted upon property owners in the states of Michigan and Ontario. These suddenly changing water levels are also known to affect the output of the Niagara power plant.

Australia has no lakes of the size or commercial importance of the Great Lakes. It does have many extremely shallow lakes, however, which would be expected to be influenced by winds. A typical example is provided by the system of Murray Mouth Lakes, South Australia, for which depths generally lie within the range 1m - 4.5m.

A detailed description of these lakes is provided in Appendix A, together with an outline of the impact of man on the system and some predictions of its future uses. In particular, planned urbanization of nearby regions could lead to the lake waters being used in diverse and possibly conflicting ways. Thus the lakes will certainly become an important recreational source; they may also be used as an outlet for wastes from the new city.

The Engineering and Water Supply Department (E. & W.S.) of South Australia has, for at least 25 years, maintained instruments for measuring wind speed and direction and corresponding water level at various points around the shoreline of the Murray Mouth Lakes. These records amply confirm the suspicion that wind effects are of considerable importance in the lakes.

This fact is well-known to farmers with property on the shores of Lake Albert who talk of considerable run-off from the lake through the Narrung Channel into Lake Alexandrina due to strong and persistent southerly winds. Indeed, high velocities characterize the currents within the Narrung Channel and often make its navigation a hazardous undertaking.

A sudden drop in the water level along the shores of Lake Albert due to an off-shore wind has occasionally prevented pastoralists from pumping the fresh water needed to irrigate their large areas of lucerne. This is also an acute problem in Lake Alexandrina where wind effects have been known to temporarily change the water level by as much as 1m, leaving inlet pipes of pumps well out of the water.

For example, a 75km/hr south wind suddenly began blowing across Lake Alexandrina just before midnight on 3 August, 1953. At Tauwitchere barrage at the south-western end of the lake, the water level had fallen by more than 1m by 2 a.m., and at Wellington, a short distance up the River Murray at the northern end of the lake, the water level had risen by over 60cms by 3 a.m. These effects are illustrated in Fig. 1.4 which shows the E. & W.S. Department's recordings of the event.

Variations of water levels in the Coorong lagoons are characterized by a _diurnal_ oscillation. These movements have been well documented by Noye (1970). Clarke (1966) contends that they are _free_ oscillations. However an examination of Fig. 1.5, showing a length of recorded water level at Seven Mile Point on the north lagoon and corresponding component of wind stress directed along the lake axis, seems to suggest that the

oscillations are wind _forced_. The diurnal oscillation of wind stress, possibly a land-sea breeze effect, gives rise to forced water level oscillations of a similar period.

Thus far in this section we have discussed the effects of surface wind stress on water levels in closed basins. Important, too, is the circulation of lake waters caused by surface wind stress.

Circulation and diffusion processes within a lake largely determine the quality of the water. In order to judge the consequences of, say, a pollution discharge into the lake, it would be necessary to have some knowledge of these processes.

Lindh and Bengtsson (1971) list the factors causing circulation of water masses in a lake as (i) wind action; (ii) inflow-outflow system; (iii) atmospheric pressure differences on the lake; (iv) astronomical forces; (v) density differences. They state, further, that wind action is by far the most important mechanism determining the lake circulation. This is so regardless of the lake depth, size or structure though such factors will alter the structure of the circulation.

Short term wind currents (time scale of 0(1 hr) or less) are of an essentially random nature, being associated with essentially random fluctuations of strength and direction in surface wind stress. There is more consistency in wind circulation of an intermediate time scale (0 (1 hr - 1 week)), since it is associated with changing weather patterns and other regular variations in wind stress. Time scales of water level changes show similar behaviour.

Associated with most closed lakes is a long term circulation (time scale of 0(1 week or more)) which in the northern hemisphere has a consistently counter-clockwise direction. (No observations are available for lakes of the southern hemisphere). Emery and Csanady (1973) have postulated that such a long term circulation is wind-induced. It must have important consequences for mixing processes within a lake.

Of course, the wind effects of different time scales cannot be rigidly categorized since the effects of one time scale interact with those of another. However the manner of this interaction is largely unknown and, in any case, is probably slight. This thesis therefore is directed towards an investigation of wind effects of the intermediate time scale which have the advantage of relative simplicity both in observation and analysis. Accordingly, the following chapter presents the mathematical equations necessary for such an analysis and briefly discusses certain types of solutions to these equations.

$$\tau_s = c_s \rho_a u_s^2$$
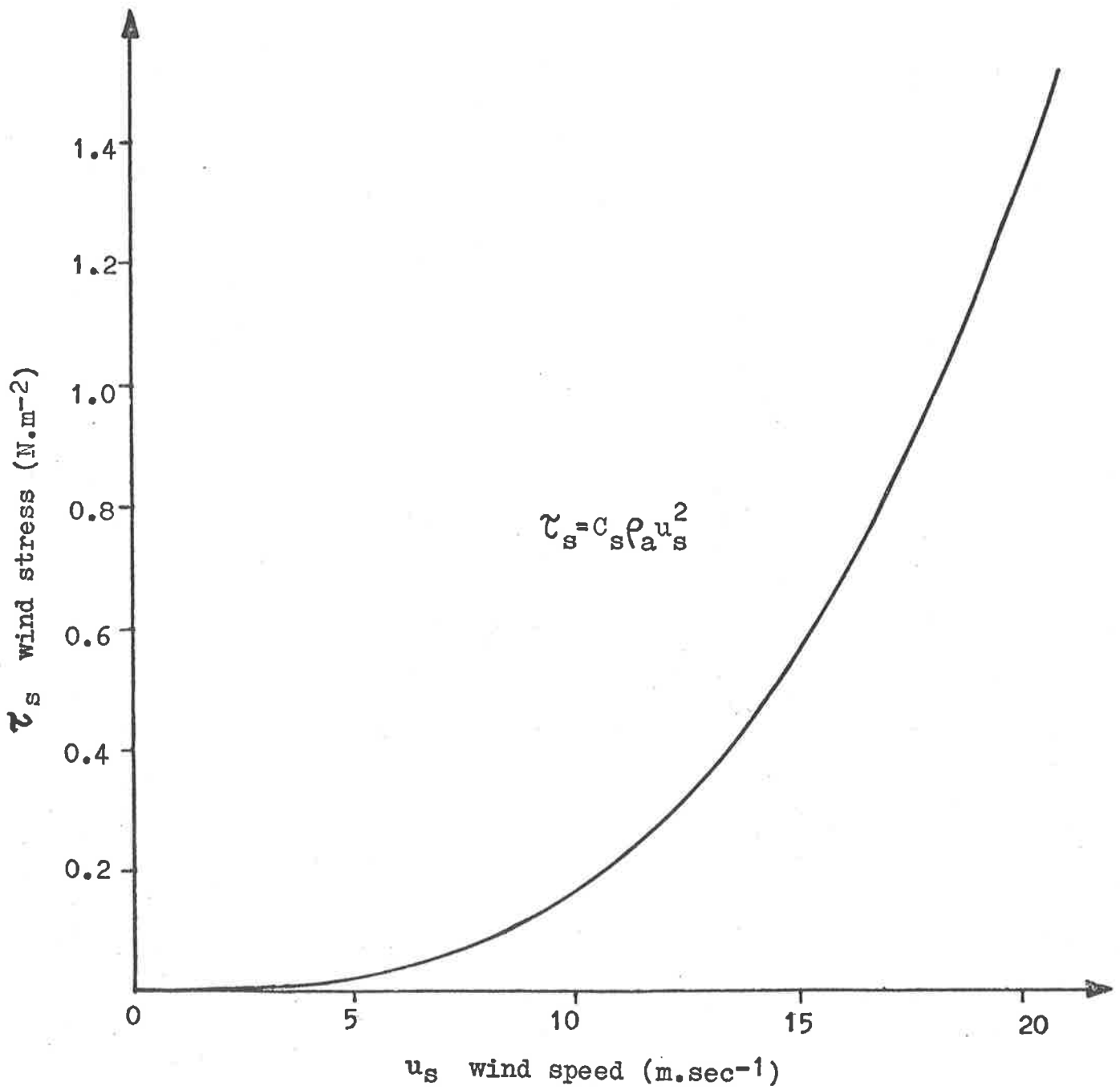
FIGURE 1.1 : RELATIONSHIP BETWEEN WIND SPEED AT 10 m
HEIGHT AND RESULTANT SURFACE WIND STRESS,
AS USED BY HEAPS AND RAMSBOTTOM (1966).

Surface wind stress τ_s

Undisturbed surface

Wind tide

A

A

Bottom friction τ_b

A

A

LAKE SURFACE

LAKE BOTTOM
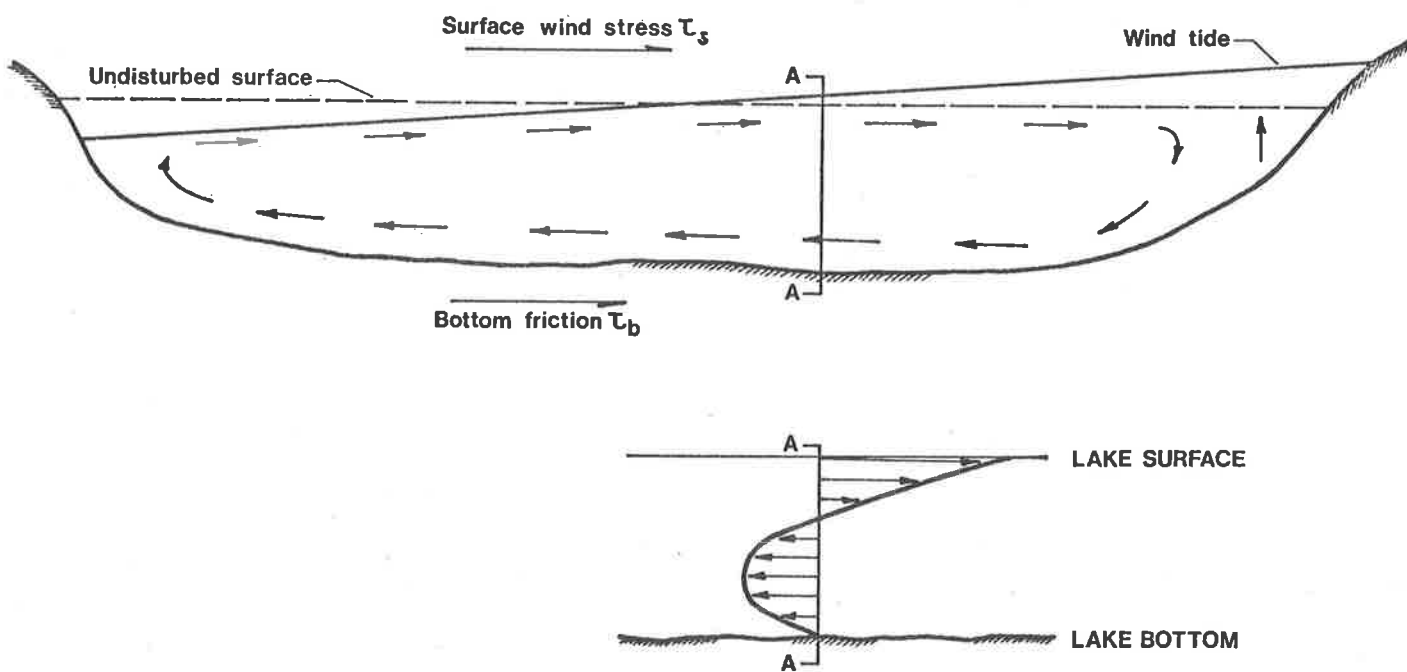
FIGURE 1.2 : SECTION OF A LAKE SHOWING WIND TIDE AND
VERTICAL CIRCULATION DUE TO THE SURFACE
WIND STRESS τ_s . SHOWN ALSO IS THE VELOCITY
PROFILE FOR THE SECTION AA NEAR THE CENTRE
OF THE LAKE.
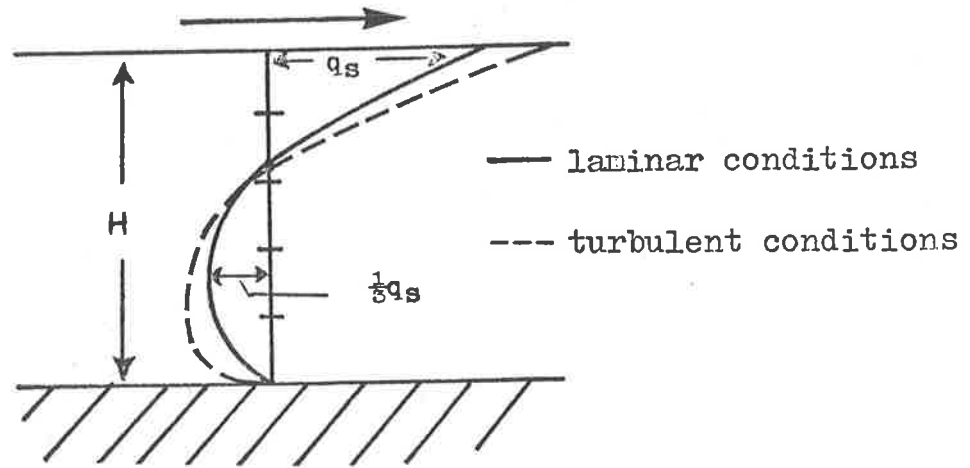
FIGURE 1.3a : EQUILIBRIUM VELOCITY PROFILE IN A LAKE
OF CONSTANT DEPTH H.
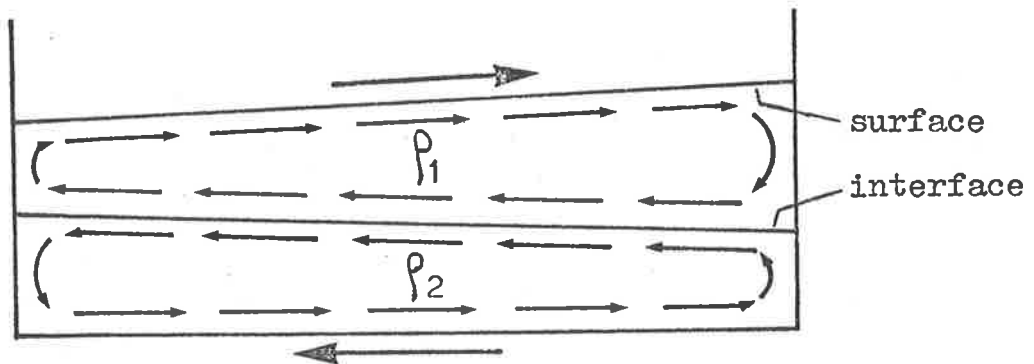
FIGURE 1.3b : WIND TIDE FORMATION IN A CONSTANT DEPTH,
TWO-LAYERED BASIN.
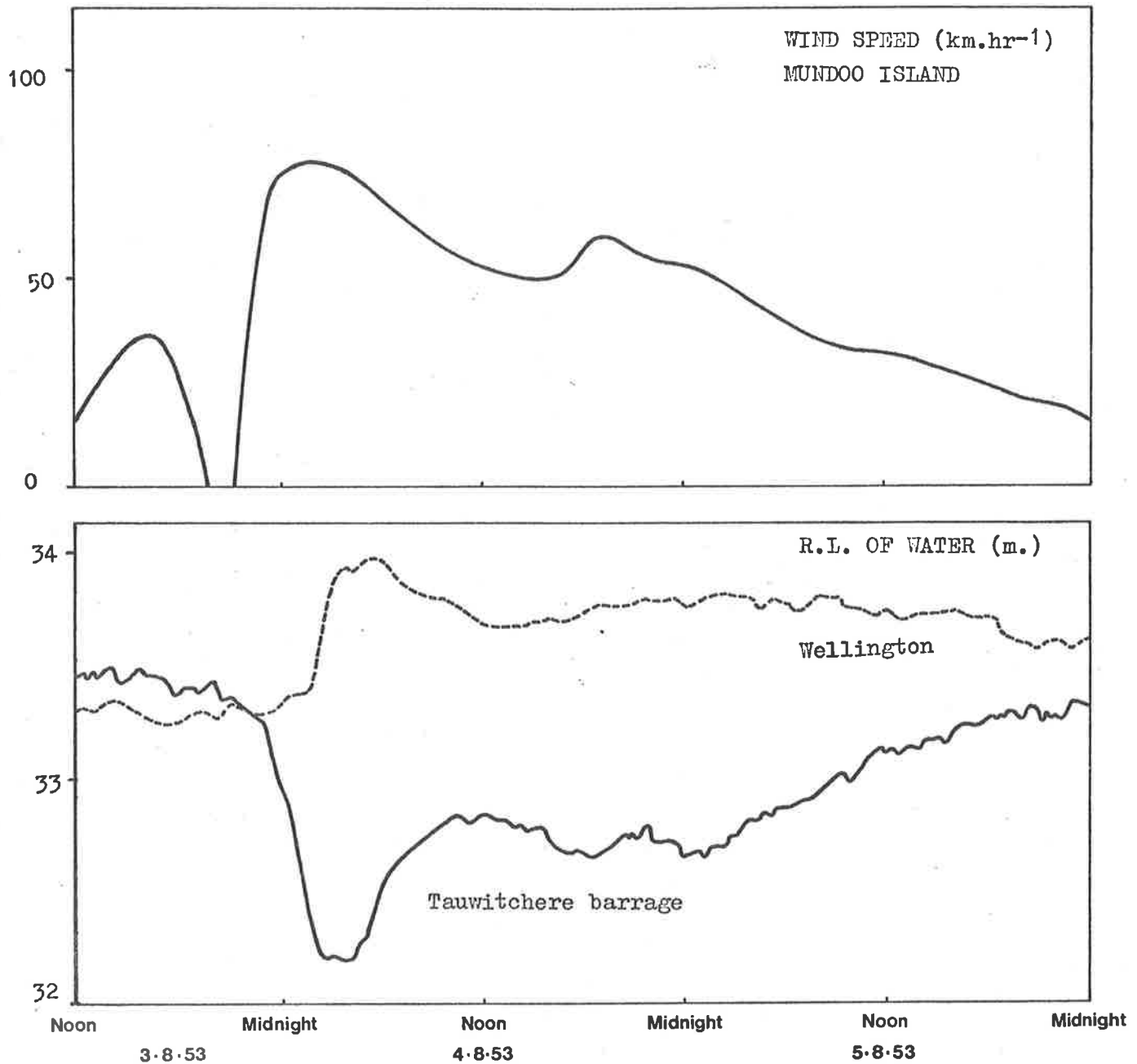
FIGURE 1.4 : E & WS DEPARTMENT'S RECORDINGS, FOR 36 HOURS
FROM 12 NOON ON 3RD AUGUST 1953, OF WIND
SPEED RECORDED AT MUNDOO ISLAND AND CORRES-
PONDING WATER LEVEL AT WELLINGTON AND
TAUWITCHERE BARRAGE. THE WIND BLEW FROM THE
SOUTH FOR MOST OF THIS TIME.
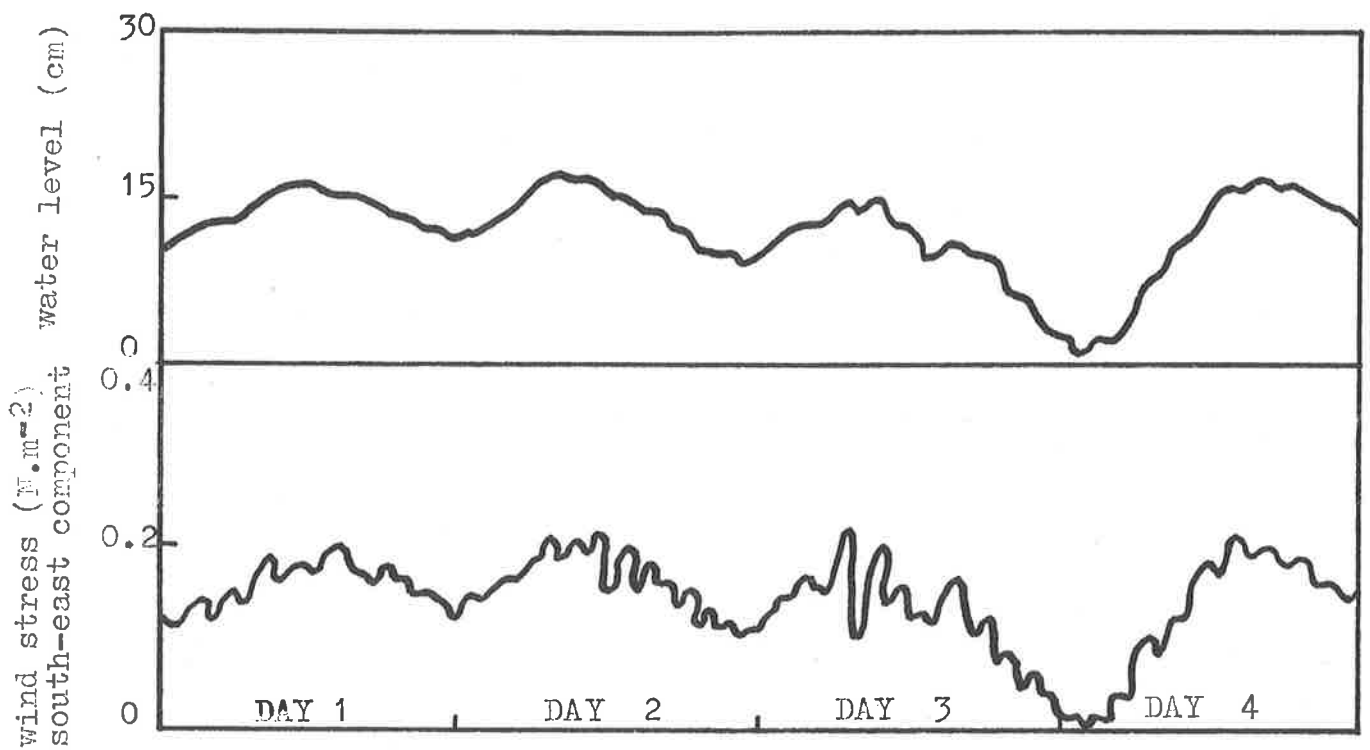
FIGURE 1.5 : EXAMPLE OF RECORDED WATER LEVEL AND
LONGITUDINAL WIND STRESS CALCULATED
FROM WIND VELOCITY RECORDS AT SEVEN
MILE POINT ON THE NORTH COORONG ,
(TAKEN FROM NOYE(1970)).

CHAPTER 2

THE WIND EFFECT EQUATIONS AND THE USE OF RESPONSE

FUNCTIONS IN THEIR SOLUTION

2.1 The Wind Effect Equations

The mathematical treatment of wind effects is accomplished by solving the Navier-Stokes equations and the equation of continuity applied to a vertical column of fluid extending from the bottom to the surface and subject to certain boundary conditions.

Consider the lake of Fig. 2.1 acted on by the wind stress vector field τ_{s}. Cartesian co-ordinate axes, fixed relative to the earth at a latitude ϕ, are placed as shown with the plane $z = 0$ in the plane of no disturbance and the z-axis directed vertically upwards. The horizontal lake contour is denoted by Γ.

The horizontal components τ_{sx}, τ_{sy} of the wind stress vector field τ_{s} are functions of x, y and t (time) as also is the displacement of water level from the $z = 0$ plane, described functionally by $z = \zeta(x,y,t)$. The bottom contour of the lake is described by $z = -h(x,y)$.

The specific equations that relate to time-dependent wind effects on shallow, homogeneous closed lakes are the Eulerian equations of motion and continuity equation used widely in oceanography; for a detailed treatment of these equations, refer, for example, Proudman (1953), Welander (1961), Fortak (1972). The equations of motion are

$$\frac{\partial u}{\partial t} - fv = -\frac{1}{\rho}\frac{\partial p}{\partial x} + \frac{\partial \tau_{xz}}{\partial z} \qquad (2.1.1a)$$

$$\frac{\partial v}{\partial t} + fu = -\frac{1}{\rho}\frac{\partial p}{\partial y} + \frac{1}{\rho}\frac{\partial \tau_{yz}}{\partial z} \qquad (2.1.1b)$$

$$0 = -\frac{1}{\rho}\frac{\partial p}{\partial z} - g \qquad (2.1.1c)$$

while the continuity equation is

$$\frac{\partial u}{\partial x} + \frac{\partial v}{\partial y} + \frac{\partial w}{\partial z} = 0 \ . \qquad (2.1.1d)$$

Here $u = u(x,y,z,t)$, $v = v(x,y,z,t)$, $w = w(x,y,z,t)$ are x-, y-, and z-components respectively of fluid velocity; $p = p(x,y,z,t)$ is fluid pressure; $\tau_{xz} = \tau_{xz}(x,y,z,t)$, $\tau_{yz} = \tau_{yz}(x,y,z,t)$ are components of the turbulent stress tensor acting in planes parallel to the $z = 0$ plane. In addition, ρ is fluid density (assumed constant), g is the acceleration due to gravity and f is the Coriolis parameter with a value calculable from

$$f = \begin{cases} 2\Omega\sin\phi, & \text{northern hemisphere} \\ -2\Omega\sin\phi, & \text{southern hemisphere} \end{cases} \qquad (2.1.2)$$

where $\Omega = 0.73 \times 10^{-4} \sec^{-1}$ is the angular velocity of the earth's rotation.

A number of important assumptions were made in forming the system of equations (2.1.1).

Firstly, in (2.1.1c), the vertical acceleration terms have been omitted. It may be shown, (Proudman (1953), Stoker (1957)), that this is valid provided that

$$\frac{h^*}{\ell^*} \ll 1$$

where h* (a typical depth) and ℓ* (a typical horizontal distance) are vertical and horizontal length scales for the motion involved. This is the so-called "long-wave" approximation and when it holds true the water is said to be "shallow".

It is clear, then, from (2.1.1c) that the fluid pressure obeys the hydrostatic relation

$$p = p_a + \rho g \ (\zeta - z) \tag{2.1.3}$$

where $p_a = p_a(x, y, t)$ is the surface (i.e. atmospheric) pressure. Since we are not interested here in the effects of surface pressure variations we assume that p_a is constant in space and time.

Secondly, we neglect horizontal convection of turbulence, an assumption which again is valid for shallow waters where movement in vertical planes is slight.

These two assumptions must clearly break down in shore regions where vertical and horizontal length scales become of the same order of magnitude. From Fig. 1.2 it is clear that considerable motion in vertical planes is generated near the shores during wind tide formation in closed basins.

Thirdly, it is assumed that convective (non-linear) acceleration terms in (2.1.1a), (2.1.1b) may be omitted. For example, a term of the form $u \frac{\partial u}{\partial x}$ may be neglected in comparison with the local acceleration term $\frac{\partial u}{\partial t}$ provided that

$$\frac{\ell^*}{t^*} \gg u^*$$

where t^*, u^* are time and fluid velocity scales for the motion under concern.

The ratio $\ell*/t* = c*$ is essentially equivalent to the velocity of long gravity waves, $\sqrt{gh*}$, in the basin.

Can we omit a term of the form $w \frac{\partial u}{\partial z}$ in comparison with $\frac{\partial u}{\partial t}$? The vertical velocity w is close to zero at the bottom, and at the free surface may be approximated by $\frac{\partial \zeta}{\partial t}$ provided that the surface slope is not too large. Thus a typical vertical velocity is $\zeta*/t*$ where $\zeta*$ is a typical surface elevation. So provided that

$$\frac{\zeta*}{h*} \ll 1$$

then the above omission is justified. It is again clear, however, that the approximation would break down near shore regions.

As shown by Greenspan (1968), the magnitude of the Rossby number, a ratio of the convective acceleration to the Coriolis acceleration, also indicates the relative importance of non linear acceleration terms. The assumption of small Rossby number has been used by, for example, Platzman (1963), Csanady (1967) and Liggett (1969), as a justification for neglecting non linear accelerations in the equations of motion.

Fourthly, we neglect the effects of spatial variation of the Coriolis parameter. Harlemann et al. (1962) have shown this to be a quite valid approximation for the Great Lakes and it will clearly hold for smaller water bodies.

Combining (2.1.1a), (2.1.1b) with (2.1.3) gives

$$\frac{\partial u}{\partial t} - fv = -g \frac{\partial \zeta}{\partial x} + \frac{1}{\rho} \frac{\partial \tau_{xz}}{\partial z} \qquad (2.1.4a)$$

$$\frac{\partial v}{\partial t} + fu = -g \frac{\partial \zeta}{\partial y} + \frac{1}{\rho} \frac{\partial \tau_{yz}}{\partial z} . \qquad (2.1.4b)$$

The continuity equation (2.1.1d) may be simplified by vertical integration from the bottom, $z = -h$, to the free surface, approximated by $z = 0$, to give

$$\int_{-h}^{0} \frac{\partial u}{\partial x} \, dz + \int_{-h}^{0} \frac{\partial v}{\partial y} \, dz = - \frac{\partial \zeta}{\partial t} . \qquad (2.1.4c)$$

The assertion that the free surface and the $z = 0$ plane closely coincide is again valid if

$$\frac{\zeta^*}{h^*} \ll 1 .$$

Equations (2.1.4) are subject to the following boundary conditions:-

(i) The flow normal to a closed boundary is zero, i.e.

$$q_n = 0 \text{ along } \Gamma \qquad (2.1.5a)$$

where $q = (u,v)$. This condition is equivalent to the assumption that the contour Γ does not alter with time, i.e. that no land is covered or uncovered with a rise or fall in water level. For particularly shallow lakes surrounded by low-lying flats, however, hurricane force winds may flood the surrounds and expose a large portion of the lake bed. Such was the case with Lake Okeechobee, Florida, during the hurricane of 26-27 August, 1949 as reported by Haurwitz (1951).

(ii) Shear stress is continuous in the plane of the free surface, again approximated by $z = 0$, i.e.

$$\tau_{xo} = \tau_{sx} \, , \quad \tau_{yo} = \tau_{sy} \tag{2.1.5b}$$

where τ_{sx}, τ_{sy} are the horizontal components of surface wind stress.

(iii) As a bottom condition we may impose the "no-slip" condition

$$u(x,y,-h,t) = v(x,y,-h,t) = 0 \, . \tag{2.1.5c}$$

The imposition of a bottom boundary layer contrasts with the absence of a boundary layer along the contour Γ due to the neglect of horizontal turbulent convection.

Before equations (2.1.4) subject to conditions (2.1.5) can be used to examine wind effect problems on a given lake system, the assumptions made in their derivation should be validated for the system. Consider, for example, the system of Murray Mouth lakes.

Taking $h* = 2m$, $\ell* = 10km$ it is clear that the long-wave approximation is quite valid. Further, since $c* = 0(5 \ m.sec^{-1})$ and wind-induced fluid velocities are typically less than $0.1 \ m.sec^{-1}$ in magnitude, then the convective term $u \frac{\partial u}{\partial x}$ may be omitted in comparison with the local derivative $\frac{\partial u}{\partial t}$. Further, we omit the term $w \frac{\partial u}{\partial z}$ on the basis that typically $\zeta* = 0(1m)$.

During periods of strong winds it is possible that $\zeta* = 0(1m)$ so that no longer does the approximation $\zeta*/h* \ll 1$ hold true. This is especially so for the Coorong (refer Appendix A) where $h*$ is closer to $1m$; near the south-eastern tip of the South lagoon depths are of $0(10cm)$. However, for purposes of mathematical simplicity, we shall neglect $\zeta*$ in comparison with $h*$.

Finally, although low-lying mud flats around Lake Albert and Lake Alexandrina are at times inundated by wind tides, the extent of the flooding is small. Further, the boundaries of the shallow extremes of the South Coorong are subject to movement under the influence of winds, but to the first approximation this is slight.

It needs to be emphasized again that equations (2.1.4) are generally invalid near shore regions, where vertical and convective accelerations become important while lateral friction may no longer be neglected. The more exact, non-linear form of the equations is needed to properly account for wind effects in these regions.

It is clear that (2.1.4) is not closed in the dependent variables u, v and ζ. Closure is effected by expressing τ_{xz}, τ_{yz} in terms of these variables. This is normally performed in one of the two following ways:-

(a) Eddy-viscosity method.

This method uses the concept of the coefficient of eddy viscosity, N, defined by analogy with laminar flow so that

$$\tau_{xz} = \rho N \frac{\partial u}{\partial z} \, , \quad \tau_{yz} = \rho N \frac{\partial v}{\partial z} \, . \qquad (2.1.6)$$

Thus, the fluid flow is assumed to be essentially quasi-laminar. The value of N varies from point to point within the fluid though a constant value for a given lake is normally assumed, this being a simple model which gives satisfactory results. The assumption of constant N is best for shallow, well-mixed waters. Density stratification in the fluid strongly influences the value of N, which may fall practically to zero in the region

of a density discontinuity (Welander (1957)).

Combining (2.1.4) and (2.1.6) gives

$$\frac{\partial u}{\partial t} - fv = -g \frac{\partial \zeta}{\partial x} + N \frac{\partial^2 u}{\partial z^2} \qquad (2.1.7a)$$

$$\frac{\partial v}{\partial t} + fu = -g \frac{\partial \zeta}{\partial y} + N \frac{\partial^2 v}{\partial z^2} \qquad (2.1.7b)$$

$$\frac{\partial}{\partial x} \int_{-h}^{0} u dz + \frac{\partial}{\partial y} \int_{-h}^{0} v dz = - \frac{\partial \zeta}{\partial t} \qquad (2.1.7c)$$

while the boundary condition (2.1.5b) becomes

$$\rho N \left(\frac{\partial u}{\partial z} \right)_{z=0} = \tau_{sx}, \quad \rho N \left(\frac{\partial v}{\partial z} \right)_{z=0} = \tau_{sy}. \qquad (2.1.8)$$

(b) Volume transport method.

This method conveniently by-passes the problem of the specification of the vertical dependence of the stress vector. It uses the technique of vertical integration of the equations of motion (2.1.4a), (2.1.4b) from the bottom to the surface to give

$$\frac{\partial U}{\partial t} - fV = -gh \frac{\partial \zeta}{\partial x} + \frac{1}{\rho} (\tau_{sx} - \tau_{bx}) \qquad (2.1.9a)$$

$$\frac{\partial V}{\partial t} + fU = -gh \frac{\partial \zeta}{\partial y} + \frac{1}{\rho} (\tau_{sy} - \tau_{by}) \qquad (2.1.9b)$$

while (2.1.4c) may be rewritten as

$$\frac{\partial U}{\partial x} + \frac{\partial V}{\partial y} = - \frac{\partial \zeta}{\partial t} . \qquad (2.1.9c)$$

In (2.1.9), $U = U(x,y,t)$ and $V = V(x,y,t)$ are the components of volume transport (or total stream), given by

$$U = \int_{-h}^{0} u\,dz, \quad V = \int_{-h}^{0} v\,dz .$$

The transport vector $\underset{\sim}{S} = (U,V)$ is related to $\underset{\sim}{q}_m$, the velocity vector averaged over depth, by

$$\underset{\sim}{S} = h\underset{\sim}{q}_m .$$

Equations (2.1.9) are subject to the boundary condition that the component of the transport vector $\underset{\sim}{S}$ normal to the contour, is zero, i.e.

$$S_n = 0 \text{ along } \Gamma . \tag{2.1.10}$$

Weenink (1958), Groen and Groves (1962) and Fortak (1962) treat in detail the assumptions made in the vertical integration to produce (2.1.9). In particular, the free surface is again assumed to coincide with the plane $z = 0$, which is true, provided that $\zeta^*/h^* \ll 1$. τ_{bx}, τ_{by} are the components of the bottom stress vector, $\underset{\sim}{\tau}_b$. The surface stress components τ_{sx}, τ_{sy} are known at any time. However, the bottom stress components are unknown, and in order to make the system (2.1.9) closed in the variables U, V and ζ, they must be expressed in terms of those variables.

Essentially, the bottom stress magnitude satisfies a drag relationship similar to (1.1.1), viz.

$$|\underset{\sim}{\tau}_b| = \rho C_b |\underset{\sim}{q}_b|^2 \tag{2.1.11a}$$

where C_b is a dimensionless drag coefficient and $\underset{\sim}{q}_b$ is the fluid velocity vector measured at the outer edge of the bottom boundary layer. Proudman (1953), p.136 gives a value for C_b of 2.5×10^{-3} .

A convenient linearized form for $\underset{\sim}{\tau}_b$ may be achieved by writing

$$\underset{\sim}{\tau}_b = \rho C_b \; |\underset{\sim}{q}_b| \; \underset{\sim}{q}_b \qquad\qquad (2.1.11b)$$

and defining a parameter r, with the dimensions of velocity, by

$$r = C_b \; |\underset{\sim}{q}_b| \; .$$

Furthermore, by approximating

$$\underset{\sim}{q}_b = \underset{\sim}{q}_m = \frac{\underset{\sim}{S}}{h}$$

then (2.1.11b) becomes

$$\underset{\sim}{\tau}_b = \frac{\rho r \underset{\sim}{S}}{h} \; . \qquad\qquad (2.1.11c)$$

The form (2.1.11c) predicts that in an equilibrium situation, i.e. when no net flow or transport is occurring, the bottom stress vanishes. However for the equilibrium wind set-up of a closed lake, there clearly is a stress exerted on the bottom by return currents near the bottom. One may think of the bottom as exerting a stress on the fluid in the direction of the surface stress (Fig. 1.2).

So for a general, non-equilibrium situation, the bottom stress is more correctly given by

$$\underset{\sim}{\tau}_b = -m\underset{\sim}{\tau}_s + \frac{\rho r \underset{\sim}{S}}{h} \qquad\qquad (2.1.11d)$$

where m is a non-dimensional parameter that essentially specifies the relative additional contribution that the bottom stress makes to the surface stress. For laminar, wind-induced flow in a lake of uniform depth,

Hellstrom (1941), Keulegan (1951) and Felsenbaum (1956) all have deduced that at equilibrium m = 0.5. Francis (1954) showed that in realistic turbulent flows m is generally less than 0.1.

Bowden (1956) and Reid (1956) give more exact treatments than that provided here of the linearized form (2.1.11d). Smith (1973) has provided a detailed comparison of the bottom stress parameterizations used by previous authors. Groen and Groves (1962) discuss the different forms of non-linear damping.

The term $\rho r \underset{\sim}{S}/h$ models turbulent dissipative effects within the fluid. For simplicity, the parameter r is generally taken as constant for a given hydrodynamical system. It is sometimes assumed that r = 0, i.e. the system is non-dissipative. However such a simple model is unrealistic for extremely shallow waters where near bottom currents meet strong resistance, so leading to high energy dissipation.

Throughout this thesis the linearized bottom stress expression (2.1.11d) is used, with r taken as constant. Combining (2.1.11d) and (2.1.9) gives the following system closed in the variables U, V and ζ :-

$$\frac{\partial U}{\partial t} + \frac{r}{h} U - fV = -gh \frac{\partial \zeta}{\partial x} + K\tau_{sx} \qquad (2.1.12a)$$

$$\frac{\partial V}{\partial t} + \frac{r}{h} V + fU = -gh \frac{\partial \zeta}{\partial y} + K\tau_{sy} \qquad (2.1.12b)$$

$$\frac{\partial U}{\partial x} + \frac{\partial V}{\partial y} = - \frac{\partial \zeta}{\partial t} \qquad (2.1.12c)$$

where $K = (1+m)/\rho$.

Let us briefly compare the eddy viscosity and transport forms of the wind effect equations.

Clearly, the system (2.1.12), the transport form of the equations, is of a simpler form than (2.1.7), the eddy viscosity form, due to the absence in the former of the independent variable z. The corresponding boundary conditions also are simpler. For these reasons the transport form is normally preferred, both for analytical and for numerical work. However by elimination of the variable z, all information concerning the vertical distribution of currents is lost. Using only the transport equations we can at best obtain the mean velocity over depth.

An inherent weakness of both (2.1.12) and (2.1.7) is the presence in each of an unknown damping parameter. Semi-empirical methods must be used to determine values of r or N for particular lakes.

Platzman (1963) determined a value for the eddy viscosity of Lake Erie, viz. $40 \mathrm{cm}^2 \mathrm{sec}^{-1}$, by measurement of the decay of the fundamental mode of surface oscillation. Much the same method was used by Heaps and Ramsbottom (1966) to estimate a value of r for the more dense, bottom layer in the stratified Lake Windermere, Scotland.

Liggett and Hadjitheodorou (1969) estimate a value of the eddy viscosity for Lake Erie, viz. $200 \mathrm{cm}^2 \mathrm{sec}^{-1}$, which correctly predicts certain measured currents. A similar method of computing eddy viscosity from observed velocities has been used by Lindh and Bengtsson (1971).

The difference in the above two estimates for the eddy viscosity of Lake Erie indicates the essentially variable nature of the parameters r

and N. It is not really sensible to assert that for a given lake system either of the parameters always takes a certain value. Perhaps the best that can be achieved is to choose values for r and N at a given time which give results compatible with observations.

It should finally be mentioned that the supreme mathematical advantage of both (2.1.12) and (2.1.7) is the property of linearity, which makes it possible to obtain some relatively simple analytical solutions and to use many of the powerful tools of linear system theory in so doing.

2.2 The Concept of the Response Function in Relation to Wind Effects

Papoulis (1962), p.81, in defining the term "system" states that:-

"The analysis of most physical systems can be reduced to the investigation of the relationship between certain causes and their effects. Any system can be viewed as a transducer, with the cause $f_i(t)$ as its input and the effect $f_o(t)$ as its output or response; $f_o(t)$ is uniquely determined in terms of $f_i(t)$. The system is completely characterized terminally if the nature of the dependence of the output on the input is known".

When solving the wind effect equations one is essentially concerned with the response of a system to given inputs. Suppose the wind stress is homogeneous over the lake surface. Then one might take as inputs to the system the wind stress components $\tau_{sx}(t)$, $\tau_{sy}(t)$ and as output the resulting surface displacement $\zeta(x_o, y_o, t)$ measured at the position (x_o, y_o). These input and output signals are functions of time only. Further, since

the system behaviour is described by linear equations, then it must be a linear system and so obey the law of superposition.

It is customary to model analytically the behaviour in real lake basins due to real wind stress fields by considering basins of simple shapes and wind stress fields of simple spatial and time variation. Then, by superposition, one may obtain the response of the model basin to a real wind stress field. Simple but realistic theoretical models of wind stress fields include:-

(a) A wind of constant strength and direction over the whole lake surface suddenly imposed at time t = 0, and maintained at that strength thereafter

In the language of systems analysis, such a wind stress field is a step input to the system, i.e. of the form $\tau_s(t) = \tau_o . \overline{U}(t)$ where $\overline{U}(t)$ is the Unit step function and τ_o is constant. It models quite realistically a large scale storm or cyclonic disturbance maintained over a lake for a considerable time. The response of the lake consists of two parts - the transient of dynamic part of the response and the equilibrium or steady state part of the response. Essentially, the response consists of damped free oscillations about the equilibrium response, the degree of damping in the oscillation depending on the extent of internal damping occurring within the system. (For later use, we define the step response of a linear system as being the response to an input function $f_i(t) = \overline{U}(t)$).

(b) <u>A wind of constant strength and alignment but varying periodically in</u> <u>time</u>

Such a wind models the effects due to changes in weather patterns, e.g. large-scale weather cycles or small-scale land-sea breeze effects. The example of the prevailing oscillating winds over the Coorong lagoons has been previously cited.

Now for a linear system, the steady state response (after starting transients have died away) to a sinusoidal input is itself sinusoidal with the same angular frequency as the input. However, the amplitude and phase will, in general, be different. Using complex number notation, if the input function has the form $f_i(t) = e^{j\omega t}$ where $j = \sqrt{-1}$ and ω is an angular frequency, i.e. a <u>unit-amplitude</u> sinusoid, then the steady-state response will be $f_o(t) = J(\omega)e^{j\omega t}$ where the function $J(\omega)$ is most commonly called the frequency response function or <u>response function</u> for the system. We may, further, write

$$J(\omega) = G(\omega)e^{-j\phi(\omega)} \qquad (2.2.1)$$

where $G(\omega)$ is the gain of the system response and $\phi(\omega)$ is its phase-lag (Fig. 2.2).

The term 'system function' is also used to describe $J(\omega)$. It is a convenient label for the input-output characteristics of a linear system, whether the components of that system be electrical, mechanical or hydrodynamic. Its chief advantages are that it may be obtained in a relatively simple manner either analytically or numerically, and that it is possible, using time series analysis, to extract the system function from a given

input-output record and so to make comparisons between theoretical and experimental response functions.

One may draw an input-output diagram (block diagram) as shown in Fig. 2.3a to describe the linear system with response function $J(\omega)$.

A system consisting of a lake acted on by a wind stress field may be viewed as a two input - single output system with block diagram shown in Fig. 2.3b. There are two response functions needed to specify the total system, viz. $Z_1 = Z_1(x_o, y_o, \omega)$ for the subsystem with $\tau_{sx}(t)$ as input and a displacement $\zeta_1(x_o, y_o, t)$ as output, and $Z_2 = Z_2(x_o, y_o, \omega)$ for the subsystem with $\tau_{sy}(t)$ as input and a displacement $\zeta_2(x_o, y_o, t)$ as output. Further, one has that

$$\zeta(x_o, y_o, t) = \zeta_1(x_o, y_o, t) + \zeta_2(x_o, y_o, t) \qquad (2.2.2)$$

i.e. the two 'sub-displacements' add to give the total displacement.

When only one component of wind stress, say τ_{sx}, affects the lake, i.e. the wind stress field is uni-directional, the 'sub'-response function $Z_1(x_o, y_o, \omega)$ becomes the 'total' response function, and may be inferred by data analysis from a given record of wind stress and corresponding surface displacement.

However, for a general two-dimensional problem, it is not a simple matter to determine $Z_1(x_o, y_o, \omega)$, $Z_2(x_o, y_o, \omega)$ by analysis of experimental data. Instead, if $\tau_{sx}(t) = \tau_{ox} e^{j\omega t}$, $\tau_{sy}(t) = \tau_{oy} e^{j\omega t}$ one has that $\zeta(x_o, y_o, t) = Z(x_o, y_o, \omega) e^{j\omega t}$, where

$$Z = \tau_{ox} Z_1 + \tau_{oy} Z_2 \ . \qquad (2.2.3)$$

The function $Z(x_o, y_o, \omega)$ _may_ be extracted by a simple analysis of the output record; however, it is not a true response function for the system.

Note that in the relation $\zeta = Ze^{j\omega t}$, ω is regarded as fixed so that we have $\zeta = \zeta(x_o, y_o, t)$. However we maintain the convention of writing $Z = Z(x_o, y_o, \omega)$, since we are specifically interested in the variation of Z with ω. Note also that we might equally well have taken either component of volume transport measured at (x_o, y_o) or, indeed, a velocity component at any depth and measured at (x_o, y_o), as being a representative output function of the system consisting of a closed lake with input functions $\tau_{sx}(t), \tau_{sy}(t)$.

A great deal of the literature in linear system theory deals with the determination of the response, $f_o(t)$, of the system to an arbitrary input $f_i(t)$, if the response to some standard input is known.

Application of the convolution theorem enables $f_o(t)$ to be expressed in terms of the step response, $a(t)$, of the system by means of the Duhamel formula

$$f_o(t) = \int_0^\infty f_i(t-\tau) \frac{d}{d\tau} a(\tau) d\tau . \qquad (2.2.4)$$

In wind effect problems, integrals of this type have been formulated and used with some success; refer, for example, Proudman and Doodson (1924), Saito (1949), Heaps and Ramsbottom (1966). For a treatment of the Duhamel formulae, refer Wylie (1966), p. 272.

It is also possible to express $f_o(t)$ directly in terms of $J(\omega)$. It may be shown (Papoulis (1962), p.86) that

$$f_o(t) = \frac{1}{2\pi} \int_{-\infty}^{\infty} J(\omega) \, F(\omega) e^{j\omega t} d\omega \qquad (2.2.5)$$

where $F_i(\omega)$ is the Fourier transform of $f_i(t)$, i.e.

$$F_i(\omega) = \int_{-\infty}^{\infty} f_i(t) e^{-j\omega t} dt.$$

Alternatively, for a periodic input function $f_i(t)$, we may write

$$f_i(t) = \sum_{n=-\infty}^{\infty} a_n e^{j\omega_n t} \qquad (2.2.6)$$

for which the steady state response is clearly given by

$$f_o(t) = \sum_{n=-\infty}^{\infty} a_n J(\omega_n) e^{j\omega_n t} \quad . \qquad (2.2.7)$$

In making practical use of this method, since the input record to be analysed is of finite length T, the continuation of period T must be used. Further, the series (2.2.6), (2.2.7) will be finite. The steady state response to this periodic input (of period T) will be close to the observed response if T is sufficiently large to have allowed the system to reach a steady state.

Using (2.2.5) we may derive a convenient form for the step response, $a(t)$, in terms of $J(\omega)$. In this case, $f_i(t) = \overline{U}(t) = \frac{1}{2}(1 + \text{sgn}(t))$, where

$$\text{sgn}(t) = \begin{cases} +1, & t > 0 \\ -1, & t < 0 \end{cases} .$$

Now the Fourier transform of 1 is $2\pi \, \delta(\omega)$, while the Fourier transform of $\text{sgn}(t)$ is $2/j\omega$. Hence, in this case,

$$F_i(\omega) = \pi \delta(\omega) + \frac{1}{j\omega}$$

so that (2.2.5) gives

$$a(t) = \frac{1}{2} \left(J(0) + \frac{1}{\pi} \left(\int_{-\infty}^{\infty} \frac{J(\omega)e^{j\omega t}}{j\omega} \, d\omega \right) \right). \qquad (2.2.8a)$$

Papoulis (1962) shows that for a causal system (2.2.8a) may be simplified to

$$a(t) = \frac{2}{\pi} \int_{0}^{\infty} \frac{R(\omega)}{\omega} \sin (\omega t) d\omega \qquad (2.2.8b)$$

where $R(\omega) = \text{Real } \{J(\omega)\}$.

Now it may be shown that $J(0) = R(0)$, i.e. the response function $J(\omega)$ assumes only real values at $\omega=0$. Further, the equilibrium response to the unit step function is given by $\lim_{t\to\infty} \{a(t)\}$, provided that the limit exists. In Appendix B it is shown that

$$\lim_{t\to\infty} \{a(t)\} = J(0) = R(0) . \qquad (2.2.9)$$

Thus, the forms (2.2.8a), (2.2.8b), (2.2.9) provide convenient means of calculating both the total step response and the equilibrium step response.

In the following chapters we shall concentrate on the calculation of response functions for various lakes of simple form using analytical techniques, and more complex form using finite difference numerical techniques. Using the methods outlined above, however, we shall, where appropriate, transfer our attention from the frequency domain to the real time domain in considering the response of such lakes to non-periodic wind stresses.
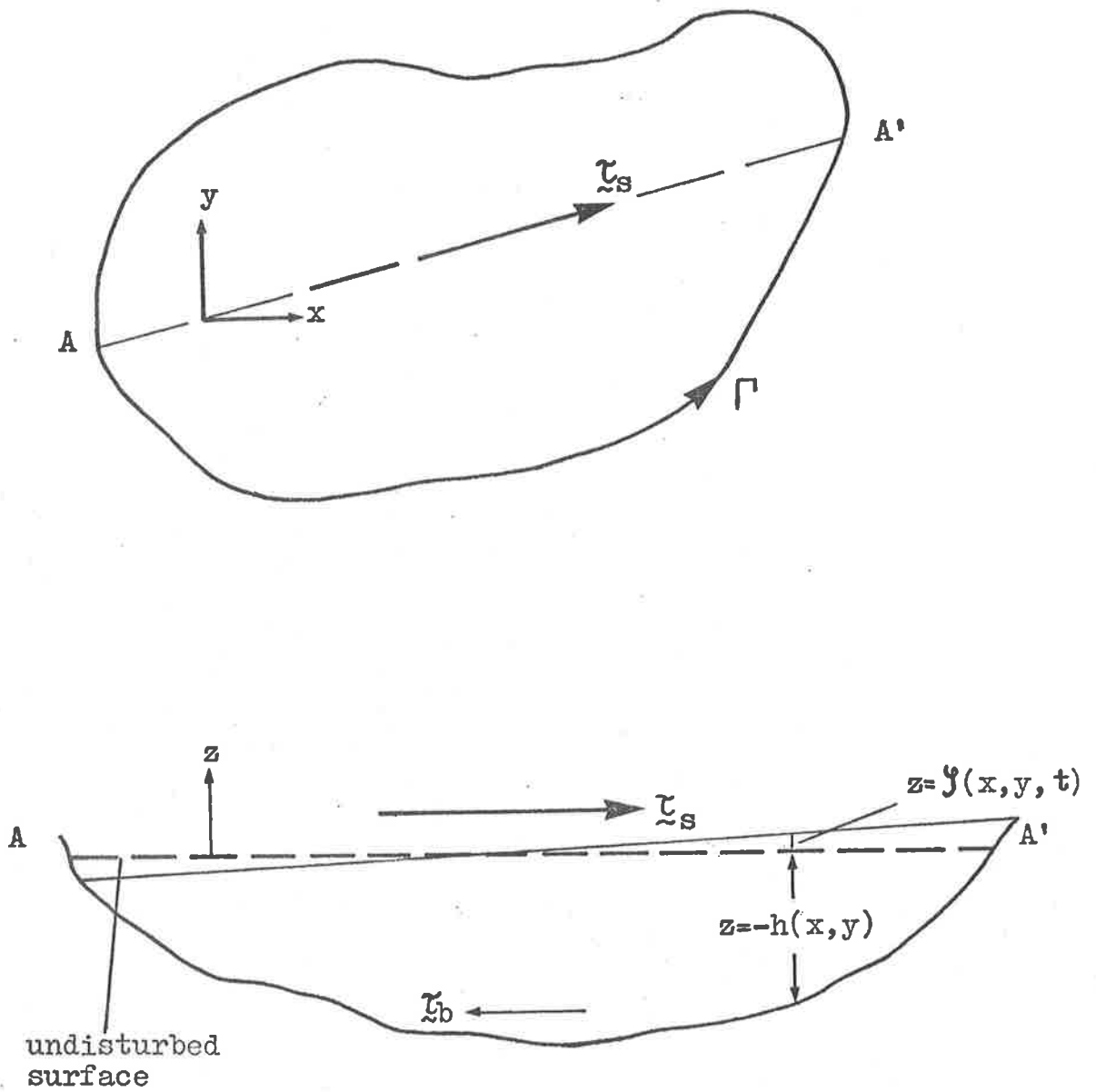
FIGURE 2.1 : PLAN AND SECTION OF A LAKE ACTED ON
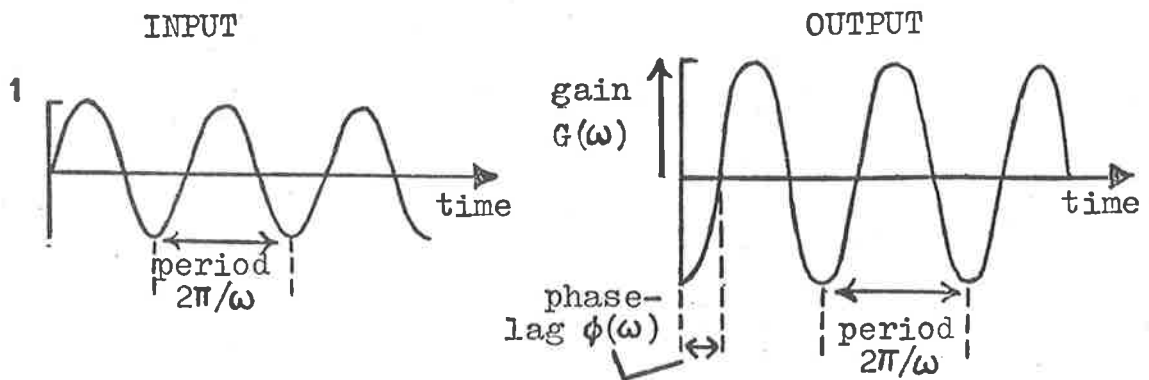BY THE WIND STRESS VECTOR $\underset{\sim}{\tau}_s$.

FIGURE 2.2 : SINGLE INPUT AND OUTPUT OSCILLATIONS FOR A
LINEAR SYSTEM, SHOWING THE GAIN AND PHASE-
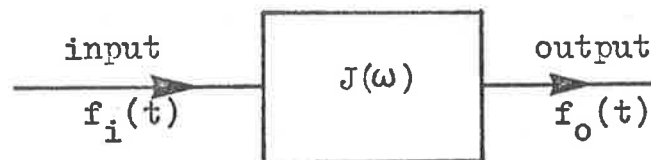LAG AT ANGULAR FREQUENCY ω .

FIGURE 2.3a : BLOCK DIAGRAM FOR THE LINEAR SYSTEM WITH
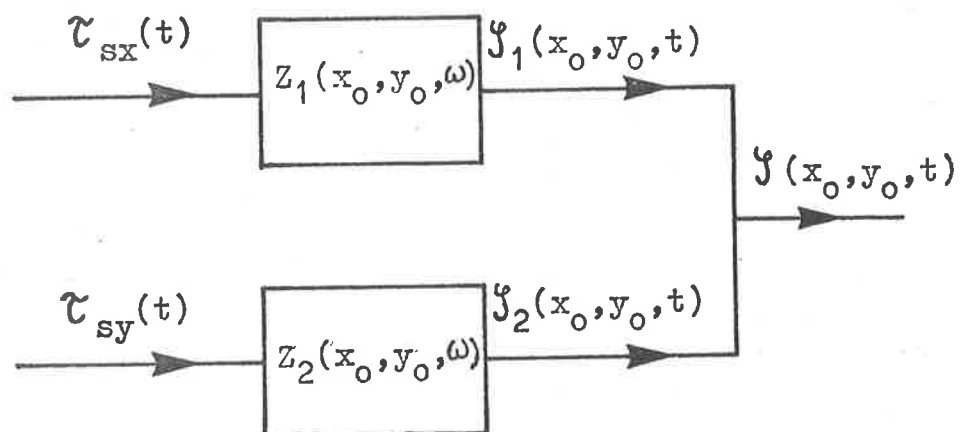RESPONSE FUNCTION $J(\omega)$.

FIGURE 2.3b : BLOCK DIAGRAM FOR THE WIND STRESS — WATER
LEVEL LINEAR SYSTEM .

CHAPTER 3

RESPONSE FUNCTIONS FOR NARROW LAKES - AN ANALYTICAL STUDY

3.1 The 'Narrow Lake' Approximation

Consider a closed lake which is significantly elongated in a particular direction. The dominant wind effects on such a lake are a result of wind stresses acting parallel to the longitudinal (lake) axis. As an example, the wind tide formed in a direction transverse to the lake axis is negligible compared with that formed along the lake axis, since the ratio of transverse wind fetch to longitudinal wind fetch is very small.

The so-called 'narrow lake' approximation consists, then, of ignoring wind-induced motions directed at right angles to the lake axis. Only the longitudinal component of wind stress need be considered in a determination of wind effects in the basin. The approximation has been often used in studying the free and forced motions of fluids in elongated, closed basins and narrow, infinite canals; refer, for example, Lamb (1932), Proudman (1953).

As part of the approximation we neglect the effects of the Coriolis force. Supposing the lake axis to be equivalent to the x-axis of the coordinate system of Fig. 2.1 (we ignore the effects of curvature in the lake axis), then $v = 0$ and $\tau_{yz} = 0$, so (2.1.4b) gives

$$fu = -g \frac{\partial \zeta}{\partial y} \tag{3.1.1}$$

i.e. Coriolis effects "are represented by transverse pressure gradients" (Proudman (1953), p. 219) which do not significantly influence the

longitudinal motion and may be ignored.

Thus, the 'narrow lake' approximation reduces the eddy viscosity form of the wind effect equations to

$$\frac{\partial u}{\partial t} = -g \frac{\partial \zeta}{\partial x} + N \frac{\partial^2 u}{\partial z^2} \qquad\qquad (3.1.2a)$$

$$\frac{\partial}{\partial x} \int_{-h}^{0} u\,dz = -\frac{\partial \zeta}{\partial t} \qquad\qquad (3.1.2b)$$

with $u = u(x,z,t)$ and $\zeta = \zeta(x,t)$, subject to

$$u = 0 \text{ at the ends of the lake}, \qquad\qquad (3.1.2c)$$

$$\rho N \left(\frac{\partial u}{\partial z}\right)_{z=0} = \tau_s , \qquad\qquad (3.1.2d)$$

$$u(x,-h,t) = 0 . \qquad\qquad (3.1.2e)$$

The transport form is reduced to

$$\frac{\partial U}{\partial t} + \frac{r}{h} U = -gh \frac{\partial \zeta}{\partial x} + K\tau_s \qquad\qquad (3.1.3a)$$

$$\frac{\partial U}{\partial x} = -\frac{\partial \zeta}{\partial t} \qquad\qquad (3.1.3b)$$

with $U = U(x,t)$ and $\zeta = \zeta(x,t)$, subject to

$$U = 0 \text{ at the ends of the lake} . \qquad\qquad (3.1.3c)$$

The systems of equations (3.1.2), (3.1.3) are the simplest possible forms of the wind effect equations. The attraction of simplicity often leads these forms to be applied even to basins for which the 'narrow lake' concept is a poor approximation. For example, (3.1.2) and (3.1.3) describe

motions in a non-rotating rectangular basin induced by a wind stress acting always parallel to one of the two lake axes. The solutions are clearly independent of the breadth of the lake (transverse to the direction of the wind) and though giving only a crude representation of effects in 'non-narrow" lakes, nevertheless form a natural starting point for a theoretical investigation of wind effects on closed lakes.

3.2 A Solution Using the Transport Form of the Equations

In this section we use the transport form of the wind effect equations to determine a response function for a rectangular, non-rotating basin of constant depth subject to forcing at the surface by a wind stress acting always parallel to one of the two lake axes. For simplicity, the surface wind stress is assumed homogeneous, a proposition which is nevertheless physically reasonable since most weather cycles and wind disturbances have length scales much larger than the lake systems they effect.

The plan and longitudinal section of the basin under consideration together with the alignment of surface wind stress are shown in Fig. 3.1, with the horizontal lake axes defined as shown. The length in the x-direction is L, while the undisturbed depth of the basin is H, a constant.

Now the boundary condition (3.1.3c) implies a form for the transport, $U(x,t)$, like

$$U(x,t) = U_p(t) \sin(\kappa_p x) \qquad (3.2.1a)$$

for integers p, where $\kappa_p = p\pi/L$. Thus (3.1.3b) gives

$$\zeta(x,t) = \zeta_p(t) \cos(\kappa_p x) \qquad (3.2.1b)$$

where

$$U_p = -\frac{1}{\kappa_p} \frac{d\zeta_p}{dt} \quad .$$

The spatial dependence of the solutions (3.2.1a), (3.2.1b) is identical to that of the one-dimensional _free_ oscillations (or seiches) of the basin (Proudman (1953), p. 225), i.e. solutions to the problem of the wind forced motion of the basin are sought in terms of its seiche modes. These forms are valid regardless of the spatial distribution of wind stress. Assume, therefore, a form of the stress $\tau_s(x,t)$, like

$$\tau_s(x,t) = \tau_p(t) \sin(\kappa_p x). \qquad (3.2.1c)$$

Now eliminating $U(x,t)$ between (3.1.3a), (3.1.3b) gives

$$\frac{\partial^2 \zeta}{\partial t^2} + 2\alpha \frac{\partial \zeta}{\partial t} - c^2 \frac{\partial^2 \zeta}{\partial x^2} = -K \frac{\partial \tau_s}{\partial x} \qquad (3.2.2)$$

while elimination of $\zeta(x,t)$ gives

$$\frac{\partial^2 U}{\partial t^2} + 2\alpha \frac{\partial U}{\partial t} - c^2 \frac{\partial^2 U}{\partial x^2} = K \frac{\partial \tau_s}{\partial t} \qquad (3.2.3)$$

where $\alpha \equiv r/2H$ is the damping parameter for the system, and $c \equiv (gH)^{1/2}$ is the characteristic long-wave velocity for the basin.

Combining (3.2.1), (3.2.2), (3.2.3) gives

$$\frac{d^2 \zeta_p}{dt^2} + 2\alpha \frac{d\zeta_p}{dt} + \omega_p^2 \zeta_p = -K \kappa_p \tau_p \qquad (3.2.4a)$$

$$\frac{d^2U_p}{dt^2} + 2\alpha \frac{dU_p}{dt} + \omega_p^2 U_p = K \frac{d\tau_p}{dt} \qquad (3.2.4b)$$

where $\omega_p \equiv \kappa_p c$ is the angular frequency of the nth mode seiche of the basin. Clearly (3.2.4a), (3.2.4b) describe the behaviour of a damped simple harmonic oscillator with a natural frequency ω_p.

Equations (3.2.4a), (3.2.4b) may be solved in a variety of ways, Laplace transform techniques being suitable for quite general time variations of wind stress.

We are here specifically interested in a homogeneous wind stress of unit strength and sinusoidal time variation. This may be written as an infinite series of terms of the form (3.2.2c), as

$$\tau_s(x,t) = \frac{4}{L} e^{j\omega t} \sum_{n=1}^{\infty} \frac{\sin(\kappa_{2n-1}x)}{\kappa_{2n-1}} \qquad (3.2.5)$$

i.e. the odd continuation of τ_s for $x \in [0,L]$. The stress configuration (3.2.5) is considered applied to an infinitely long lake (Fig. 3.2). Since the wind stress changes direction at the points $x = kL$, $k = 0, \pm 1, \pm 2, \ldots$ but maintains the same (unit) strength, then there can be no flow across these vertical sections in the infinite lake. Hence the behaviour of the section [0,L] of the infinite lake will be the same as for the actual lake. Such a method has been used previously by Haurwitz (1951), Tickner (1961), Heaps and Ramsbottom (1966).

Clearly then,

$$\tau_p(t) = \begin{cases} \dfrac{4}{L\kappa_{2n-1}} & \text{for } p = 2n-1, \; n = 1,2, \ldots \\ \\ 0 & \text{for } p = 2n, \; n = 1,2, \ldots \end{cases} \qquad (3.2.6)$$

Thus only the <u>odd</u> harmonics of the fundamental seiche mode will be present in the steady state forcing of the basin by such a wind stress, i.e. $U_{2n}(t) = \zeta_{2n}(t) = 0$ while, from (3.2.4) it is clear that steady state (particular) solutions are

$$\zeta_{2n-1}(t) = \frac{-4Ke^{j\omega t}}{L(\omega_{2n-1}^2 + 2j\alpha\omega - \omega^2)} \qquad (3.2.7a)$$

$$U_{2n-1}(t) = \frac{4Kj\omega e^{j\omega t}}{L\kappa_{2n-1}(\omega_{2n-1}^2 + 2j\alpha\omega - \omega^2)} \qquad . \qquad (3.2.7b)$$

Finally, the steady state solutions to (3.2.3) become (by superposition)

$$\zeta(x,t) = \frac{-4Ke^{j\omega t}}{L} \sum_{n=1}^{\infty} \frac{\cos(\kappa_{2n-1}x)}{(\omega_{2n-1}^2 + 2j\alpha\omega - \omega^2)} \qquad (3.2.8a)$$

$$U(x,t) = \frac{4Kj\omega e^{j\omega t}}{L} \sum_{n=1}^{\infty} \frac{\sin(\kappa_{2n-1}x)}{(\omega_{2n-1}^2 + 2j\alpha\omega - \omega^2)} \qquad . \qquad (3.2.8b)$$

Consider, now, the linear system with input consisting of surface wind stress (homogeneous), and output the resultant surface displacement at the same position. Clearly the function $Z(x_0,\omega)$ defined by

$$Z(x_0,\omega) = \frac{-4K}{L} \sum_{n=1}^{\infty} \frac{\cos(\kappa_{2n-1}x_0)}{(\omega_{2n-1}^2 + 2j\alpha\omega - \omega^2)} \qquad (3.2.9)$$

represents the frequency response function for such a system.

Some important features of the response function defined by (3.2.9) should be noted. Rewriting $Z(x_o,\omega)$ in terms of the system gain $G = G(x_o,\omega)$ and phase-lag $\phi = \phi(x_o,\omega)$, one has that

$$G = (A^2 + B^2)^{1/2} = A\sec(\phi) \qquad (3.2.10a)$$

$$\phi = -\arctan\left[\frac{B}{A}\right] \qquad (3.2.10b)$$

where

$$A = \frac{-4K}{L} \sum_{n=1}^{\infty} \frac{\cos(\kappa_{2n-1}x_o)\gamma_{2n-1}}{\gamma_{2n-1}^2 + 4\alpha^2\omega^2} \qquad (3.2.11a)$$

$$B = \frac{8K\omega\alpha}{L} \sum_{n=1}^{\infty} \frac{\cos(\kappa_{2n-1}x_o)}{\gamma_{2n-1}^2 + 4\alpha^2\omega^2} \qquad (3.2.11b)$$

$$\gamma_n = \omega_n^2 - \omega^2 \quad . \qquad (3.2.11c)$$

For the gain, infinite response (resonance) occurs for real, positive frequencies when $\alpha = 0$ and $\omega = \omega_{2n-1}$, i.e. the frequency of the wind stress coincides with the odd-mode seiche frequencies of the basin. For $\alpha \neq 0$ the infinite peaks at resonance become turning points and for sufficiently large α the resonance phenomenon vanishes entirely. Note that the limiting gain as $\omega \to \infty$ is zero, provided $\alpha \neq 0$.

The behaviour of phase-lag is more complicated. For $\alpha = 0$, the response function is always real and ϕ assumes the value 0° or 180°, points of discontinuity occurring wherever the response changes sign. For $\alpha \neq 0$, phase-lag values vary continually between 0° and 180°, and the behaviour changes greatly as $\omega \to \infty$. However the limiting behaviour is simple; asymptotically,

$$A \sim \frac{4K}{L\omega^2} \sum_{n=1}^{\infty} \cos(\kappa_{2n-1}x_0) , \quad B \sim \frac{8K\alpha}{L\omega^3} \sum_{n=1}^{\infty} \cos(\kappa_{2n-1}x_0)$$

so that

$$\phi \sim 2\ell\pi - \frac{2\alpha}{\omega}$$

where ℓ is an integer.

The north lagoon of the Coorong (Fig. 3.3) may be regarded, in the first approximation, as being closed at its shallow north-western end (Tauwitchere Island) and also near the narrow Hells Gate Channel which therefore forms its south-eastern extremity. As shown by Noye (1970), tidal influences extend only a short distance south-east along the Coorong from the Murray Mouth, while flows between the north and south lagoons do not significantly affect water levels inside either.

Further, the 'narrow lake' approximation may be quite justifiably applied to the North Coorong. Its length is approximately 50km while its average width is about 2km. In summer, its mean depth is 1.25m. The longitudinal axis closely coincides with the north-west, south-east alignment.

Fig. 3.4 shows a plot of gain and phase-lag for various values of α for a rectangular lake with these dimensions, subject to wind stress forcing along the lake axis. The non-dimensional parameter m, defined in (2.1.11d), is assigned the value 0.05 (Francis (1954)). The station for output measurement is $x_0 = 0.75L$ (with $L = 50$km) which corresponds to Seven Mile Point on the North Coorong with the origin at the north-western end of the basin. The frequency range considered is 0 - 24 cycles per day

(cpd). The first 50 terms in the series (3.2.11a), (3.2.11b) were evaluated, these being quite sufficient for convergence. The resonant frequencies are odd multiples of 3.04 cpd which is the frequency of the fundamental seiche for the basin.

In the vicinity of the resonance peak near $\omega = \omega_{2n-1}$, the system behaviour is due almost entirely to the response of the $(2n-1)$th seiche mode to wind forcing. We may write

$$Z(x_0, \omega) \sim \frac{-4K}{L} \frac{\cos(\kappa_{2n-1} x_0)}{(\gamma_{2n-1} + 2j\alpha\omega)} \qquad (3.2.12)$$

so that

$$G \sim \frac{-4K}{L} \cos(\kappa_{2n-1} x_0)(\gamma_{2n-1}^2 + 4\alpha^2\omega^2)^{-1/2}$$

$$\frac{dG}{d\omega} \sim \frac{8K\omega}{L} \cos(\kappa_{2n-1} x_0)(2\alpha^2 - \gamma_{2n-1})(\gamma_{2n-1}^2 + 4\alpha^2\omega^2)^{-3/2} .$$

The resonance peak occurs when $\frac{dG}{d\omega} = 0$, i.e. $\omega^2 = \omega_{2n-1}^2 - 2\alpha^2$.

Two things become clear from this result. First, the position of the resonance peak which occurs at $\omega = \omega_{2n-1}$ for $\alpha = 0$ shifts gradually towards the origin, $\omega = 0$, as α increases. For $\alpha > \omega_{2n-1}/\sqrt{2}$, the peak is no longer present. Second, the lowest frequency peak is the first to disappear.

For sufficiently large α, the gain is dominated by low frequencies, i.e. the water level oscillations are most strongly influenced by the low frequency components in a wind stress of general time variation.

Such behaviour is evident in Fig. 1.5 where the water level at Seven Mile Point closely 'follows' the dominant diurnal component of wind stress

variation, and is influenced to only a minor degree by oscillations of smaller period. This suggests that the response of the North Coorong surface to time-varying wind stresses is heavily damped, a suggestion which is confirmed later in Chapter 8 by more precise analysis.

It is to be noted from (3.2.8a) that the surface response is always zero in the middle of the basin, $x_o = 0.5L$, and is symmetric about this position, regardless of the value of α. This corresponds closely with behaviour observed in both North and South Coorong by Noye (1970).

In Fig. 3.5 is shown the steady state real time response of the surface of the North Coorong basin to a periodic wind stress of the form $\tau_o \sin(2\pi t/T)$, T being the period of the wind stress cycle. The response is given by $\tau_o \text{Im}\{Z(x,\omega)e^{j\omega t}\}$ where $\omega = 2\pi/T$. Values used for T are 1 day, 0.2 day, 0.1 day (corresponding to frequencies 1 cpd, 5 cpd and 10 cpd respectively), while τ_o is taken as 0.1 N.m^{-2}, this being a typical value for the amplitude of the wind stress cycle. The response is shown only at times 0, T/8, T/4 and 3T/8 of the wind stress cycle - the response at times T/2, 5T/8, 3T/4 and 7T/8 is identical in magnitude,but opposite in sign.

When $\alpha = 0$, the surface always assumes a sinusoidal shape. The proof of this result is given in the following chapter. For T = 1 day, the wavelength of the sinusoid is far greater than the basin length. The surface response at t = T/4 is, in fact, close to the equilibrium (wind tide) response, since a slowly oscillating wind allows a near equilibrium situation to be achieved at all times. For lower values of T the

sinusoidal surface shape with $\alpha = 0$ is quite evident.

As α increases the surface response is seen to lag behind the surface wind stress. Further, the surface profile becomes flatter as larger values of α decrease the amplitude of displacement at each point along the lake axis.

The equilibrium surface response due to a steady, uniform wind is found (from (2.2.9)) by putting $\omega = 0$ in (3.2.8a) to give

$$Z(x,0) \equiv Z_0(x) = \frac{-4K}{L} \sum_{n=1}^{\infty} \frac{\cos(\kappa_{2n-1}x)}{\omega_{2n-1}^2}$$

$$= \frac{K}{c^2}\left(x - \frac{L}{2}\right), \quad x\epsilon \ [0,L] \tag{3.2.13}$$

i.e. a plane of slope $(1+m)/\rho gH$. This result is well-known; refer, for example, Hellstrom (1941), Haurwitz (1951), Keulegan (1951), Felsenbaum (1956). It is valid regardless of the value of α. Further, as will be shown in the following chapter, it has a wider application than simply to the elongated rectangular basin.

Let us now look briefly at the <u>mean velocity response function</u> $q_m(x_0,\omega)$, defined by

$$q_m = \frac{4Kj\omega}{LH} \sum_{n=1}^{\infty} \frac{\sin(\kappa_{2n-1}x_0)}{\kappa_{2n-1}(\omega_{2n-1}^2 + 2j\alpha\omega - \omega^2)} \ . \tag{3.2.14}$$

Shown in Fig. 3.6 are the gain and phase-lag of the mean velocity response for the North Coorong rectangular basin at $x_0 = 0.75L$. Resonance again occurs when $\alpha = 0$ and ω is an odd multiple of 3.04 cpd. For the case $\alpha = 0$, phase-lag assumes only the values 270° or 90°, so that the mean velocity

either leads the surface wind stress by 90° (equivalent to 270° lag) or lags by 90°.

The equilibrium mean velocity is zero, as seen by putting $\omega = 0$ in (3.2.14). Clearly as $\omega \to \infty$, the gain approaches zero, though its rate of doing so is far slower than for the gain of surface response. In fact, for values of $\alpha > 10^{-3}$ sec^{-1}, the mean velocity gain is virtually constant for the North Coorong system over the frequency range 0-24 cpd.

Using (2.2.8a) we may proceed to a determination of the surface step response, $a(x_o, t)$, of the system. The integral

$$I(x_o, t) \equiv \int_{-\infty}^{\infty} \frac{Z(x_o, \omega)}{j\omega} e^{j\omega t} d\omega \tag{3.2.15}$$

can be evaluated by contour integration in the complex ω-plane. We may write (3.2.9) as

$$Z(x_o, \omega) = \frac{4K}{L} \sum_{n=1}^{\infty} \frac{\cos(\kappa_{2n-1} x_o)}{(\omega - \psi_{2n-1})(\omega - \chi_{2n-1})} \tag{3.2.16}$$

where $\psi_{2n-1} = j\alpha + \delta_{2n-1}$, $\chi_{2n-1} = j\alpha - \delta_{2n-1}$, and $\delta_{2n-1} = (\omega_{2n-1}^2 - \alpha^2)^{1/2}$. Thus, the poles of the integrand $f(\omega)$ in (3.2.15) occur for $\omega = 0$ and $\omega = \psi_{2n-1}$, χ_{2n-1} for $n = 1, 2, \ldots$. Choose the contour of integration as shown in Fig. 3.7, allowing the radius of the outer circle, R_o, to approach infinity and the radius of the inner circle, r_i, to approach zero.

Denoting $\mu_i = r_i e^{j\theta}$, then the integral

$$I_s \equiv \int_\pi^0 \left\{ \frac{Z(x_o,\mu_i)e^{j\mu_i t}j\mu_i}{j\mu_i} \right\} d\theta$$

$$= \int_\pi^0 \left\{ Z(x_o,\mu_i)e^{j\mu_i t} \right\} d\theta$$

$$\rightarrow -\pi \, Z_o(x_o) \text{ as } r_i \rightarrow 0 \ ,$$

while denoting $\mu_o = R_o e^{j\theta}$, then the integral

$$I_s = \int_0^\pi \left\{ \frac{Z(x_o,\mu_o)e^{j\mu_o t}j\mu_o}{j\mu_o} \right\} d\theta$$

$$= \int_0^\pi \left\{ Z(x_o,\mu_o)e^{j\mu_o t} \right\} d\theta$$

$$\rightarrow 0 \text{ as } R_o \rightarrow \infty$$

since $Z(x_o,\mu_o) \rightarrow 0$ as $R_o \rightarrow \infty$. Further, defining

$$I_- = \int_{-R_o}^{r_i} \left\{ \frac{Z(x_o,\omega)e^{j\omega t}}{j\omega} \right\} d\omega, \quad I_+ = \int_{-r_i}^{R_o} \left\{ \frac{Z(x_o,\omega)e^{j\omega t}}{j\omega} \right\} d\omega$$

then

$$\lim_{r_i \rightarrow 0, R_o \rightarrow \infty} (I_- + I_+) = I \ .$$

Thus, by the residue theorem we have

$$I(x_o,t) = \pi Z_o(x_o) + 2\pi j \sum_{n=1}^\infty \left\{ \text{Res}[f(\omega);\psi_{2n-1}] + \text{Res}[f(\omega);\chi_{2n-1}] \right\}$$

$$= \pi Z_o(x_o) + \frac{8Ke^{-\alpha t}}{L} \sum_{n=1}^\infty \left\{ \frac{\cos(\kappa_{2n-1}x_o)}{\omega_{2n-1}^2} \left(\cos(\delta_{2n-1}t) \right. \right.$$

$$\left. \left. + \frac{\alpha}{\delta_{2n-1}} \sin(\delta_{2n-1}t) \right) \right\}$$

so that,

$$a(x_o, t) = Z_o(x_o) + \frac{4Ke^{-\alpha t}}{L} \sum_{n=1}^{\infty} \{ \frac{\cos(\kappa_{2n-1} x_o)}{\omega_{2n-1}^2} (\cos(\delta_{2n-1} t)$$

$$+ \frac{\alpha}{\delta_{2n-1}} \sin(\delta_{2n-1} t)) \} . \qquad (3.2.17a)$$

The general solution (3.2.17a) has been obtained previously by Saito (1949), who solved an initial value problem. Putting $\alpha = 0$ in (3.2.17a) gives

$$a(x_o, t) = Z_o(x_o) + \frac{4K}{L} \sum_{n=1}^{\infty} \frac{\cos(\kappa_{2n-1} x_o) \cos(\omega_{2n-1} t)}{\omega_{2n-1}^2} \qquad (3.2.17b)$$

as obtained by Haurwitz (1951) and Tickner (1961).

Fig. 3.8 shows the form of the step response at positions $x_o = 0.75L$, $x_o = 0.99L$ of the North Coorong basin previously considered, from time $t = 0$ to $t = 4T_s$, where $T_s (\equiv 2L/C)$, the period of the fundamental seiche, is 7.90 hr. It consists of seiches of odd nodality superimposed on the equilibrium wind set-up.

For $\alpha = 0$ the step response overshoots the equilibrium response by a factor of 2. For much larger values of α the response is essentially over-damped. The nth mode seiche is overdamped if

$$\alpha > \omega_{2n-1} = \frac{(2n-1)\pi c}{L} \qquad (3.2.18)$$

in which case the $\cos(\delta_{2n-1} t)$, $\sin(\delta_{2n-1} t)$ terms in (3.2.17a) become exponentials of real argument. So, for the fundamental seiche in the North Coorong to be damped out, it is required that

$$\alpha > 2.20 \times 10^{-4} \text{ sec}^{-1} .$$

The shape of the step response curve as a function of time for $\alpha = 0$ bears some explanation. It is clear that (3.2.17b) may be rewritten as

$$a(x_o, t) = Z_o + \frac{2K}{L} \sum_{n=1}^{\infty} \frac{1}{\omega_{2n-1}^2} \{\cos(\kappa_{2n-1}(x_o + ct)) + \cos(\kappa_{2n-1}(x_o - ct))\}$$

i.e. a superposition of the equilibrium response and two oppositely directed and equal amplitude travelling waves, each with speed $c = \sqrt{gH}$. Thus, the surface shape at times 0, $T_s/8$, $T_s/4$, $3T_s/8$, $T_s/2$ has the form shown in Fig. 3.9. It is observed that the effect of the step input is first felt at the lake edges, while the centre portion reacts only after a time lag. Such behaviour is still evident for those non-zero values of α for which the response is underdamped, as is clear from Fig. 3.8. It remains a matter of speculation, however, as to whether this could possibly be observed in real lakes.

3.3 A Solution using the Eddy Viscosity Form of the Equations

Here the same problem dealt with in the previous section is reconsidered. This time we seek to solve the equations

$$\frac{\partial u}{\partial t} = -g \frac{\partial \zeta}{\partial x} + N \frac{\partial^2 u}{\partial z^2} \tag{3.3.1a}$$

$$\frac{\partial}{\partial x} \int_{-h}^{0} u\, dz = -\frac{\partial \zeta}{\partial t} \tag{3.3.1b}$$

subject to

$$u(0,t) = u(L,t) = 0 \ , \tag{3.3.1c}$$

$$\rho N \left(\frac{\partial u}{\partial z}\right)_{z=0} = \tau_s' \tag{3.3.1d}$$

$$u(x,-H,t) = 0 \ . \tag{3.3.1e}$$

The end conditions (3.3.1c) imply

$$u(x,z,t) = u_p(z,t)\sin(\kappa_p x) \tag{3.3.2a}$$

$$\zeta(x,t) = \zeta_p(t)\cos(\kappa_p x) \tag{3.3.2b}$$

for integers p, and we again assume that

$$\tau_s(x,t) = \tau_p(t)\sin(\kappa_p x) \ .$$

Combining (3.3.1), (3.3.2) gives

$$\frac{\partial u_p}{\partial t} = g\kappa_p\zeta_p + N \frac{\partial^2 u_p}{\partial z^2} \tag{3.3.3a}$$

$$\kappa_p \int_{-H}^{0} u_p \, dz = - \frac{d\zeta_p}{dt} \tag{3.3.3b}$$

subject to

$$\rho N \left(\frac{\partial u_p}{\partial z}\right)_{z=0} = \tau_p \tag{3.3.3c}$$

$$(u_p)_{z=-H} = 0 \ . \tag{3.3.3d}$$

Now again assume the form (3.2.6) for $\tau_p(t)$, i.e. $\tau_p(t) = T_p e^{j\omega t}$ where

$$T_p = \begin{cases} \dfrac{4}{L\kappa_n} & \text{for } p = 2n-1, \ n=1,2, \ \ldots \\[2mm] 0 & \text{for } p = 2n, \ n=1,2, \ \ldots \end{cases} \tag{3.3.4}$$

and look for solutions to (3.3.3) of the form

$$\zeta_p(t) = Z_p(\omega)e^{j\omega t} \tag{3.3.5a}$$

$$u_p(z,t) = \eta_p(z,\omega)e^{j\omega t} \; . \tag{3.3.5b}$$

Then (3.3.3a), (3.3.3b) become

$$\frac{\partial^2 \eta_p}{\partial z^2} - b^2 \eta_p = -\epsilon_p Z_b \tag{3.3.6a}$$

$$\kappa_p \int_{-H}^{0} \eta_p \, dz = -Nb^2 \tag{3.3.6b}$$

where $b^2 = j\omega/N$ and $\epsilon_p = g\kappa_p/N$, subject to

$$\rho N \left(\frac{\partial \eta_p}{\partial z}\right)_{z=0} = T_p \tag{3.3.6c}$$

$$(\eta_p)_{z=-H} = 0 \; . \tag{3.3.6d}$$

The general solution to (3.3.6) may be written as

$$\eta_p(z,\omega) = A_p \cosh(bz) + B_p \sinh(bz) + \frac{\epsilon_p}{b^2} Z_p \tag{3.3.7}$$

where $A_p(\omega)$, $B_p(\omega)$ are to be determined. Furthermore from (3.3.6d) we have

$$Z_p(\omega) = \frac{b^2}{\epsilon_p} \left(B_p \sinh(bH) - A_p \cosh(bH)\right) \tag{3.3.8}$$

so (3.3.7) becomes

$$\eta_p(z,\omega) = A_p(\cosh(bz) - \cosh(bH)) + B_p(\sinh(bz) + \sinh(bH)). \tag{3.3.9}$$

Condition (3.3.6c) gives

$$B_p(\omega) = \frac{T_p}{\rho Nb} \tag{3.3.10a}$$

so combining (3.3.6b), (3.3.9), (3.3.10a) gives

$$A_p(\omega) = \frac{T_p R_p}{\rho Nb} \qquad (3.3.10b)$$

where

$$R_p(\omega) = \frac{\sinh(bH)[Nb^5 + \varepsilon_p \kappa_p bH] + \varepsilon_p \kappa_p [1 - \cosh(bH)]}{\cosh(bH)[Nb^5 + \varepsilon_p \kappa_p bH] - \varepsilon_p \kappa_p \sinh(bH)} \; .$$

Thus

$$Z_p(\omega) = \frac{bT_p}{\rho N\varepsilon_p} \; [\sinh(bH) - R_p \cosh(bH)] \qquad (3.3.11a)$$

$$\eta_p(z,\omega) = \frac{T_p}{\rho Nb} \; [(\sinh(bz) + \sinh(bH)) + R_p(\cosh(bz) - \cosh(bH))] \; . $$

$$(3.3.11b)$$

Again only the odd harmonics of the fundamental natural mode of the basin will be excited by the wind stress, due to the form of the expression (3.3.4). The solutions to (3.3.1) may thus be written as

$$\zeta(x,t) = \frac{4b}{L\rho g} \sum_{n=1}^{\infty} \left\{ \frac{\cos(\kappa_{2n-1} x)}{\kappa_{2n-1}^2} \; (\sinh(bH) - R_{2n-1}\cosh(bH)) \right\} e^{j\omega t} \qquad (3.3.12a)$$

$$u(x,z,t) = \frac{4}{L\rho Nb} \sum_{n=1}^{\infty} \frac{\sin(\kappa_{2n-1} x)}{\kappa_{2n-1}} \; (\sinh(bz) - \sinh(bH))$$

$$- R_{2n-1}(\cosh(bz) - \cosh(bH)) \} e^{j\omega t} \; . \qquad (3.3.12b)$$

Writing $\zeta(x_o,t) = Z(x_o,\omega)e^{j\omega t}$, then (3.3.12a), defines the surface response function $Z(x_o,\omega)$ for the basin at station x_o as determined from the eddy viscosity form of the equations. Shown in Fig. 3.10 is the gain and phase-lag for the North Coorong basin at $x_o = 0.75L$ for various values of the coefficient of eddy viscosity, N. Clearly, there is little difference in form between the plots of Fig. 3.4 and those of Fig. 3.10.

In fact, from (3.3.12a) we have

$$Z(x_o,\omega) = \frac{4b}{L\rho N}(1-\cosh(bH))\sum_{n=1}^{\infty}\left\{\frac{\cos(\kappa_{2n-1}x_o)}{(Nb^5+\varepsilon_{2n-1}\kappa_{2n-1}bH)\cosh(bH)-\varepsilon_{2n-1}\kappa_{2n-1}\sinh(bH)}\right\}$$

$$(3.3.13)$$

from which, in the limit $N \rightarrow 0$, we have

$$Z(x_o,\omega) \rightarrow \frac{-4}{L\rho}\sum_{n=1}^{\infty}\frac{\cos(\kappa_{2n-1}x_o)}{\omega_{2n-1}^2-\omega^2}$$

equivalent to the response function obtained from the transport equations with $m = 0$ and $\alpha = 0$. In particular, it is to be noted that in the limit $N \rightarrow 0$, resonance occurs again at the frequencies $\omega = \omega_{2n-1}$.

The equilibrium response due to a steady uniform wind is found by letting $\omega \rightarrow 0$ in (3.3.12a) to give

$$Z_o(x) = \frac{3}{2\rho gH}\left(x - \frac{L}{2}\right) ,x \in [0,L] \qquad (3.3.14)$$

equivalent to (3.2.13) with $\alpha = 0$ and $m = 0.5$.

We turn now to the velocity response function $s(x_o,z_o,\omega)$ at station (x_o,z_o) where $u(x_o,z_o,t) = s(x_o,z_o,\omega)e^{j\omega t}$. Shown in Figs. (3.11a), (3.11b), (3.11c) are gain and phase-lag for the North Coorong rectangular basin at depths $z_o = 0$ (surface velocity), $z_o = -H/3$ and $z_o = -2H/3$ respectively, with $x_o = 0.75L$ in each. (Note that the velocity gains shown in Fig. 3.11 have been normalized with respect to the zero-frequency gain with $N = 10^{-5}m^2.sec^{-1}$ for the surface velocity, viz. $31.5m.sec^{-1}$).

The equilibrium response is found by letting $\omega \rightarrow 0$ in (3.3.12b) to give

$$s_0(x,z) = \frac{H}{\rho N} \left\{ \frac{1}{4} + \frac{z}{H} + \frac{3}{4} \left(\frac{z}{H}\right)^2 \right\}, \quad x \in [0,L] \qquad (3.3.15)$$

i.e. the quasi-laminar equilibrium velocity profile is parabolic, a result mentioned in Chapter 1 and depicted in Fig. 1.3a. We note that the magnitude of $s_0(x,z)$ is dependent on the coefficient of eddy viscosity, N, whereas the magnitude of $Z_0(x)$ is independent of N.

An interesting feature of the graphs of Fig. 3.11 is that for $N \gtrsim 10^{-3} m^2 sec^{-1}$, the velocity gain remains relatively constant at a given depth over the frequency range 0-24 cpd, except for a sharp increase at very low frequencies. This suggests that, at least for heavily damped systems, the equilibrium velocities given by (3.3.15) are probably not typical of measured velocities in a given lake system.

We shall not consider here in detail the surface step response of the rectangular, constant depth basin as deduced from the eddy viscosity equations. The problem has been previously examined by Proudman and Doodson (1924) and requires far more computational effort than for the transport solution.

Again, from (2.2.8a), the integral

$$I(x_0, z_0) \equiv \int_{-\infty}^{\infty} \frac{Z(x_0, \omega)}{j\omega} e^{j\omega t} d\omega$$

must be evaluated, where $Z(x_0, \omega)$ is given by (3.3.13).

The method of contour integration requires that the poles of $Z(x_0, \omega)$ be determined. This is clearly equivalent to finding the roots of the equation

$$(Nb^5 + \varepsilon_{2n-1} \kappa_{2n-1} bH) \cosh(bH) = \varepsilon_{2n-1} \kappa_{2n-1} \sinh(bH), n=1,2, \ldots.$$

i.e. roots of

$$\frac{\tan\sigma - \sigma}{\sigma^5} = \theta_{2n-1}, \quad n = 1,2, \ldots \qquad (3.3.16)$$

where $\sigma = j.bH$, $\theta_n = N/\varepsilon_n \kappa_n H^5 = N^2 L^2/gH^5 n^2 \pi^2$. The function $f(\sigma) = (\tan\sigma - \sigma)/\sigma^5$ is even in σ. Fig. 3.12 shows a plot of $f(\sigma)$ for real, positive σ. For $\sigma < \pi/2$ the function has a turning point (a minimum) at (1.11, 0.54). For $\sigma > \pi/2$, the factor $1/\sigma^5$ ensures that $f(\sigma)$ is always close to zero and < 0 except near the poles of $\tan\sigma$.

Proudman (1924) investigated the solutions of (3.3.16) and showed that in the positive half of the complex σ-plane:-

- for $|\sigma| < \pi/2$ and $\theta_{2n-1} > 0.54$, 2 real roots only;
- for $|\sigma| < \pi/2$ and $\theta_{2n-1} < 0.54$, 2 complex conjugate roots only;
- for $|\sigma| > \pi/2$, the only roots are real and are $\sim \dfrac{(2n-1)\pi}{2}$, n=1,2, ...

The position of the roots must, in each case, be determined numerically.

The step response thus obtained again consists of damped seiches of odd nodality, superimposed this time on the equilibrium response $Z_o(x_o)$ given by (3.3.14).

Such similarity may seem surprising in view of the fact that for the eddy viscosity case, $Z(x_o, \omega)$ has an infinite number of poles for each n, whereas for the transport case, the number is only 2. However for the former case it is only the poles with modulus less than $\pi/2$ that are

important in determining the type of the step response - these correspond

closely to the poles of $Z(x_o, \omega)$ in the transport form. Thus if $\theta_{2n-1} >$

0.54 all roots of (3.3.17) will be real so that the poles of $Z(x_o, \omega)$ will

occur for purely imaginary values of ω. This is then the condition for

overdamping of the seiche of (2n-1)th nodality. It may be rewritten as

$$N > \frac{(2n-1)\pi}{L} \ (0.54 \ g_H{}^5)^{1/2} . \qquad (3.3.17)$$

For the North Coorong rectangular basin, the condition for the fundamental

seiche to be overdamped becomes

$$N > 2.58 \times 10^{-4} m^2.sec^{-1} .$$

3.4   Some Conclusions Concerning Wind Effects on the North Coorong

It was stated earlier that internal damping processes appear to

dominate the surface response of the North Coorong to time varying wind

stresses. The extent of this dominance may be gauged by suitably estima-

ting values for the damping parameters α and N for the system. In Chapter

8, time-series analysis of wind stress and water level data suggests, in

fact, that $\alpha = 2.5 \times 10^{-4} m.sec^{-1}$ and $N = 4.0 \times 10^{-4} m^2.sec^{-1}$.

The gain of surface response is, therefore, dominated by frequency

components in the range 0 - 6 cpd. Velocity gains, however, retain the

same order of magnitude over a much wider frequency band, say 0 - 24 cpd.

An important conclusion drawn from these estimates of α and N is that

the surface step response is likely to be close to a critically damped

situation. This result we infer from the inequalities (3.2.18) and (3.3.17). From Fig. 3.8 it seems that the surface of the North Coorong basin, in response to a wind stress of the step form, will reach a state very close to equilibrium only 1 fundamental seiche period (7.9 hr) after the onset of the wind .

The appearance of the fundamental longitudinal seiche ('sloshing mode') in response to surface wind stress is therefore unlikely in the North Coorong, though secondary seiches of very small amplitude probably will occur. We conclude that the characteristic diurnal water level oscillations observable in both Coorong lagoons are not free seiches, as postulated by Clarke (1966). Instead, the theoretical <u>forced</u> surface response to wind stresses of the form $\tau_s = \tau_o \sin(2\pi t/T)$ with T = 1 day, as shown in Fig. 3.5, satisfactorily models the phenomenon.

From the above estimate of α for the North Coorong, a value for the parameter r ($\equiv 2\alpha H$) is calculated as $6.3 \times 10^{-4} m.sec^{-1}$. Smith (1973) uses values of r ranging from $10^{-4} m.sec^{-1}$ to $10^{-3} m.sec^{-1}$ in a series of numerical experiments on Lake Michigan (noting little change in computed transports with these variations). Heaps and Ramsbottom (1966) determine that for the bottom layer (depth = 21m) of the stratified Lake Windermere. Scotland, $\alpha = 1.2 \times 10^{-5} sec^{-1}$, so that $r = 5.1 \times 10^{-4} m.sec^{-1}$.

We infer that r assumes a value of the order of $5 \times 10^{-4} m.sec^{-1}$ regardless of lake contour or depth. This does not seem surprising since the quantity q_b in (2.1.11a) probably is largely invariant of such factors. In regions of strong tidal flow, on the other hand, q_b is probably much larger and, indeed, values of r for the southern part of the North Sea

and the Straits of Dover (Bowden (1956)) may be higher than $5 \times 10^{-3} m.sec^{-1}$.

We, therefore, conclude that the parameter α (rather than r), through the 1/H factor, determines the degree of damping within a given lake system. For extremely shallow lakes, such as the Murray Mouth lakes where H = 0 (1m), damping forces dominate the motions. For deeper lakes, damping forces do not play such an important role.

In mathematical models of the Great Lakes, where H = 0 (50m), it is quite common to neglect damping forces completely, especially in a consideration of transient motions (Birchfield (1969)) which may persist for up to 1 week. For the Murray Mouth lakes and, indeed, for most Australian lakes, it seems that such a simplifying assumption will not suffice.
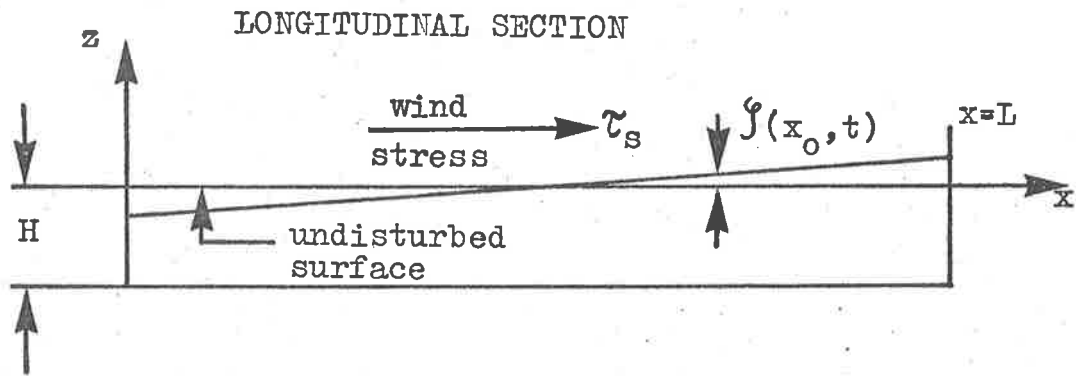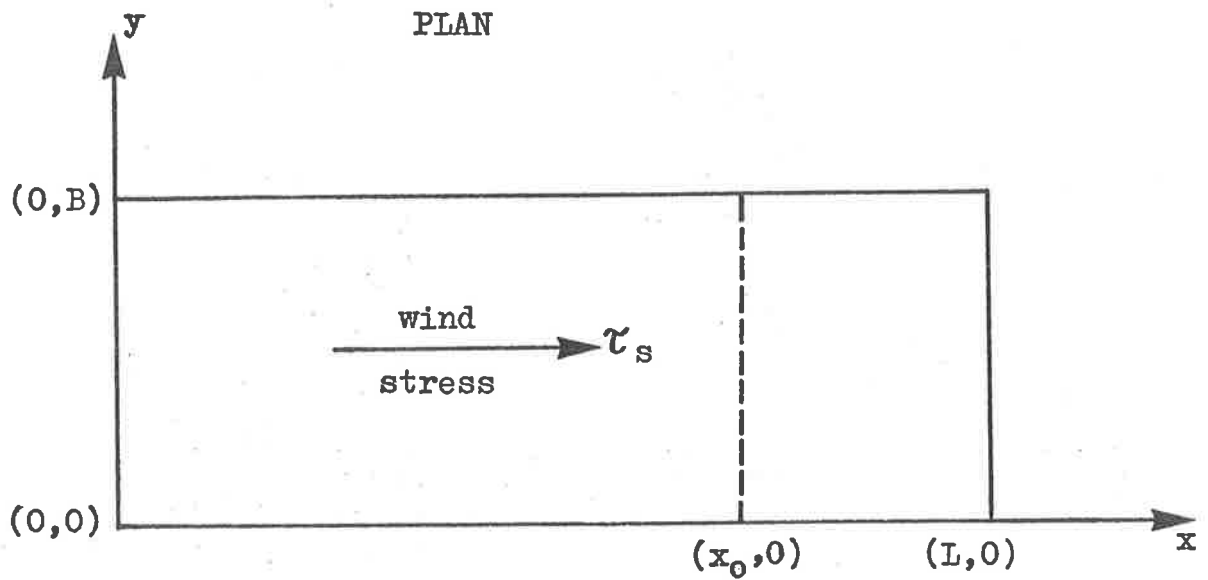
FIGURE 3.1 : PLAN AND LONGITUDINAL SECTION OF RECTANGULAR BASIN
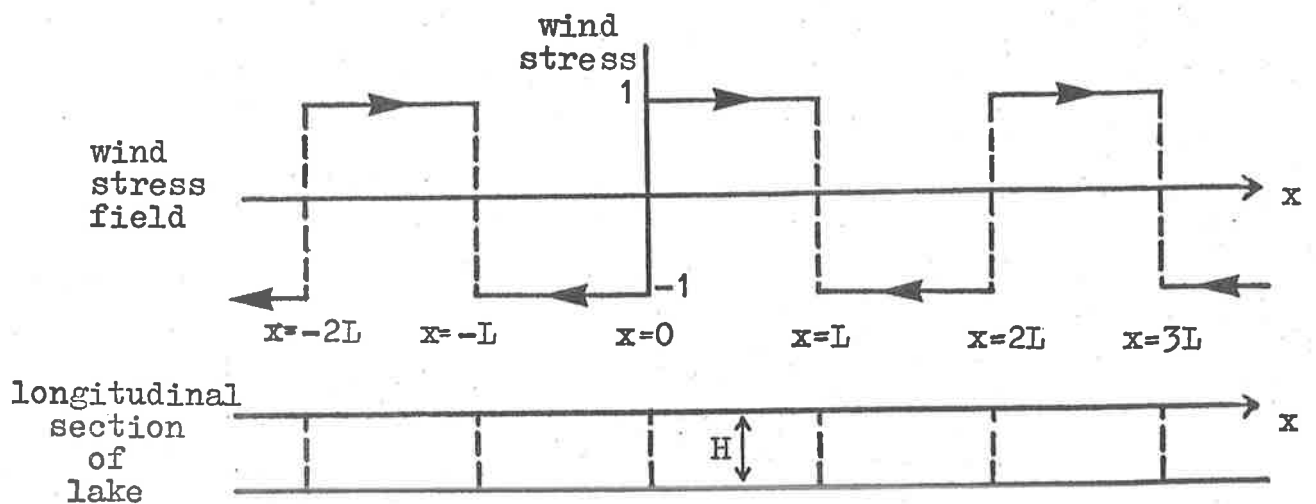OF CONSTANT DEPTH H, ACTED ON BY WIND STRESS τ_s.

FIGURE 3.2 : SECTION OF INFINITE LAKE OF DEPTH H, ACTED ON BY
WIND STRESS FIELD OF FORM (3.2.5) .

NORTH COORONG

Tauwitchere
Island

Seven Mile Point

Southern Ocean

N

mean depth of
section (m.)

2

1

Mean Depth

0

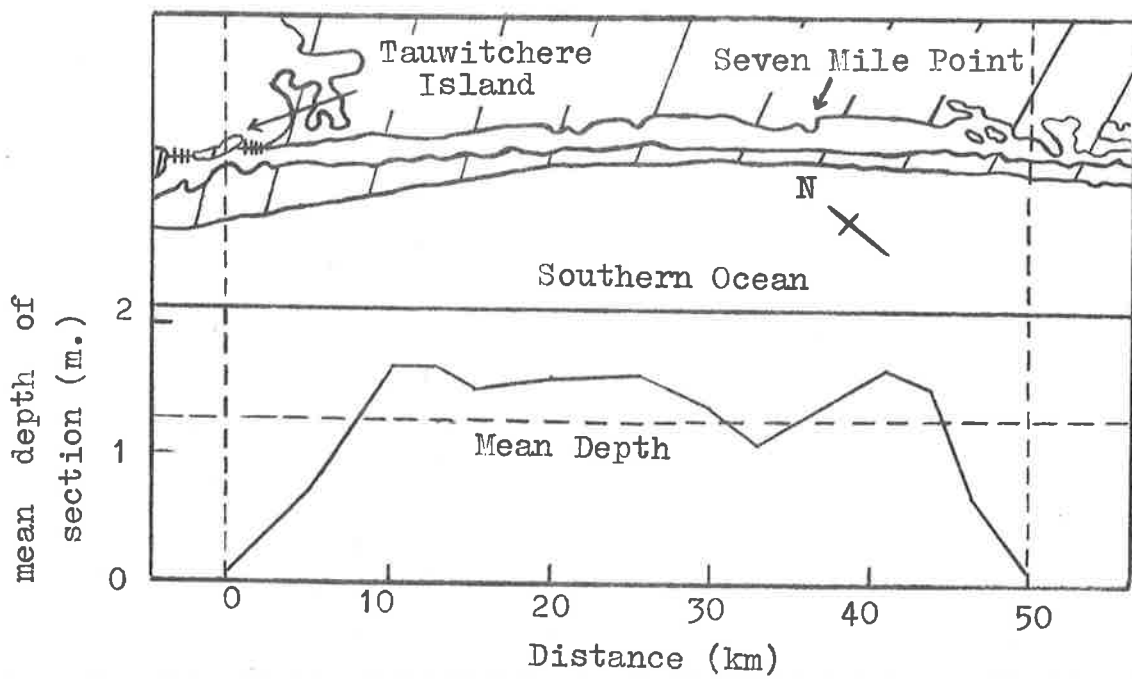0   10   20   30   40   50

Distance (km)

FIGURE 3.3 : MAP OF THE NORTH COORONG, WITH MEAN DEPTHS OF
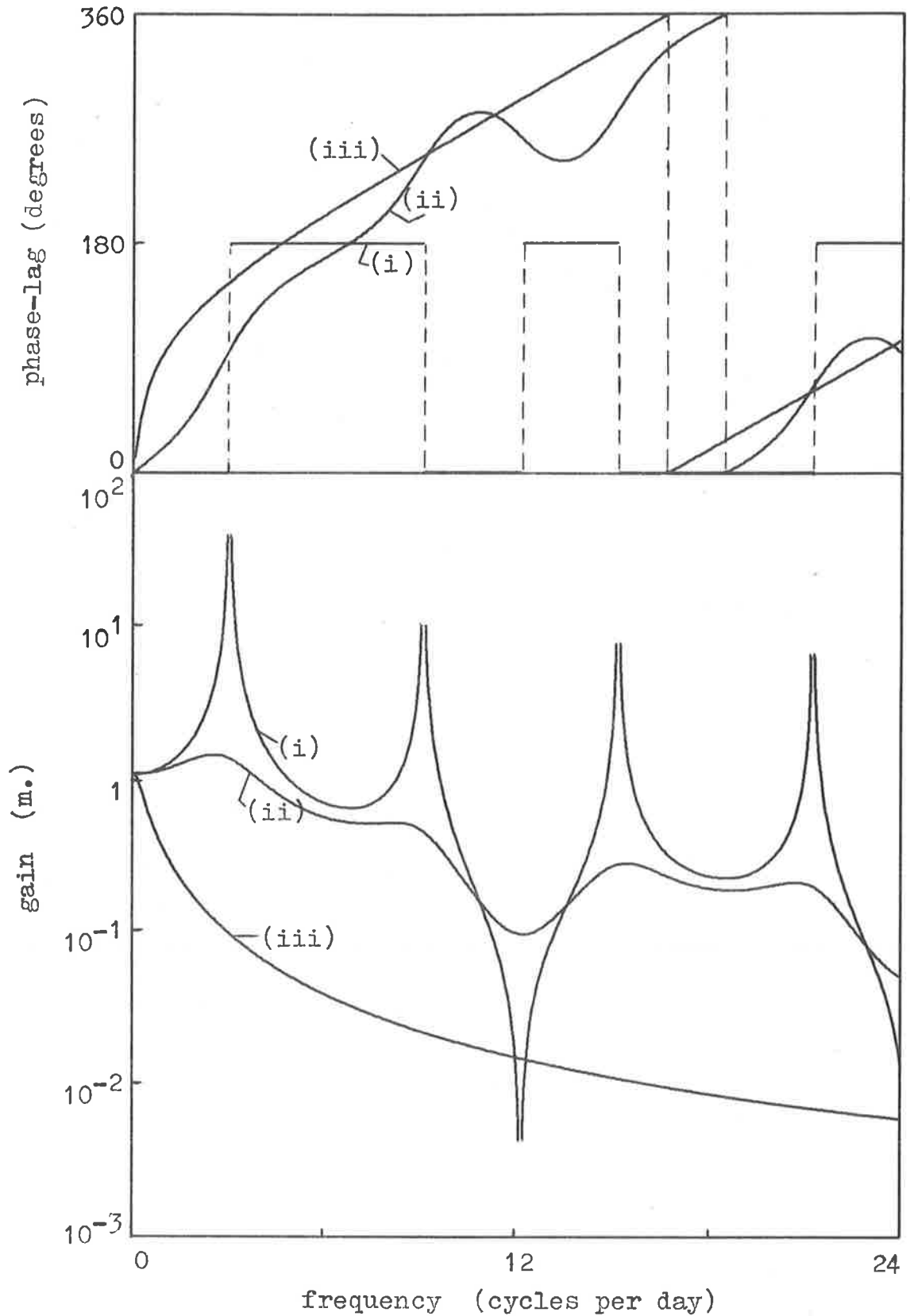SECTIONS ALONG THE LAKE AXIS ALSO SHOWN .

FIGURE 3.4 : RESPONSE FUNCTIONS FOR SURFACE DISPLACEMENT AT
SEVEN MILE POINT, NORTH COORONG, AS CALCULATED
FROM (3.2.9), FOR (i)α=0 sec^{-1}, (ii)α=10^{-4} sec^{-1},
(iii)α=10^{-3} sec^{-1} . EQUILIBRIUM RESPONSE IS
1.063 M. GAIN AND PHASE-LAG ARE SHOWN AS FUNCTIONS
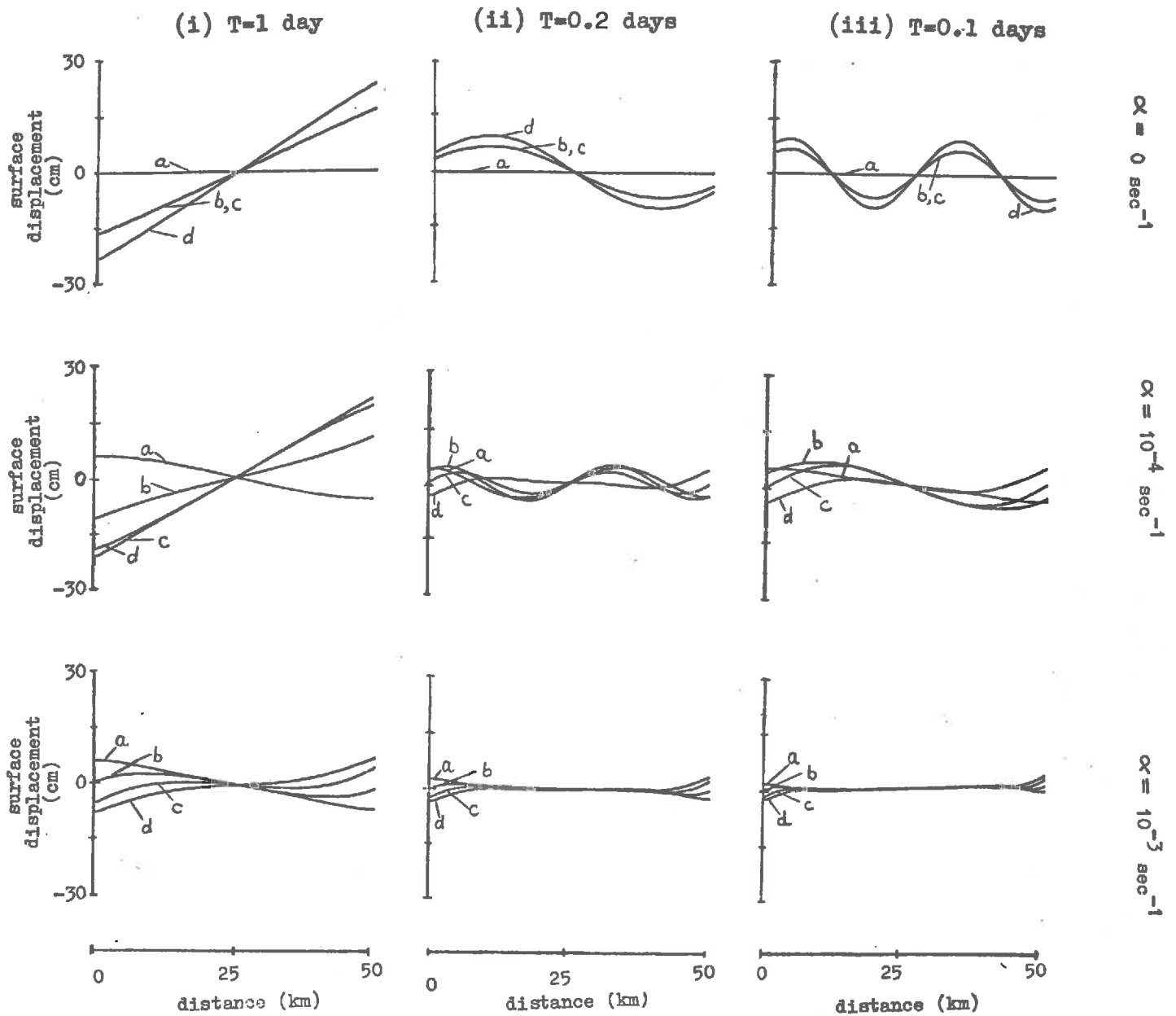OF LINEAR FREQUENCY $\omega/2\pi$, WITH UNITS CPD .

FIGURE 3.5 : REAL TIME RESPONSE OF NORTH COORONG BASIN TO WIND
STRESS OF FORM $\tau_o SIN(2\pi t/T)$ WITH $\tau_o = 0.1 \ N.m^{-2}$.
SURFACE RESPONSE IS SHOWN FOR 3 DIFFERENT VALUES
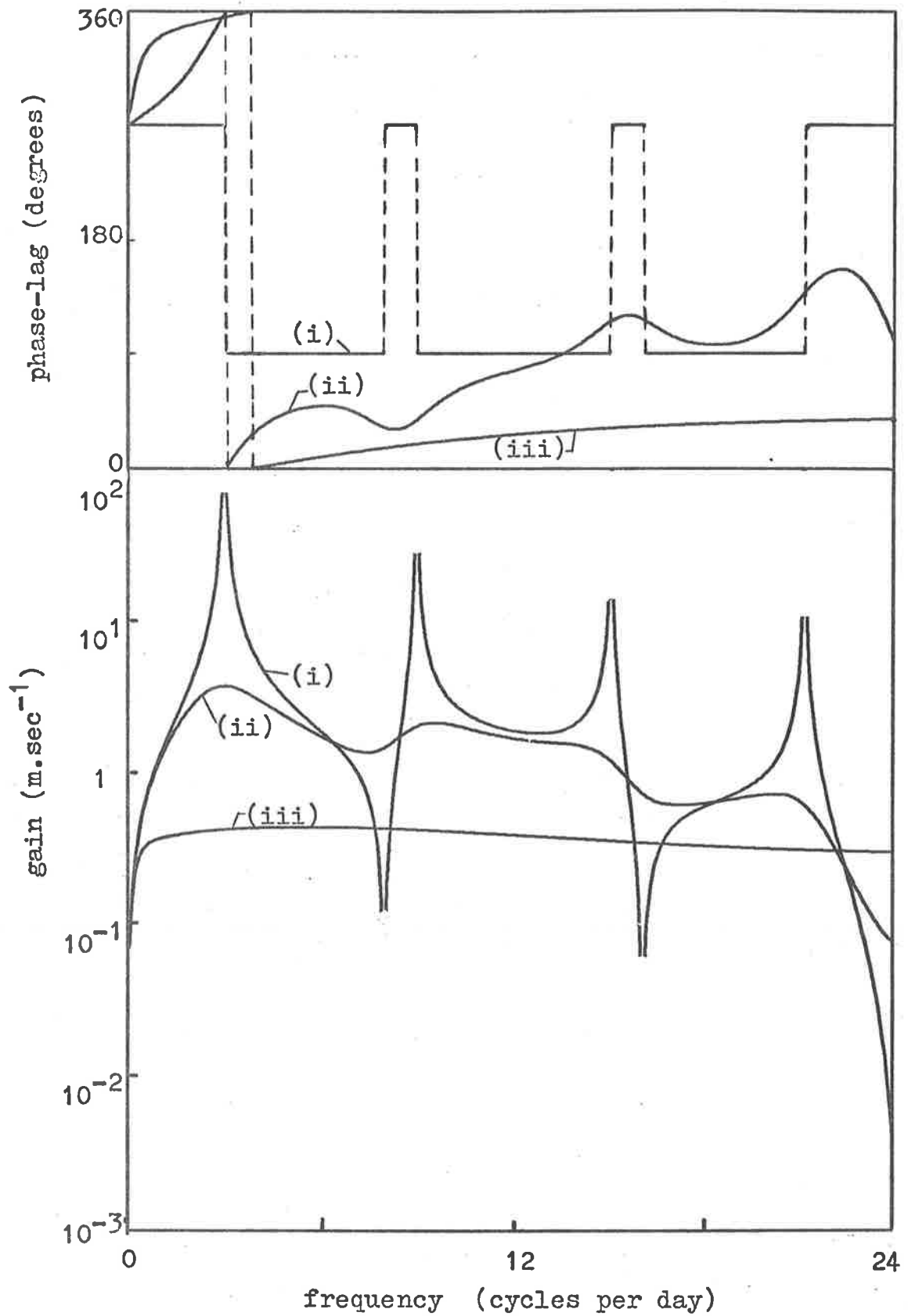EACH OF T AND α, AT TIMES (a) t=0, (b) t=T/8,
(c) t=T/4, (d) t=3T/8.

FIGURE 3.6 : RESPONSE FUNCTIONS FOR MEAN VELOCITY AT SEVEN MILE
POINT, NORTH COORONG, AS CALCULATED FROM (3.2.14),
FOR (i)α=0 sec^{-1}, (ii)α=10^{-4} sec^{-1}, (iii)α=10^{-3} sec-1.
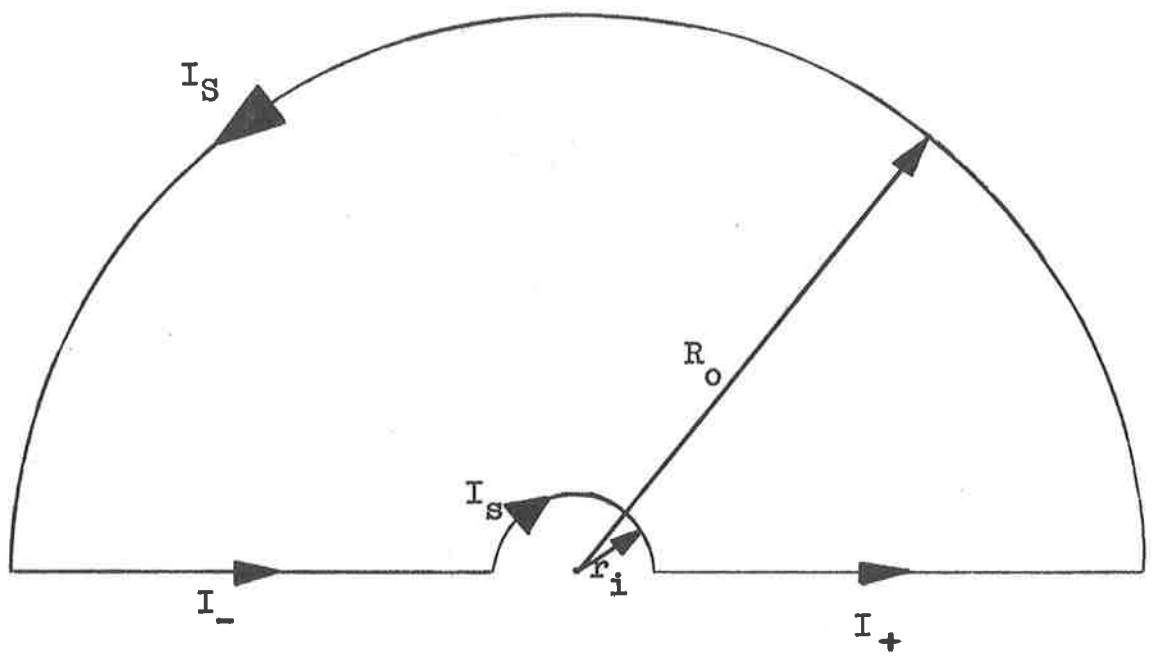
FIGURE 3.7 : CONTOUR OF INTEGRATION IN THE COMPLEX ω-PLANE FOR EVALUATION OF THE INTEGRAL (3.2.15).
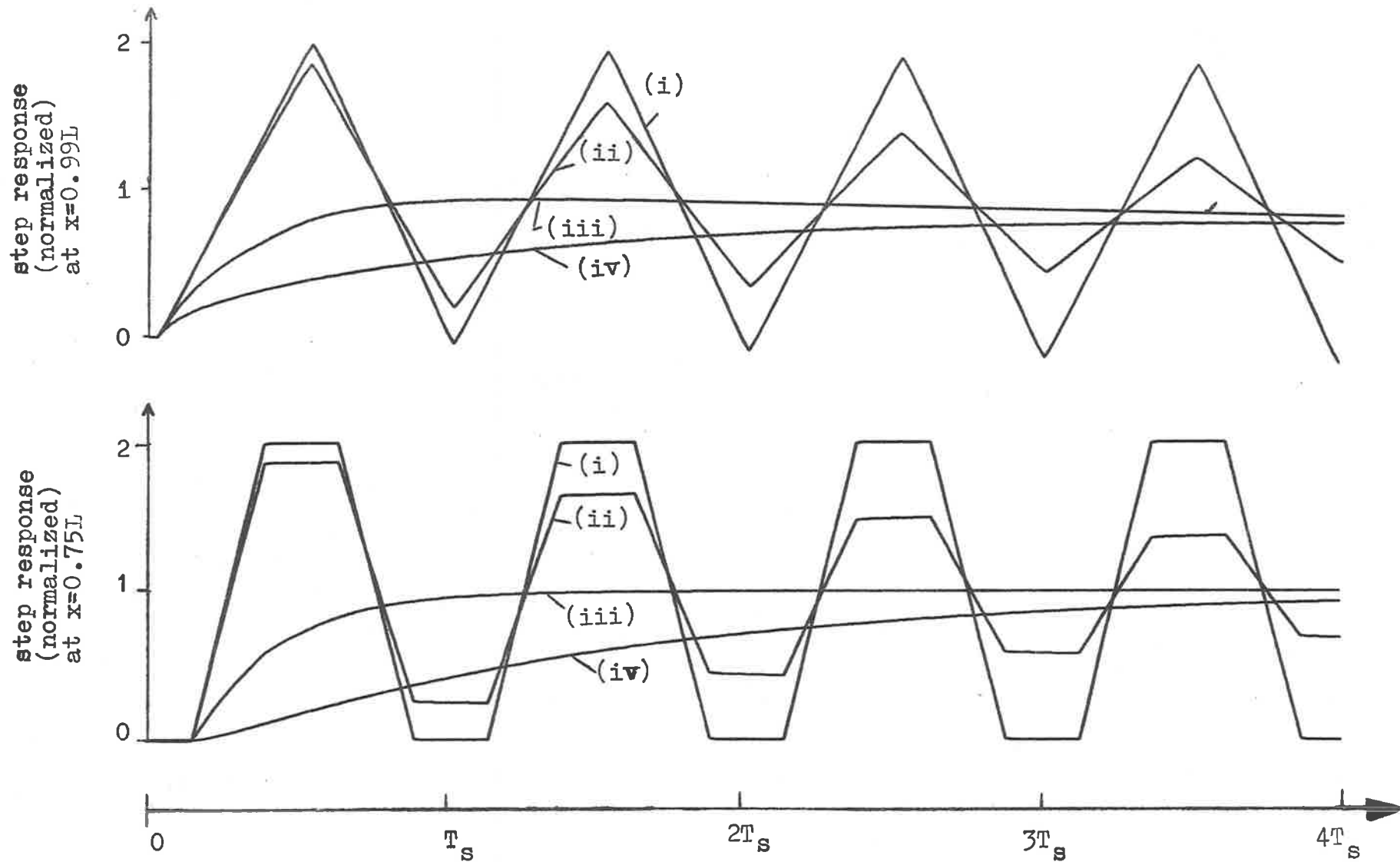
FIGURE 3.8: STEP RESPONSE OF NORTH COORONG AT (a)x=0.99L and (b)x=0.75L (SEVEN MILE POINT) FOR (i)α=0 sec^{-1}, (ii)α=10^{-5} sec^{-1}, (iii)α=2.5 x 10^{-4} sec^{-1}, (iv)α≈10^{-3} sec^{-1}. RESPONSES HAVE BEEN NORMALIZED WITH RESPECT TO THE EQUILIBRIUM RESPONSE FOR EACH, VIZ. 2.083 m AND 1.063 m RESPECTIVELY.
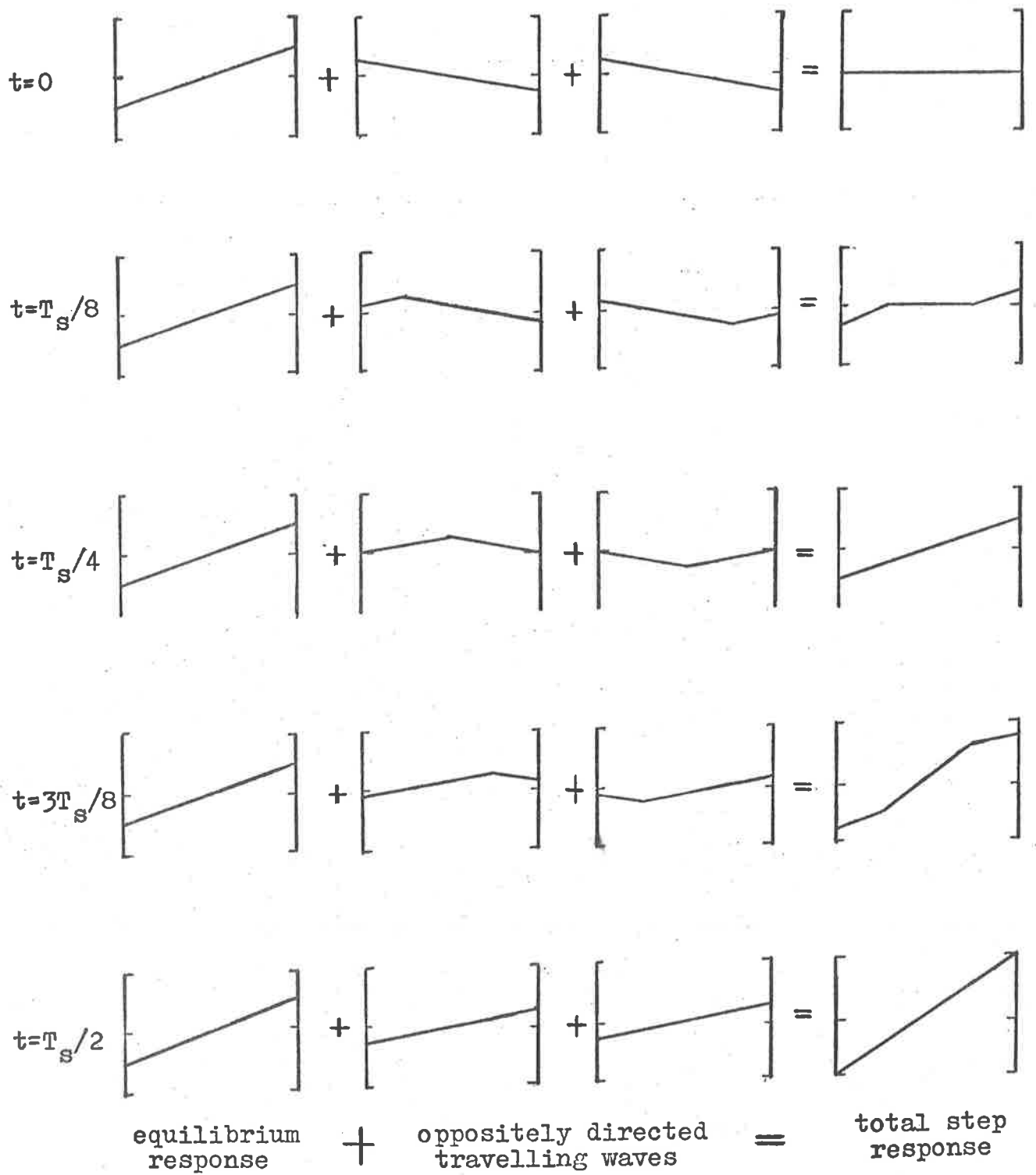
FIGURE 3.9 : SURFACE SHAPE OF RECTANGULAR, CONSTANT DEPTH BASIN (WITH ZERO DAMPING) IN RESPONSE TO A STEP WIND APPLIED AT t=0. THE RESPONSE BEGINS AT THE LAKE EDGES. AT t = $T_s/2$, THE LAKE SURFACE OVERSHOOTS THE EQUILIBRIUM RESPONSE BY A FACTOR OF 2 .
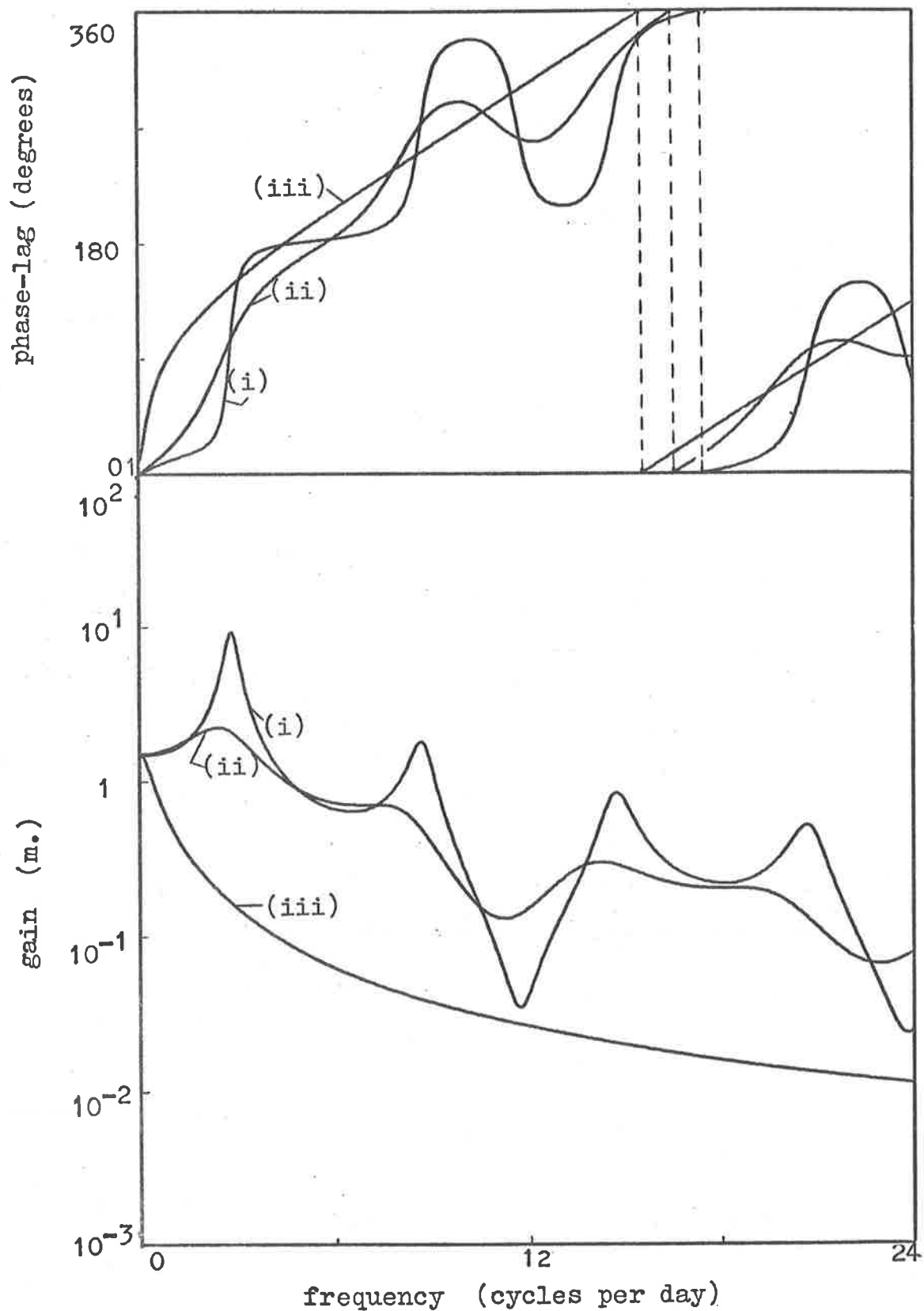
FIGURE 3.10 : RESPONSE FUNCTIONS FOR SURFACE DISPLACEMENT AT SEVEN MILE POINT, NORTH COORONG, AS CALCULATED FROM (3.3.12a), FOR (i) $N=10^{-5}$ m^2. sec^{-1}, (ii) $N=10^{-4}$ m^2. sec^{-1}, (iii) $N=10^{-3}$ m^2. sec^{-1}. EQUILIBRIUM RESPONSE IS 1.519 M.
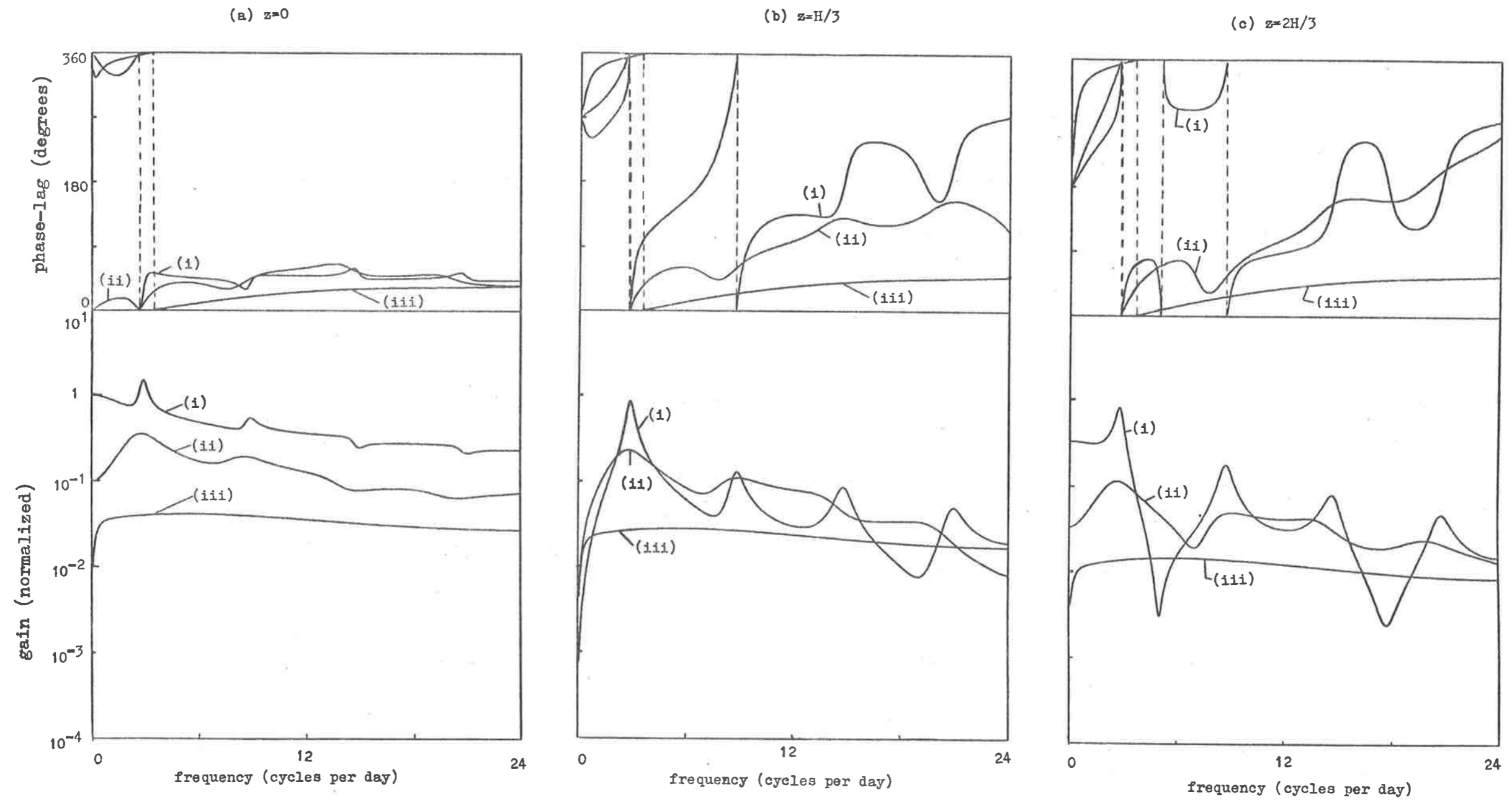
FIGURE 3.11 : RESPONSE FUNCTIONS FOR VELOCITY AT DEPTHS (a) 0, (b) H/3,
(c) 2H/3, AT SEVEN MILE POINT, NORTH COORONG, AS CALCULATED
FROM (3.3.12b), FOR (i) $N=10^{-5}$ $m^2.sec^{-1}$, (ii) $N=10^{-4}$ $m^2.sec^{-1}$
(iii) $N=10^{-3}$ $m^2.sec^{-1}$.   ALL GAINS ARE NORMALIZED WITH
RESPECT TO THE ZERO FREQUENCY GAIN OF SURFACE VELOCITY FOR
$N=10^{-5}$ $m^2.sec^{-1}$, VIZ. 31.5 $m.sec^{-1}$.
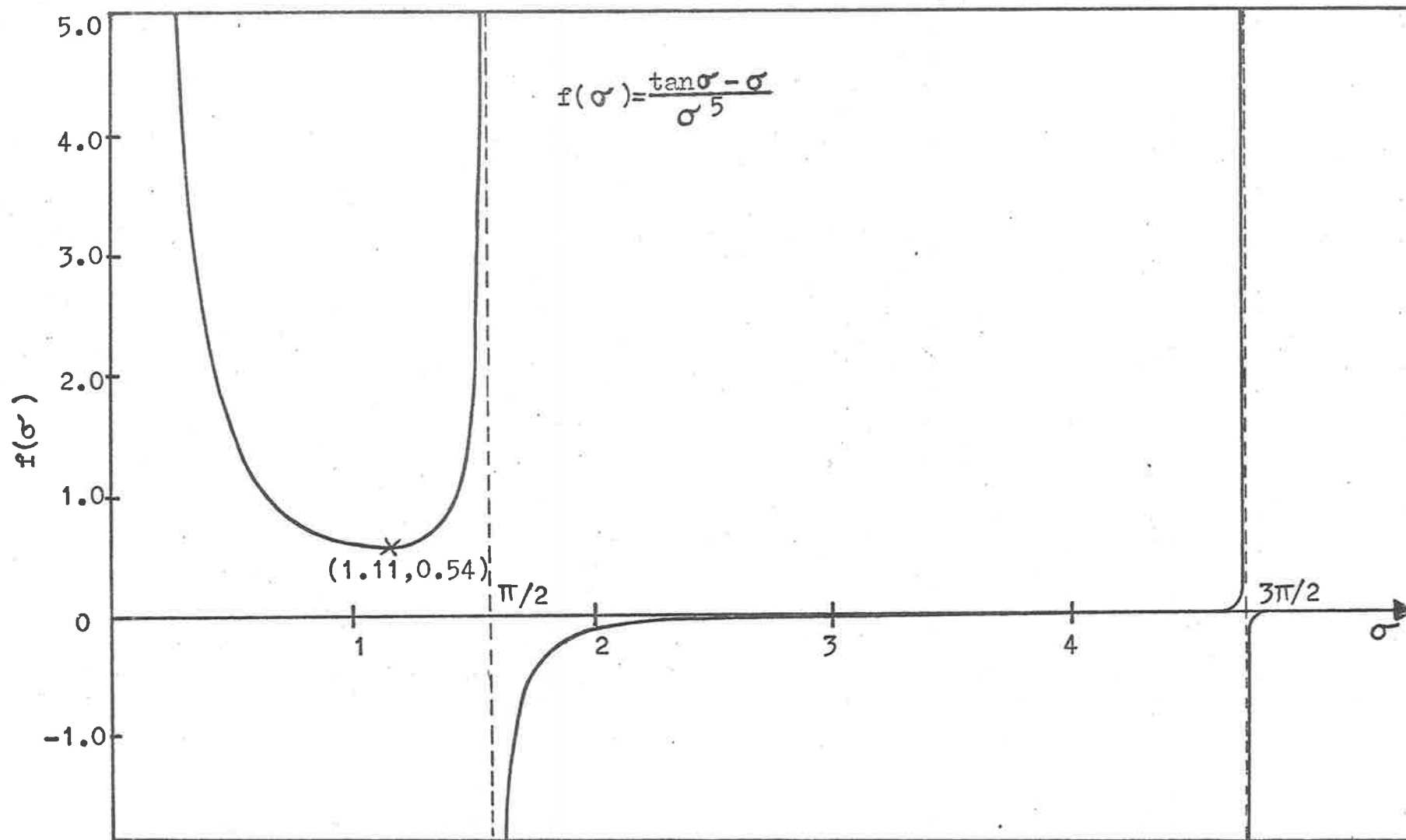
FIGURE 3.12 : PLOT OF $f(\sigma) = (\tan\sigma - \sigma)/\sigma^5$ FOR REAL σ .

CHAPTER 4

A GENERALIZED THEORY FOR WIND EFFECTS

4.1 The Theory

We develop here a generalized theory for time varying wind effects on a lake of arbitrary contour and constant depth. The steady state periodic response for such a system is the solution of a Helmholtz equation subject to certain boundary bonditions.

Consider the transport equations (2.1.12) with constant depth, H, viz.

$$\frac{\partial U}{\partial t} + 2\alpha U - fV = -c^2 \frac{\partial \zeta}{\partial x} + K\tau_{sx} \qquad (4.1.1a)$$

$$\frac{\partial V}{\partial t} + 2\alpha V + fU = -c^2 \frac{\partial \zeta}{\partial y} + K\tau_{sy} \qquad (4.1.1b)$$

$$\frac{\partial U}{\partial x} + \frac{\partial V}{\partial y} = -\frac{\partial \zeta}{\partial t} \qquad (4.1.1c)$$

with c, α having their previous meanings.

Assume that wind stress components have the form

$$\tau_{sx}(x,t) = \tau_{ox}(x,y)e^{j\omega t} \qquad (4.1.2a)$$

$$\tau_{sy}(x,t) = \tau_{oy}(x,y)e^{j\omega t} \qquad (4.1.2b)$$

where $\tau_{ox}(x,y)$, $\tau_{oy}(x,y)$ are amplitudes of wind stress components and, in general, vary with position across the lake surface. Then the steady state response of the lake is expressible in the form

$$\zeta(x,y,t) = Z(x,y,\omega)e^{j\omega t} \tag{4.1.3a}$$

$$U(x,y,t) = P(x,y,\omega)e^{j\omega t} \tag{4.1.3b}$$

$$V(x,y,t) = Q(x,y,\omega)e^{j\omega t} \quad . \tag{4.1.3c}$$

Combining (4.1.1), (4.1.3) gives

$$\beta P - fQ = -c^2 \frac{\partial Z}{\partial x} + K\tau_{ox} \tag{4.1.4a}$$

$$\beta Q + fP = -c^2 \frac{\partial Z}{\partial y} + K\tau_{oy} \tag{4.1.4b}$$

$$\frac{\partial P}{\partial x} + \frac{\partial Q}{\partial y} = -j\omega Z \tag{4.1.4c}$$

where $\beta(\omega) = j\omega + 2\alpha$. Eliminating P, Q in turn from (4.1.4a), (4.1.4b) gives

$$P = \frac{1}{(f^2 + \beta^2)} \left[K(\beta\tau_{ox} + f\tau_{oy}) - c^2(\beta \frac{\partial Z}{\partial x} + f \frac{\partial Z}{\partial y}) \right] \tag{4.1.5a}$$

$$Q = \frac{1}{(f^2 + \beta^2)} \left[K(\beta\tau_{oy} - f\tau_{ox}) - c^2(\beta \frac{\partial Z}{\partial y} - f \frac{\partial Z}{\partial x}) \right], \tag{4.1.5b}$$

and combining (4.1.5), (4.1.4c) we have

$$(\nabla^2 + k^2)Z = \frac{K}{c^2\beta} (\beta D + fC) \tag{4.1.6}$$

where $\nabla^2 \equiv \frac{\partial^2}{\partial x^2} + \frac{\partial^2}{\partial y^2})$, i.e. the steady state, periodic response is the solution of an inhomogeneous Helmholtz equation.

In (4.1.6),

$$k^2 = \frac{-j\omega\beta}{c^2} (1 + \frac{f^2}{\beta^2}) \tag{4.1.7}$$

$$D = \frac{\partial\tau_{ox}}{\partial x} + \frac{\partial\tau_{oy}}{\partial y} \tag{4.1.8a}$$

$$C = \frac{\partial\tau_{oy}}{\partial x} - \frac{\partial\tau_{ox}}{\partial y} \quad . \tag{4.1.8b}$$

D, C are respectively the divergence and the magnitude of the curl of the wind stress amplitude vector $\underset{\sim}{\tau}_o = (\tau_{ox}, \tau_{oy})$.

The boundary condition (2.1.10), when subject to (4.1.3b), (4.1.3c) becomes

$$(S*)n = 0 \text{ along } \Gamma \tag{4.1.9a}$$

where $\underset{\sim}{S}* = (P, Q)$. We may write

$$\underset{\sim}{S}* = K\underset{\sim}{a} - c^2\underset{\sim}{b}$$

where

$$\underset{\sim}{a} = (\beta\tau_{ox} + f\tau_{oy}, \beta\tau_{oy} - f\tau_{ox}) = \beta\underset{\sim}{\tau}_o + f\underset{\sim}{\tau}_o \times \hat{\underset{\sim}{k}}$$

$$\underset{\sim}{b} = (\beta Z_x + fZ_y, \beta Z_y - fZ_x) = \beta\underset{\sim}{\nabla}Z + f\underset{\sim}{\nabla}Z \times \hat{\underset{\sim}{k}}$$

and $\hat{\underset{\sim}{k}}$ is the unit vector in the +z direction (Fig. 4.1). Thus (4.1.9a) becomes

$$\frac{K}{c^2} \; (\underset{\sim}{a} \cdot \hat{\underset{\sim}{n}})_\Gamma = (\underset{\sim}{b} \cdot \hat{\underset{\sim}{n}})_\Gamma$$

or

$$(\beta\underset{\sim}{\nabla}Z \cdot \hat{\underset{\sim}{n}} + f\underset{\sim}{\nabla}Z \times \hat{\underset{\sim}{k}} \cdot \hat{\underset{\sim}{n}})_\Gamma = \frac{K}{c^2} \; (\beta\underset{\sim}{\tau}_o \cdot \hat{\underset{\sim}{n}} + f\underset{\sim}{\tau}_o \times \hat{\underset{\sim}{k}} \cdot \hat{\underset{\sim}{n}})_\Gamma \tag{4.1.9b}$$

where $\hat{\underset{\sim}{n}}$ is the outward unit vector normal to the lake contour, Γ, (Fig. 4.1). Further, define $\hat{\underset{\sim}{e}}$ the unit vector in the positive (counter-clockwise) direction of the lake contour, Γ, (Fig. 4.1). Now the following relationships are easily established:

$$\underset{\sim}{\nabla}Z \cdot \hat{\underset{\sim}{n}} = \frac{\partial Z}{\partial n}$$

$$\underset{\sim}{\nabla}Z \times \hat{\underset{\sim}{k}} \cdot \hat{\underset{\sim}{n}} = \frac{\partial Z}{\partial e}$$

$$\underset{\sim}{\tau}_o \cdot \hat{\underset{\sim}{n}} = \tau_{on}$$

$$\underset{\sim}{\tau}_O \times \hat{\underset{\sim}{k}} \cdot \hat{\underset{\sim}{n}} = \tau_{oe}$$

where ∂n, ∂e are elements of length in the directions of the unit vectors $\hat{\underset{\sim}{n}}$, $\hat{\underset{\sim}{e}}$ respectively. Thus (4.1.9b) becomes

$$(\beta \frac{\partial Z}{\partial n} + f \frac{\partial Z}{\partial e})_\Gamma = \frac{K}{c^2} (\beta \tau_{on} + f \tau_{oe})_\Gamma , \qquad (4.1.9c)$$

a generalized boundary condition for the wind forced, periodic and steady state motion of a closed lake, with Coriolis and damping parameters included.

In the work which follows we assume, as in the previous chapter, that the wind stress is homogeneous over the lake surface, so that $C = D = 0$.

Recently, Emery and Csanady (1973) have postulated that the long-term, consistently counter-clockwise circulation of surface waters in many lakes, lagoons and marginal seas of the northern hemisphere, is due to a positive (cyclonic) wind stress curl acting on the lake. The proposed mechanism is as follows.

Surface wind drift currents have a component directed to the right of the wind (looking downwind) in the northern hemisphere (Ekman drift) and in the presence of surface heating this leads to a displacement of warmer water to the right. Greater surface turbulence and thus greater surface drag is produced to the right of the wind, i.e. a wind stress curl across the lake is established. In addition, upwelling of cold water to the left of the wind would accentuate the temperature gradient across the lake and hence the magnitude of the wind stress curl.

Now a wind stress curl of this form blowing for a considerable period of time produces counter-clockwise circulation(Tareyev (1958)). Further, regardless of the speed or direction of the wind, the circulation has counter-clockwise sense so that if the lake motion is averaged over a long period of time, the portion due directly to the wind stress curl would remain while that due to other, more conventional effects (wind drift, seiches, etc) would be averaged out. Emery and Csanady show that velocities equivalent in magnitude to observed velocities $(0(0.1 \text{ cm.sec}^{-1}))$ can be induced in a circular, constant depth model lake by a temperature gradient of 1°C across a 50 km lake diameter.

In the southern hemisphere, the theory predicts Ekman drift of warmer waters to the left of the wind (looking downwind) with a consequent, long-term clockwise circulation. Unfortunately there is no available data to substantiate this supposition. Australian lakes, subject to considerable surface heating, might be expected to exhibit such a circulation.

Wunsch (1973) has provided another possible explanation for the phenomenon. He relates the long-term circulation to second-order Lagrange drift associated with internal waves generated by impulsive wind changes over the lake.

The requirement of a wind stress field of zero divergence and curl reduces (4.1.6) to

$$(\nabla^2 + k^2) \ Z = 0 \qquad\qquad (4.1.10)$$

still subject to boundary condition (4.1.9c).

The assumption of constant depth made at the beginning of this section is relatively unrestrictive; solutions obtained are likely to reproduce closely the main features of wind effects in real basins provided there is no sudden variation in bottom contour. Smith (1973) in a study of the wind-forced and seiche-forced motion of Grand Traverse Bay, Lake Michigan, has shown, using numerical models, that unusual bottom topographic features of this kind may result in the formation of velocity gyres which correspond closely to observed velocity patterns.

We proceed, in later sections of this chapter, to solve (4.1.10) making one final simplifying assumption, viz. that the wind stress is unidirectional, its direction being that of the x-axis, i.e. we have

$$\tau_{sx}(t) = \tau_o e^{j\omega t} \qquad\qquad (4.1.11a)$$

$$\tau_{sy}(t) = 0 \qquad\qquad (4.1.11b)$$

where τ_o is a constant. With unit amplitude this allows $Z(x_o, y_o, \omega)$ to be interpreted as the response function of the system with $\tau_{sx}(t)$ as input and $\zeta(x_o, y_o, t)$ as output. Note that generally the function $Z(x_o, y_o, \omega)$ is a linear combination of the sub-response functions which together specify the system (refer Chapter 2).

Since in this case $\underset{\sim}{\tau}_O = (\tau_o, 0)$, then the components τ_{on}, τ_{oe} satisfy $\tau_{on} = \tau_o \underset{\sim}{\hat{i}} \cdot \underset{\sim}{\hat{n}}$, $\tau_{oe} = \tau_o \underset{\sim}{\hat{i}} \cdot \underset{\sim}{\hat{e}}$ where $\underset{\sim}{\hat{i}}$ is the unit vector in the positive x-direction (Fig. 4.1).

The particularization of (4.1.10) obtained with f = 0 should be noted.

It is

$$(\nabla^2 + k_o^2) \; Z = 0 \tag{4.1.12a}$$

where $k_o^2 = -j\omega\beta/c^2$. Boundary condition (4.1.9c) becomes

$$\left(\frac{\partial Z}{\partial n}\right)_\Gamma = \frac{K}{c^2} \; (\tau_{on})_\Gamma \; . \tag{4.1.12b}$$

4.2 Equilibrium Solutions

Let us examine, firstly, the equilibrium solutions to (4.1.10), i.e. the zero frequency solutions assuming the uni-directional wind stress field (4.1.11). We consider the solutions under the following headings:-

(a) The non-rotating case, $f = 0$

Here $k = k_o$ and in the limit $\omega \to 0$ we have $k_o \to 0$. Thus, the equilibrium response $\overline{Z}(x,y)$, defined as $\lim\limits_{\omega \to 0} \{Z(x,y,\omega)\}$, satisfies

$$\nabla^2 \; \overline{Z} = 0 \tag{4.2.1a}$$

subject to

$$\left(\frac{\partial \overline{Z}}{\partial n}\right)_\Gamma = \frac{K}{c^2} \; (\tau_{on})_\Gamma \; . \tag{4.2.1b}$$

A particular solution to this problem is clearly $K\tau_o x/c^2$, so the general solution to (4.2.1) may be written

$$\overline{Z}(x,y) = \frac{K\tau_o x}{c^2} + \phi(x,y) \tag{4.2.2}$$

where $\phi(x,y)$ satisfies

$$\nabla^2\phi = 0 \tag{4.2.3a}$$

subject to

$$\left(\frac{\partial \phi}{\partial n}\right)_{\Gamma} = 0 \ . \qquad\qquad (4.2.3b)$$

The unique solution to this Neumann problem is $\phi = \phi_o$, a constant, (Chester (1971), p.70), so the unique solution to (4.2.1) is

$$\overline{Z}(x) = \frac{K\tau_o x}{c^2} + \phi_o \qquad\qquad (4.2.4)$$

where the constant ϕ_o is to be determined by the condition of mass conservation, i.e. the integral of $\overline{Z}$ over the lake surface must be zero.

From (4.1.5) we see that $Z = \overline{Z}(x)$ implies $P = Q = 0$, i.e. (4.2.4) is a static equilibrium solution. Further, we note that the slope of the equilibrium surface is independent of the shape of the basin contour. So the classical one-dimensional equilibrium wind set-up, explained physically in Chapter 1 and derived in Chapter 2 for the case of a non-rotating rectangular basin of constant depth, is theoretically achievable for a much wider class of wind effect problems.

We note that (4.1.4a), (4.1.4b) (with $\tau_{ox} = \tau_o$, $\tau_{oy} = 0$) may be written as

$$\beta P - fQ = -c^2 \frac{\partial}{\partial x} (Z - \overline{Z}) \qquad\qquad (4.2.5a)$$

$$-\beta Q + fP = -c^2 \frac{\partial}{\partial y} (Z - \overline{Z}) \ . \qquad\qquad (4.2.5b)$$

Lamb (1932), p.319 uses an equivalent form in his investigation of the general forced motion of a rotating basin. Using Lamb's relation (4) of §207, the potential of the disturbing forces is

$$\Omega = - \overline{Z}g \qquad\qquad (4.2.6)$$

so the potential of the wind stress (4.1.11) acting on a closed basin of constant depth H, is

$$\Omega = - \frac{K\tau_o x}{H} . \qquad\qquad (4.2.7)$$

Finally we note that the generalized boundary condition (4.1.9c) may be rewritten in the form

$$(\beta\frac{\partial}{\partial n} (Z-\overline{Z}) + f \frac{\partial}{\partial e} (Z-\overline{Z}))_\Gamma = 0 . \qquad\qquad (4.2.8)$$

(b) The Rotating Case, $f \neq 0$

It proves useful in this case to form, from (4.1.4a) and (4.1.4b), the vorticity equation

$$\beta M = j\omega f Z \qquad\qquad (4.2.9a)$$

where $M = \left(\frac{\partial Q}{\partial x} - \frac{\partial P}{\partial y}\right)$ is the amplitude of the integrated vorticity $W = \left(\frac{\partial v}{\partial x} - \frac{\partial u}{\partial y}\right)$ imparted to the fluid by the rotation of the earth.

Then for $\underline{\alpha = 0}$, (4.2.9a) gives

$$M = fZ \qquad\qquad (4.2.9b)$$

at all frequencies, including zero frequency. Now if the equilibrium state were static, (4.2.9b) would imply that the surface equilibrium response $\tilde{Z}(x,y)$, defined as $\underset{\omega \to 0}{\lim} \{Z(x,y,\omega)\}$, is everywhere zero, which is unlikely. Rather, a non-trivial form for $\tilde{Z}(x,y)$ implies the presence of vorticity at equilibrium giving rise to a quasistatic equilibrium circulation pattern.

In this case $k \to j/R$ as $\omega \to 0$, where

$$R = \frac{c}{f} , \qquad\qquad (4.2.10)$$

so the equilibrium response $\tilde{Z}(x,y)$ satisfies

$$(\nabla^2 - \frac{1}{R^2}) \, \tilde{Z} = 0 \qquad\qquad (4.2.11a)$$

subject to

$$\left(\frac{\partial \tilde{Z}}{\partial e}\right)_\Gamma = \frac{K}{c^2} \, (\tau_{oe})_\Gamma \cdot \qquad\qquad (4.2.11b)$$

From (4.2.5), the equilibrium transport components $\tilde{P}(x,y)$, $\tilde{Q}(x,y)$ are given by

$$\tilde{P} = - \frac{c^2}{f} \frac{\partial}{\partial y} (\tilde{Z}-\overline{Z}) = - \frac{\partial \psi}{\partial y} \qquad\qquad (4.2.12a)$$

$$\tilde{Q} = \frac{c^2}{f} \frac{\partial}{\partial x} (\tilde{Z}-\overline{Z}) = \frac{\partial \psi}{\partial x} \qquad\qquad (4.2.12b)$$

where $\psi(x,y)$ is a stream function defined to satisfy (4.1.4c) with $\omega = 0$. Its contours define the quasistatic circulation pattern.

Clearly we may write

$$\psi(x,y) = \frac{c^2}{f} (\tilde{Z}-\overline{Z}) \qquad\qquad (4.2.13)$$

since this gives the required equilibrium transports defined in (4.2.12). Further, since the lake contour, Γ, must itself form a streamline, then along Γ it is clear that $\tilde{Z}(x,y)$ and $\overline{Z}(x)$ differ by only an additive constant.

The differential equation satisfied by $\psi(x,y)$ is obtained by combination of (4.2.11) and (4.2.13). It is

$$(\nabla^2 - \frac{1}{R^2})\psi = \frac{K\tau_0 fx}{c^2}$$

(4.2.14a)

subject to

$$\left(\frac{\partial\psi}{\partial e}\right)_\Gamma = 0 ,$$

i.e.

$$\psi = 0 \text{ along } \Gamma ,$$

(4.2.14b)

where the contour ψ is arbitrarily chosen as the streamline $\psi = 0$.

In Appendix C it is shown that solutions to (4.2.11) and (4.2.14) are respectively unique to within an additive constant and completely unique. In the former case, the correct additive constant for a given basin is determined by the condition of mass conservation.

In later sections of this chapter, the quasistatic equilibrium response of basins of specific form will be considered.

Rossby (1938), Cahn (1945) and Veronis (1955) have shown that the parameter R is of extreme importance in determining the (theoretical) extent of the quasistatic adjustments (deformations) of mass and velocity distributions for a wind-induced oceanic current system of finite width and infinite length. It has dimensions of length and Rossby termed it the radius of deformation . The magnitude of R is the radius of the inertia circle (Proudman (1953), p.74) for long waves in a channel of depth, H.

Recently Csanady (1967, 1968a, 1968b, 1972) and Birchfield (1969) have shown that R is also important in determining the extent of the equivalent

adjustments in closed basins. These works are examined in greater detail later in this chapter.

Let us briefly consider the case $\alpha \neq 0$. In the limit $\omega \to 0$, the vorticity equation (4.2.9a) gives $M = 0$, i.e. in the presence of damping forces the equilibrium motion is irrotational. We may thus write

$$(\tilde{P}, \tilde{Q}) \equiv \underset{\sim}{S}^* = \nabla \chi \tag{4.2.15}$$

where the function $\chi(x,y)$ satisfies

$$\nabla^2 \chi = 0 \quad \text{within } \Gamma \tag{4.2.16a}$$

(this follows by combining (4.2.15) and (4.1.4c) with $\omega = 0$), subject to

$$\left(\frac{\partial \chi}{\partial n}\right)_\Gamma = 0 . \tag{4.2.16b}$$

The solution to boundary value problem (4.2.16) is $\chi = \chi_o$, a constant, and thus (4.2.15) gives $\underset{\sim}{S}^* = \underset{\sim}{0}$, i.e. the equilibrium response is a static response. Finally, integration of (4.2.5) with $\tilde{P} = \tilde{Q} = 0$ gives

$$\tilde{Z}(x) = \overline{Z} + \phi_o$$

i.e. solution (4.2.4) again. Thus, even for the case of a rotating basin, the familiar equilibrium wind tide is established, provided some damping forces act within the fluid.

4.3 The Rectangular Lake

We now apply the theory developed in the two previous sections to the case of the constant depth rectangular lake considered in Sections 3.2, 3.3. The coordinate system of Fig. 3.1 is again used here. The basin has length L (x-direction) and breadth B (y-direction) and is subject to the wind stress field (4.1.11) which acts always parallel to the side of length L.

We write (4.1.10) as

$$\frac{\partial^2 Z}{\partial x^2} + \frac{\partial^2 Z}{\partial y^2} + k^2 Z = 0 \qquad (4.3.1a)$$

subject to boundary conditions

$$\beta \frac{\partial}{\partial x} (Z-\overline{Z}) + f \frac{\partial}{\partial y} (Z-\overline{Z}) = 0 \text{ for } x = 0, L \qquad (4.3.1b)$$

$$-f \frac{\partial}{\partial x} (Z-\overline{Z}) + \beta \frac{\partial}{\partial y} (Z-\overline{Z}) = 0 \text{ for } y = 0, B. \qquad (4.3.1c)$$

The general solution to system (4.3.1) has not been attempted here. The difficulty results from the complicated nature of the boundary conditions (4.3.1b), (4.3.1c). The comment of Rao (1966) that

"the solution of the problem of free oscillations in rotating rectangular basins is far from complete"

is equally applicable to the forced problem.

However the simplification f = 0 reduces the problem to the one-dimensional situation of Section 3.2, described now by the equation

$$\frac{d^2 Z}{dx^2} + k_o^2 Z = 0 \qquad (4.3.2a)$$

subject to

$$\frac{\partial}{\partial x} (Z-\bar{Z}) = 0 \text{ for } x = 0, L .$$

(4.3.2b)

The solution to (4.3.2) is

$$Z(x,\omega) = \frac{K\tau_o \sin\{k_o(x - \frac{L}{2})\}}{k_o c^2 \cos(k_o L/2)}$$

(4.3.3)

identical (at station x_o and with $\tau_o = 1$) to (3.2.9), as may be seen by expanding (4.3.3) as a Fourier cosine-series over the range $[0,L]$. We note, too, that

$$\bar{Z}(x) = \frac{K\tau_o}{c^2} (x - \frac{L}{2}),$$

(4.3.4)

equivalent to (3.2.13).

With $\alpha = 0$ we have $k_o = \omega/c$, so resonance occurs when $\cos(\omega L/2c) = 0$, i.e. $\omega = (2n-1)\pi c/L$, $n = 1, 2, \ldots$, as determined in Section 3.2. We note that the real time response to a wind stress of the form $\tau_s = \tau_o \sin(\omega t)$ is $\zeta(x,t) = \tau_o I_m\{Z(x,\omega)e^{j\omega t}\}$. With $\alpha = 0$ this becomes

$$\zeta(x,t) = \frac{K\tau_o}{\omega c} \frac{\sin\{\frac{\omega}{c}(x - \frac{L}{2})\}}{\cos(\omega L/2c)} \sin(\omega t)$$

(4.3.5)

i.e. the surface response has a sinusoidal shape (a result referred to though not proved in Section 3.2) and has the form of a standing wave. (Alternatively, we might regard the response as a superposition of oppositely directed travelling waves, each with speed c).

Noye (1973) has previously obtained and discussed the solution (4.3.3) in the case $\alpha = 0$.

Let us examine the quasistatic equilibrium circulation pattern for the

case of the rectangular lake. The stream function $\psi(x,y)$ satisfies
(4.2.14a) within the lake contour, while boundary condition (4.2.14b) may
be written as

$$\psi = 0 \text{ for } x = 0,L$$

$$\psi = 0 \text{ for } y = 0,B.$$

The solution to this boundary value problem may be obtained by use of
finite Fourier transforms (Tranter (1971)).

Specifically, define the finite sine transform $\psi_n(x)$ by

$$\psi_n(x) = \int_0^B \psi(x,y)\sin(\theta_n y)\,dy$$

where $\theta_n = n\pi/B$, $n = 1,2, \dots$. Then

$$\int_0^B \frac{\partial^2\psi}{\partial y^2}\sin(\theta_n y)\,dy = -\theta_n^2\,\psi_n$$

so that (4.3.14a) transforms to

$$\frac{\partial^2\psi_n}{\partial x^2} - \delta_n^2\,\psi_n = \frac{-K\tau_o fx((-1)^n - 1)}{c^2\theta_n} \tag{4.3.6a}$$

where $\delta_n^2 = \theta_n^2 + 1/R^2$, subject to

$$\psi_n(0) = \psi_n(L) = 0 . \tag{4.3.6b}$$

The solution to (4.3.6) is

$$\left.\begin{aligned}
\psi_{2p} &= 0 \\
\psi_{2p-1} &= \frac{-2K\tau_o f}{c^2\theta_n\delta_n^2}\left[x - L\,\frac{\sinh(\delta_n x)}{\sinh(\delta_n L)}\right]
\end{aligned}\right\} \quad p = 1,2, \dots \tag{4.3.7}$$

So from the inversion formula

$$\psi(x,y) = \frac{2}{B} \sum_{p=1}^{\infty} \psi_p(x) \sin(\theta_p y)$$

we have

$$\psi(x,y) = \frac{-4K\tau_o f}{Bc^2} \sum_{p=1}^{\infty} \frac{\sin(\theta_{2p-1} y)}{\theta_{2p-1} \, \delta_{2p-1}^2} \left[x - L \frac{\sinh(\delta_{2p-1} x)}{\sinh(\delta_{2p-1} L)} \right]. \quad (4.3.8)$$

Lake Alexandrina may be approximated as a rectangular basin with axes in north-east and north-west directions; we take length L (north-east direction) as 30km, breadth B as 15km and depth H as 3.5m. Further, we take $f = -8.5 \times 10^{-5} \text{sec}^{-1}$, obtainable from (2.1.2) with $\phi = 35°$ which is the latitude appropriate to the area of the Murray Mouth lakes. The quasistatic circulation pattern obtainable from (4.3.8) for this model due to a steady south-west wind is shown in Fig. 4.2. The series was found to converge sufficiently after 50 terms.

In the portion of the basin from $x = 0$ to $x = L/2$, the circulation consists of slow Ekman drift to the left of the wind (looking downwind), the flow then moving in a clockwise direction around the basin. It is to be noted that the flow is more concentrated along the sides and the down-wind end of the basin than along the upwind end – such concentrations are commonly termed coastal jets . Also, the flow involves the entire basin, and, regardless of the direction of wind, is always in the clockwise sense. For the Northern hemisphere, a counter-clockwise circulation pattern is predicted. Circulation of this form offers another plausible explanation for the long-term counter-clockwise circulation observable in many lakes of the Northern hemisphere. Evaluation of the velocities associated with

the pattern of Fig. 4.2 with $\tau_o = 0.1$ N.m^{-2} shows that typical velocity magnitudes are of $0(0.1$ cm.sec^{-1} - 1 cm.sec$^{-1})$, though within the highly concentrated coastal jets they may be as high as $0(10$ cm.sec$^{-1})$.

The quasistatic equilibrium surface response is, from (4.2.14), given by

$$\tilde{Z} = \frac{f}{c^2} \psi + \frac{K\tau_o x}{c^2} + \phi_o$$

where ϕ_o is determined so that mass is conserved, i.e.

$$\phi_o = -\frac{1}{c^2} \left\{ \frac{K\tau_o L}{2} + \frac{f}{BL} \int_0^B \int_0^L \psi(x,y)\,dxdy \right\}.$$

Thus we may write

$$\tilde{Z} = \frac{f}{c^2} \left\{ \psi - \frac{1}{BL} \int_0^B \int_0^L \psi(x,y)\,dxdy \right\} + \frac{K\tau_o}{c^2} \left(x - \frac{L}{2} \right). \qquad (4.3.9)$$

Evaluation of (4.3.9) shows, in fact, that the quasistatic equilibrium response for the Lake Alexandrina model is dominated by the term $K\tau_o (x-L/2)/c^2$, i.e. is almost equivalent to the static response. This is why the velocities associated with the pattern of Fig. 4.2 are generally small.

4.4 The Circular Lake

The problem of the undamped free and forced motions of a rotating, circular, single-layer basin is treated in detail by Lamb (1932), §209 - §211.

Recently, Csanady (1967, 1968a, 1968b, 1972) and Birchfield (1969) have extended Lamb's work to the case of a rotating, circular, two-layer

basin, a simple model shown to exhibit some of the main features of the summer motions of the Great Lakes.

Here we examine the damped, wind-forced motion of a rotating, circular, single-layer basin using the generalized theory developed in previous sections. Such a model should allow some of the important features of wind forced motions in the shallow (and therefore heavily damped) and well-mixed Murray Mouth Lakes to be deduced. The methods used are applicable also to the two-layer model developed by Csanady and Birchfield, but discussion of this is left to a later chapter.

The plan of the lake under consideration is shown in Fig. 4.3. The origin of coordinates is positioned in the centre of the lake; the radius is denoted by a. Again the wind stress (4.1.11) acts on the lake. Clearly we achieve considerable simplification in this case by using polar coordinates r, θ such that $x = r\cos\theta$, $y = r\sin\theta$. Then the wind stress vector may be written

$$\underline{\tau}_s = \tau_r \hat{\underline{e}}_r + \tau_\theta \hat{\underline{e}}_\theta$$

where $\hat{\underline{e}}_r$, $\hat{\underline{e}}_\theta$ are unit vectors in the r- and θ- directions respectively (Fig. 4.3) and τ_r, τ_θ are the r- and θ- components respectively of the wind stress vector. From (4.1.11) it is clear that

$$\tau_r = \tau_o \cos\theta \qquad\qquad (4.4.1a)$$

$$\tau_\theta = -\tau_o \sin\theta . \qquad\qquad (4.4.1b)$$

Further (4.1.10) may be written as

$$\left(\frac{\partial^2}{\partial r^2} + \frac{1}{r}\frac{\partial}{\partial r} + \frac{1}{r^2}\frac{\partial^2}{\partial \theta^2} + k^2\right) Z = 0 \qquad (4.4.2a)$$

while boundary condition (4.2.8) becomes

$$(\beta \frac{\partial}{\partial r}(Z-\bar{Z}) + \frac{f}{r}\frac{\partial}{\partial \theta}(Z-\bar{Z}))_{r=a} = 0 \qquad (4.4.2b)$$

where the static equilibrium response is

$$\bar{Z}(r,\theta) = \frac{K\tau_o r\cos\theta}{c^2} \ . \qquad (4.4.3)$$

The solution of the boundary value problem (4.4.2) is not difficult to achieve for arbitrary ω. The general solution to (4.4.2a) has the form

$$Z(r,\theta,\omega) = J_m(kr)(A_m\cos(m\theta) + B_m\sin(m\theta))$$

where m is an integer and $J_m(kr)$ is the mth order ordinary Bessel function of the first kind, with (in general) complex argument. However from the form of the boundary condition (4.4.2b) it is clear that only azimuthal wave number m = 1 is present in the solution to (4.4.2a), i.e. $A_m = B_m = 0$ for all m $\neq$ 1. On the other hand, if the strength of the wind stress, τ_o, varied over the surface then other values of m would also be appropriate.

The solution correctly satisfying (4.4.2b) is

$$Z(r,\theta,\omega) = \frac{K\tau_o J_1(kr)\{(\beta^2 kL_2+f^2 L_1/a)\cos\theta+\beta f(L_1/a-kL_2)\sin\theta\}}{c^2\{(\beta kL_2)^2+(fL_1/a)^2\}}$$

$$(4.4.4)$$

where $L_1(\omega) = J_1(ka)$, $L_2(\omega) = \left(\frac{d}{dz}J_1(z)\right)_{z=ka} = J_o(ka)-J_1(ka)/ka$. With f = 0, (4.4.4) reduces to

$$Z(r,\theta,\omega) = \frac{K\tau_o J_1(k_o r)\cos\theta}{c^2(J_o(k_o a)-J_1(k_o a)/k_o a)} \qquad (4.4.5)$$

which may be checked as a solution to the boundary value problem (4.1.12).

We may approximate Lake Albert (closed at the Narrung channel entrance) as a circular lake of radius a = 7.5 km and depth H = 2m. The behaviour of this model lake might be expected to correspond, at least in its gross features, to the wind-induced behaviour of the actual lake. Shown in Fig. 4.4a are the gain and phase-lag for the response function $Z(r_o, \theta_o, \omega)$ (unit τ_o) at station (a/2,0), with $f = -8.5 \times 10^{-5} sec^{-1}$, and for various values of α. In Fig. 4.4b are shown the curves of gain and phase-lag at the same station with Coriolis parameter f set to zero. To achieve effective comparison between the response curves of Fig. 4.4a and Fig. 4.4b, the gains in each have been normalized with respect to the static equilibrium response at (a/2,0) as given by (4.4.3), with $\tau_o = 1$ $N.m^{-2}$, viz. 0.201m. Typically $\tau_o = 0.1$ $N.m^{-2}$, so that for Lake Albert, surface displacements are generally of 0(5cm).

In Figs. 4.5a, 4.5b are shown similar curves obtained from the station (a/2, π/4). The normalization factor for gains is again 0.201m.

In the absence of rotation, and with $\alpha = 0$ so that $k_o = \frac{\omega}{c}$, resonance occurs at frequencies $\omega = \frac{c}{a} z_n$ (n = 1,2, ...) = 1.9 $\frac{c}{a}$, 5.3 $\frac{c}{a}$, 8.5 $\frac{c}{a}$, 11.7 $\frac{c}{a}$, etc. where z_n is the nth successive positive zero of the function $\frac{d}{dz} J_1(z)$. These are the frequencies of the natural modes of oscillation of azimuthal wave number 1 for a non-rotating circular basin of depth H, and radius a, (see Lamb (1932), §191). For comparison, a non-rotating rectangular basin of length 2a, and depth H, exhibits resonance, when subject to the lengthwise wind stress field (4.1.11), at the frequencies

$\omega = \frac{c}{a} (n - \frac{1}{2})\pi, (n = 1, 2, \ldots) = 1.6 \frac{c}{a}, 4.7 \frac{c}{a}, 7.9 \frac{c}{a}, 11.0 \frac{c}{a}$, etc. Further, as $z \to \infty$, $\frac{d}{dz} J(z)$ tends to $\left(\frac{2}{\pi z}\right)^{1/2} \cos\left(z - \frac{\pi}{4}\right)$, so as $n \to \infty$, $z_n \to (n - \frac{1}{4})\pi$. Hence the difference in value of the nth resonant frequencies of the two basins approaches the constant $\frac{\pi c}{4a}$ as $n \to \infty$.

Consider now the response curves in the presence of rotation, i.e. $f \neq 0$. Clearly the nature of (4.4.4) is dependent on the relative values of ω and f. Since $k \equiv k_1 = \left(\left(\frac{\omega}{f}\right)^2 - 1\right)^{1/2}/R$ with $\alpha = 0$, where R is Rossby's radius of deformation, then with $\omega < f$ the Bessel functions in (4.4.4) have imaginary argument and are thus modified Bessel functions, I_1, of the first kind with real argument; but with $\omega > f$ the arguments are real and so the Bessel functions in (4.4.4) are ordinary Bessel functions, J_1, of the first kind with real argument.

Now resonance will occur at frequencies, ω, coinciding with the natural modes of azimuthal wave number 1 in the absence of friction. From (4.4.4) we have that with $\omega < f$ this occurs when

$$(ak_1 I_1')^2 = (\frac{f}{\omega} I_1)^2$$

where $I_1 \equiv I_1(k_1 a)$, $I_1' \equiv \left(\frac{d}{dz} I_1(z)\right)_{z=k_1 a}$. But since $I_1 > 0$, $I_1' > 0$ for all ω, then in fact there is the <u>possibility</u> of resonance only when

$$ak_1 I_1' = \frac{f}{\omega} I_1. \qquad (4.4.6a)$$

When $\omega > f$, resonance <u>will</u> occur at the 'frequency pairs' given by

$$(ak_1 J_1') = \pm \left(\frac{f}{\omega} J_1\right)$$

where $J_1 \equiv J_1(k_1 a)$, $J_1' \equiv \left(\frac{d}{dz} J_1(z)\right)_{z=k_1 a}$, i.e. each resonance peak in the zero rotation case (at frequency given by $J_1' = 0$) splits into a pair of resonant frequencies upon the introduction of rotation, at least for $\omega > f$.

Lamb (1932), §210 shows that (4.4.6a), (4.4.6b) properly describe the frequencies of the natural modes of the roating basin. Those natural modes with frequency less than the inertial frequency, f, are termed

Kelvin modes following the notation of Defant (1961), Csanady (1967); modes with frequency greater than the inertial are termed Poincare modes.

In his treatment of the natural modes, Lamb shows that there will always be at most 1 Kelvin mode for each azimuthal wave number m. Further, the condition for there to be one Kelvin mode for each m is that

$$\frac{a^2}{R^2} > m(m + 1) \ .$$

Thus there will always be at most one resonant frequency for (4.4.4) with $\omega < f$ and there will be exactly one if

$$\frac{a}{R} > \sqrt{2} \ . \tag{4.4.7}$$

No such restrictions apply to the Poincare modes of which there are an infinite number for each m.

For the Lake Albert model, R = 52.1 km, a = 7.5 km so that, from (4.4.7), there are no resonant frequencies below the inertial frequency, as is clear from Fig. 4.4a. Only the first pair of resonant frequencies with $\omega > f$ are discernibly different; higher frequency pairs are negligibly different.

Note that (4.4.3) is obtainable from (4.4.5) in the limit $\omega \to 0$. Further, the quasi-static equilibrium response is obtainable from (4.4.4), with $\alpha = 0$, by allowing $\omega \to 0$, giving

$$\tilde{Z}(r,\theta) = \frac{K\tau_0 a I_1\left(\frac{r}{R}\right)\cos\theta}{c^2 I_1\left(\frac{a}{R}\right)} \tag{4.4.8}$$

which may be verified as the solution to the boundary value problem

(4.2.11) for the case of a circular lake.

The quasi-static transport components $\tilde{P}(r,\theta)$, $\tilde{Q}(r,\theta)$ are thus (from (4.2.12)) obtainable from the stream function

$$\psi(r,\theta) = \frac{K\tau_O}{f} \left[a \frac{I_1\left(\frac{r}{R}\right)}{I_1\left(\frac{a}{R}\right)} - r \right] \cos\theta . \qquad (4.4.9)$$

Results (4.4.8), (4.4.9) have been previously obtained by Csanady (1968b).

A plot of the streamlines for the Lake Albert model basin are shown in Fig. 4.6. Essentially the circulation consists of a slow Ekman drift to the left of the wind direction (looking downwind) away from the centre of the basin with concentrated coastal jets returning fluid to the right half of the basin both at the upwind and downwind ends. Unlike the rectangular basin circulation, the flow in the circular basin entails separate vortices with identical shape but oppositely directed flow in each.

The difference between the solutions for the rectangular and circular basins is so striking, that it is a matter of considerable speculation as to whether either type of flow could possibly be observed in a real lake, or whether they are not both simply analytical curiosities. Of course, in no lake is the damping parameter, α, ever zero; neither is a true equilibrium situation ever reached. But it is possible that for lakes in which damping influences are slight, flows of either type (or possibly both) might be induced by strong, almost steady winds.

For $R > a$, the arguments of the Bessel functions in (4.4.8) will be less than unity and the approximations $I_1(r/R) \sim \frac{1}{2} r/R$, $I_1(a/R) \sim \frac{1}{2} a/R$ may be applied. Thus $\tilde{Z} \sim \bar{Z}$ for $R > a$, i.e. the static equilibrium response and quasi-static equilibrium response are approximately equivalent when the

radius of deformation exceeds the radius of the basin. In Figs. 4.4, 4.5 the zero frequency gain is in fact 0.999 times the equivalent static equilibrium response.

Let us briefly comment on the differences between the response functions for the rotating and non-rotating basins, i.e. the differences between the solutions (4.4.4) and (4.4.5). Firstly, for the case $\alpha = 0$ ($k \equiv k_1$), it is clear from Figs. 4.4, 4.5 that for the response of the Lake Albert model at (a/2, 0), the only significant differences occur in the vicinity of the resonant frequencies. At frequencies less than 3 cpd (including the inertial frequency), the response is essentially an equilibrium response, so that the small value of the ratio a/R for the Lake Albert model ($\sim$ 0.15) largely determines the similarity between the curves here. At frequencies much greater than the inertial, it is clear that $k_1 \rightarrow k_0$ so equations (4.1.10), (4.1.12a) become equivalent as do boundary conditions (4.1.9c), (4.1.12b). Thus for sufficiently large ω the response curves for the rotating and non-rotating basins with zero α will be negligibly different, regardless of the value of the ratio a/R.

The effect of non-zero α is to reduce further the significance of the Coriolis force. That this should be so becomes clear by observing that for large values of α (greater than $10^{-4} \sec^{-1}$), $|f/\beta| \ll 1$. Thus again equations (4.1.10) and (4.1.12a) become equivalent as do the appropriate boundary conditions. Physically, the integrated vorticity induced by the earth's rotation is dissipated by damping forces (refer (4.2.9a)) and is negligible for sufficiently large α.

To make these points clearer let us examine the real time surface response of the basin to a wind stress of the form $\tau_{sx}(t) = \tau_o \cos(\omega t)$. The surface response at position (r_o, θ_o) is $\zeta(r_o, \theta_o, t) = \text{Re}\{ Z(r_o, \theta_o, \omega) e^{j\omega t} \}$ $\equiv \text{Re}\{Z\}\cos(\omega t) - \text{Im}\{Z\}\sin(\omega t)$. Now with $\alpha = 0$, and assuming $\omega > f$, we have

$$\text{Re}\{Z\} = \frac{K\tau_o a J_1(k_1 r_o)\{f^2 J_1 - \omega^2 a k_1 J_1'\}\cos\theta_o}{c^2\{(fJ_1)^2 - (ak_1\omega J_1')^2\}}$$

$$\text{Im}\{Z\} = \frac{K\tau_o a J_1(k_1 r_o)\omega f\{J_1 - aJ_1'\}\sin\theta_o}{c^2\{(fJ_1)^2 - (ak_1\omega J_1')^2\}}$$

where J_1, J_1' are as defined in (4.4.6b). (With $\omega < f$, J_1 and J_1' are replaced by I_1, I_1'). Thus after some manipulation we have

$$\zeta(r_o, \theta_o, t) = \frac{K\tau_o a J_1(k_1 r_o)}{2c^2}\left[\frac{(1-f/\omega)\cos(\theta_o - \omega t)}{(ak_1 J_1' - fJ_1/\omega)} + \frac{(1+f/\omega)\cos(\theta_o + \omega t)}{(ak_1 J_1' + fJ_1/\omega)}\right] \cdot$$

$$(4.4.10)$$

Csanady (1968a) obtained a similar result which, however, appears to be in error by a factor of $\frac{1}{2}$. Recognizing, finally, that

$$\frac{1 \mp f/\omega}{ak_1 J_1' \pm fJ_1/\omega} = \frac{1}{akJ_1'} \pm \frac{f(1 - J_1/ak_1 J_1')}{(\omega ak_1 J_1' \pm fJ_1)}$$

we have that

$$\zeta(r_o, \theta_o, t) = \frac{K\tau_o a J_1(k_1 r_o)}{2c^2}\left[\frac{-2\cos\theta_o\cos(\omega t)}{ak_1 J_1'}\right.$$

$$\left. -f(1 - J_1/ak_1 J_1')\left(\frac{\cos(\theta_o - \omega t)}{\omega ak_1 J_1' - fJ_1} - \frac{\cos(\theta_o + \omega t)}{\omega ak_1 J_1' + fJ_1}\right)\right] \cdot \qquad (4.4.11)$$

Thus, from (4.4.10), the surface response consists of 2 travelling waves of differing amplitudes travelling in opposite (i.e. $+\theta$, $-\theta$)

directions around the basin. With $f = 0$, the two waves are of identical amplitude, so the response becomes the standing wave.

$$\frac{K\tau_o J_1(kr_o)\cos\theta_o\cos(\omega t)}{c^2 k(J_o(ka) - J_1'(ka)/ka)}$$

with $k = \omega/c$. This zero rotation result is analogous to the result for the forced, 1-dimensional response in a rectangular basin; there, the surface response consists of two identical, but oppositely directed, progressive waves forming a standing wave.

One may alternatively, from (4.4.11), regard the response in the case $\alpha = 0$ as consisting of two travelling waves of differing amplitude superimposed on the standing wave

$$\frac{K\tau_o J_1(k_1 r_o)\cos\theta_o \cos(\omega t)}{c^2 k_1 J_1'}$$

In fact, for the Lake Albert model, the progressive waves make a quite negligible contribution to the forced surface response at all frequencies, except near resonant frequencies when α assumes small values.

The steady state mean velocities due to the same wind are easily calculable from (4.4.4). Rewriting (4.1.5a), (4.1.5b) in terms of polar coordinates, we have

$$Q_r = \frac{-c^2}{(f^2+\beta^2)} [\beta \frac{\partial z}{\partial r} + \frac{f}{r} \frac{\partial z}{\partial \theta} - \frac{K}{c^2} (\beta\tau_{or} + f\tau_{o\theta})] \qquad (4.4.12a)$$

$$Q_\theta = \frac{-c^2}{(f^2+\beta^2)} [-f \frac{\partial z}{\partial r} + \frac{\beta}{r} \frac{\partial z}{\partial \theta} - \frac{K}{c^2} (-f\tau_{or} + \beta\tau_{o\theta})] \qquad (4.4.12b)$$

where Q_r, Q_θ are the amplitudes of the r-, θ- components respectively of the transport vector. Further, the amplitudes of the components of mean velocities are simply $q_r = Q_r/H$, $q_\theta = Q_\theta/H$. Substitution of (4.4.1), (4.4.4) in (4.4.12) enables calculation of Q_r, Q_θ for the particular problem of this section. The steady state mean velocity components at time t due to the wind $\tau_{sx}(t) = \tau_o \cos(\omega t)$ are then simply $Re\{q_r\}\cos(\omega t)$ - $Im\{q_r\}\sin(\omega t)$ and $Re\{q_\theta\}\cos(\omega t)$ - $Im\{q_\theta\}\sin(\omega t)$. Again explicit expressions are obtainable when α = 0, but they have not been written here.

In Fig. 4.7 we show the mean velocity response to a wind stress of this form for the Lake Albert model in the four cases (i) α = 0 sec^{-1}, f = 0 sec^{-1}; (ii) α = 10^{-4}sec^{-1}, f = 0 sec^{-1}; (iii) α = 0 sec^{-1}, f = -8.5 x 10^{-5}sec^{-1}; (iv) α = 10^{-4} sec^{-1}, f = -8.5 x 10^{-5}sec^{-1}. The period T of the wind stress is 1 day; the amplitude, τ_o, of the wind stress is 0.1 N.m^{-2}; and the response is shown at times t = 0, T/8, T/4, 3T/8 of the wind stress cycle. Of most interest in these diagrams is the comparison of the velocity structures at time t = 0.

For the case (i), the velocities are everywhere zero since the surface response is at a maximum. For (ii), the velocity structure is largely unchanged, there being only very small velocities at t = 0. However, for the case (iii), the velocity pattern at t = 0 is clearly similar to the streamline patterns of (4.4.9), the velocity magnitudes being comparable to the magnitudes obtained in the cases (i), (iii). It is clear that at each instant of time, the lake response is almost an equilibrium response and thus, at time t = 0, when the wind stress is acting with maximum strength, the velocity patterns are similar to the equilibrium velocity patterns due

to a steady wind acting in that direction. Finally for the case (iv), we see that any influence of the Coriolis force on the velocity pattern has become of secondary importance.

From the analysis of this section, we may make some conclusions regarding the importance of the Coriolis force in the wind-induced motions of the Murray Mouth Lakes.

For Lake Albert, a value of α is calculable from r/2H where r = $0(5 \times 10^{-4} \text{m.sec}^{-1})$ and H = 2m; thus we take $\alpha = 1.25 \times 10^{-4} \text{m.sec}^{-1}$.

Consider, firstly, the surface response. At frequencies within the equilibrium regime, the small value of the ratio a/R determines that inclusion of the Coriolis parameter is inconsequential, regardless of the value of α. At frequencies outside the equilibrium regime, the ratio $|f/\beta|$ is very small due to a combination of large α and large ω, so that again the Coriolis force makes a negligible contribution to the forced surface response.

Considering the velocity response, the near-equilibrium velocity pattern induced at low frequencies is of no significance compared with non-geostrophic velocities, due to the dominance of the damping term. At frequencies away from the equilibrium regime, the smallness of the ratio $|f/\beta|$ again determines that there is negligible difference between the rotating and non-rotating cases.

Similar reasoning may also be applied to Lake Alexandrina, for which typical horizontal and vertical length scales are of a similar order of magnitude to those of Lake Albert. Remembering that both Coorong lagoons

obey the 'narrow lake' approximations, we conclude that the effects of the Coriolis force may be neglected in a consideration of wind effects on the lakes of the Murray Mouth.
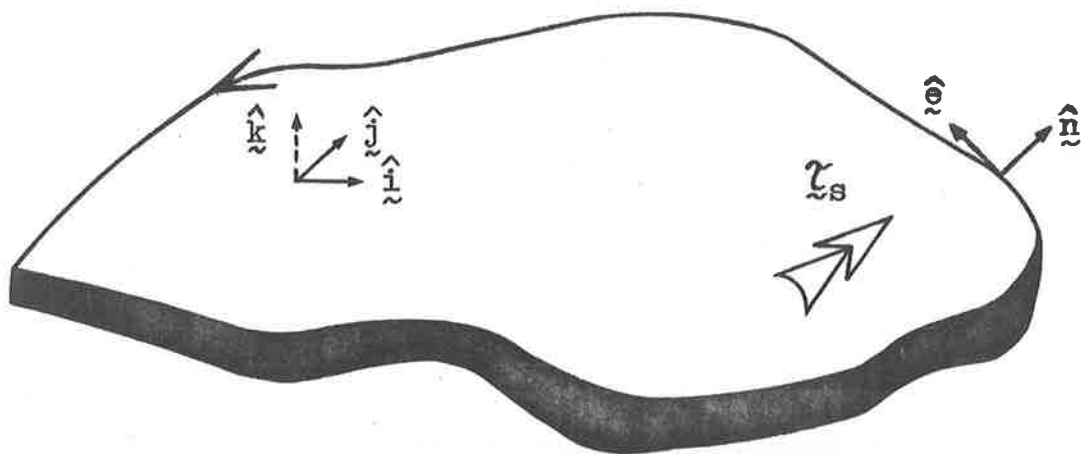
FIGURE 4.1 : THREE-DIMENSIONAL ASPECT OF CLOSED BASIN ACTED
ON BY WIND STRESS VECTOR $\underset{\sim}{\tau}_s$. ALL THE VECTORS
SHOWN, LIE IN THE PLANE OF THE UNDISTURBED LAKE
SURFACE, EXCEPT FOR THE UNIT VECTOR IN THE
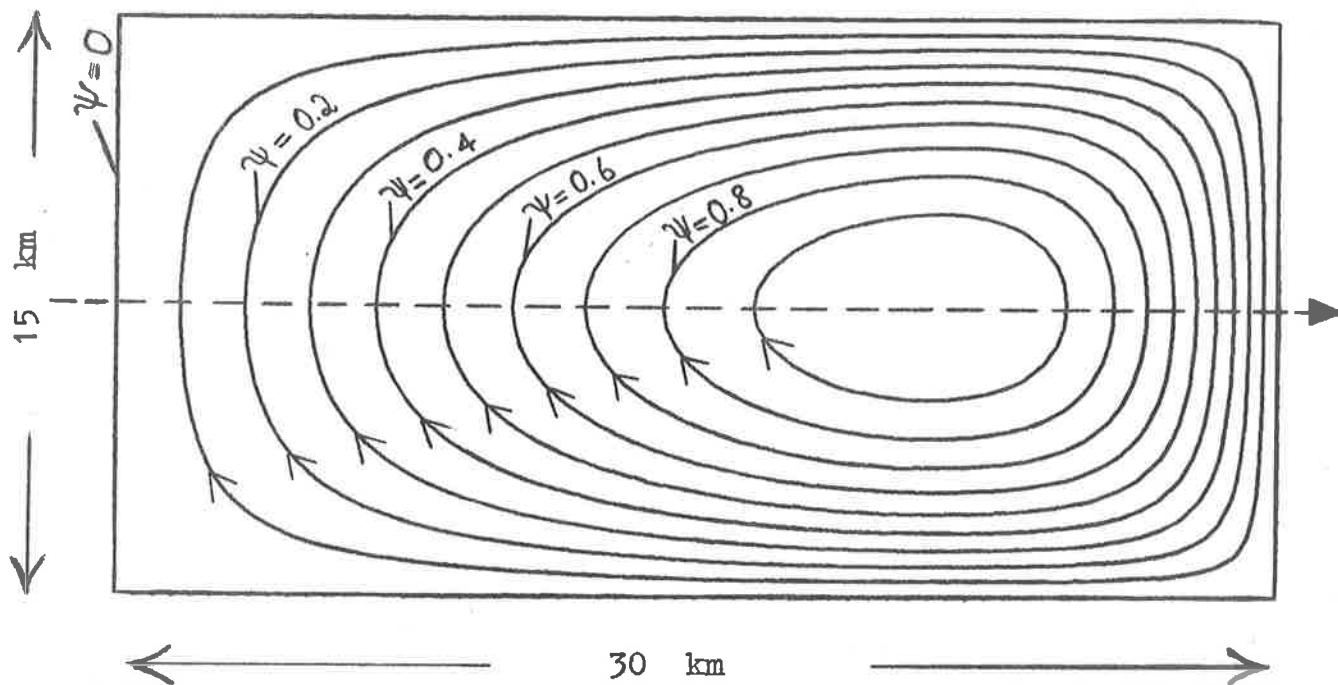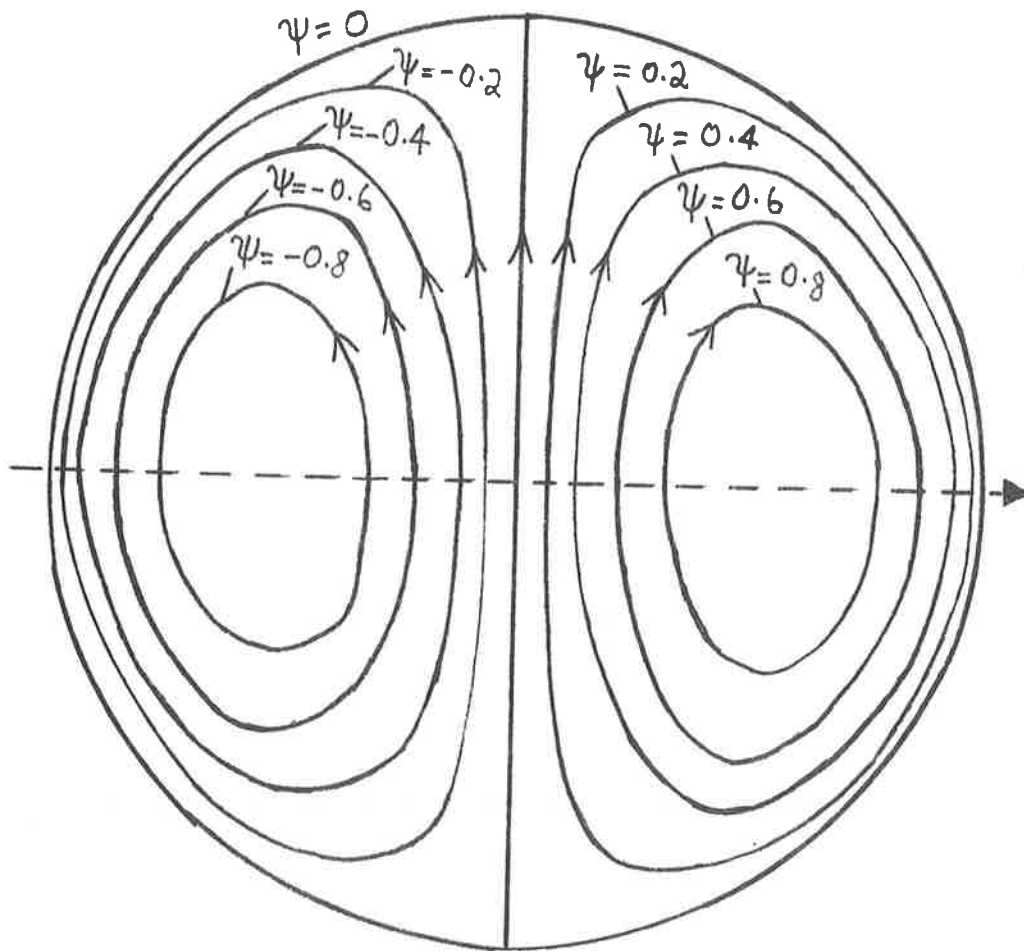POSITIVE Z-DIRECTION WHICH IS PERPENDICULAR TO
THIS PLANE .

FIGURE 4.2 : STREAMLINE PATTERN (NORMALIZED VALUES) FOR THE
QUASISTATIC EQUILIBRIUM CIRCULATION OF A MODEL
LAKE ALEXANDRINA . THE WIND DIRECTION (SOUTH-
WEST) IS INDICATED BY THE DASHED ARROW FROM
LEFT TO RIGHT. THE CIRCULATION ALWAYS HAS A
CLOCKWISE SENSE .
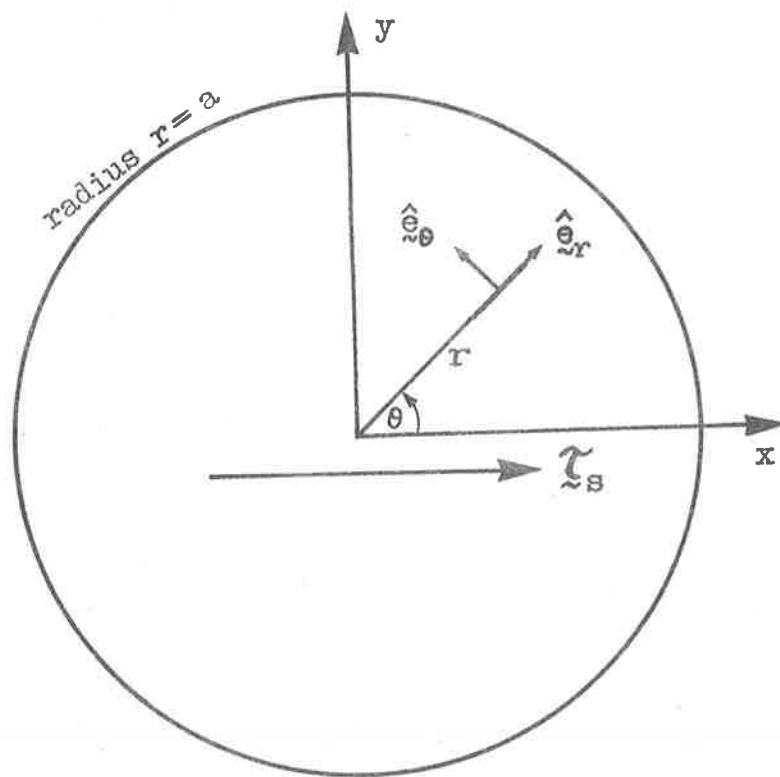
FIGURE 4.3 : PLAN OF A CIRCULAR, CONSTANT DEPTH, SINGLE-
LAYERED BASIN ACTED ON BY THE WIND STRESS
VECTOR $\underset{\sim}{\tau}_s$.
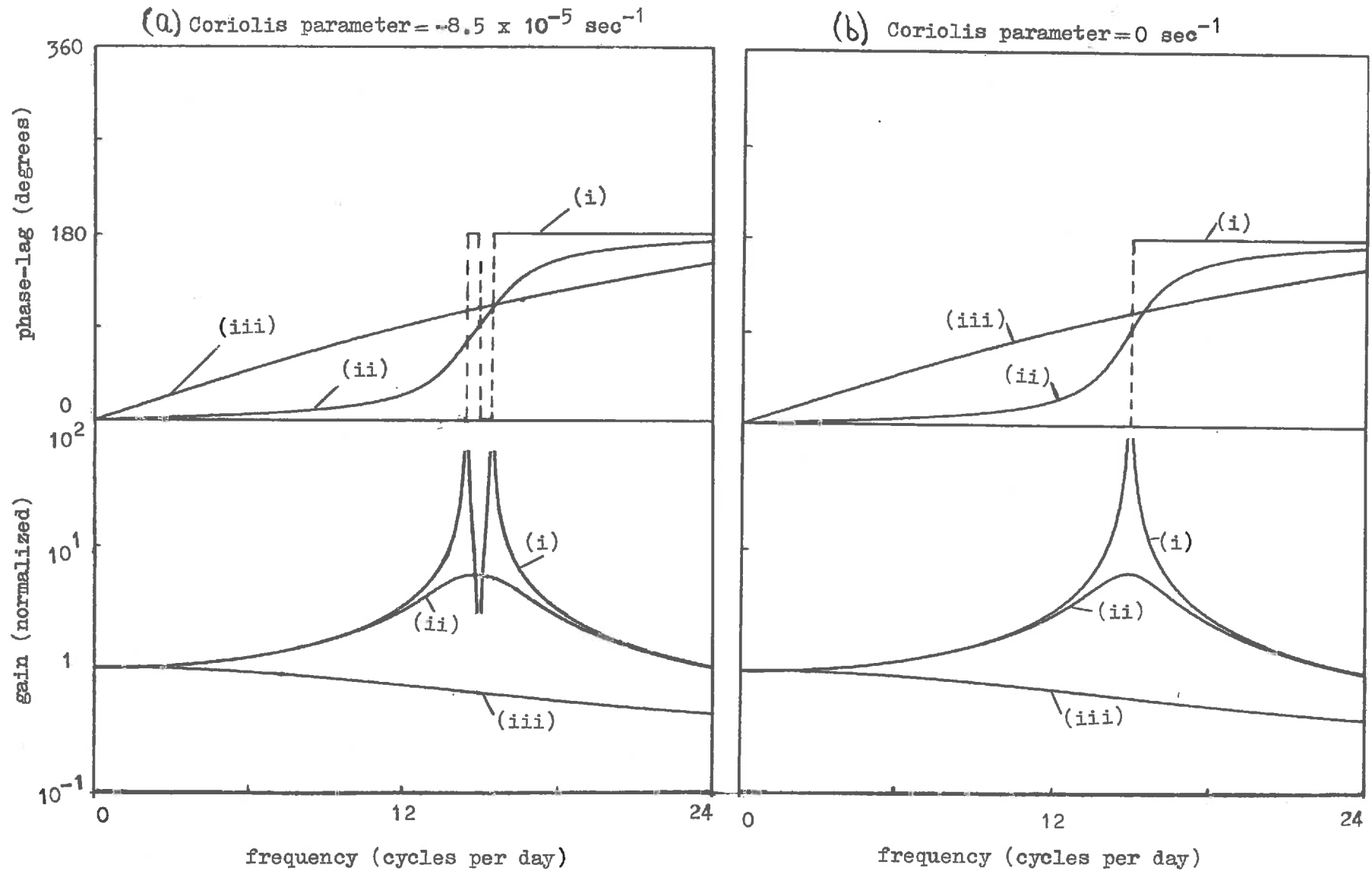
FIGURE 4.4 : RESPONSE FUNCTIONS FOR A CIRCULAR LAKE ALBERT AT STATION
(a/2,0) IN BOTH ROTATING AND NON-ROTATING CASES, FOR
(i)α=0 sec^{-1}, (ii)α=10^{-4} sec^{-1}, (iii)α=10^{-3} sec^{-1}.
GAINS ARE NORMALIZED WITH RESPECT TO THE EQUILIBRIUM
RESPONSE FOR THE NON-ROTATING CASE, VIZ. 0.201 M.
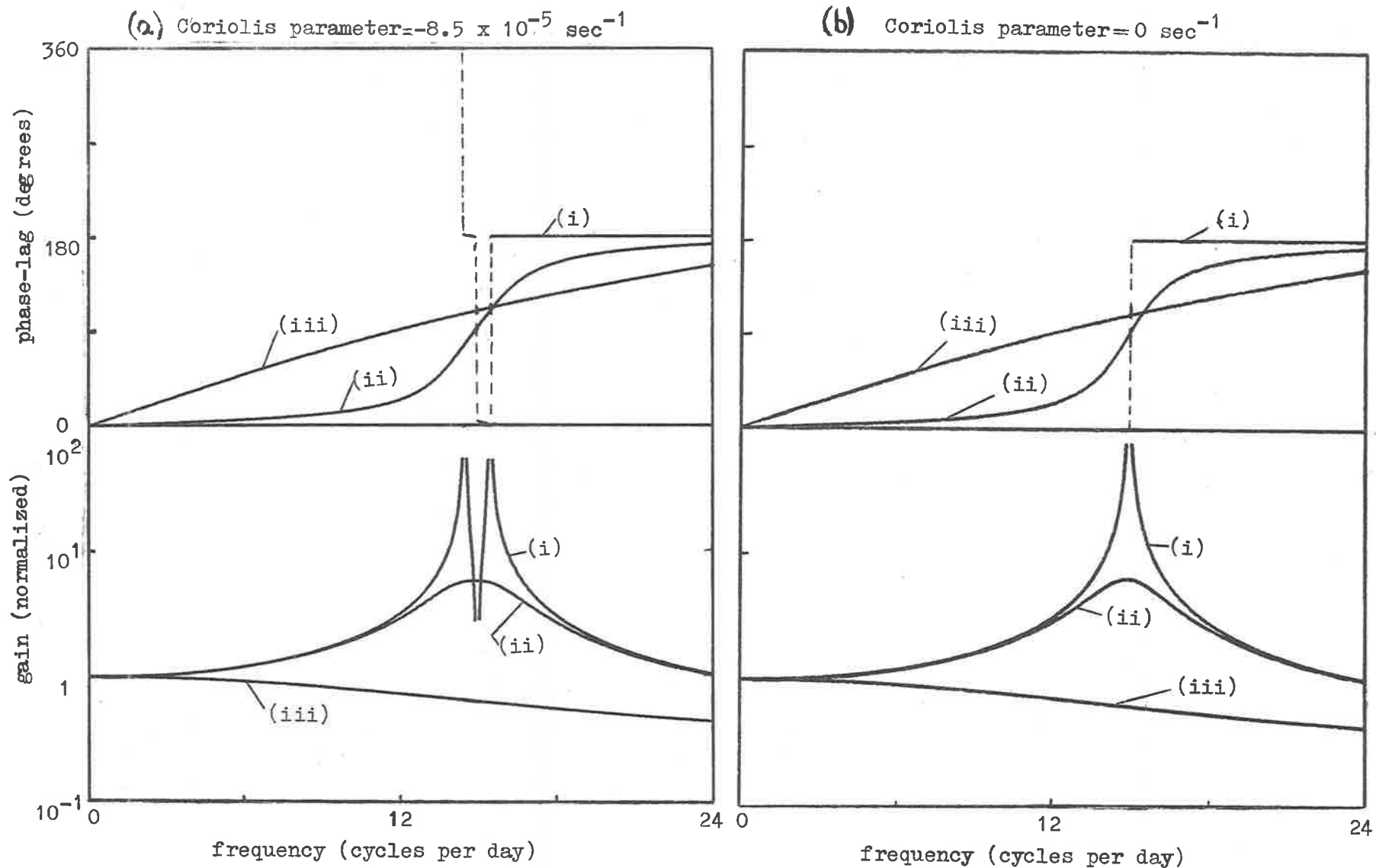
FIGURE 4.5 : RESPONSE FUNCTIONS FOR A CIRCULAR LAKE ALBERT AT
STATION $(a/2, \pi/4)$.   THE NORMALIZATION FACTOR FOR
GAINS IS AGAIN 0.201 M .   THE CURVES ARE ALMOST
IDENTICAL TO THOSE OF FIG. 4.4. NOTE THAT WHEN $\alpha =$
0 sec^{-1} IN THE ROTATING CASE, THE PHASE-LAG
ASSUMES VALUES VERY CLOSE TO 0° AND 180° .

FIGURE 4.6 : STREAMLINE PATTERN (NORMALIZED VALUES) FOR
THE QUASISTATIC EQUILIBRIUM CIRCULATION OF
A CIRCULAR MODEL LAKE ALBERT, RADIUS 7.5 km.
THE WIND DIRECTION IS INDICATED BY THE
DASHED ARROW FROM LEFT TO RIGHT .
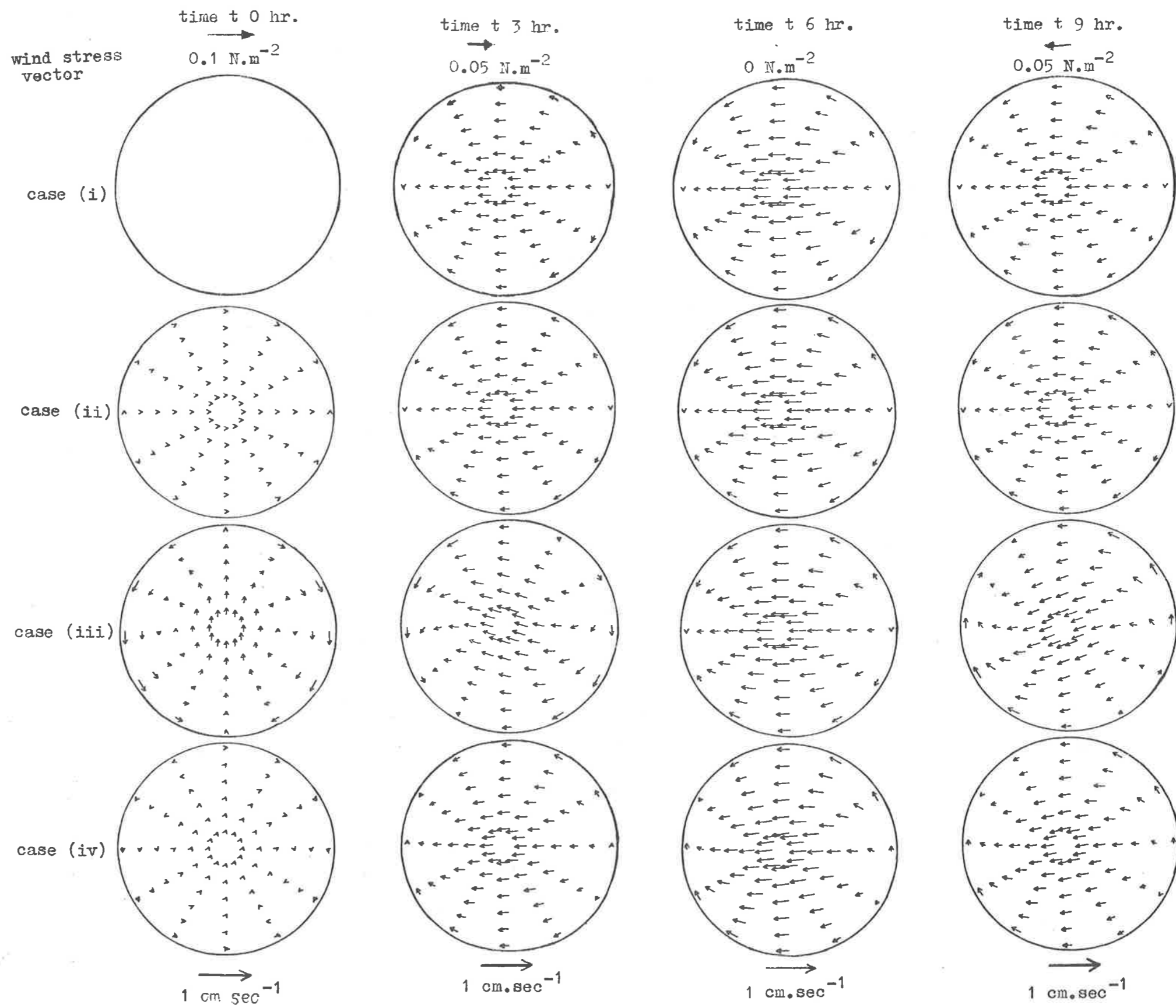
FIGURE 4.7 : MEAN VELOCITY RESPONSE OF A CIRCULAR LAKE ALBERT TO A WIND
STRESS OF THE FORM $\tau_0 \cos(2\pi t/T)$ WITH $\tau_0 = 0.1$ N.m^{-2}, T=1 day,
AND ALIGNMENT AS SHOWN, FOR CASES (i) $\alpha = 0$ sec^{-1}, f=0 sec^{-1};
(ii) $\alpha = 10^{-4}$ sec^{-1}, f=0 sec^{-1}; (iii) $\alpha = 0$ sec^{-1}, f=-8.5 x 10^{-5}
sec^{-1}; (iv) $\alpha = 10^{-4}$ sec^{-1}, f=-8.5 x 10^{-5} sec^{-1} .

CHAPTER 5

NUMERICAL SOLUTION OF THE WIND EFFECT EQUATIONS

5.1 Introduction

As a means of solving wind effect problems, analytical techniques are restricted to basins of simple form. Their usefulness lies in the fact that they allow certain physical features of the motions in arbitrary closed basins to be deduced. Thus, for example, Csanady (1967, 1968a, 1968b, 1972) and Liggett (1969) consider, respectively, circular and rectangular constant depth lakes in studying the motions of the Great Lakes.

Analytical techniques, however, will not give results of a sufficiently precise nature for predictive purposes unless the form of the particular lake closely approximates a basin of simple form. Thus rectangular or circular model basins are insufficient for a detailed description of wind effects on Lakes Albert and Alexandrina; the problem here is compounded by the flow exchange between the two lakes. It is clear that in this instance numerical techniques are required for satisfactory results.

The numerical treatment of wind effects on closed basins has received great impetus from the widely studied coastal storm surge problem, for which basically the same equations must be solved. The majority of models have been of the finite difference type, centered differences in space and forward in time. A typical example is the model developed by Heaps (1969) with which very successful simulation of North Sea surges was achieved.

Similar finite-difference, time-stepping models have been used by many

workers to study the motions of the North American Great Lakes. The behaviour of these lakes is almost ocean-like; indeed, storm surges similar to coastal surges in the open sea are common, and often result in severe property damage and even loss of life. Among the numerical studies undertaken have been those of Platzman (1958, 1965) - prediction of Lake Michigan storm surges; Platzman (1963) - wind tides on Lake Erie; Murty, Tadepalli and Rao (1970) - wind generated circulation in Lakes Erie, Huron, Michigan and Superior; Freeman, Hale and Danard (1971) - a variable density model of Lake Huron; Simons (1972) - three-dimensional numerical models; Smith (1973) - motions of Grand Traverse Bay, Lake Michigan.

Lakes with horizontal lengths scales of much smaller magnitude (and thus of lesser commercial importance) have, by comparison, received little in the way of numerical treatment, though similar sorts of methods ought to be applicable. Lindh and Bengtsson (1971) have developed both homogeneous and stratified numerical models and have applied them to Lake Valen, Sweden, which has horizontal dimensions of 1 km x 7 km. The work of Smith (1973) also falls into the 'small lake' category as it treats the motions within a small bay connected to Lake Michigan.

One difficulty with the closed bay problem is that of satisfactorily ensuring conservation of mass. Finite difference specification of conditions at closed boundaries is susceptible to considerable error, which results in an effective flow across the boundary and hence a net loss or gain of fluid from the model if all boundaries are closed. This difficulty is not encountered in the coastal surge problem where, due to the presence of open boundaries, mass is not conserved.

Finite element methods appear to offer the means of more accurately treating irregular boundaries and have already been used in a number of steady state Great Lakes models; refer Cheng and Tung (1970); Cheng (1972) and Gallagher, Liggett and Chan (1973).

In this chapter we develop systematic one- and two- dimensional implicit finite difference methods to calculate the steady state response of closed basins of arbitrary form to wind stresses of periodic time variation. Since the time variation of the steady state response is known, the models are not of the time stepping variety, i.e. only finite differences in space are required.

The one-dimensional method enables extremely rapid and accurate calculations to be made of the response for basins of elongated form such as the Coorong lagoons. The two-dimensional method, using a grid scheme similar to that of Heaps (1969), enables realistic computations to be made of wind effects on two-dimensional spatial models. Using these methods we construct several models of the Murray Mouth Lakes. In particular, a model combining both Lake Albert and Lake Alexandrina enables a realistic assessment to be made of the importance of Narrung channel flow in the wind-forced motions of the combined system. In all these models the effects of the Coriolis force have been ignored. For one-dimensional models, the 'narrow lake' approximations are applied; for two-dimensional models, the conclusions of Section 4.4 justify the neglect of the Coriolis force.

5.2 One-dimensional Numerical Solution

We present here a finite difference method to solve the transport form of the one-dimensional wind effect equations for a wind stress field varying periodically in time. As with the analytical treatment of Chapter 3, the method outlined in this section is strictly applicable only to elongated lakes (channels) such as the Coorong lagoons. Specifically, we seek to take into account variations in channel cross-sectional area in determining the response of the lake to time varying wind stresses.

Shown in Fig. 5.1 is the plan of the South Coorong lagoon. Any effects due to the curvature of the channel, which is slight, will be ignored. The channel axis (denoted the x-axis) points in the north-west direction, with the origin at the south-east end of the channel. The length, L, of the channel is 39.9km. The wind stress, $\tau_s(t)$, blows parallel to the channel axis and again is assumed homogeneous over the lake surface. We denote by $A(x)$ the area of channel cross-section, by $b(x)$ the (undisturbed surface) breadth of channel cross-section and by $h(x)$ the mean depth of channel cross-section, where

$$A = hb .$$

(5.2.1)

Now (3.1.3a), (3.1.3b) may be written as

$$\frac{\partial W}{\partial t} + \frac{r}{h} W = -gA \frac{\partial \zeta}{\partial x} + Kb\tau_s$$

(5.2.2a)

$$\frac{\partial W}{\partial x} = -b \frac{\partial \zeta}{\partial t}$$

(5.2.2b)

subject to

$$W = 0 \text{ at } x = 0, L \qquad (5.2.2c)$$

where $W(x,t)$ is the total flow through a channel cross-section and is given in terms of the transport $U(x,t)$ by

$$W = bU . \qquad (5.2.3)$$

Further, $\zeta(x,t)$ represents the mean surface displacement across a channel cross-section.

In deriving (5.2.2a), (5.2.2b) we assume that $h(x)$ in (3.1.3a) refers to the mean depth of cross-section; further, a term $Q \frac{1}{b} \frac{db}{dx}$ has been omitted from (5.2.2b) on the grounds that $\frac{db}{dx}$ is small. Equations (5.2.2a), (5.2.2b) are the hydrodynamical channel equations with a linear damping term and a wind stress forcing term.

Now assuming that $\tau_s(t) = \tau_o e^{j\omega t}$, with τ_o constant, we look for steady state solutions to (5.2.2), like

$$\zeta(x,t) = Z(x,\omega) e^{j\omega t} \qquad (5.2.4a)$$

$$W(x,t) = \xi(x,\omega) e^{j\omega t} \qquad (5.2.4b)$$

so that (5.2.2) becomes

$$\beta\xi = -gA \frac{\partial Z}{\partial x} + Kb\tau_o \qquad (5.2.5a)$$

$$\frac{\partial \xi}{\partial x} = -j\omega b Z \qquad (5.2.5b)$$

$$\xi = 0 \text{ at } x = 0, L \qquad (5.2.5c)$$

where $\beta(x,\omega) = (j\omega + r/h)$.

Platzman and Rao (1964) and Noye (1973) used a similar finite differ-
ence method to solve the system (5.2.5) without the damping term, for the
case of free and forced oscillations respectively. This method is here
extended to include frictional forces.

Fig. 5.2 shows the type of grid scheme used, here applied to the
South Coorong basin. Also shown is the variation of cross-sectional mean
depth and area along the channel as calculated from summer contours for
the South Coorong presented by Noye (1974). The average depth is 1.01m
while average breadth is 2.82 km. Along the lake axis is positioned a
one-dimensional array with an odd number, NP, of equispaced grid points,
the first and last points corresponding to the ends of the lake; the
distance between adjacent stream points is the grid length, d. For the
South Coorong model, NP = 109 and d = 370m. At the odd-numbered points
(1,3, ... , NP), only $\xi(x,\omega)$ is evaluated; these are known as 'stream
points" and denoted "x". At the even-numbered points (2,4, ... , (NP-1)),
known as 'elevation points' and denoted '0', only $Z(x,\omega)$ is evaluated.

We use subscript notation to denote the value of a particular quan-
tity at a given array point; e.g. h_i denotes cross-sectional mean depth at
array point i. Further, we approximate spatial derivatives by centred
finite differences; thus

$$\left(\frac{\partial \xi}{\partial x}\right)_{i+1} \sim \frac{\xi_{i+2}-\xi_i}{2d} \qquad (5.2.6a)$$

$$\left(\frac{\partial Z}{\partial x}\right)_{i+2} \sim \frac{Z_{i+3}-Z_{i+1}}{2d} \quad . \qquad (5.2.6b)$$

Note that elevation derivatives are evaluated at stream points, transport derivatives at elevation points. So evaluating (5.2.5b) at elevation point $(i + 1)$ and (5.2.5a) at stream point $(i + 2)$ gives

$$\frac{\xi_{i+2} - \xi_i}{2d} = -j\omega b_{i+1} \, z_{i+1}$$

$$\beta_{i+2} \, \xi_{i+2} = -gA_{i+2} \left(\frac{z_{i+3} - z_{i+1}}{2d} \right) + Kb_{i+2}\tau_o$$

and upon rearranging

$$\xi_{i+2} = \xi_i - 2dj\omega b_{i+1} \, z_{i+1} \qquad (5.2.7a)$$

$$z_{i+3} = z_{i+1} + (\beta_{i+2}\xi_{i+2} - K\tau_o b_{i+2})/\gamma_{i+2} \qquad (5.2.7b)$$

where $\gamma_i = -gA_i/2d$; (5.2.5c) becomes simply

$$\xi_1 = \xi_{NP} = 0 \, . \qquad (5.2.7c)$$

The system of difference equations (5.2.7) forms the basis of an iteration scheme to solve the system of differential equations (5.2.5). Specifically, knowing that $\xi_1 = 0$ and assuming a value for z_2 we may calculate ξ_3 from (5.2.7a), z_4 from (5.2.7b) and so on, right through the grid. (Note that we only require values for h_i at stream points $i = 1,3, \ldots , NP$). Then ξ_{NP} will be zero only if z_2 has been correctly chosen. Whatever its value, ξ_{NP} is a linear function of the value chosen for z_2, i.e.

$$\xi_{NP} = C_1 + C_2 z_2$$

where the constants C_1, C_2 are independent of z_2. Clearly the correct choice for z_2 is

$$Z_2 = -C_1/C_2.$$

C_1 and C_2 (in general complex-valued) may be determined by calculating ξ_{NP} for any two different choices of Z_2. For example, choosing $Z_2 = 0$ gives $\xi^0_{NP} = C_1$; choosing $Z_2 = 1$ gives $\xi^1_{NP} = C_1 + C_2$. Thus

$$Z_2 = \xi^0_{NP}/(\xi^0_{NP} - \xi^1_{NP}) \ .$$

Using the correct value for Z_2, a final run may be made through the array to determine values for ξ, Z at alternate grid points.

A stability criterion for this scheme has been determined using the method of stability analysis of Noye (1973). The basis of this analysis is to introduce a small roundoff error at one step of the computation of ξ (or Z) and to examine the manner in which the error propagates through the array as values of ξ (or Z) are calculated at further steps.

Thus, suppose an error $\Delta\xi_i$ is introduced in the computation of ξ_i, so that we obtain instead

$$\xi^*_i = \xi_i + \Delta\xi_i$$

and further

$$Z^*_{i+1} = Z_{i+1} - \beta_i \Delta\xi_i/\gamma_i$$

$$\xi^*_{i+2} = \xi_{i+2} + (1 + 2dj\omega b_{i+1}\beta_i/\gamma_i)\Delta\xi_i \ .$$

The error, $\Delta\xi_i$, introduced at stream point i, will clearly propagate with diminished magnitude through the remainder of the array if

$$\left| 1 + 2dj\omega b_{i+1}\beta_i/\gamma_i \right| < 1$$

which upon rearrangement gives

$$d < \left[\frac{gh_i b_i}{2b_{i+1}(\omega^2+r^2/h_i^2)} \right]^{1/2} . \tag{5.2.9a}$$

The introduction of an error ΔZ_{i+1} at elevation point $i + 1$ leads to a similar condition for the diminished propagation of the error. It is clear then that by choosing grid length such that

$$d < d_o = \left[\frac{g\delta_o h_o}{2(\omega^2+r^2/h_o^2)} \right]^{1/2} \tag{5.2.9b}$$

where h_o = min. $\{h_i, i = 2,4, \ldots (NP-1)\}$, δ_o = min. $\{(b_i/b_{i+1}), i = 1,2, \ldots NP\}$, the stability of the iterative scheme will be guaranteed. Condition (5.2.9b) is a sufficient stability condition, but is not a necessary condition. This is because the scheme may (according to (5.2.9a)) be unstable at one step but, because of changing breadths and depths, be stable at the next. In fact, it may be more accurate to suggest that a necessary stability condition for the scheme is

$$d < d_o = \left[\frac{gH}{2(\omega^2+r^2/H^2)} \right]^{1/2} \tag{5.2.9c}$$

where H is the average depth of the basin, viz. 1.01m for the South Coorong.

To demonstrate this fact, consider the South Coorong model of Fig. 5.2 for which $d = 370$m. The value for h_o is 0.06m at grid point 1 (the very shallow extremes of the South Coorong) while $\delta_o = 0.5$ (between grid points 1 and 2 the breadth increases from 300m to 600m). Fig. 5.3 shows a plot of d_o as calculated from (5.2.9b) and (5.2.9c) for various values of r and a frequency range 0 - 24 cpd. It is clear that (5.2.9b) predicts stability over a limited range of frequencies for $r = 0$ m.sec^{-1} while for

$r = 10^{-4} \text{m.sec}^{-1}$, $10^{-2} \text{m.sec}^{-1}$ it is unstable at all frequencies. However, it is certain that in this case (5.2.9b) is unreasonable as h_o is not of the same order of magnitude as H, i.e. errors generated at the first two steps are quickly damped out in regions where the scheme is stable. However, (5.2.9c) predicts stability throughout the range of frequencies and for all values of $\dot{r}$ shown in Fig. 5.3. It is probable that a necessary stability condition is more closely approximated by (5.2.9c) than by (5.2.9b). Several test runs revealed indeed that the scheme becomes grossly unstable only for exceptionally high values of r, say $r = 0(10^{-1} \text{m.sec}^{-1})$.

The numerical scheme was used to examine the surface response functions of three types of test basins, viz. (i) rectangular plan (sides L,B) and constant depth, H; (ii) rectangular plan and a depth variation symmetric about the centre of the basin, of the form

$$h(x) = H + \frac{H}{2} \cos\{2\pi(x-L/2)/L\};$$

(iii) rectangular plan and a depth variation asymmetric about the centre of the basin, of the form

$$h(x) = H - \frac{H}{L}(x-L/2) .$$

For each, $H = 1.01\text{m}$, $L = 39.9\text{km}$ and $B = 2.82\text{km}$, the average dimensions of the South Coorong, while again $NP = 109$ and $d = 370\text{m}$. (Of course the solution for (i) is that obtained in Section 3.2; a comparison of responses obtained analytically and numerically revealed negligible differences over a wide range of frequencies and for values of r less than $10^{-1} \text{m.sec}^{-1}$). For each basin, the average depth is H.

Shown in Fig. 5.4 are the surface response functions for all three test basins at the Salt Creek Point station (grid point 20) with $r = 0 \text{ m.sec}^{-1}$. We know that for the constant depth basin, resonance peaks coincide with the frequencies of the odd free modes.. For the South Coorong constant

depth basin, the resonant frequencies are odd multiplies of 3.41 cpd. Further, it is clear from Fig. 5.4 that resonance occurs at approximately the same frequencies for the test basin with depth symmetric about $x = L/2$. However, for the test basin with depth asymmetric about $x = L/2$, resonance occurs for frequencies corresponding approximately to all the multiples of the free modes of the constant depth basin.

Finally, we examine the response of the South Coorong model of Fig. 5.2, i.e. using actual depths and breadths. Since the depth contour is asymmetric about the centre of the basin, we might naively expect that resonance would occur at frequencies corresponding approximately to multiples of 3.41 cpd. (Of course, the variation of breadth also must play a part here). This is, indeed, seen to be the case from Fig. 5.5 which shows the surface response at the Salt Creek Point station for $r = 0$ m.sec^{-1}, 10^{-4} m.sec^{-1} and 10^{-3} m.sec^{-1}. The computations involved here may be performed extremely rapidly; the Central Processor time required to calculate the response at a single frequency is estimated at 0.15 seconds using the CDC 6400 machine of the University of Adelaide.

In Fig. 5.6 is shown the steady state time response of the South Coorong surface at times $t = 0$, $T/8$, $T/4$, $3T/8$ of the wind stress cycle of the form $\tau_s = \tau_o \sin(2\pi t/T)$ with $\tau_o = 0.1$ N.m^{-2}, for $T = 1$ day, 0.2 day and 0.1 day. A dominant feature of the response is the excessively large surface displacement occuring at the shallow extremes of the South Coorong, particularly at the south-east end where depths are of O(10 cm). Clearly in these regions the basin response is highly non-linear since the ratio ζ^*/h^* (Section 2.1) is greater than unity. The linear theory predicts, in fact, a daily cycle of flooding of low-lying areas at the south-east end

of the basin followed by an exposure of a considerable portion of the bed of the basin at that end. Such an effect has been documented by Noye (1970).

We note that displacements are generally greater in the south-east half of the basin than in the north-west half. This is a result of mass continuity which requires that the surface displacement integrated over the whole surface be zero, i.e. approximately that

$$\sum_{i=2(2)}^{(NP-1)} \{\zeta_i b_i\} = 0 . \tag{5.4.1}$$

Tests carried out on the displacements of Fig. 5.6 showed that negligible errors of this type were involved. Since breadths are generally smaller in the south-east half, then the average displacement across each section is generally bigger in order that the relation (5.4.1) be satisfied.

Finally, we present results for the step response of the South Coorong surface as calculable from (2.2.8b), i.e.

$$a(t) = \frac{2}{\pi} \int_0^\infty \frac{R(\omega)}{\omega} \sin(\omega t) d\omega$$

where $R(\omega)$ is the real part of the surface response function. An approximate method of calculating the above integral is to truncate the range of integration and apply a suitable quadrature.

Such a method was found to work well for systems with a reasonable degree of damping. Using Simpson's quadrature, tests were carried out on rectangular constant depth basins and the results compared with the known analytical results of Chapter 3 for the North Coorong basin at Seven Mile Point, where the equilibrium step response is 1.063 metres. Numerical integration

over the range 0 - 24 cpd with an interval length for the quadrature of 0.25 cpd gave values to within 1cm at all times for $r = 10^{-4}$ m.sec^{-1}, and to within 2mm for $r = 10^{-3}$ m.sec^{-1}. Using a range of 0 - 48 cpd with the same interval length gave values to withi.. 5mm for $r = 10^{-4}$ m.sec^{-1}, and to within 1mm for $r = 10^{-3}$ m.sec^{-1}.

In Fig. 5.7 is shown the step response of the South Coorong basin at the Salt Creek Point station and the Noye's Island station (grid point 92) up to 12 hours after the onset of the wind. We observe that with $r = 5.0$ x 10^{-4} m.sec^{-1} the response is almost exactly critically damped. In fact (3.2.18) with L = 39.9km and H = 1.01m gives

$$r > 5.0 \times 10^{-4} \text{ m.sec}^{-1}$$

for the fundamental seiche of the South Coorong to be damped out.

5.3 Two-Dimensional Numerical Solution

Here we generalize the method of the previous section to enable realistic computations to be made for the response of lakes of arbitrary shape and depth to periodic wind stresses.

We wish to solve by a finite difference technique, the system of equations (4.1.4) with Coriolis parameter, f, set to zero, i.e.

$$\beta P = -gh \frac{\partial Z}{\partial x} + K\tau_{ox} \tag{5.3.1a}$$

$$\beta Q = -gh \frac{\partial Z}{\partial y} + K\tau_{oy} \tag{5.3.1b}$$

$$\frac{\partial P}{\partial x} + \frac{\partial Q}{\partial y} = -j\omega Z \tag{5.3.1c}$$

subject to the boundary condition (4.1.9a). We shall assume that τ_{ox}, τ_{oy} are spatially constant, though the technique can simply incorporate wind stress inhomogeneities.

The two-dimensional grid scheme here is similar to that used in the models of Heaps (1969) to study storm surges in the North Sea. In Fig. 5.8a is shown a model of Lake Albert, considered closed at the Narrung channel entrance, constructed from the scheme.

Again $Z(x,y,\omega)$ is evaluated only at points marked "0", while $P(x,y,\omega)$, $Q(x,y,\omega)$ are evaluated only at points marked "X". A rectangular array of consecutive rows of elevation and stream points completely covers the lake in question. For the Lake Albert model the array size is 11 x 13, i.e. 11 rows and 13 columns of both elevation and stream points. The horizontal and vertical array axes (x- and y-axes respectively) of the Lake Albert model coincide with the west-east and south-north directions respectively. The array is bounded to the north and west by elevation points and to the south and east by stream points. The distance between consecutive columns is denoted Δx, while Δy denotes the distance between consecutive rows. Unlike the scheme of Heaps (1969), we shall assume that $\Delta x = \Delta y = d$. For the Lake Albert model of Fig. 5.8a, d = 630 metres.

It can be seen that the basic "building units" of the array are

```
    O        O                      X        X
         X                                O
    O        O                      X        X
```

i.e. a stream point surrounded by four elevation points, and an elevation
point surrounded by four stream points. For an m x n array, both eleva-
tion and stream points are numbered 1, 2, ..., mn starting from the first
row and proceeding from west to east along each row. A typical cluster
of points is thus numbered

$$X^{i-n-1} \quad X^{i-n}$$
$$O^{i} \qquad\quad O^{i+1}$$
$$X^{i-1} \quad X^{i}$$
$$O^{i+n} \qquad O^{i+n+1} \qquad .$$
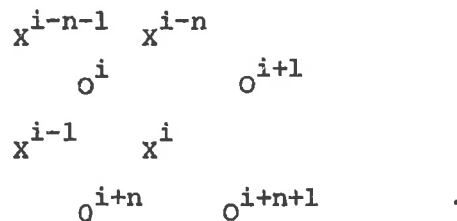
Further, each stream point and each elevation point is classified as
a particular <u>type</u> of point. This classification of points into groups
is simpler than the classification of Heaps (1969) since here all bound-
aries are closed. Specifically there are 14 groups of stream points and
3 groups of elevation points, listed in Table 5.1. In Fig. 5.8b, each
array point of the Lake Albert model of Fig. 5.8a has been designated by
its group number.

For all array points <u>interior</u> to the lake boundary (i.e. group 2
points, groups 16 and 17 points), spatial derivatives may be approximated
by centred differences. Thus, at the interior stream point i,

$$\left(\frac{\partial z}{\partial x}\right)_i \sim \frac{1}{4d} (z_{i+1} - z_i + z_{i+n+1} - z_{i+n})$$

TABLE 5.1

GROUPING OF ARRAY POINTS FOR THE TWO-DIMENSIONAL SCHEME

Assume horizontal and vertical array axes coincide with
west-east and south-north directions respectively.

STREAM POINTS
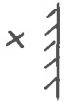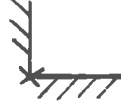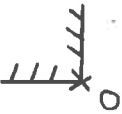
Group number	Type	
1	EXTERIOR POINT	
2	INTERIOR POINT	
3	NORTH BOUNDARY POINT	
4	SOUTH BOUNDARY POINT	
5	WEST BOUNDARY POINT	
6	EAST BOUNDARY POINT	
7	NORTH-WEST 90° CORNER POINT	
8	NORTH-WEST 270° CORNER POINT	
9	SOUTH-WEST 90° CORNER POINT	
10	SOUTH-WEST 270° CORNER POINT	
11	SOUTH-EAST 90° CORNER POINT	

TABLE 5.1 (cont.)

Group number	Type	
12	SOUTH-EAST 270° CORNER POINT	
13	NORTH-EAST 90° CORNER POINT	
14	NORTH-EAST 270° CORNER POINT	

ELEVATION POINTS

Group number	Type	
15	EXTERIOR POINT	
16	POINT IMMEDIATELY SOUTH OF NORTH BOUNDARY	
	or IMMEDIATELY EAST OF WEST BOUNDARY	
	or IMMEDIATELY SOUTH-EAST OF GROUP 8 POINT	
17	ALL OTHER INTERIOR POINTS	

$$\left(\frac{\partial Z}{\partial y}\right)_i \sim \frac{1}{4d} \; (Z_i - Z_{i+n} + Z_{i+1} - Z_{i+n+1})$$

while at the interior elevation point i,

$$\left(\frac{\partial P}{\partial x}\right)_i \sim \frac{1}{4d} \; (P_i - P_{i\;1} + P_{i-n} - P_{i-n-1})$$

$$\left(\frac{\partial Q}{\partial y}\right)_i \sim \frac{1}{4d} \; (Q_{i-n} - Q_i + Q_{i-n-1} - Q_{i-1}).$$

Using these approximations we transform (5.3.1) into a system of difference equations evaluated at interior array points. (Note that, as with the one-dimensional numerical method of the previous section, values for depth h are required only at stream points. Shown in Fig. 5.8c are depth values at each of the interior or boundary stream points of the Lake Albert model as inferred from the contour map Fig. A2 of Appendix A).

System (5.3.1) becomes

$$\beta_i P_i = \frac{-gh_i}{4d} \; (Z_{i+1} - Z_i + Z_{i+n+1} - Z_{i+n}) + K\tau_{ox} \qquad (5.3.2a)$$

$$\beta_i Q_i = \frac{-gh_i}{4d} \; (Z_i - Z_{i+n} + Z_{i+1} - Z_{i+n+1}) + K\tau_{oy} \qquad (5.3.2b)$$

evaluated at interior stream point i, and

$$\frac{1}{4d} \; (P_i - P_{i-1} + P_{i-n} - P_{i-n-1}) + \frac{1}{4d} \; (Q_{i-n} - Q_i + Q_{i-n-1} - Q_{i-1}) = j\omega Z_i \quad (5.3.2c)$$

evaluated at interior elevation point i. System (5.3.2) may be written in the alternative form

$$\beta_i S_i = - \gamma_i (Z_{i+1} - Z_{i+n}) + A \qquad (5.3.3a)$$

$$\beta_i D_i = - \gamma_i (Z_{i+n+1} - Z_i) + B \qquad\qquad (5.3.3b)$$

$$-4dj\omega Z_i = D_i - S_{i-1} + S_{i-n} - D_{i-n-1} \qquad\qquad (5.3.3c)$$

where $\gamma_i = -gh_i/2d$, $A = K(\tau_{ox} + \tau_{oy})$, $B = K(\tau_{ox} - \tau_{oy})$ and unknowns S_i, D_i are given in terms of P_i, Q_i by

$$S_i = P_i + Q_i \qquad\qquad (5.3.4a)$$

$$D_i = P_i - Q_i . \qquad\qquad (5.3.4b)$$

The degenerate forms of the difference equations satisfied by each type of boundary stream point are described in detail in Appendix D. Use of a condition at 270° corner points equivalent to that of Heaps (1969) was found to produce erroneous results. The errors were clearly revealed in non-conservation of mass, i.e. any inaccuracy in the specification of the boundary condition at 270° corner points leads to a flow across the lake boundary at that point and hence a net loss or gain of fluid from the basin. Such losses, in a closed basin model, are intolerable. Similar effects were noticed by Smith (1973), and his method of introducing the unnatural boundary condition of $(P_i, Q_i) = (0,0)$ at 270° corner points has been adopted here. Such a condition is unnatural in the sense that our model does not incorporate a lateral boundary layer, i.e. the effects of horizontal turbulent diffusion have been neglected. It has the advantage of simplicity, however, and was found to reduce non-conservation of mass to acceptable proportions in all the models described here.

The difference equations (5.3.3) form the basis of an iterative scheme to determine the appropriate value for Z, S and D at each stream or

elevation point within or on the lake boundary. Rewriting (5.3.3) as

$$S_i = \frac{1}{\beta_i} \{- \gamma_i (Z_{i+1} - Z_{i+n}) + A\} \qquad (5.3.5a)$$

$$D_i = D_{i-n-1} + S_{i-1} - S_{i-n} - 4dj\omega Z_i \qquad (5.3.5b)$$

$$Z_{i+n+1} = Z_i - \frac{1}{\gamma_i} (\beta_i D_i - B_i) , \qquad (5.3.5c)$$

then knowing values for S and D at stream points i-n-1, i-n and i-1, and also values for Z at elevation points i, i+1 and i+n, we may calculate values for S_i (from (5.3.5a)), D_i (from (5.3.5b)), and Z_{i+n+1} (from (5.3.5c)).

In order to initiate such a scheme and to enable it to proceed through the array, we assume a value for Z at each group 16 point, the assumed values being known as 'starting values'. Values for S and D for all points belonging to groups 3, 5, 7, 8, 9 and 13 are computed using the difference equations of Appendix D. Next, proceeding west to east along each row and treating each row successively, we calculate values for S and D at each group 2 point and a value for Z at each group 17 point. The order of calculations is indicated by the direction of arrows in Fig. 5.9. Along each row, stream points belonging to any one of groups 4, 6, 10, 11, 12 and 14 may be encountered; values for S and D at such points are computed according to the equations of Appendix D.

Now values for S and D at group 3, 5, 7, 8, 9 and 13 points have been calculated so that the relevant boundary condition at each point is satisfied, regardless of the starting values. This is not the case for group 4, 6, 10, 11, 12 and 14 points - the relevant boundary conditions

will only be satisfied at each of these if the correct starting values have been chosen. At each such point one may define a so-called 'end value' which, if zero, ensures that the relevant boundary condition is satisfied, as shown in Appendix D. For example, for group 4 points the boundary condition is that

$$S_i = D_i$$

so we define the end value as being S-D.

For a consistent system the number of starting values and the number of end values are the same, say p. We may thus form vectors $\underset{\sim}{s}$ and $\underset{\sim}{e}$, both of dimension (p x 1), consisting of starting values and end values respectively. The vector elements are numbered according to the position in the array of the point to which they refer. For the Lake Albert model, p = 24. In Fig. 5.8a the relevant vector element number (1-24) has been assigned to each array point at which a starting value or end value is defined. For a general m x n array in which the lake boundaries coincide with the first and last rows and first and last columns, i.e. a rectangular lake with sides 2(m-1)d and 2(n-1)d, we may easily show that p = (m+n-3).

An additional complication, as with the one-dimensional numerical method, results from that fact that Z, S and D are, in general, complex valued. Thus at each group 16 point we define two starting values, corresponding to the real and imaginary parts of Z; while at each point belonging to one of groups 4, 6, 10, 11, 12 or 14, two end values will be arrived at. Let us define vectors $\underset{\sim}{t}$ and $\underset{\sim}{f}$, both of dimension (2p x 1), such that

$$t_{2i-1} = \text{Re } \{s_i\} \ , \ t_{2i} = \text{Im}\{s_i\}$$

$$f_{2i-1} = \text{Re } \{e_i\} \ , \ f_{2i} = \text{Im}\{e_i\}.$$

Each end value is linearly related to the starting values. We may thus write

$$\underset{\sim}{f} = \Phi \underset{\sim}{t} + \underset{\sim}{k} \tag{5.3.6}$$

where Φ is a matrix (2p x 2p), with (real) elements, which determines the effect of the starting values on the end values, and $\underset{\sim}{k}$ is a vector (2p x 1) which describes the effect of the forcing functions τ_{ox}, τ_{oy} on the end values. The correct starting values are thus determined by solving (5.3.6) for $\underset{\sim}{t}$, with $\underset{\sim}{f} = \underset{\sim}{0}$, i.e.

$$\underset{\sim}{t} = -(\Phi)^{-1} \underset{\sim}{k} \ . \tag{5.3.7}$$

The elements of Φ and $\underset{\sim}{k}$ must first be determined. Clearly each column of Φ may be generated by setting $\underset{\sim}{k} = \underset{\sim}{0}$ and choosing a starting vector of the Kronecker delta form, so that

$$f_i = \Phi_{ik} \delta_{kj} = \Phi_{ij} \ .$$

Further, $\underset{\sim}{k}$ is equivalent to the end vector obtained by setting $\underset{\sim}{t} = \underset{\sim}{0}$ and using the particular forcing functions that act upon the given lake.

Having determined the correct starting values, a final run of the iteration scheme is performed to determine the correct values of Z, S and D at each elevation or stream point over the lake. The simplified flow diagram of Fig. 5.10 summarizes the total iterative procedure.

The matrix Φ is generally non-sparse. Its size (and thus the array

size used to specify a given lake) is therefore limited by the storage

capacity of the machine in use, as there are no simple means of inverting

large, non-sparse matrices. For the relatively coarse Lake Albert model,

Φ has dimensions (48 x 48) so that the solution of (5.3.6) with $\underset{\sim}{f} = \underset{\sim}{0}$

presents no great difficulties.

A stability criterion for the scheme may be determined in a manner

similar to the one-dimensional stability procedure. The complicated

nature of the two-dimensional scheme, however, makes the analysis far

more difficult, and it is presented only briefly here.

Suppose that a small roundoff error, ΔZ_i, is introduced to the value

for Z_i. Neither Z_{i+1} nor Z_{i+n} is affected by the error in Z_i since

neither is given in terms of Z_i by a difference equation of the form

(5.3.5c). Similarly, S_i is unaffected. However, D_i is affected; the

error involved in a calculation of D_i is $-(4dj\omega + \nu_{i-1} + \nu_{i-n})\Delta Z_i$, where

$\nu_i = \gamma_i/\beta_i$. This in turn affects the value for Z_{i+n+1} (from (5.3.5c)),

for which the error is $\{1 + (\nu_{i-1} + \nu_{i-n} + 4dj\omega)/\nu_i\}\Delta Z_i$.

Thus referring again to the fundamental unit

$$0^i \qquad 0^{i+1}$$
$$x^i$$
$$0^{i+n} \qquad 0^{i+n+1}$$

it is clear that an error in Z_i propagates only in a diagonal direction.

For stability it is then required that

$$\left| 1 + (4dj\omega + \nu_{i-1} + \nu_{i-n})/\nu_i \right| < 1 \qquad (5.3.9a)$$

for all interior elevation points i. Further analysis shows that the error ΔZ_i <u>does</u> propagate to elevation points i+2 and i+2n, the errors being $-(\nu_{i-n}/\nu_{i-n+1})\Delta Z_i$ and $-(\nu_{i-1}/\nu_{i-n+1})\Delta Z_i$ respectively. (Clearly if the depth is constant then this represents only a change of sign of ΔZ_i rather than a change of magnitude). The error, in fact, 'leap-frogs' along rows and columns of elevation points (Fig. 5.11) affecting only every second point. The error, however, affects each succeeding point in the same diagonal as elevation point i, so we expect that in an unstable scheme diagonals will harbour the greatest accumulated error.

Let us examine the stability of the Lake Albert model of Fig. 5.8a. We follow the pattern of the one-dimensional scheme by supposing that the depth is a constant, H ($\equiv$ 1.94m), the average depth of the actual basin. The resultant stability condition will then approximate a necessary condition of stability for the model with variable depths. With depth constant, no round-off error propagates along verticals or horizontals and we need consider only errors propagating diagonally through the grid. Then (5.3.9a) becomes

$$\left| 3 + \frac{4dj\omega}{\nu} \right| < 1 \tag{5.3.9b}$$

where $\nu = gH/(2d\{j\omega+r/H\})$.

Evaluation of the quantity $\left| 3+4dj\omega/\delta \right|$ over the frequency range 0 - 96 cpd revealed that the scheme was <u>unstable</u> according to (5.3.9b) at all frequencies below about 48 cpd and above 68 cpd, for values of r from 0 $m.sec^{-1}$ to $10^{-3} m.sec^{-1}$.

The property of instability does not render the scheme ineffectual;

however, the array size must be limited to ensure that any accumulated round-off error is kept within reasonable bounds. Clearly, the precision of number specification of the machine in use plays an important role in containing accumulated errors. Single precision specification, accurate to approximately 14 decimal digits, has been used in all the two-dimensional numerical calculations reported here. Use of double precision unfortunately increases significantly the amount of time required for the iterative scheme to be performed, as well as placing bigger demands on storage capacity. Use of single precision means that all the models developed are relatively 'coarse', but they nevertheless have been found to give reasonable results and, importantly, are able to contain round-off errors.

Each model must be individually tested for its degree of instability. It was found that instabilities manifested themselves largely in the form of non-zero flows across the closed boundaries of the lake model, especially in the regions of terminating diagonals. For the Lake Albert model of Fig. 5.8a, tests revealed that in the frequency range 0 - 24 cpd the accumulated round-off errors involved were insignificant.

Fig. 5.12 shows the surface response function due to a southerly wind (i.e. $\tau_{ox} = 1$, $\tau_{oy} = 0$) at elevation point number 15 in the Lake Albert model of Fig. 5.8a. We note that for $r = 5 \times 10^{-4} \text{m.sec}^{-1}$ resonance peaks are still quite apparent, so that the response of Lake Albert to changing wind stresses is not as low-frequency dominated as is the response of the Coorong lagoons. Further, if we assume Lake Albert to be rectangular (sides 15km, 12km) with constant depth (1.94m) then for the fundamental

longitudinal seiche (south-north direction) to be overdamped, it is
required from (3.2.18) that

$$r > 3.6 \times 10^{-3} m.sec^{-1}$$

which is of an order of magnitude greater than the expected value of r.
Similar general reasoning applied to Lake Alexandrina, assumed closed at
the Narrung channel entrance, shows that here too none of the free
oscillations of the basin is likely to be overdamped.

Let us examine the steady state time response of the Lake Albert model
to a periodic westerly wind of diurnal frequency. The wind stress takes
the form $\tau_s = \tau_o \cos(2\pi t/T)$ with T = 1 day and $\tau_o = 0.1 N.m^{-2}$. Shown in
Fig. 5.13a are the surface contours and mean velocity vectors at times
t = 0, T/8, T/4, and 3T/8 for the Lake Albert model with depth taken as
constant and equal to 1.94m; and in Fig. 5.13b the same using actual
depths. In both we take $r = 5 \times 10^{-4} m.sec^{-1}$.

We note a general similarity between the response of the circular model
lake of Section 4.4 and that shown in Fig. 5.13a. At each instant an
approximately equilibrium response is attained, the velocities reaching a
maximum at about T/4 when the surface elevation is at a minimum.

With the variable depth model we note little change in elevation
patterns but a large alteration in velocity structures. The order of the
velocity magnitudes $(0(0.1-0.5 cm.sec^{-1}))$ in the centre of the basin is
the same for both constant- and variable-depth models, but there is consid-
erable difference in directions. In the velocity response at time t = 0

for the variable depth model there is evidence of flow separation about
Campbell Point on the western shore of Lake Albert, with resultant gyre
formation in the southern and northern halves of the basin.

We note that velocities reach a maximum much earlier in the wind stress
cycle for the variable depth model. Further the maximum velocities
$(0(1-2 \text{ cm.sec}^{-1}))$ are attained in the shallower coastal regions - these
magnitudes seem exaggerated and may be the result of a peculiarity of the
numerical model which is unlikely to be observed in practice. Tronson
(1973) reported similar effects in a series of time-stepping experiments
on the South Australian gulf system.

5.4 A Combined Model of Lake Albert - Lake Alexandrina

In this section a finite difference model of the combined Lake
Albert - Lake Alexandrina system which incorporates both the one-dimension-
al and two-dimensional schemes outlined in the previous sections is des-
cribed, and results of a series of numerical experiments carried out on
the model are discussed. This model was constructed in order to give an
indication of the importance of Narrung channel flow in determining the
water levels and current patterns within each lake.

A grossly simplified model of the combined system, as reported by
Walsh and Noye (1974), was initially constructed to examine the flow inter-
action between Lake Albert and Lake Alexandrina. This consisted of model-
ling the two lakes as rectangular basins joined by a straight channel of
constant breadth. The combined system was set on a two-dimensional array

of the type reported in the previous section, and the depth was constant

throughout. The channel breadth was taken as 2d, where d is the array grid

length. (This is the narrowest possible width that the channel can take

if it is to remain part of the two-d¹mensional scheme with constant grid

length).

The results from this model have not been presented here; they have

little quantitative value due to the simplicity of the model. Qualita-

tively, however, it was shown that subjecting the model to various forms

of wind stress invariably induced channel velocities that were consider-

ably greater in magnitude than velocities in either of the two lakes. It

seems that a narrow channel or opening between two lakes is a region in

which wind-induced velocities undergo considerable amplification. This

feature is consistent with the observations referred to in Chapter 1.

A more accurate representation of the combined system requires, most

importantly, that conditions in the channel be better specified. It was

decided that this could best be done by modelling the channel flow one-

dimensionally using the scheme of Section 5.2. This flow was then matched

onto two-dimensional flows in each of the lakes by deriving suitable

conditions at the ends of the channel.

Shown in Fig. 5.14a is a two-dimensional array (17 x 15, with grid

length = 1275m) for modelling Lakes Alexandrina and Albert, and also the

depths at non-exterior stream points as inferred from Fig. A2 (Appendix A).

Again the directions of the array axes coincide with the west-east and

south-north directions. The one-dimensional array (25 points, with grid

length = 425m) for modelling the Narrung channel is shown in Fig. 5.14b;
further details of the array are provided in Appendix E together with the
conditions used to match the one-dimensional channel flow onto the two-
dimensional flows in the separate lakes. Little data is available con-
cerning channel depths. For simplicity it is assumed that the channel
slopes uniformly from a depth of 3m at the Lake Alexandrina end to 2m at
the Lake Albert end. The numbering of the two-dimensional array points
follows the normal convention; the channel points are numbered 1 - 25
beginning at the Lake Alexandrina end.

We note that for reasons mentioned in the previous section, the two-
dimensional finite difference specification of the separate lakes (parti-
cularly of Lake Albert) is necessarily coarse, though it provides a
reasonable representation of the basic features of the lakes.

Within the Narrung channel there is considerable reed growth which,
in all probability, reduces the effective surface wind stress in the
channel. Such a phenomenon has been investigated by Saville (1952) and
Tickner (1957). We assume here that the wind stress is homogeneous sep-
arately over the two lakes and the channel, and that the ratio of the
wind stress amplitude, τ_c, over the channel to that, τ_ℓ, over the two
lakes assumes the value 0.5. Variation of the ratio τ_c/τ_ℓ was shown to
influence only marginally the response of the combined system.

We expect, further, that the damping parameter r assumes a greater
value within the channel than in either of the two lakes. Excessive
bottom growth is likely to increase the channel value of the drag

coefficient C_b (refer (2.1.11a)); further, the observed high velocities within the channel indicate that the quantity q_b is likely to be of a higher order of magnitude here than within either of the separate lakes. Denoting by r_ℓ, r_c the value of r within the lakes and the channel respectively, we assume for simplicity, that the ratio r_ℓ/r_c has the value 0.5. Since typically we expect that $r_\ell = 5 \times 10^{-4}$ m.sec^{-1}, this indicates that typically $r_c = 10^{-3}$ m.sec^{-1}.

It is clear from the above discussion that among important parameters to be chosen before an analysis of the combined system is attempted, are the ratios τ_c/τ_ℓ and r_ℓ/r_c. The quite moderate choice of 0.5 for each is shown in Chapter 8 to give a reasonable comparison between predicted and measured water levels. However, much experimental work remains to be done to properly elucidate the nature of conditions within the Narrung channel.

Using the above values for r_ℓ and r_c, the surface response functions (due to a <u>south-east</u> wind, with $\tau_\ell = 1$ N.m^{-2}, $\tau_c = 0.5$ N.m^{-2}) for the <u>combined</u> system at elevation points 89 (approximating the response at Wellington), 107 (Milang), 129 (Narrung 1 - the Lake Alexandrina end of the channel), 177 (Narrung 2 - the Lake Albert end of the channel), 184 (Tauwitchere barrage) and 255 (Meningie) are shown in Fig. 5.15. For comparison, the response functions at the same stations for the <u>uncombined</u> system, i.e. assuming neither lake is connected to the channel (appropriate boundary conditions detailed in Appendix E), are also shown in Fig. 5.15.

Resonance peaks are observed in each of the gains for the combined

system. Generally, the most significant differences between the response functions for the combined and uncombined systems occur for frequencies less than 3 cpd. For higher frequencies, curves of gain and phase-lag are shaped similarly for both systems. However, the differences at all stations are sufficient to suggest that a consideration of the independent behaviour of Lakes Alexandrina and Albert would be inadequate in a description of wind effects in the total system. This suggestion is strengthened by an examination of characteristic wind induced velocities within the system.

Consider the response of the combined system to a diurnal wind stress with constant alignment, of the form $\tau_s = \tau_\ell \cos(2\pi t/T)$ with $T = 1$ day and $\tau_\ell = 0.1$ N.m^{-2} (and thus $\tau_c = 0.05$ N.m^{-2}). We may examine a variety of alignments for such a wind stress, corresponding to different possible types of prevailing winds in the area of the Murray Mouth lakes. For convenience, we assume that within Lakes Alexandrina and Albert depths are constant at 3m and 2m respectively, while again the channel depths slope uniformly from one end to the other. Such a simplification eliminates exaggerated velocities in shallow coastal regions produced in a variable depth model and allows the effects of channel flow to be considered in isolation. It would be desirable for later models to incorporate depth variations.

Shown in Fig. 5.16a are the mean velocity vectors and surface contours due to a wind stress of this form with a south-east alignment, at times t = 0, T/8, T/4 and 3T/8. In Fig. 5.16b we show the response of the uncombined system to the same wind stress field.

The most obvious feature of the response of the combined system is that typical channel velocities $(0(1-30 \text{ cm.sec}^{-1}))$ are very large, relative to typical velocities in the separate lakes $(0(0.1 - 0.5 \text{ cm.sec}^{-1}))$. It is apparent that water is continuously being 'pushed' from one lake to the other through the channel. Thus, at time $t = T/4$, the surface of the uncombined model is almost equivalent to the plane of no disturbance; for the combined model, the Lake Alexandrina and Lake Albert water levels are approximately constant at +1.5cm and -5cm respectively. Clearly, in the portion of the wind stress cycle from (approximately) $t = T/8$ to $t = 5T/8$, water is pushed from Lake Alexandrina to Lake Albert; the channel flow is oppositely directed for the remainder of the cycle.

The response of the combined system to a wind stress of similar form and south-west alignment is shown in Fig. 5.17. Even though the wind is always directed at right angles to much of the channel axis, it is apparent that very large channel velocities are still induced.

A type of wind commonly observed in the region of the Murray Mouth lakes is a diurnally rotating wind which has been observed to persist for several days at a time (Noye (1970)). Fig. 5.18 shows wind speed and directions on the South Coorong as recorded at Noye's Island and Salt Creek over a period of four days in December, 1967. For the first two days the direction was approximately constant, for the remaining two days it exhibited a slow, daily rotation in a counter-clockwise direction.

A simple model for a counter-clockwise rotating wind is given by

$$\tau_{sx} = \text{Re}\{T_\ell e^{j\omega t}\} = \tau_\ell \cos(\omega t)$$

$$\tau_{sy} = \text{Re}\{-j\tau_\ell e^{j\omega t}\} = \tau_\ell \sin(\omega t .$$

Haurwitz (1951) examined analytically the <u>transient</u> response of a square, constant depth lake to such a wind stress. In Fig. 5.19 is shown the <u>steady state</u> response of the combined Lake Alexandrina - Lake Albert model to a rotating wind stress of this form with $\tau_\ell = 0.1 \text{ N.m}^{-2}$ ($\tau_c = 0.05$ N.m^{-2}) and period T = 1 day.

For a closed basin subject to a diurnally rotating wind the surface contours rotate with the wind while the directions of the mean velocities <u>lead</u> the wind by approximately 90°, a result clear from our analyses of previous chapters and shown numerically by Walsh and Noye (1974). This phenomenon is observable in the separate lakes of Fig. 5.19, with some modification due to channel flow. We note that the strongest channel flows occur when the direction of the wind is at right angles to the average direction of the channel axis (i.e. T/8 - T/4) since then characteristic velocities in the lakes are aligned with the channel direction.

The response of the combined system to periodic wind stresses of south-east and south-west alignment as well as to a rotating wind were re-examined using $r_\ell = 10^{-3} \text{ m.sec}^{-1}$ and $r_c = 2 \times 10^{-3} \text{ m.sec}^{-1}$. Channel velocities were reduced in magnitude but were still significantly greater than velocities in the separate lakes.

In summary, it appears that no matter what the form of the wind stress, Narrung channel flows are an indispensable part of the wind-induced motions

of Lakes Alexandrina and Albert. It appears, indeed, that the lakes act very much as a single unit in their response to wind stresses. Further, the numerical experiments of this section confirm the local observations regarding the very intense flows in the Narrung channel.
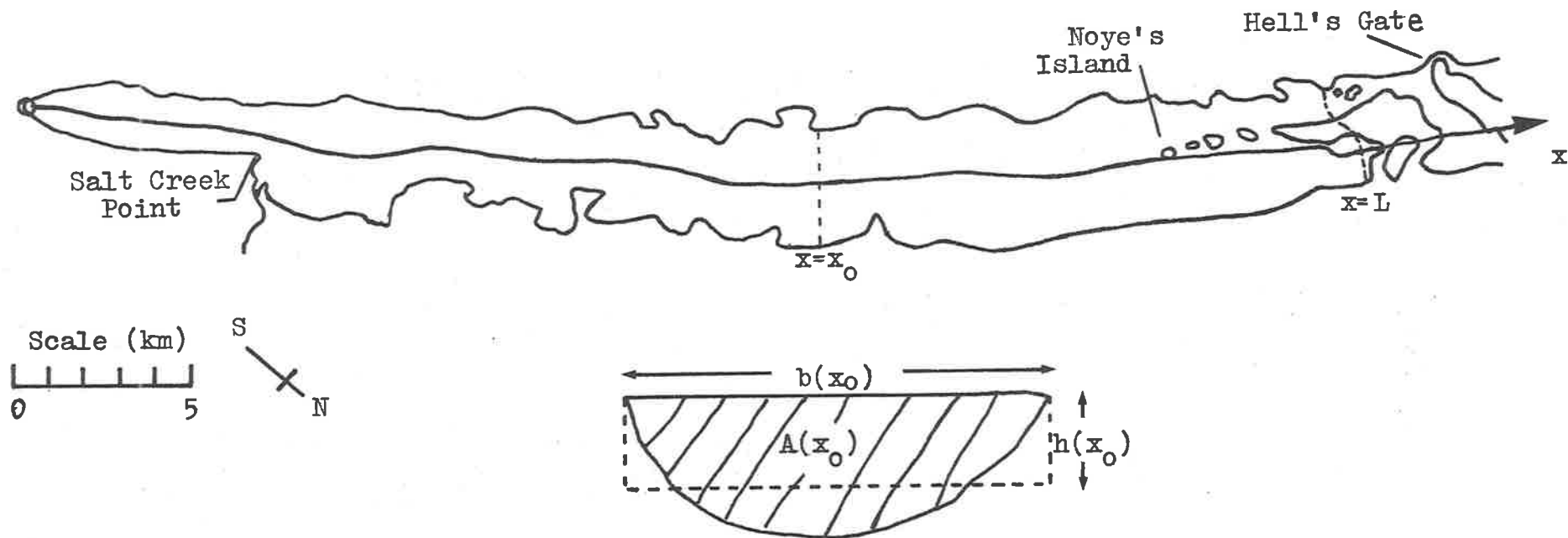
FIGURE 5.1 : PLAN OF SOUTH COORONG LAGOON CONSIDERED CLOSED NEAR
HELL'S GATE.   THE CHANNEL AXIS EXTENDS FROM THE
SOUTH-EASTERN END. ALSO SHOWN IS THE CHANNEL CROSS-
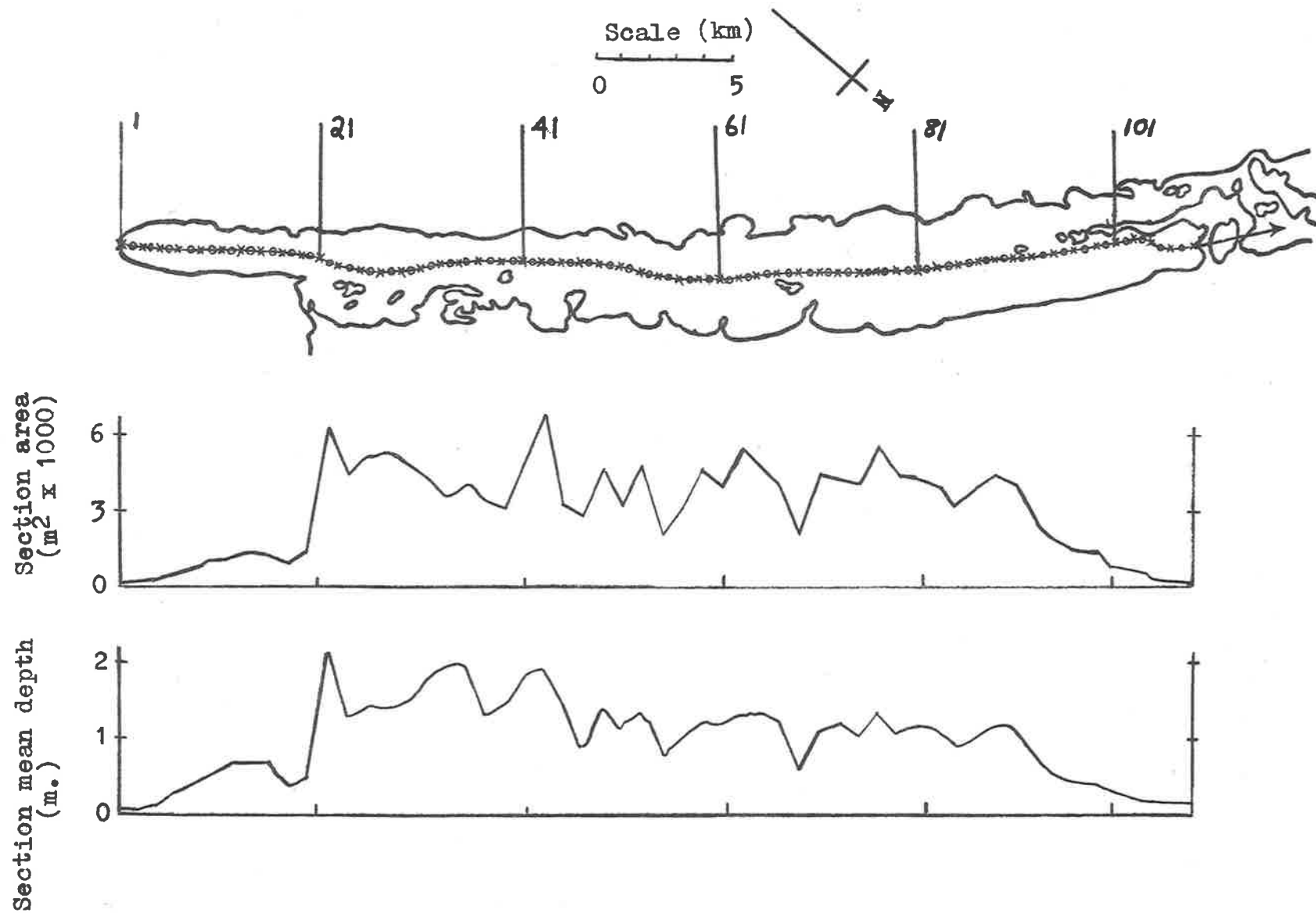SECTION AT STATION X_0 .

FIGURE 5.2 : ONE-DIMENSIONAL GRID FOR THE SOUTH COORONG. ALSO SHOWN IS THE VARIATION OF SECTION AREA AND SECTION MEAN DEPTH ALONG THE LAKE AXIS
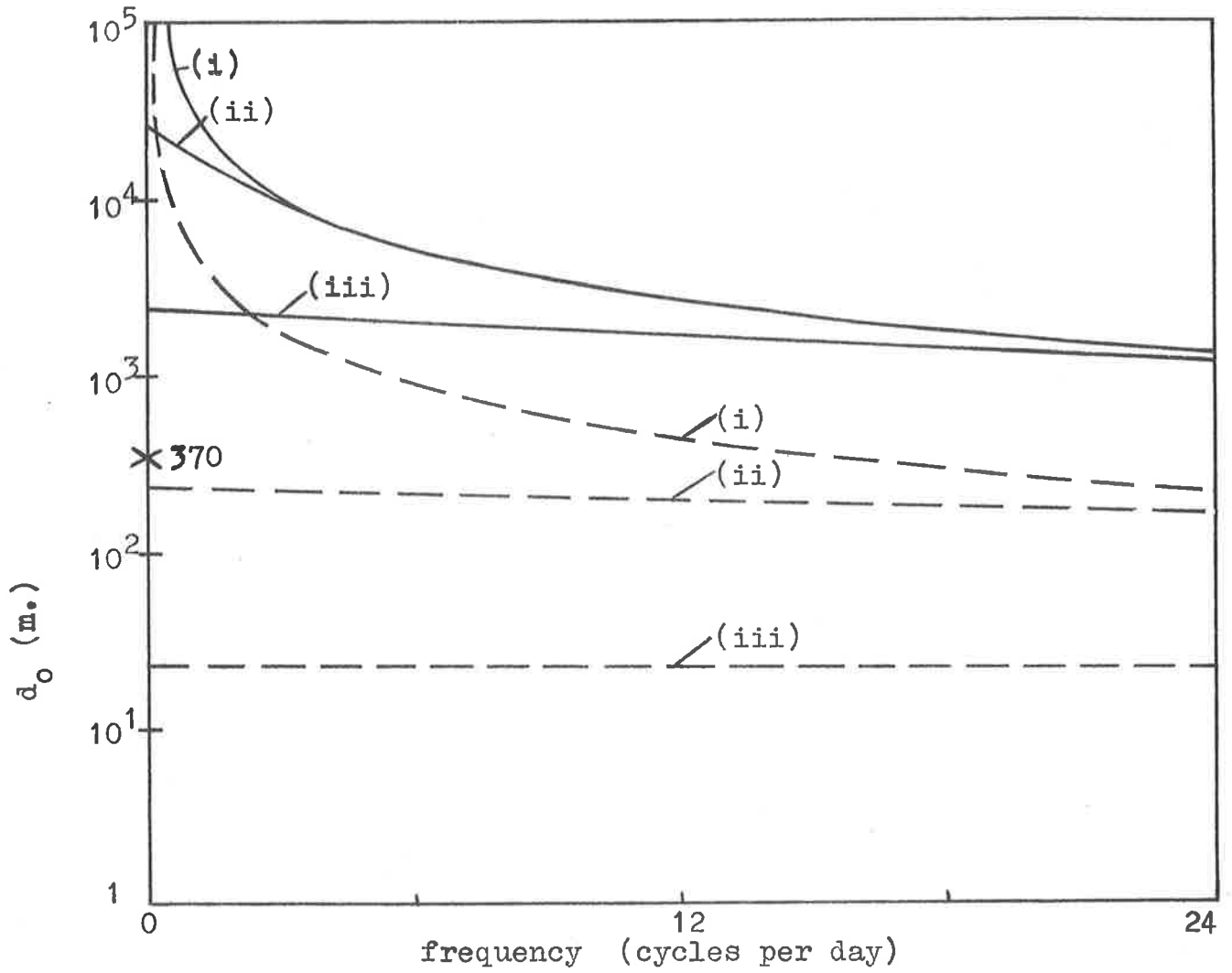
FIGURE 5.3 : PLOT OF d_0 AS CALCULATED FROM (5.2.9b) – DASHED
CURVES, AND FROM (5.2.9c) – SOLID CURVES, USING
ACTUAL CONTOURS FROM THE SOUTH COORONG, FOR
(i)$r=0$m.sec^{-1}, (ii)$r=10^{-4}$ m.sec^{-1}, (iii)$r=$
10^{-3} m.sec^{-1}. THE NUMERICAL SCHEME IS UNSTABLE
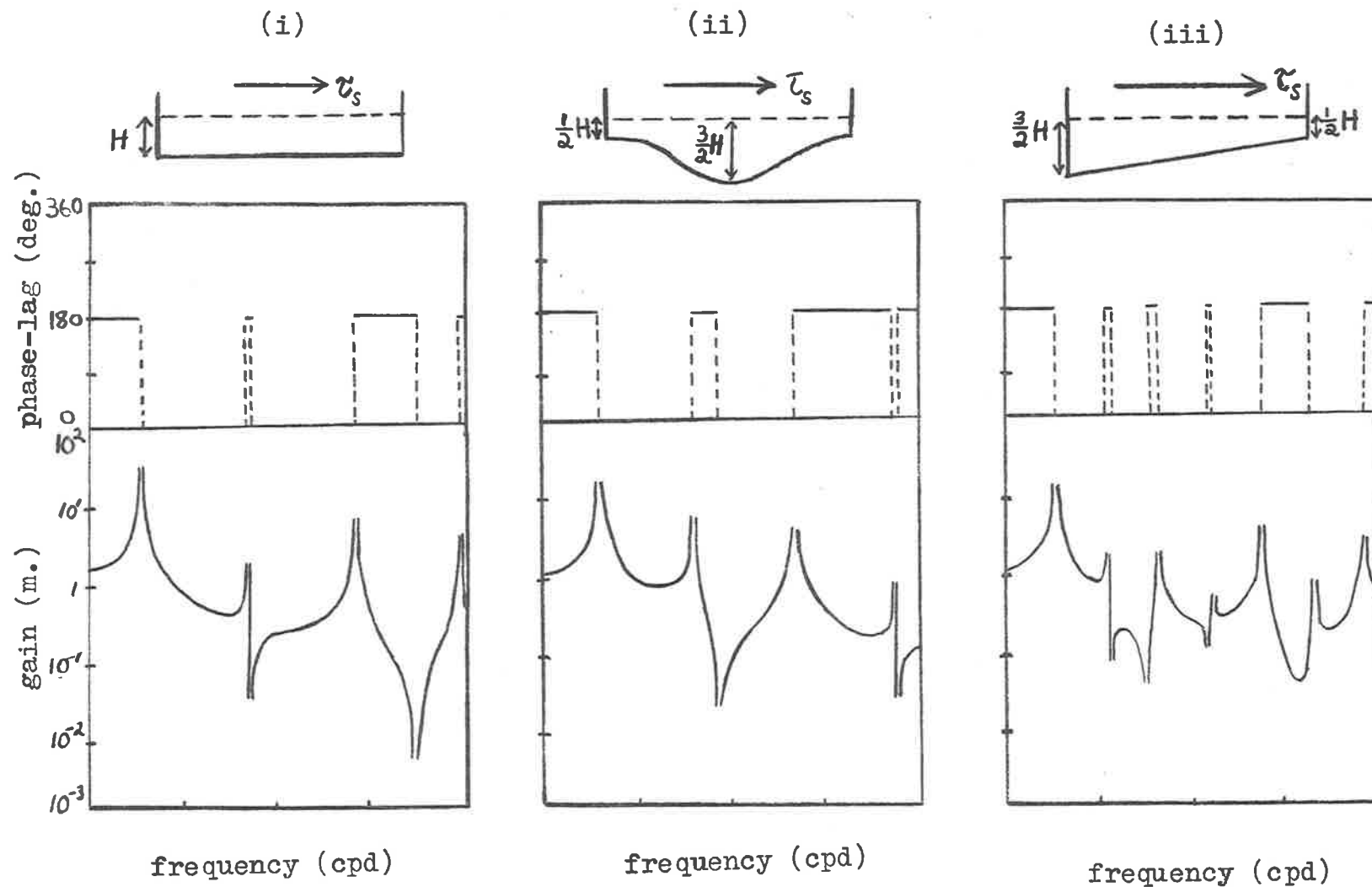AT A GIVEN FREQUENCY IF $d_0 < 370$ m.

FIGURE 5.4 : RESPONSE FUNCTION DUE TO LONGITUDINAL WIND STRESS
τ_s FOR A BASIN WITH RECTANGULAR PLAN AND
(i) DEPTH CONSTANT, (ii) DEPTH SYMMETRIC ABOUT
BASIN CENTRE, (iii) DEPTH ASYMMETRIC ABOUT BASIN
CENTRE. IN EACH CASE, AVERAGE DEPTH (H) AND
BASIN LENGTH ARE EQUIVALENT TO AVERAGE DIMENSIONS
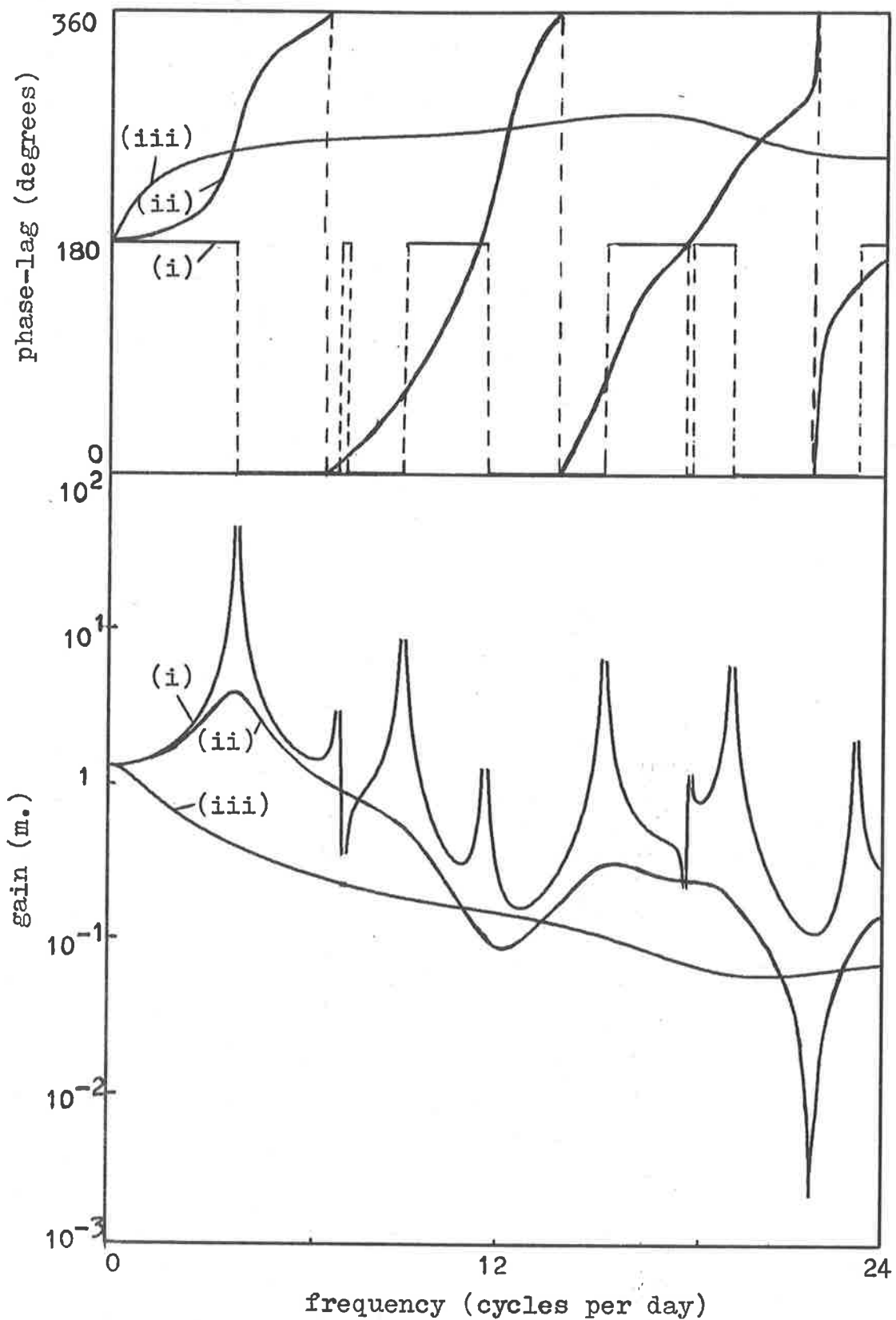OF THE SOUTH COORONG, WHILE $r = 0$ m.sec^{-1}.

FIGURE 5.5: RESPONSE FUNCTIONS FOR SURFACE DISPLACEMENT AT
SALT CREEK POINT, SOUTH COORONG, USING ACTUAL
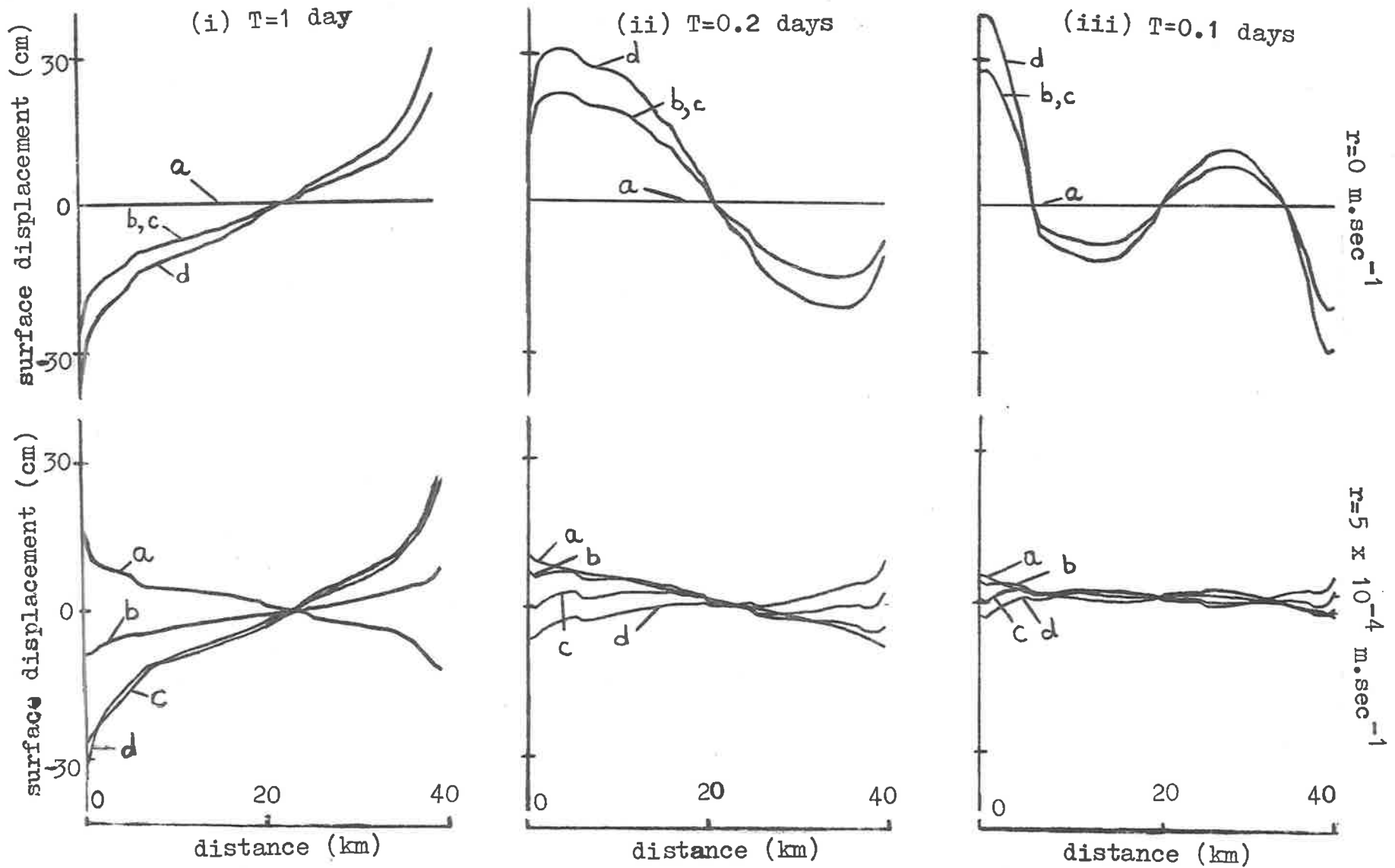BASIN CONTOURS, FOR (i) r=0 m.sec-1, (ii) r=
10-4 m.sec-1, (iii) r=10-3 m.sec-1.

FIGURE 5.6 : REAL TIME RESPONSE OF SOUTH COORONG BASIN TO WIND
STRESS OF FORM $\tau_o\text{SIN}(2\pi t/T)$ WITH τ_o=0.1 N.m^{-2} , AT
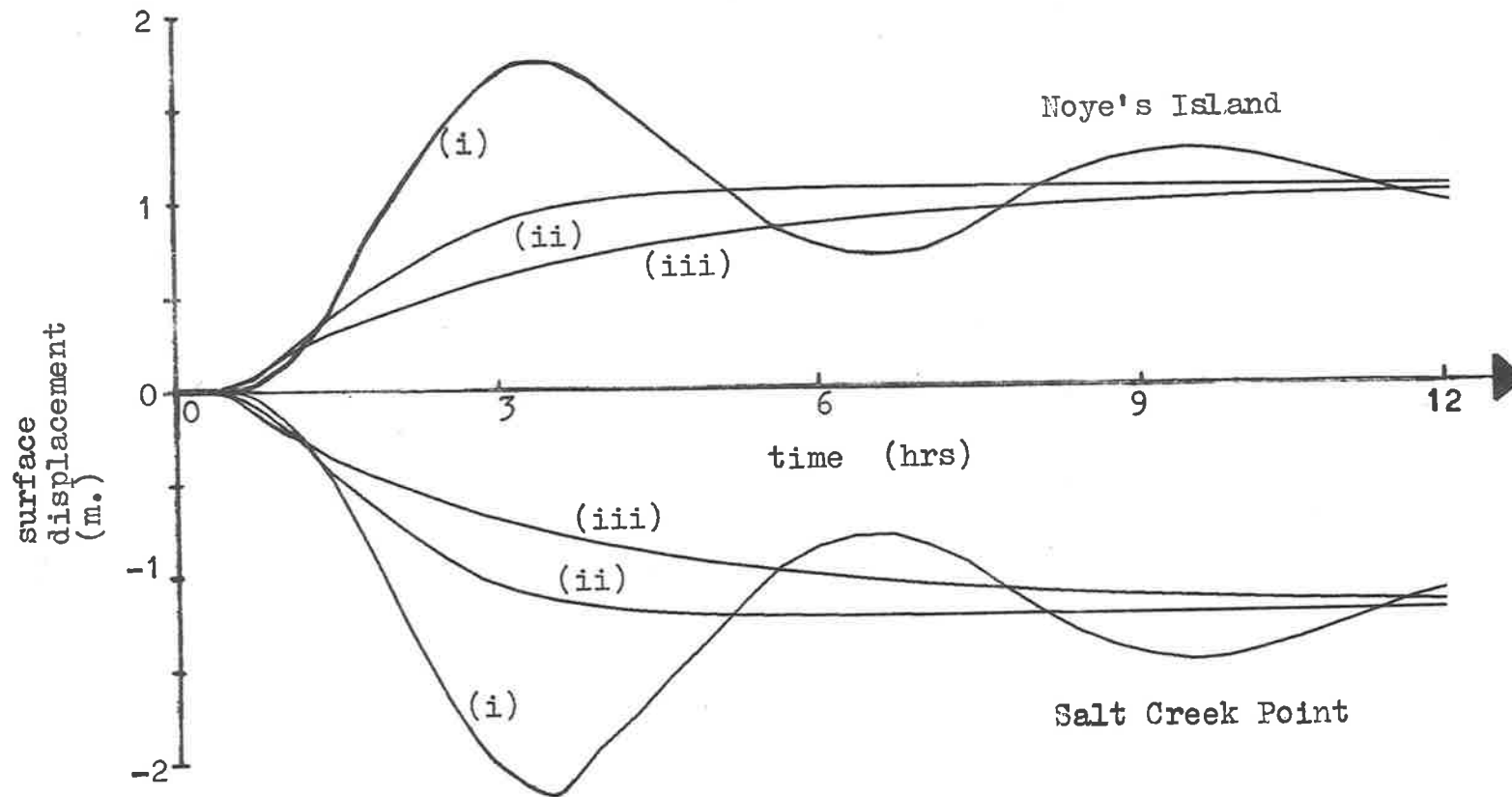(a) t=0, (b) t=T/8, (c) t=T/4, (c) t=3T/8 .

FIGURE 5.7 : STEP RESPONSE FOR SOUTH COORONG USING ACTUAL CONTOURS
AT NOYE'S ISLAND AND SALT CREEK POINT, FOR (i) $r=$
0 m.sec^{-1}, (ii) $r=5 \times 10^{-4}$ m.sec^{-1}, (iii) $r=10^{-3}$ m.sec^{-1}.

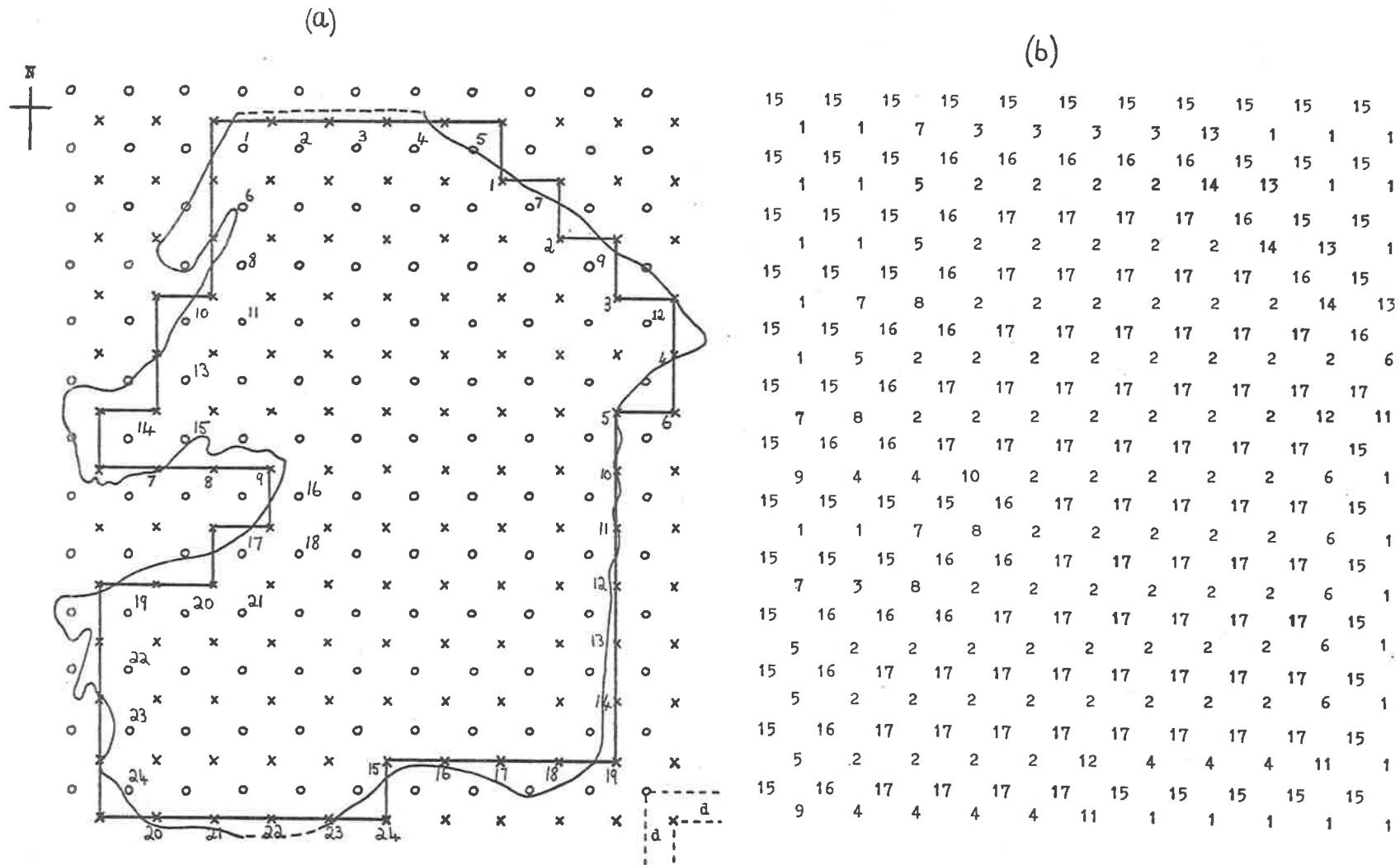FIGURE 5.8 : (a) TWO-DIMENSIONAL MODEL OF LAKE ALBERT; (b) CORRESPOND-
GROUP NUMBER FOR EACH ARRAY POINT OF THE MODEL, THE GRID
LENGTH, d, IS 630 m . STARTING AND END VALUES MAY BE
DEFINED AT CERTAIN ELEVATION AND STREAM POINTS, RESPECT-
IVELY. FOR THE LAKE ALBERT MODEL THERE ARE 24 SUCH POINTS
(IN EACH CASE), NUMBERED AS SHOWN IN (a).

(c)

```
                 1.5   1.5   1.5   1.5   1.5   1.5

                 1.5   2.0   2.3   2.3   2.0   1.5   1.5

                 1.5   2.0   2.3   2.3   2.3   2.0   1.5   1.5

           1.5   1.5   2.0   2.3   2.4   2.4   2.4   2.3   1.5   1.5

           1.5   1.8   2.2   2.3   2.4   2.5   2.5   2.3   2.0   1.5

     1.5   1.5   1.8   2.1   2.3   2.4   2.8   2.8   2.4   1.5

     1.5   1.5   1.5   1.5   2.3   2.4   2.9   2.9   2.4   1.5

                 1.5   1.5   2.2   2.4   2.9   2.9   2.4   1.5

     1.5   1.5   1.5   2.0   2.2   2.4   2.7   2.7   2.2   1.5

     1.5   1.8   2.0   2.2   2.3   2.4   2.5   2.4   2.2   1.5

     1.5   1.7   2.0   2.2   2.3   2.3   2.2   2.0   1.8   1.5

     1.5   1.7   2.0   2.0   1.9   1.5   1.5   1.5   1.5   1.5

     1.5   1.5   1.5   1.5   1.5   1.5
```

FIGURE 5.8 : (c) DEPTHS (METRES) AT EACH BOUNDARY OR
INTERIOR STREAM POINT OF (a).
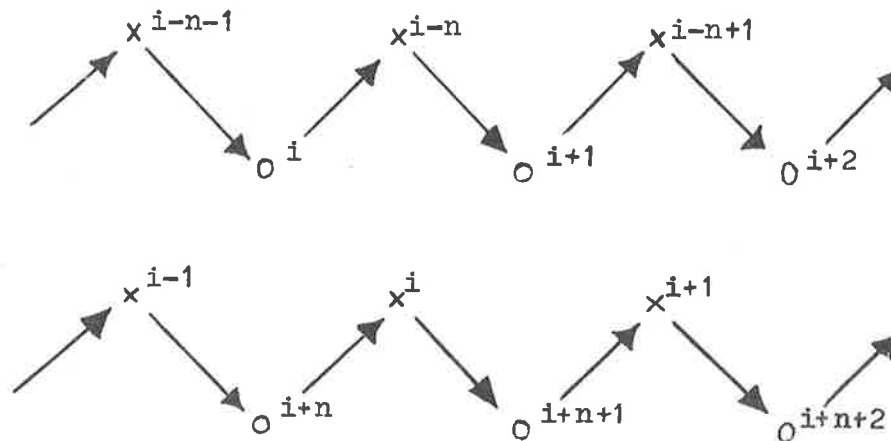
FIGURE 5.9 : ORDER OF CALCULATION OF Z (AT ELEVATION POINTS) AND S,D (AT **STREAM** POINTS) FOR INTERIOR POINTS OF THE TWO-DIMENSIONAL ARRAY, AS INDICATED BY THE DIRECTION OF ARROWS. THE CALCULATION PROCEEDS FROM LEFT TO RIGHT WITHIN EACH ROW OF ELEVATION AND STREAM POINTS .
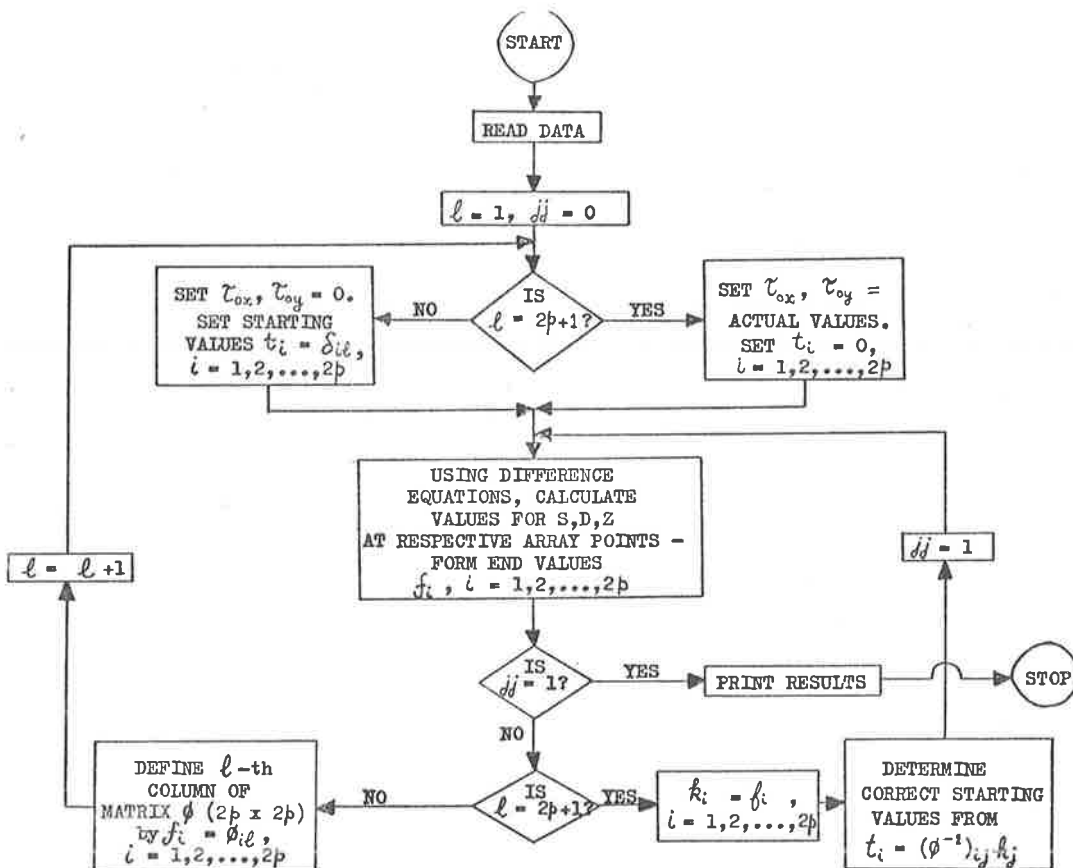
FIGURE 5.10 : FLOW DIAGRAM OF THE ITERATIVE PROCEDURE TO CALCULATE THE RESPONSE OF THE TWO-DIMENSIONAL ARRAY AT A SINGLE FREQUENCY .
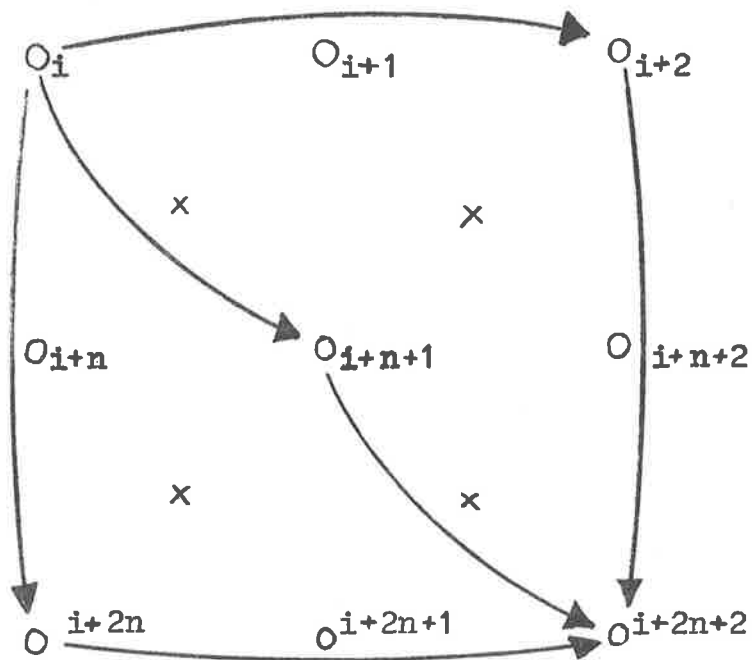
FIGURE 5.11 : SHOWING HOW AN ERROR AT ELEVATION POINT i IS
              TRANSMITTED TO NEIGHBOURING ELEVATION POINTS .
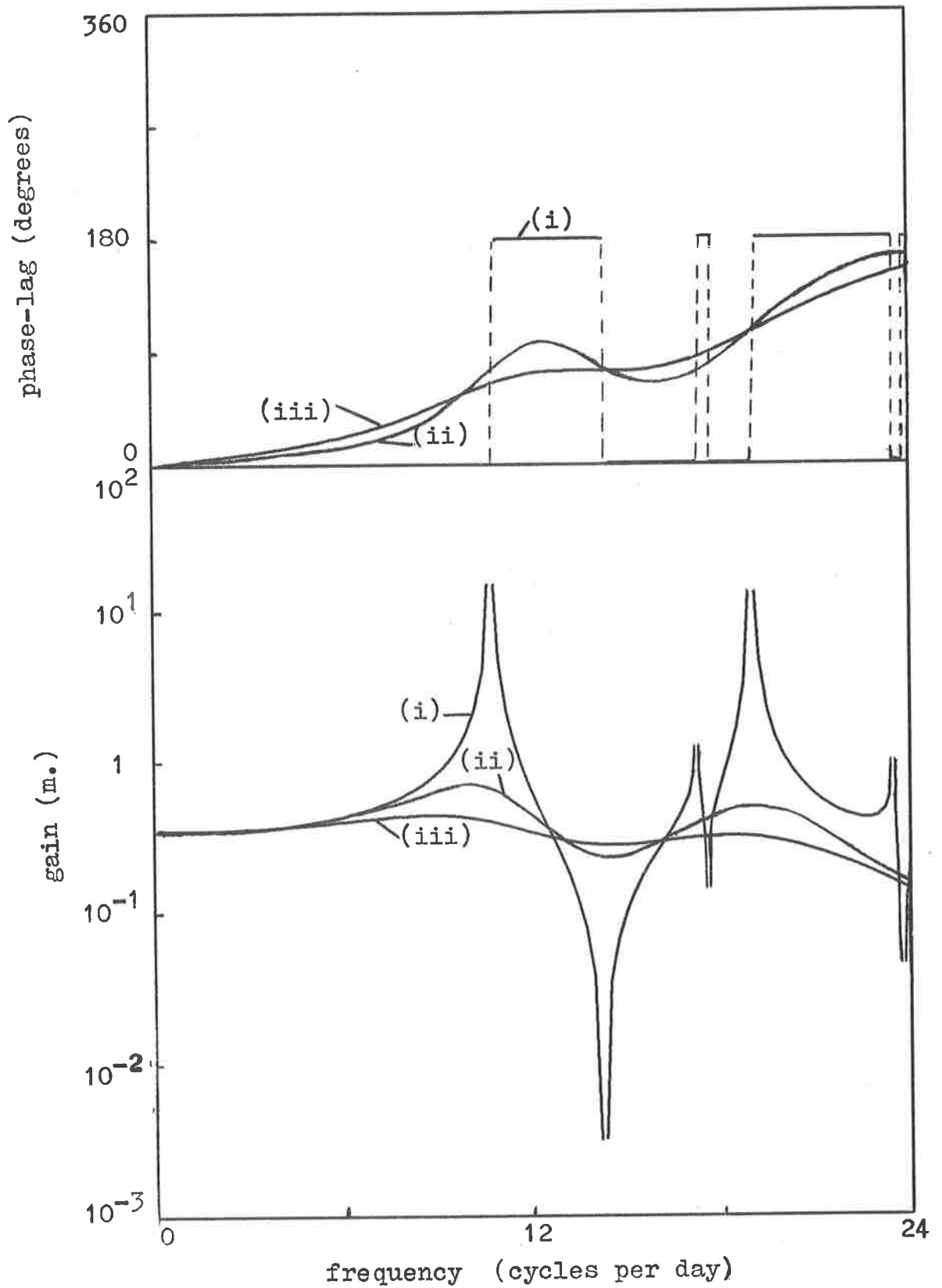
FIGURE 5.12 : RESPONSE FUNCTIONS FOR SURFACE DISPLACEMENT
AT ELEVATION POINT NUMBER 15 OF THE LAKE
ALBERT MODEL, FOR (i) r=0m.sec^{-1}, (ii) r=
5 x 10^{-4} m.sec^{-1}, (iii) r=10^{-3} m.sec^{-1}.

FIGURE 5.13 : (a) RESPONSE OF CONSTANT DEPTH LAKE ALBERT MODEL (1.94 m.) TO
WIND STRESS $\tau_o \cos(2\pi t/T)$ WITH T = 1 day AND $\tau_o = 0.1$ N.m^{-2}.
NOTE THE SLIGHT DISPLACEMENT OF THE BOUNDARY OF THE MODEL TO
ALLOW BOUNDARY VELOCITIES TO BE PROPERLY SEEN .
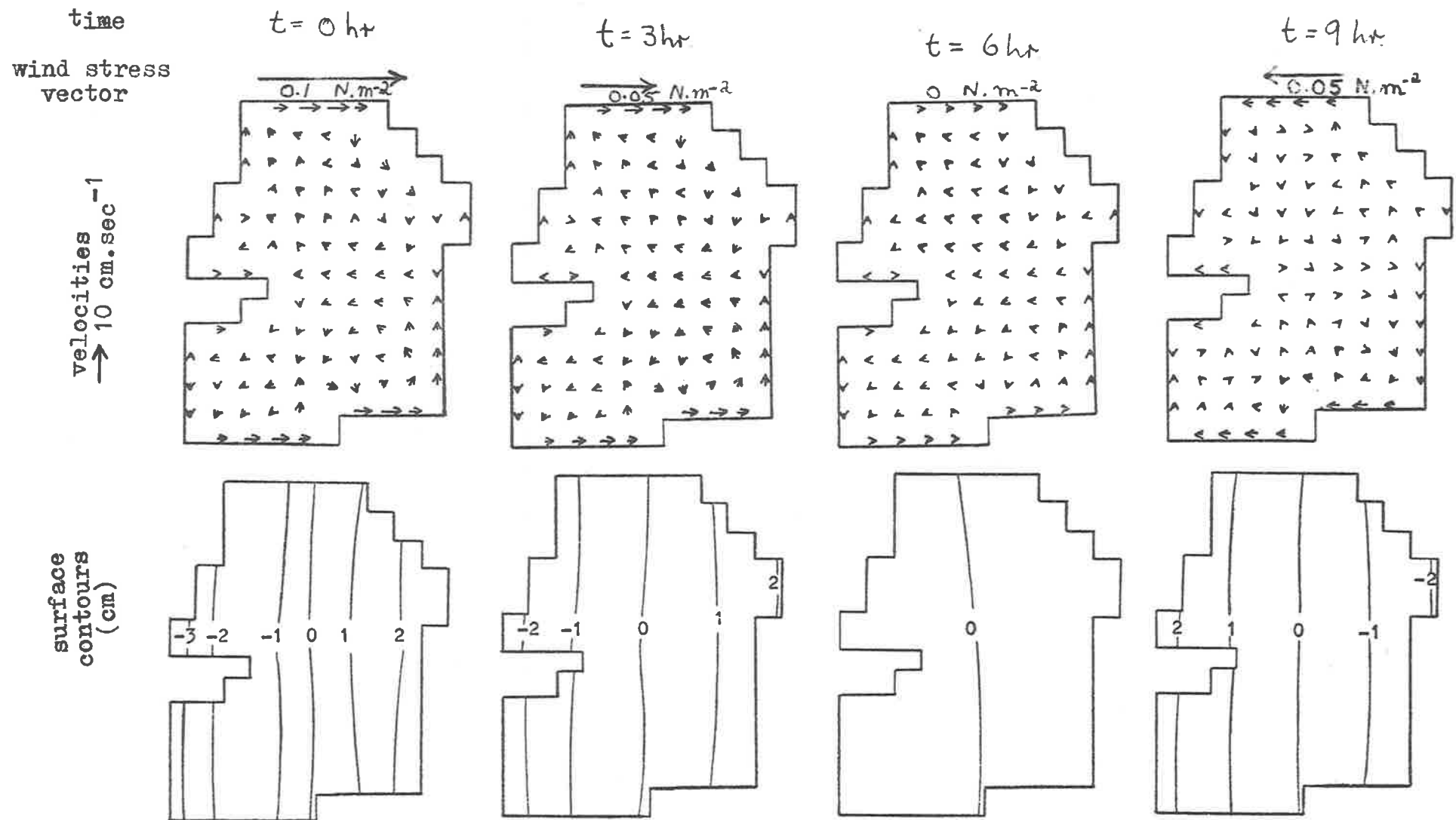
FIGURE 5.13 : (b) RESPONSE OF THE LAKE ALBERT MODEL USING ACTUAL DEPTHS TO THE SAME WIND STRESS. NOTE THE HIGHER VELOCITY SCALE DUE TO EXAGGERATED BOUNDARY VELOCITIES.

1.50 1.50 1.50 1.50

1.50 3.00 3.25 3.50 1.50 1.50

1.50 1.50 3.25 3.50 3.70 3.50 1.50

1.50 1.50 1.50 1.50 1.50 3.50 3.75 3.80 3.80 3.40 1.50

1.50 1.50 1.50 3.20 3.50 4.10 4.20 4.30 4.30 4.30 4.20 4.00 1.50 1.50 1.50

1.50 2.50 3.50 4.00 4.15 4.30 4.45 4.60 4.55 4.50 4.25 3.50 2.00 2.00 1.50

1.50 3.00 3.70 4.00 4.20 4.30 4.30 4.30 4.30 4.20 3.50 2.70 3.00 2.50 1.50

1.50 1.50 3.50 3.90 4.10 4.10 4.20 4.10 4.05 1.50 1.50 1.50 1.50 1.50 1.50

1.50 1.50 1.50 3.30 1.50 1.50 1.50 3.00 1.50

1.50 1.50 3.00 1.50

1.50 2.00 1.50 1.50   1.50 2.00 1.50 1.50

1.50 1.50 1.50   1.50 2.20 2.30 1.50 1.50

1.50 1.50   1.50 1.50 2.20 2.30 2.40 1.50

1.50 1.50 1.50 2.50 2.90 1.50

1.50 1.50 1.50 2.40 2.50 1.50

1.50 1.50 2.20 2.30 2.20 1.50

1.50 1.50 1.50 1.50 1.50

FIGURE 5.14 : (a) TWO-DIMENSIONAL ARRAY FOR MODELLING BEHAVIOUR
IN LAKES ALEXANDRINA AND ALBERT. GRID LENGTH IS
1275 m ; ALSO SHOWN ARE CORRESPONDING DEPTHS
(METRES) .
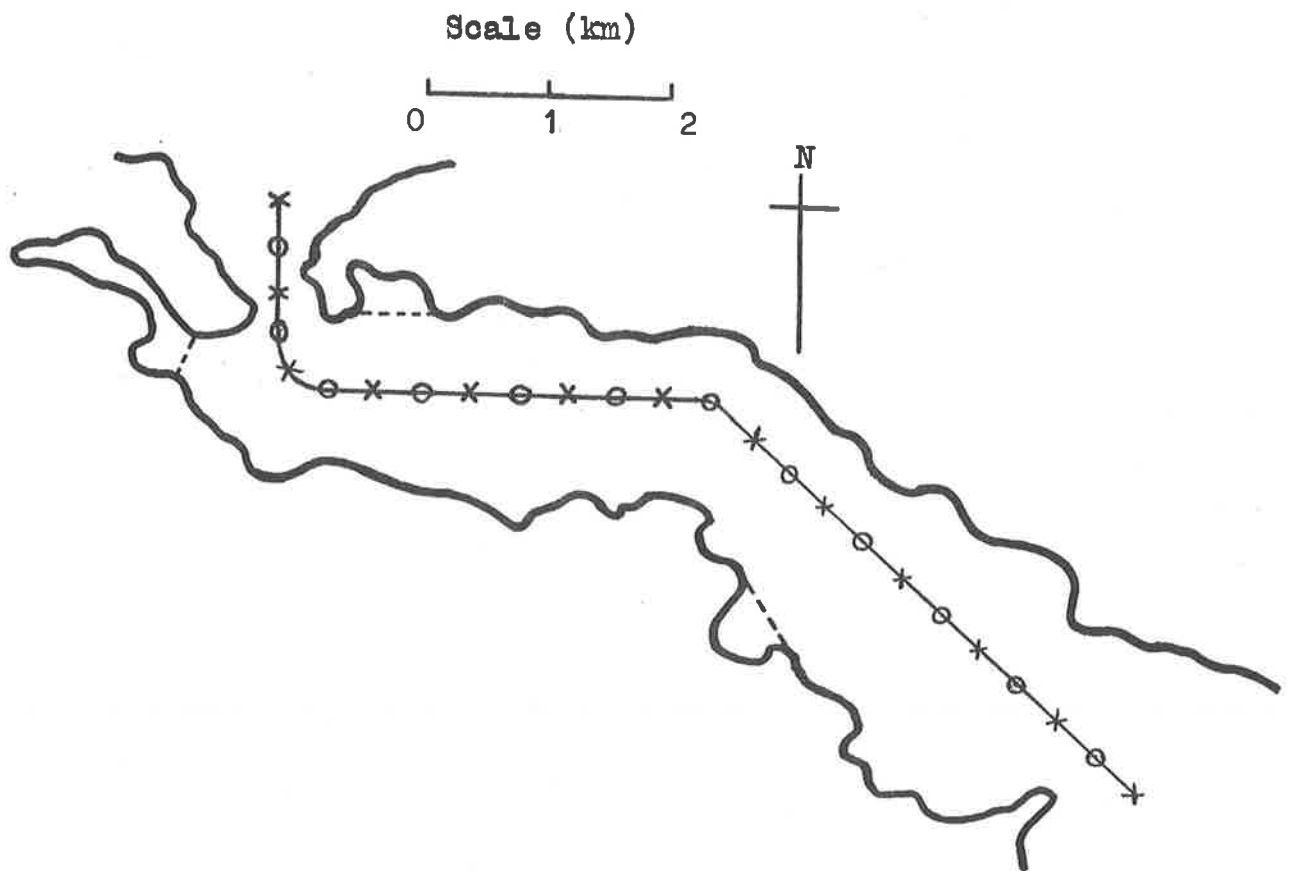
FIGURE 5.14 : (b) ONE-DIMENSIONAL ARRAY FOR MODELLING
NARRUNG CHANNEL BEHAVIOUR. GRID LENGTH
IS 425 m .
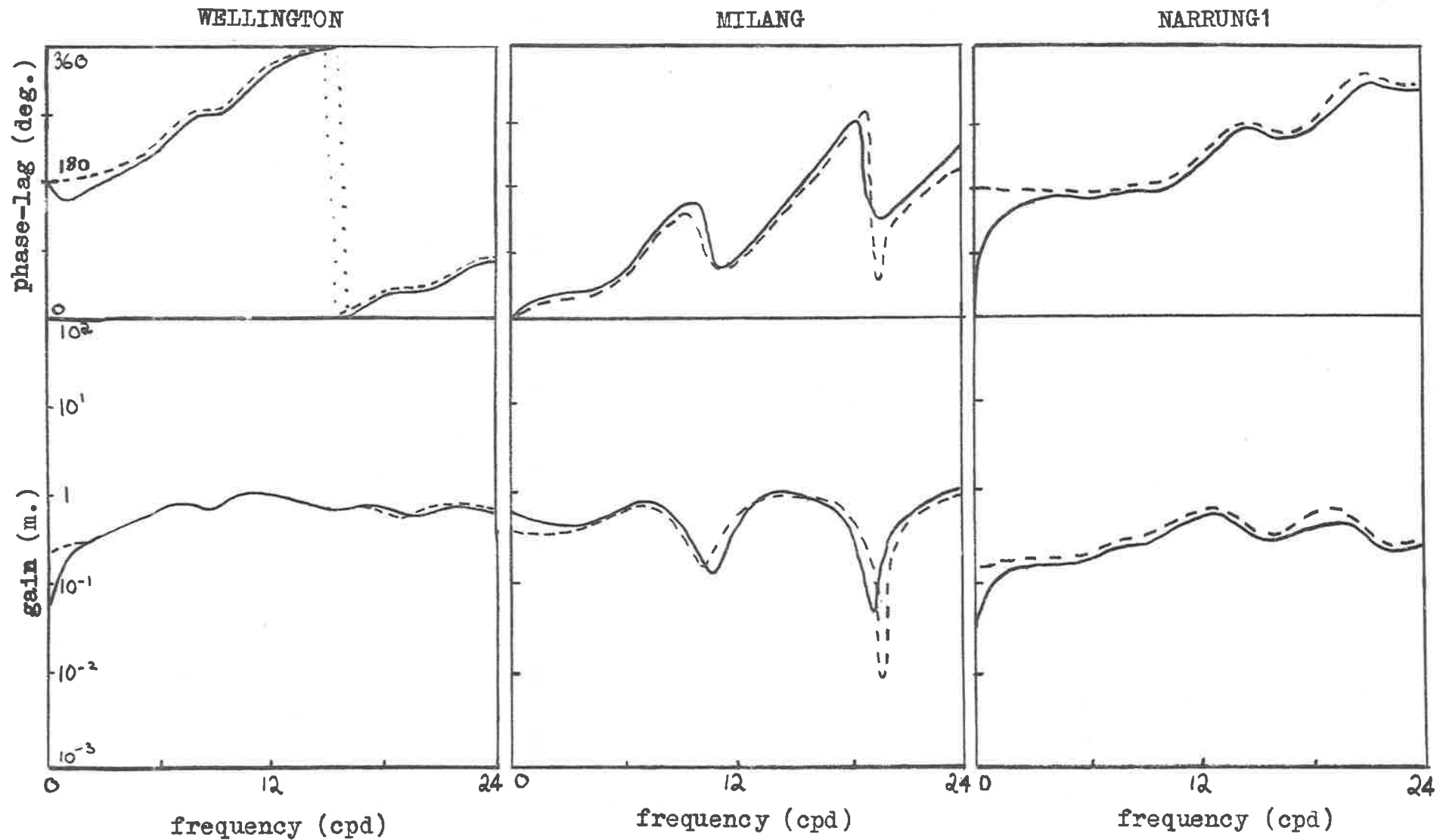
FIGURE 5.15 : RESPONSE FUNCTIONS AT VARIOUS STATIONS AROUND LAKES ALEX-
ANDRINA AND ALBERT FOR THE CONNECTED MODEL (SOLID CURVE)
AND THE UNCONNECTED MODEL (DASHED CURVE), WITH $r_1 = 5 \times 10^{-4}$
$m.sec^{-1}$ and $r_c = 10^{-3}$ $m.sec^{-1}$. CONTINUED OVERLEAF.
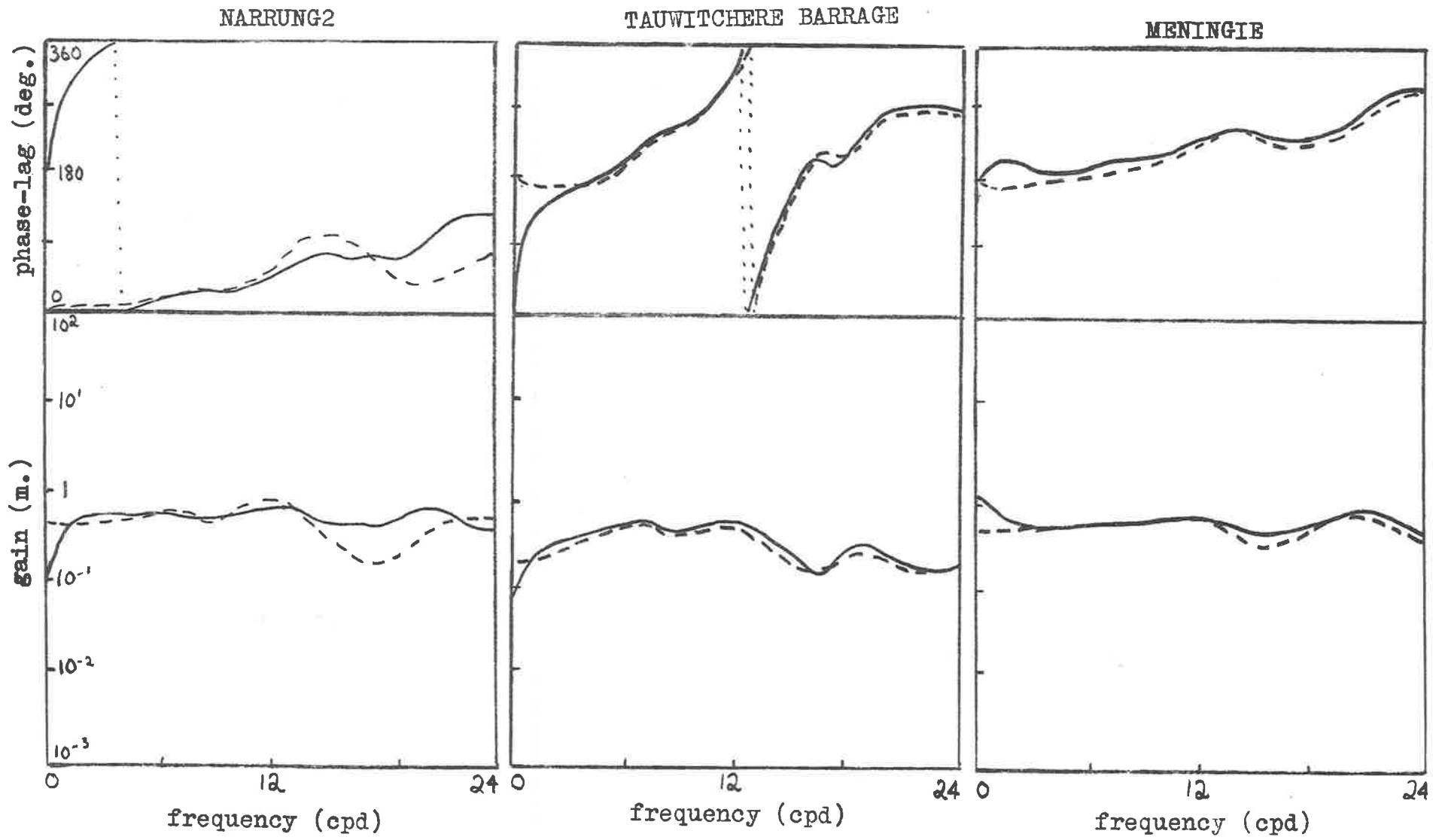
FIGURE 5.15 (CONTINUED) .
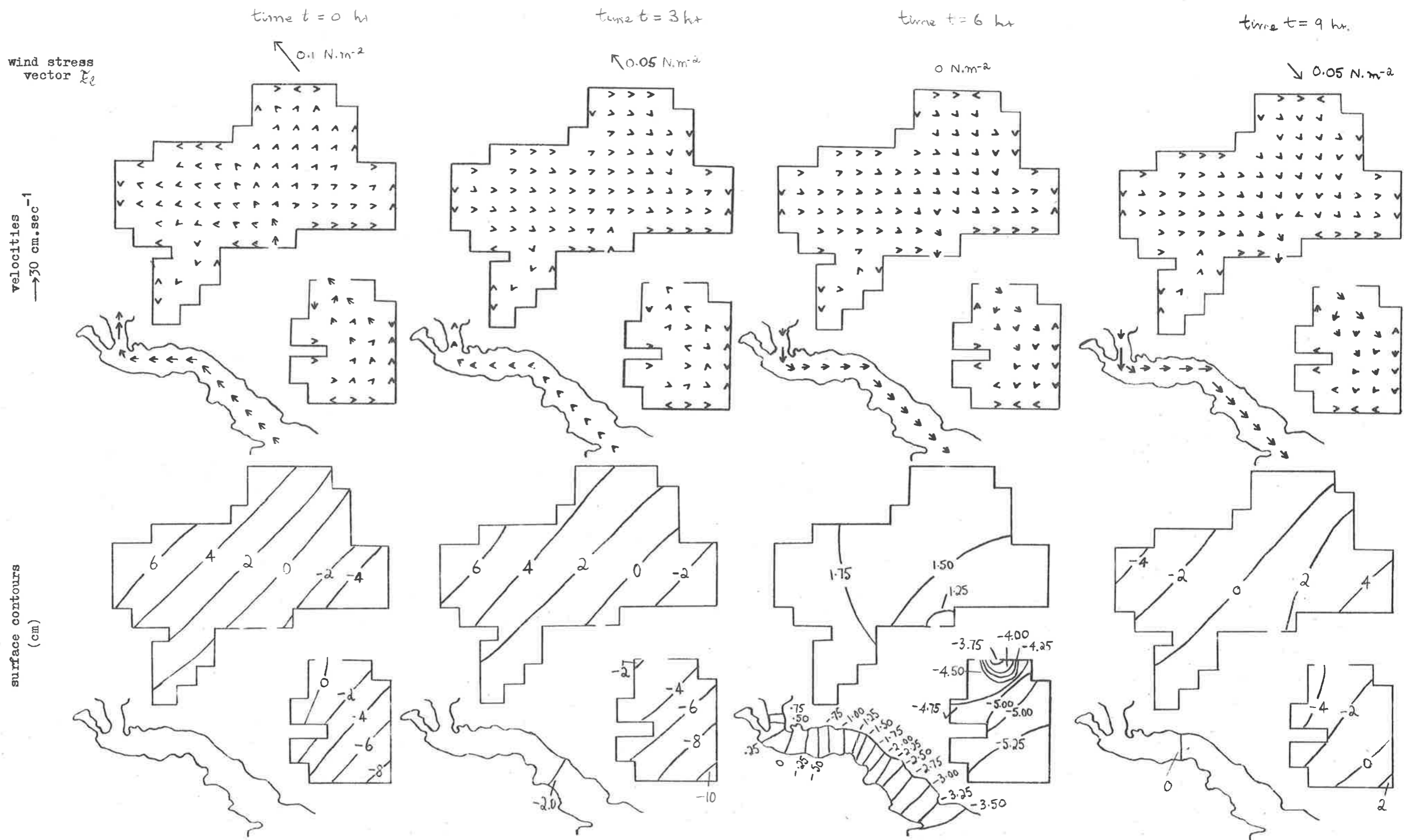
FIGURE 5.16 : (a) RESPONSE OF THE COMBINED SYSTEM TO A WIND STRESS OF THE FORM $\tau_\ell \cos(2\pi t/T)$ WITH SOUTH-EAST ALIGNMENT AND T = 1 DAY, τ_ℓ=0.1 N.m^{-2}. AGAIN THE MODEL BOUNDARY IS SLIGHTLY DISPLACED. CONTOURS ARE SHOWN AT 2 cm INTERVALS, EXCEPT AT TIME 6 hrs WHEN THE INTERVAL IS 0.25 cm.
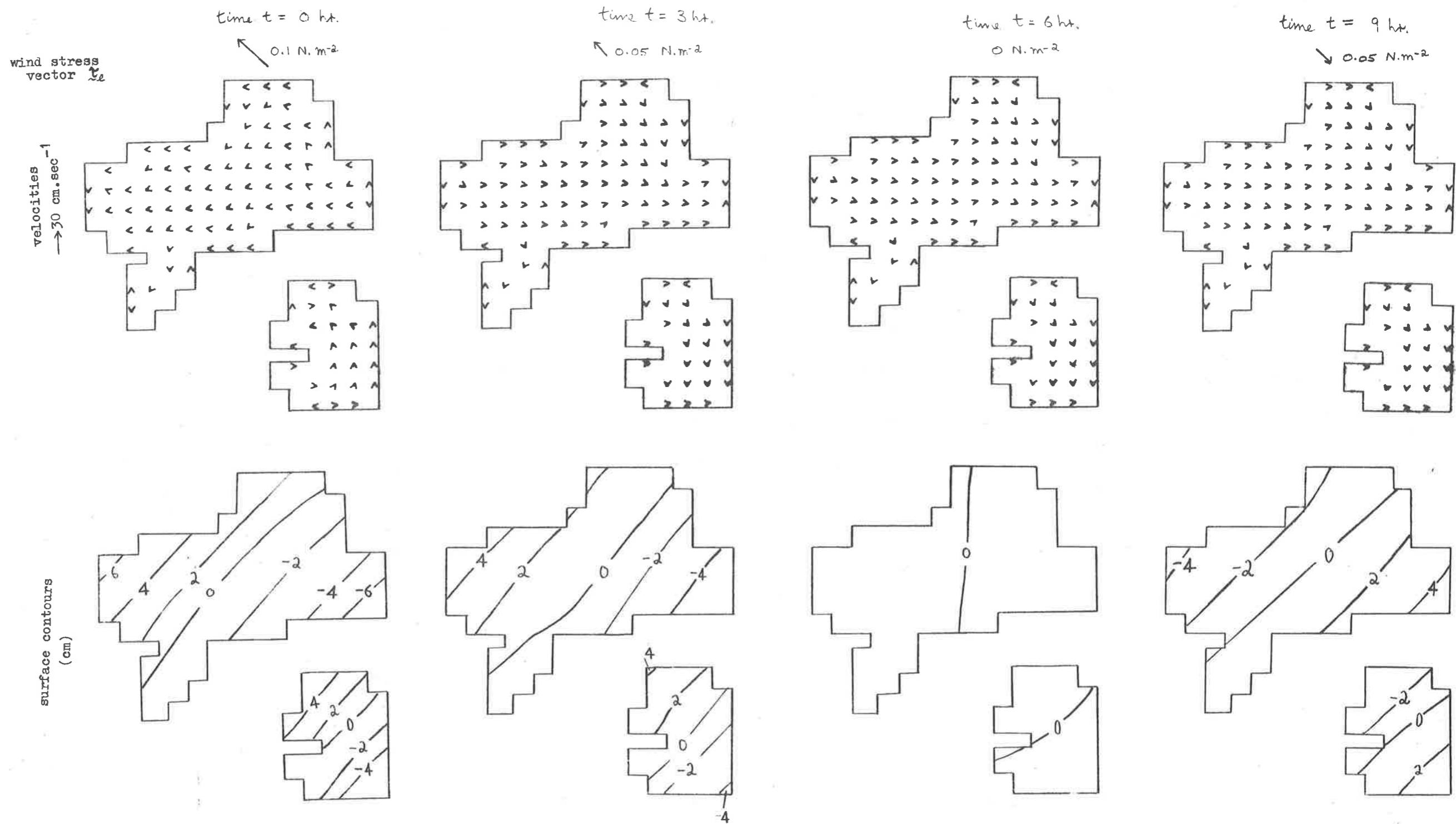
FIGURE 5.16 : (b) RESPONSE OF THE UNCOMBINED SYSTEM TO THE SAME WIND STRESS.
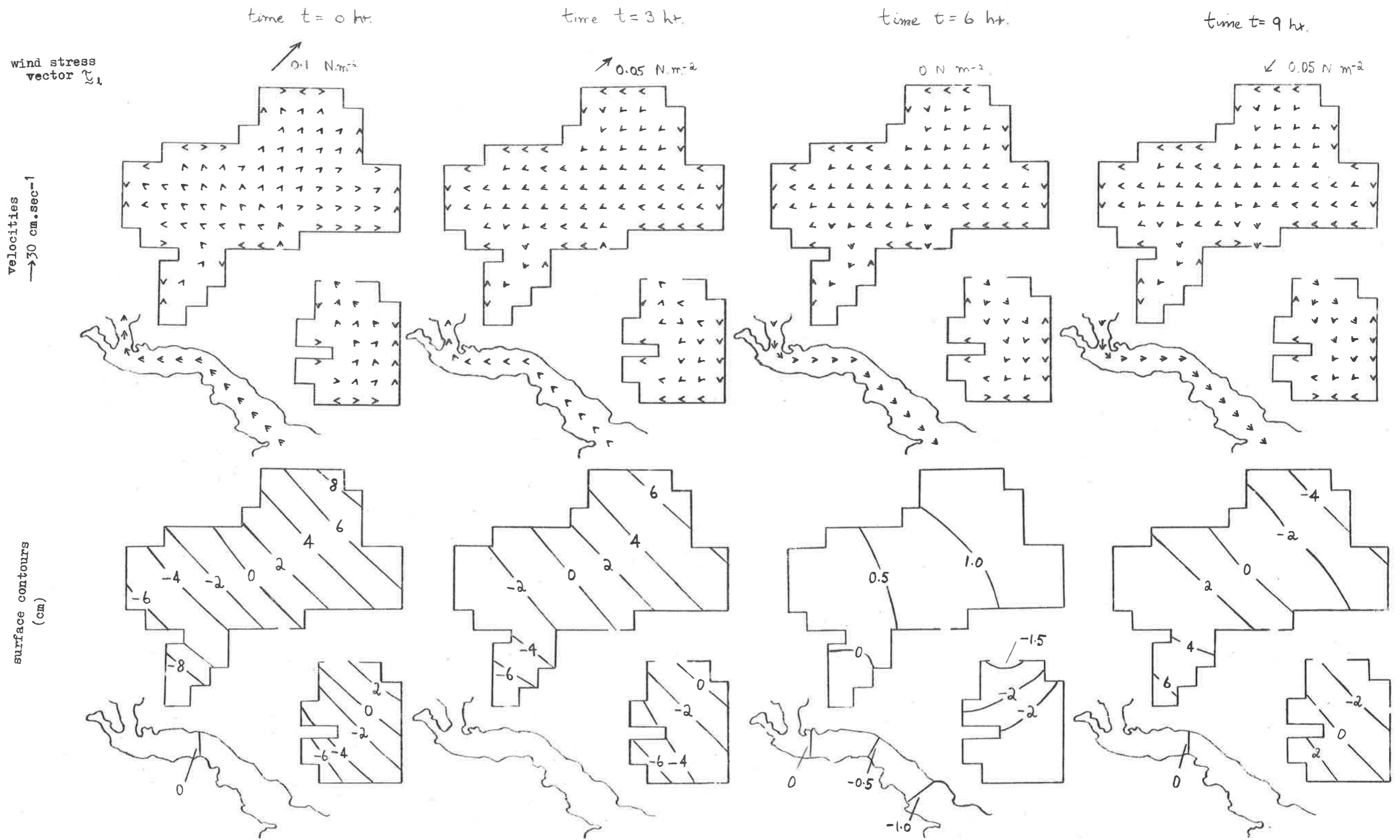
FIGURE 5.17 : RESPONSE OF THE COMBINED SYSTEM TO A WIND STRESS OF THE FORM $\tau_\ell \cos(2\pi t/T)$ WITH SOUTH-WEST ALIGNMENT AND T=1 DAY, $\tau_\ell =$ 0.1 N.m^{-2} . (AT TIME 6 hrs, CONTOUR INTERVAL IS 0.5 cm.)
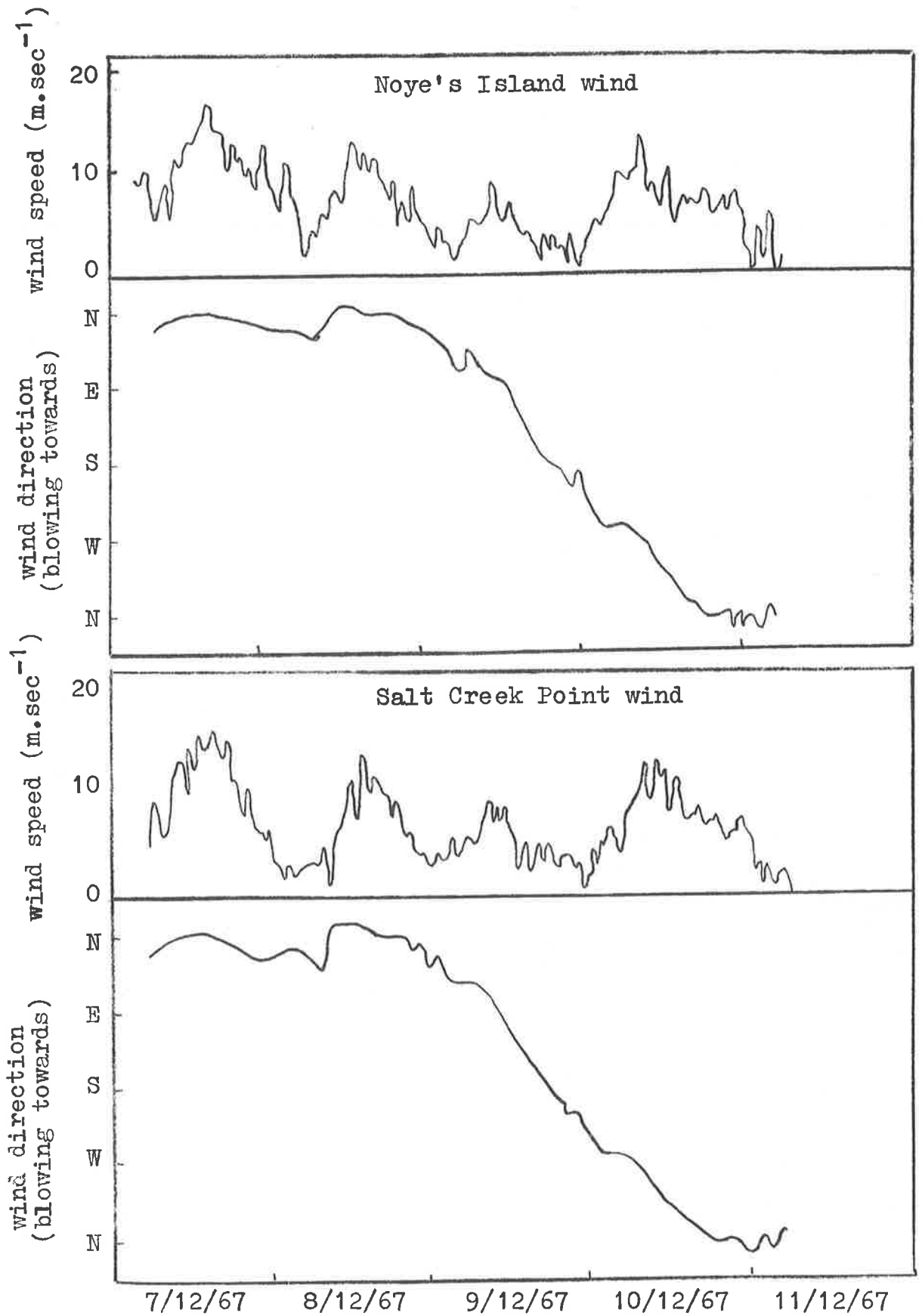
FIGURE 5.18 : EXAMPLE OF A ROTATING WIND — SOUTH
COORONG, DECEMBER 1967 .

time t = 0 hr.

time t = 3 hr.

time t = 6 hr.

time t = 9 hr.

wind stress vector τ_ℓ

velocities

surface contours (cm)
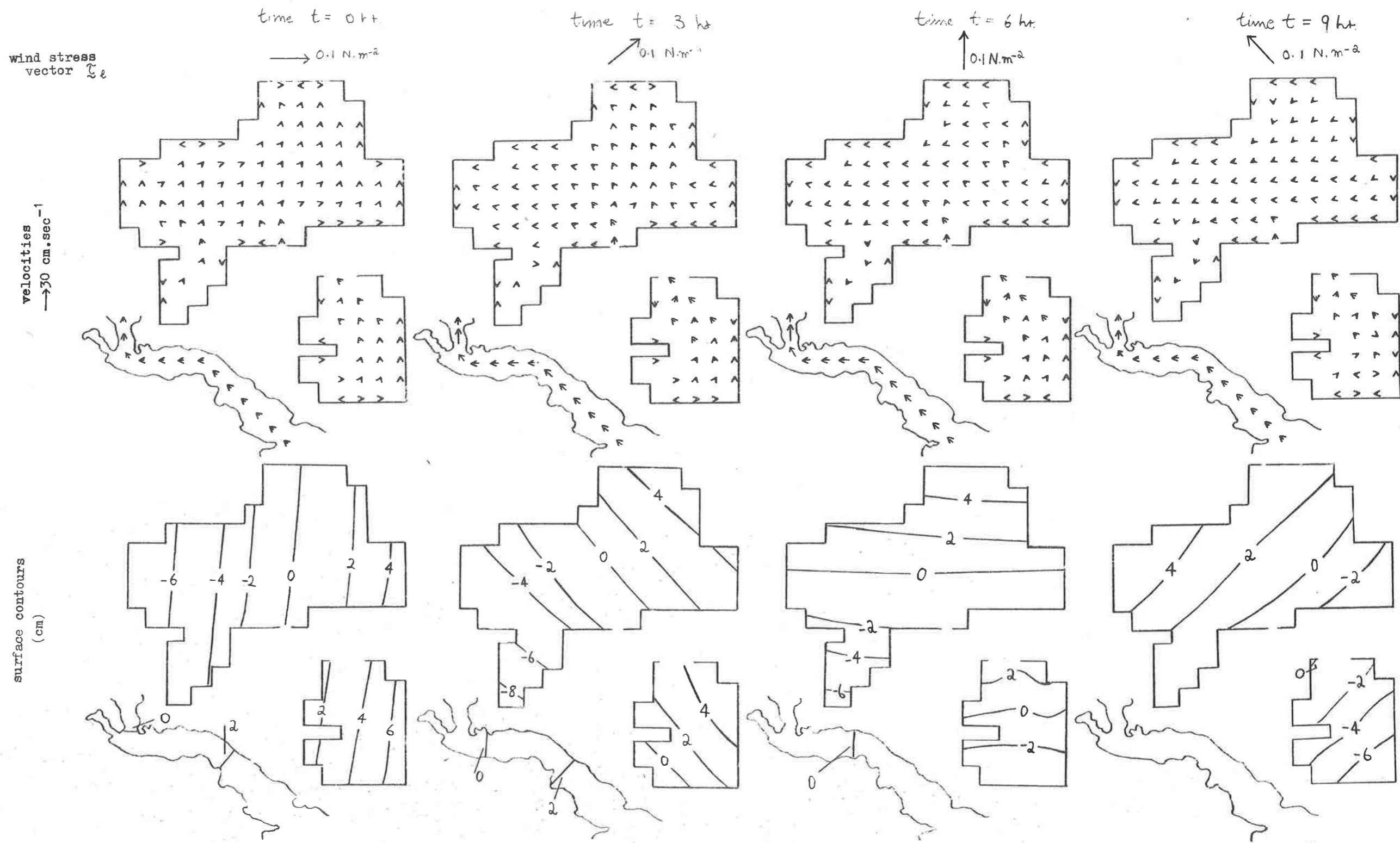
FIGURE 5.19 : RESPONSE OF THE COMBINED SYSTEM TO A COUNTER-CLOCKWISE ROTATING WIND WITH STRENGTH 0.1 N.m^{-2}.

CHAPTER 6

WIND EFFECTS ON STRATIFIED LAKES

6.1 Introduction

As mentioned earlier, the waters of the Murray Mouth lakes are well-mixed throughout the seasonal cycle. This is due to a combination of the intense surface heating to which they are subjected for most of the year and the extreme shallowness of the lakes. Shallowness permits the effects of wind-induced convective and diffusive mixing to be felt even in the deepest regions ($\sim$ 4.5m) of the lakes.

However, since the analytical methods of the previous chapters are applicable to stably stratified as well as to homogeneous fluids, it is worthwhile, for the sake of completeness, to devote a single chapter to wind effects on stratified lakes.

Where stratification (i.e. density variation) does occur it results largely from temperature (rather than salinity) differences within the fluid. (For simplicity, we neglect the extremely difficult area of convection currents). Often, a region of high temperature gradient, known as the thermocline, forms the interface between two approximately homogeneous layers of fluid. The Great Lakes, for example, have an annual cycle of partial winter freezing (during which time the fluid is relatively homogeneous) followed by summer heating, with a resultant warming of surface waters and hence thermocline formation. The process of thermocline formation in the Great Lakes is described in detail by Harleman et al. (1964). The difference in density between the two layers is slight; a

density difference typical of summer conditions in Lake Michigan is

2 kgm.m^{-3}, the density in the upper layer being about 998 kgm.m^{-3} and the

density in the lower layer about 1000 kgm.m^{-3}. Temperature differences

are more marked; typically in Lake Michigan the upper layer temperature

varies between 18°C and 22°C while temperatures in the lower layer vary

between 4°C and 6°C.

So it appears that a simple yet physically realistic model of a

stratified lake is that in which two homogeneous layers with a small

density difference are separated by an interfacial region of zero thick-

ness. In this chapter we confine ourselves to a consideration of this

model.

One of the major theoretical difficulties is that of determining a

suitable condition at the interface. The difficulty results from the fact

that the process of turbulent diffusion at a density discontinuity is not

well understood. A common assumption is that frictional stress in the

interfacial region is negligible. Proudman (1953), p. 101 comments:

> "When [the density gradient] is very great, there will be very
> little vertical turbulence, and hence very little vertical
> mixing or internal friction across horizontal surfaces. In the
> limiting case of a surface of discontinuity of density, it [is
> normally], for the sake of simplicity, ... assumed that there
> is neither mixing nor friction across the surface."

Fig. 6.1 shows the plan and vertical section of the general two-

layered basin under consideration. For purposes of simplicity we restrict

our attention to a lake for which both total depth h_2 and the depth h_1 of

the undisturbed interface between the two layers are constant. Coordinate
axes are positioned as for the homogeneous lake of Fig. 2.1. The basin is
acted on by the wind stress vector $\underset{\sim}{\tau}_s = (\tau_{sx}, \tau_{sy})$ where the components are
known functions of x, y and t.

The equations of motion and continuity again assume <u>in each layer</u>
<u>separately</u> the form (2.1.1), provided the approximations used in arriving
at the form (2.1.1) are assumed valid for each layer. We use subscript
1 to denote quantities in the upper layer, subscript 2 to denote quanti-
ties in the lower layer (e.g. densities ρ_1, ρ_2).

In the upper layer, the fluid pressure $p_1(x,y,z,t)$ is again of the
form (2.1.3), viz.

$$p_1 = p_a + \rho_1 g(\zeta_1 - z).$$

However in the lower layer the fluid pressure $p_2(x,y,z,t)$ assumes at the
surface a value equal to the value of p_1 at the bottom of the upper layer.
Hence p_2 takes the form

$$p_2 = p_a + \rho_2 g(\zeta_2 - h_1 - z) + \rho_1 g(\zeta_1 + h_1 - \zeta_2).$$

Similarly, the vertical velocity $w_1(x,y,z,t)$ is again approximately equal
to $\frac{\partial \zeta_1}{\partial t}$ at the surface of the upper layer. At the surface of the lower
layer (bottom of the upper layer) however, vertical velocities $w_1(x,y,z,t)$,
$w_2(x,y,z,t)$ are both equal to $\frac{\partial \zeta_2}{\partial t}$.

Thus in each layer the equations of motion and continuity assume a
form analogous to the form (2.1.4) valid for the homogeneous lake, viz.

for the upper layer:

$$\frac{\partial u_1}{\partial t} - f v_1 = -g \frac{\partial \zeta_1}{\partial x} + \frac{1}{\rho_1} \frac{\partial (\tau_{xz})_1}{\partial z} \qquad (6.1.1a)$$

$$\frac{\partial v_1}{\partial t} + f u_1 = -g \frac{\partial \zeta_1}{\partial y} + \frac{1}{\rho_1} \frac{\partial (\tau_{yz})_1}{\partial z} \qquad (6.1.6b)$$

$$\int_{-h_1}^{0} \frac{\partial u_1}{\partial x} \, dz + \int_{-h_1}^{0} \frac{\partial v_1}{\partial y} \, dz = \frac{\partial \zeta_2}{\partial t} - \frac{\partial \zeta_1}{\partial t} \quad . \qquad (6.1.1c)$$

for the lower layer:

$$\frac{\partial u_2}{\partial t} - f v_2 = -g\{(1-\varepsilon) \frac{\partial \zeta_1}{\partial x} + \varepsilon \frac{\partial \zeta_2}{\partial x}\} + \frac{1}{\rho_2} \frac{\partial (\tau_{xz})_2}{\partial z} \qquad (6.1.1d)$$

$$\frac{\partial v_2}{\partial t} + f u_2 = -g\{(1-\varepsilon) \frac{\partial \zeta_1}{\partial y} + \varepsilon \frac{\partial \zeta_2}{\partial y}\} + \frac{1}{\rho_2} \frac{\partial (\tau_{yz})_2}{\partial z} \qquad (6.1.1e)$$

$$\int_{-h_2}^{-h_1} \frac{\partial u_2}{\partial x} \, dz + \int_{-h_2}^{-h_1} \frac{\partial v_2}{\partial y} \, dz = - \frac{\partial \zeta_2}{\partial t} \quad . \qquad (6.1.1f)$$

Here, the quantity $\varepsilon = 1-\rho_1/\rho_2$ is a 'small' parameter, i.e. $\varepsilon = o(1)$. We note that the equations are coupled in the dependent variables $\zeta_1(x,y,t)$ and $\zeta_2(x,y,t)$ which presents difficulties in determining solutions.

As with the equations valid for the homogeneous lake, one may simplify the equations using either the eddy viscosity method or the volume transport method. We confine ourselves to a treatment of the simpler transport method. (Heaps and Ramsbottom (1966) have considered both forms of the resultant equations in a treatment of the response of a narrow, two-layered lake to a suddenly imposed wind stress).

Thus, defining components of volume transport for each layer as

$$U_1(x,y,t) = \int_{-h_1}^{0} u_1 dz, \quad V_1(x,y,t) = \int_{-h_1}^{0} v_1 dz$$

$$U_2(x,y,t) = \int_{-h_2}^{-h_1} u_2 dz, \quad V_2(x,y,t) = \int_{-h_2}^{-h_1} v_2 dz,$$

then vertical integration of the above equations of motion gives

$$\frac{\partial U_1}{\partial t} - fV_1 = -gh_1 \frac{\partial \zeta_1}{\partial x} + \frac{1}{\rho_1} (\tau_{sx} - \tau_{ix}) \tag{6.1.2a}$$

$$\frac{\partial V_1}{\partial t} + fU_1 = -gh_1 \frac{\partial \zeta_1}{\partial y} + \frac{1}{\rho_1} (\tau_{sy} - \tau_{iy}) \tag{6.1.2b}$$

$$\frac{\partial U_2}{\partial t} - fV_2 = -g(h_2-h_1) \left\{ (1-\epsilon) \frac{\partial \zeta_1}{\partial x} + \epsilon \frac{\partial \zeta_2}{\partial x} \right\} + \frac{1}{\rho_2} (\tau_{ix} - \tau_{bx})$$

$$\tag{6.1.2c}$$

$$\frac{\partial V_2}{\partial t} + fU_2 = -g(h_2-h_1) \left\{ (1-\epsilon) \frac{\partial \zeta_1}{\partial y} + \epsilon \frac{\partial \zeta_2}{\partial y} \right\} + \frac{1}{\rho_2} (\tau_{iy} - \tau_{by})$$

$$\tag{6.1.2d}$$

$$\frac{\partial U_1}{\partial x} + \frac{\partial V_1}{\partial y} = \frac{\partial \zeta_2}{\partial t} - \frac{\partial \zeta_1}{\partial t} \tag{6.1.2e}$$

$$\frac{\partial U_2}{\partial x} + \frac{\partial V_2}{\partial y} = - \frac{\partial \zeta_2}{\partial t} \tag{6.1.2f}$$

where $\underset{\sim}{\tau}_i = (\tau_{ix}, \tau_{iy})$ is the interfacial stress vector and $\underset{\sim}{\tau}_b = (\tau_{bx}, \tau_{by})$ is the bottom stress vector. We make here similar assumptions to those made in the vertical integration to produce (2.1.9). The equations are subject to the usual lateral boundary condition of zero flow normal to the lake contour, Γ, viz.

$$S_{1n} = S_{2n} = 0 \text{ along } \Gamma \qquad\qquad (6.1.2g)$$

where $\underset{\sim}{S}_1 = (U_1, V_1)$, $\underset{\sim}{S}_2 = (U_2, V_2)$.

We may, following Proudman (1954), Heaps and Ramsbottom (1966), and by analogy with expression (2.1.11c) for the homogeneous lake, assume for the bottom stress vector the form

$$\underset{\sim}{\tau}_b = \rho_2 r \underset{\sim}{S}_2 / (h_2 - h_1) = 2\alpha\rho_2 \underset{\sim}{S}_2 \qquad\qquad (6.1.3a)$$

where r is constant. Furthermore, on the basis of our previous discussion,

$$\underset{\sim}{\tau}_i = \underset{\sim}{0} \quad . \qquad\qquad (6.1.3b)$$

Combining (6.1.2), (6.1.3) thus gives

$$\frac{\partial U_1}{\partial t} - fV_1 = -gh_1 \frac{\partial \zeta_1}{\partial x} + \frac{1}{\rho_1} \tau_{sx} \qquad\qquad (6.1.4a)$$

$$\frac{\partial V_1}{\partial t} + fU_1 = -gh_1 \frac{\partial \zeta_1}{\partial y} + \frac{1}{\rho_1} \tau_{sy} \qquad\qquad (6.1.4b)$$

$$\frac{\partial U_2}{\partial t} + 2\alpha U_2 - fV_2 = -g(h_2 - h_1) \left\{ (1-\epsilon) \frac{\partial \zeta_1}{\partial x} + \epsilon \frac{\partial \zeta_2}{\partial y} \right\} \quad (6.1.4c)$$

$$\frac{\partial V_2}{\partial t} + 2\alpha V_2 + fU_2 = -g(h_2 - h_1) \left\{ (1-\epsilon) \frac{\partial \zeta_1}{\partial y} + \epsilon \frac{\partial \zeta_2}{\partial y} \right\} \quad (6.1.4d)$$

$$\frac{\partial U_1}{\partial x} + \frac{\partial V_1}{\partial y} = \frac{\partial \zeta_2}{\partial t} - \frac{\partial \zeta_1}{\partial t} \qquad\qquad (6.1.4e)$$

$$\frac{\partial U_2}{\partial x} + \frac{\partial V_2}{\partial y} = - \frac{\partial \zeta_2}{\partial t} \qquad\qquad (6.1.4f)$$

subject to

$$S_{1n} = S_{2n} = 0 \text{ along } \Gamma \quad . \qquad\qquad (6.1.4g)$$

In the following two sections we provide some simple solutions to (6.1.4) utilizing the theory of response function and the methods built up over previous chapters.

6.2 A Solution for 'Narrow' Two-Layered Lakes

Let us first solve the system (6.1.4) for the case of a rectangular (constant depth) non-rotating basin over which the wind stress acts always parallel to one of the two lake axes - the x-axis (Fig. 3.1). The results obtained from an analysis of this situation are clearly most applicable to elongated, two-layered lakes for which the 'narrow lake' approximation is satisfied in each layer, i.e. only the component of wind stress, $\tau_s(x,t)$, acting along the lake axis significantly influences wind effects in the basin, and the effects of the Coriolis force may be neglected.

The 'narrow lake' assumptions enable (6.1.4) to be written as

$$\frac{\partial U_1}{\partial t} = -c_1^2 \frac{\partial \zeta_1}{\partial x} + \frac{1}{\rho_1} \tau_s \qquad (6.2.1a)$$

$$\frac{\partial U_2}{\partial t} + 2\alpha U_2 = -(c_2^2 - c_1^2) \left\{ (1-\epsilon) \frac{\partial \zeta_1}{\partial x} + \epsilon \frac{\partial \zeta_2}{\partial x} \right\} \qquad (6.2.1b)$$

$$\frac{\partial U_1}{\partial x} = \frac{\partial \zeta_2}{\partial t} - \frac{\partial \zeta_1}{\partial t} \qquad (6.2.1c)$$

$$\frac{\partial U_2}{\partial x} = - \frac{\partial \zeta_2}{\partial t} \qquad (6.2.1d)$$

subject to

$$U_1 = U_2 = 0 \text{ at } x = 0, L \qquad (6.2.1e)$$

where $c_{1,2} = (gh_{1,2})^{1/2}$.

Firstly, we eliminate $U_1(x,t)$, $U_2(x,t)$ from (6.2.1) and obtain partial differential equations for both $\zeta_1(x,t)$, $\zeta_2(x,t)$ in terms of the forcing function $\tau_s(x,t)$. This may be done in the following manner.

Elimination of $U_1(x,t)$ between (6.2.1a), (6.2.1c) gives

$$\frac{\partial^2 \zeta_2}{\partial t^2} - \frac{\partial^2 \zeta_1}{\partial t^2} + c_1^2 \frac{\partial^2 \zeta_1}{\partial x^2} = \frac{1}{\rho_1} \frac{\partial \tau_s}{\partial x} \qquad (6.2.2a)$$

while eliminating $U_2(x,t)$ between (6.2.1b), (6.2.1d) gives

$$\frac{\partial^2 \zeta_2}{\partial t^2} + 2\alpha \frac{\partial \zeta_2}{\partial t} + (c_1^2 - c_2^2) \frac{\partial^2}{\partial x^2} \{(1-\epsilon)\zeta_1 + \epsilon \zeta_2\} = 0. \qquad (6.2.2b)$$

Further, elimination of $\zeta_2(x,t)$ between (6.2.2a), (6.2.2b) gives

$$\left[\frac{\partial^4}{\partial t^4} - c_2^2 \frac{\partial^4}{\partial t^2 \partial x^2} + 2\alpha \frac{\partial}{\partial t} \left(\frac{\partial^2}{\partial t^2} - c_1^2 \frac{\partial^2}{\partial x^2} \right) - \epsilon c_1^2 (c_1^2 - c_2^2) \frac{\partial^4}{\partial x^4} \right] \zeta_1$$

$$= - \frac{1}{\rho_1} \frac{\partial}{\partial x} \left(\frac{\partial^2}{\partial t^2} + \epsilon (c_1^2 - c_2^2) \frac{\partial^2}{\partial x^2} + 2\alpha \frac{\partial}{\partial x} \right) \tau_s \qquad (6.2.3a)$$

while eliminating $\zeta_1(x,t)$ between (6.2.2a), (6.2.2b) gives

$$\left[\frac{\partial^4}{\partial t^4} - c_2^2 \frac{\partial^4}{\partial t^2 \partial x^2} + 2\alpha \frac{\partial}{\partial t} \left(\frac{\partial^2}{\partial t^2} - c_1^2 \frac{\partial^2}{\partial x^2} \right) - \epsilon c_1^2 (c_1^2 - c_2^2) \frac{\partial^4}{\partial x^4} \right] \zeta_2$$

$$= \frac{(1-\epsilon)(c_1^2 - c_2^2)}{\rho_1} \frac{\partial^3 \tau_s}{\partial x^3} . \qquad (6.2.3b)$$

Equations (6.2.3a), (6.2.3b) may be solved using the same methods employed in the one-dimensional case of Section 3.2. Specifically, given again a wind stress field of the form (3.2.5), i.e. periodic in time and with constant unit strength across the lake surface, the steady state surface and interface responses are given by

$$\zeta_1(x,t) = \frac{4e^{j\omega t}}{L\rho_1} \sum_{n=1}^{\infty} \{(\omega^2 - 2j\alpha\omega + \epsilon(c_1^2 - c_2^2)\kappa_{2n-1}^2)\cos(\kappa_{2n-1}x)/\nu_n\} \qquad (6.2.4a)$$

$$\zeta_2(x,t) = -4(1-\epsilon)(c_1^2 - c_2^2)e^{j\omega t} \sum_{n=1}^{\infty} \{\kappa_{2n-1}^2 \cos(\kappa_{2n-1}x)/\nu_n\} \qquad (6.2.4b)$$

where $\nu_n(\omega) = \omega^4 - c_2^2\omega^2\kappa_{2n-1}^2 - 2j\alpha\omega(\omega^2 - c_1^2\kappa_{2n-1}^2) - \epsilon c_1^2(c_1^2 - c_2^2)\kappa_{2n-1}^4$.

It is clear that a two-layered lake subject to wind stress forcing may be considered as two interdependent systems, each with input consisting of surface wind stress measured at station x_o, and one with output $\zeta_1(x_o,t)$, the other with output $\zeta_2(x_o,t)$. Further, from (6.2.4) we may define response functions $Z_1(x_o,\omega)$, $Z_2(x_o,\omega)$ for the respective systems.

It is noted that, except for very large values of angular frequency, ω, and damping parameter, α, the interface response has much greater magnitude than the surface response, i.e. $|Z_2| \gg |Z_1|$, a result alluded to in Section 1.2. In fact, since

$$Z_1(x,0) = \frac{-4}{L\rho_1 c_1^2} \sum_{n=1}^{\infty} \frac{\cos(\kappa_{2n-1}x)}{\kappa_{2n-1}^2} \equiv \frac{(x-L/2)}{g\rho_1 h_1} \ , x \epsilon[0,L]$$

$$\hspace{9cm} (6.2.5a)$$

$$Z_2(x,0) = \frac{4(1-\epsilon)}{L\rho_1 c_1^2 \epsilon} \sum_{n=1}^{\infty} \frac{\cos(\kappa_{2n-1}x)}{\kappa_{2n-1}^2} \equiv \frac{-(1-\epsilon)(x-L/2)}{\epsilon g\rho_1 h_1} \ , x \epsilon[0,L]$$

$$\hspace{9cm} (6.2.5b)$$

and also since typically $\epsilon = O(10^{-3})$, then

$$|Z_1(x,0)/Z_2(x,0)| = O(10^{-3}) \ .$$

Such large movements of the thermocline constitute one of the most conspicuous features of the summer behaviour of the Great Lakes (Csanady (1968a)). The movements may be detected even by a casual observer through the upwelling of cold water from the lower layer. Such an upwelling is always associated with an appropriate wind pattern which, if

strong enough, may even cause the thermocline to intersect the surface. Under such conditions, of course, the interface response becomes highly non-linear; we chose to ignore non-linearities of this type in our formulation of the equations (6.1.4).

From (6.2.5) it is clear that the surface and interface equilibrium responses are both planar, with slopes $1/g\rho_1 h_1$ and $-(1-\epsilon)/\epsilon g \rho_1 h_1$ respectively. We note that the equilibrium interface slopes in the opposite direction to the equilibrium surface, as shown in Fig. 1.3b.

Resonant frequencies for $Z_1(x_o, \omega), Z_2(x_o, \omega)$ are identical and may be obtained by solution of

$$\omega^4 - c_2^2 \omega^2 \kappa_{2n-1}^2 - \epsilon c_1^2 (c_1^2 - c_2^2) \kappa_{2n-1}^4 = 0, \quad n=1,2, \ldots$$

i.e.

$$(\phi_{1n,2n})^2 = \frac{1}{2} c_2^2 \kappa_{2n-1}^2 \left[1 \pm \{1 + 4\epsilon \left(\frac{h_1}{h_2}\right) (\left(\frac{h_1}{h_2}\right) - 1)\}^{1/2}\right]. \quad (6.2.6)$$

Since $\left(\frac{h_1}{h_2}\right) - 1 < 0$, then both ϕ_{1n}^2, ϕ_{2n}^2 are positive. Hence for each positive integer n, there exists a pair of resonance peaks about the resonant peak at $\omega = c_2 \kappa_{2n-1} \equiv \omega_{2n-1}$ for the equivalent homogeneous lake with depth h_2.

These two resonant frequencies are very widely spaced, however. Clearly, we have

$$(\phi_{1n})^2 = \omega_{2n-1}^2 + O(\epsilon^2)$$

$$(\phi_{2n})^2 = \omega_{2n-1}^2 \left\{\epsilon \left(\frac{h_1}{h_2}\right)\left(1 - \left(\frac{h_1}{h_2}\right)\right)\right\} + O(\epsilon^2)$$

so that

$$\frac{\phi_{1n}}{\phi_{2n}} \sim \epsilon^{-1/2} \left\{ \left(\frac{h_1}{h_2} \right) \left(1 - \left(\frac{h_1}{h_2} \right) \right) \right\} \gg 1 \quad .$$

The resonant frequencies ϕ_{1n}, ϕ_{2n} are the frequencies of the normal free modes of the two-layered basin. The modes ϕ_{1n} are known as the bartotropic or external modes of the basin (Veronis (1956), Csanady (1967)) since they are close to the free modes that would exist without stratification. The modes ϕ_{2n} are known as baroclinic or internal modes, and are approximately the free modes that would exist in a homogeneous lake of length L and 'equivalent depth' $h' = \epsilon h_1 (h_2 - h_1)/h_2$.

For the stratified Lake Windermere, Heaps and Ramsbottom (1966) take $h_1 = 15m$, and $h_2 = 36m$, while typically $\rho_1 = 999$ kgm.m^{-3} and $\rho_2 = 1000$ kgm.m^{-3}. Further, the basin is sufficiently elongated for the 'narrow lake' approximation to be applied.

In Fig. 6.2a are shown the gain and phase-lag of the surface response $Z_1(x_O, \omega)$ (as calculated from (6.2.4a)) at station $x_O = 0.75L$, for the frequency ranges 0 - 24 cpd and 108 - 132 cpd. Values of α for which the responses are shown are 0 sec^{-1} and 10^{-4} sec^{-1}. In Fig. 6.2b are shown the gain and phase-lag of interface response (as calculated from (6.2.4b)) at the same station and over the same frequency range. The gains in each have been normalized against the respective zero frequency gains, viz. 0.0112m for the surface gain and 11.2m for the interface gain.

Now the first barotropic resonant frequency for Lake Windermere is approximately 122.9 cpd, while the baroclinic resonance peaks occur at odd multiples of 1.92 cpd. Thus 32 baroclinic resonance peaks precede the

first barotropic resonance peak.

The dominant feature of the surface response as shown in Fig. 6.2a is the intensity of the first barotropic mode relative to the baroclinic modes preceding it. In fact the baroclinic resonance peaks close to the first barotropic peak appear almost as infinitesimal 'spikes' superimposed on the barotropic response. Similarly the interface response is dominated by the baroclinic modes. The evidence of Fig. 6.2 points to the general conclusion that the maximum displacements associated with the barotropic modes occur at the surface (hence the alternative name external) while for the baroclinic (internal) modes, maximum displacements occur at the interface. Such a conclusion may also be reached by 'a priori' means (refer, for example, Csanady (1967)).

6.3 A Generalized Theory

Let us construct a theory, analogous to that of Chapter 4, for wind effects on two-layered, closed basins of arbitrary contour and constant depth. Again assume that wind stress components $\tau_{sx}(x,y,t)$, $\tau_{sy}(x,y,t)$ have the form (4.1.2), from which it follows that steady state surface response and transport components in each layer have the form (4.1.3).

Thus system (6.1.3) becomes

$$j\omega P_1 - fQ_1 = -c_1^2 \frac{\partial Z_1}{\partial x} + K_1 \tau_{ox} \tag{6.3.1a}$$

$$j\omega Q_1 + fP_1 = -c_1^2 \frac{\partial Z_1}{\partial y} + K_1 \tau_{oy} \tag{6.3.1b}$$

$$\beta_2 P_2 - f Q_2 = -(c_2^2 - c_1^2) \frac{\partial}{\partial x} \{(1-\epsilon)Z_1 + \epsilon Z_2\} \tag{6.3.1c}$$

$$\beta_2 Q_2 + f P_2 = -(c_2^2 - c_1^2) \frac{\partial}{\partial y} \{(1-\epsilon)Z_1 + \epsilon Z_2\} \tag{6.3.1d}$$

$$\frac{\partial P_1}{\partial x} + \frac{\partial Q_1}{\partial y} = j\omega(Z_2 - Z_1) \tag{6.3.1e}$$

$$\frac{\partial P_2}{\partial x} + \frac{\partial Q_2}{\partial y} = -j\omega Z_2 \tag{6.3.1f}$$

where (as indicated previously) subscript 1 refers to the upper layer, subscript 2 to the lower layer and we have $K_1 = 1/\rho_1, \beta_2 = (j\omega + 2\alpha)$.

From (6.3.1) we obtain

$$P_1 = \frac{1}{(f^2 - \omega^2)} \{K_1(j\omega\tau_{ox} + f\tau_{oy}) - c_1^2(j\omega \frac{\partial}{\partial x} + f \frac{\partial}{\partial y}) Z_1\} \tag{6.3.2a}$$

$$Q_1 = \frac{1}{(f^2 - \omega^2)} \{K_1(j\omega\tau_{oy} - f\tau_{ox}) - c_1^2(j\omega \frac{\partial}{\partial y} - f \frac{\partial}{\partial x}) Z_1\}$$

$$P_2 = \frac{-(c_2^2 - c_1^2)}{(f^2 + \beta_2^2)} \left[\beta_2 \frac{\partial}{\partial x} + f \frac{\partial}{\partial y}\right] \{(1-\epsilon) Z_1 + \epsilon Z_2\} \tag{6.3.2c}$$

$$Q_2 = \frac{(c_2^2 - c_1^2)}{(f^2 + \beta_2^2)} \left[f \frac{\partial}{\partial x} - \beta_2 \frac{\partial}{\partial y}\right] \{(1-\epsilon) Z_1 + \epsilon Z_2\}. \tag{6.3.2d}$$

Finally, combining (6.3.1e), (6.3.1f) with (6.3.2) gives

$$\nabla^2 Z_1 + \ell_1^2 (Z_1 - Z_2) = \frac{K_1}{j\omega c_1^2} (j\omega D + fC) \tag{6.3.3a}$$

$$\nabla^2\{(1-\epsilon)Z_1 + \epsilon Z_2\} + \ell_2^2 Z_2 = 0 \tag{6.3.3b}$$

where D, C are defined by (4.1.7) and further

$$\ell_1^2 = \frac{(\omega^2 - f^2)}{c_1^2} , \quad \ell_2^2 = \frac{-j\omega\beta_2(1 + f^2/\beta_2^2)}{(c_2^2 - c_1^2)} .$$

Equations (6.3.3a), (6.3.3b) are coupled in the unknowns $Z_1(x,y,\omega)$,

$Z_2(x,y,\omega)$ just as the original equations for the upper layer ((6.1.1.) a-c) and lower layer ((6.1.1.)d-f) are coupled in the unknowns $\zeta_1(x,y,t)$, $\zeta_2(x,y,t)$. We achieve some simplification by assuming, as in Chapter 4, that the wind stress field is homogeneous over the lake surface, so $D = C = 0$, and (6.3.3b) becomes

$$\nabla^2 Z_1 + \ell_1^2 (Z_1 - Z_2) = 0 .$$
(6.3.3c)

It then remains to uncouple (6.3.3b), (6.3.3c). This may be done in a manner similar to that of Charney (1955), Veronis (1956) and Csanady (1967). In their equations, however, damping forces in the bottom layer are neglected, so that $\beta_2 = j\omega$. Essentially, if (6.3.3c) is multiplied by an unknown, σ, and the resultant equation added to (6.3.3b) we obtain

$$\nabla^2 \{\sigma Z_1 + (1-\varepsilon) Z_1 + \varepsilon Z_2\}$$
$$+ \sigma \ell_1^2 (Z_1 - Z_2) + \ell_2^2 Z_2 = 0.$$
(6.3.4)

Now σ is chosen so that the quantities $\{\sigma Z_1 + (1-\varepsilon) Z_1 + \varepsilon Z_2\}$, $\{\sigma \ell_1^2 (Z_1 - Z_2) + \ell_2^2 Z_2\}$ are in proportion, i.e.

$$\mu^2 \{\sigma Z_1 + (1-\varepsilon) Z_1 + \varepsilon Z_2\} = \{\sigma \ell_1^2 (Z_1 - Z_2) + \ell_2^2 Z_2\}$$

which is satisfied if

$$\mu^2 [\sigma + (1-\varepsilon)] = \sigma \ell_1^2$$

$$\mu^2 \varepsilon = \ell_2^2 - \sigma \ell_1^2 .$$

Thus σ must satisfy the quadratic equation

$$\sigma^2 + \sigma(1-\delta) - \delta(1-\varepsilon) = 0$$
(6.3.5)

where $\delta = \ell_2^2 / \ell_1^2$. (Note that (6.3.5) is equivalent to (22) of Charney

(1955) if $\beta_2 = j\omega$, when δ becomes equivalent to $h_1/(h_2-h_1)$). The roots of (6.3.5) are

$$\sigma_{1,2} = \frac{1}{2}(\delta-1) \pm \left[\frac{1}{4}(\delta-1)^2 + \delta(1-\epsilon)\right]^{1/2} \qquad (6.3.6a)$$

so that

$$(\mu_{1,2})^2 = \frac{\ell_1^2(\delta-\sigma_{1,2})}{\epsilon} . \qquad (6.3.6b)$$

Defining Z_3, Z_4 by

$$Z_3 = (\sigma_1+1-\epsilon)Z_1 + \epsilon Z_2 \qquad (6.3.7a)$$

$$Z_4 = (\sigma_2+1-\epsilon)Z_1 + \epsilon Z_2 \qquad (6.3.7b)$$

then (6.3.4) gives

$$(\nabla^2+\mu_1^2)Z_3 = 0 \qquad (6.3.8a)$$

$$(\nabla^2+\mu_2^2)Z_4 = 0 \qquad (6.3.8b)$$

i.e. (6.3.4) has been uncoupled into a pair of tractable equations. Finally, $Z_1(x,y,\omega)$ and $Z_2(x,y,\omega)$ may be recovered from

$$Z_1 = \frac{Z_3-Z_4}{\sigma_1-\sigma_2} \qquad (6.3.9a)$$

$$Z_2 = \frac{(\sigma_1+1-\epsilon)Z_4-(\sigma_2+1-\epsilon)Z_3}{\epsilon(\sigma_1-\sigma_2)} . \qquad (6.3.9b)$$

Charney (1955) shows that for the case in which $\beta_2 = j\omega$, i.e. neglecting damping forces in the bottom layer, then the transformation $(Z_1, Z_2) \rightarrow (Z_3,Z_4)$ is, in fact, a separation of the motion into its normal modes, i.e. the barotropic (external) and baroclinic (internal) modes.

System (6.3.8) may be regarded as the generalization of (4.1.10) to the case of a two-layered lake. Further, appropriate boundary conditions analogous to (4.1.9c) are not difficult to achieve.

For the upper layer we have that

$$(S_1^*)_n = 0 \text{ along } \Gamma$$

where $\underline{S}_1^* = (P_1, Q_1)$, which is shown, in the manner of Section 4.1 for the boundary condition in the homogeneous case, to be equivalent to

$$(j\omega \frac{\partial z_1}{\partial n} + f \frac{\partial z_1}{\partial e})_\Gamma = \frac{K_1}{c_1^2} (j\omega\tau_{on} + f\tau_{oe})_\Gamma. \tag{6.3.10a}$$

Similarly, from

$$(S_2^*)_n = 0 \text{ along } \Gamma$$

we have that

$$[(\beta_2 \frac{\partial}{\partial n} + f \frac{\partial}{\partial e}) \{(1-\epsilon)z_1 + \epsilon z_2\}]_\Gamma = 0. \tag{6.3.10b}$$

It is not in general possible to uncouple (6.3.10) so that boundary conditions are obtained in terms of $z_3(x,y,\omega)$, $z_4(x,y,\omega)$ alone. However, having found general solutions to (6.3.8a) and (6.3.8b), then use of (6.3.9a) and substitution into (6.3.10) easily allows the appropriate arbitrary constants to be determined.

Let us now briefly examine some particularization of this method.

(a) The Rectangular Lake

For simplifcation we shall again neglect the Coriolis force, and suppose that the wind stress acts always parallel to the x-axis, so that the problem becomes equivalent to that of Section 6.1.

Then, (6.3.8a), (6.3.8b) become

$$\left(\frac{\partial^2}{\partial x^2} + \mu_1^2\right) Z_3 = 0 \qquad (6.3.11a)$$

$$\left(\frac{\partial^2}{\partial x^2} + \mu_2^2\right) Z_4 = 0 \qquad (6.3.11b)$$

subject to

$$\frac{\partial Z_1}{\partial x} = \frac{K_1 \tau_0}{c_1^2} \text{ at } x = 0, L \qquad (6.3.11c)$$

$$\frac{\partial}{\partial x} \{(1-\varepsilon)Z_1 + \varepsilon Z_2\} = 0 \text{ at } x = 0, L. \qquad (6.3.11d)$$

In this case we __may__ express the end conditions (6.3.11c), (6.3.11d) in terms of $Z_3(x,\omega)$ and $Z_4(x,\omega)$ alone. Clearly we obtain

$$\frac{\partial Z_3}{\partial x} = \frac{\sigma_1 K_1 \tau_0}{c_1^2} \text{ at } x = 0, L \qquad (6.3.11e)$$

$$\frac{\partial Z_4}{\partial x} = \frac{\sigma_2 K_1 \tau_0}{c_1^2} \text{ at } x = 0, L . \qquad (6.3.11f)$$

The solutions to (6.3.11a), (6.3.11b) satisfying (6.3.11e), (6.3.11f) respectively are

$$Z_3(x,\omega) = \frac{\sigma_1 K_1 \tau_0 \sin\{\mu_1(x-L/2)\}}{c_1^2 \mu_1 \cos(\mu_1 L/2)} \qquad (6.3.12a)$$

$$Z_4(x,\omega) = \frac{\sigma_2 K_1 \tau_0 \sin\{\mu_2(x-L/2)\}}{c_1^2 \mu_2 \cos(\mu_2 L/2)} , \qquad (6.3.12b)$$

and thus, from (6.3.9), we have

$$Z_1(x,\omega) = \frac{K_1 \tau_0}{c_1^2(\sigma_1 - \sigma_2)} \left[\frac{\sigma_1 \sin\{\mu_1(x-L/2)\}}{\mu_1 \cos(\mu_1 L/2)} - \frac{\sigma_2 \sin\{\mu_2(x-L/2)\}}{\mu_2 \cos(\mu_2 L/2)} \right]$$

$$(6.3.13a)$$

$$Z_2(x,\omega) = \frac{K_1\tau_0}{c_1^2(\sigma_1-\sigma_2)}\left[\frac{(\sigma_1+1-\epsilon)\sigma_2\sin\{\mu_2(x-L/2)\}}{\mu_2\cos(\mu_2L/2)}\right.$$

$$\left. - \frac{(\sigma_2+1-\epsilon)\sigma_1\sin\{\mu_1(x-L/2)\}}{\mu_1\cos(\mu_1L/2)}\right]. \qquad (6.3.13b)$$

Expressions (6.3.13a), (6.3.13b) may be expanded as Fourier cosine-series over the range $[0,L]$ and be shown to be completely equivalent to the expressions for $Z_1(x,\omega)$, $Z_2(x,\omega)$ obtained from (6.2.4).

Result (6.3.13) is, further, the two-layered equivalent of (4.3.3). Since we are not specifically interested in stratified lakes, however, we shall not dwell on its properties.

(b) The Circular Lake

Let us retain the Coriolis term in this case and assume, as in the homogeneous case of Section 4.4, that the wind stress always acts in the direction $\theta = 0$. Again, polar co-ordinates are used; the radius of the basin is denoted by a.

The general solutions to (6.3.8a), 6.3.8b) then become

$$Z_3(r,\theta,\omega) = J_1(\mu_1r)(A_3\cos\theta+B_3\sin\theta) \qquad (6.3.14a)$$

$$Z_4(r,\theta,\omega) = J_1(\mu_2r)(A_4\cos\theta+B_4\sin\theta) \qquad (6.3.14b)$$

so that (6.3.9) gives

$$Z_1(r,\theta,\omega) = [\cos\theta\{A_3J_1(\mu_1r) - A_4J_1(\mu_2r)\}$$

$$+ \sin\theta\{B_3J_1(\mu_1+) - B_4J_1(\mu_2r)\}]/(\sigma_1-\sigma_2) \qquad (6.3.15a)$$

$$Z_2(r,\theta,\omega) = [\{\sigma_1+1-\varepsilon\}J_1(\mu_2 r)(A_4\cos\theta+B_4\sin\theta)$$

$$- \{\sigma_2+1-\varepsilon\}J_1(\mu_1 r)(A_3\cos\theta+B_3\sin\theta)]/\varepsilon(\sigma_1-\sigma_2). \quad (6.3.15b)$$

Boundary condition (6.3.10) becomes

$$\left[j\omega\frac{\partial Z_1}{\partial r} + \frac{f}{r}\frac{\partial Z_1}{\partial \theta}\right]_{r=a} = \frac{K_1\tau_0}{c_1^2}(j\omega\cos\theta-f\sin\theta) \quad (6.3.16a)$$

$$\left[(\beta_2\frac{\partial}{\partial r} + \frac{f}{r}\frac{\partial}{\partial \theta})\{(1-\varepsilon)Z_1+\varepsilon Z_2\}\right]_{r=a} = 0. \quad (6.3.16b)$$

Combination of (6.3.15) and (6.3.16) allows a determination of the four constants to be made.

Again these results are not discussed here. It has been merely our intention in this chapter to show how readily applicable is the response function method to the analytical determination of wind effects on strati-fied lakes of simple form.
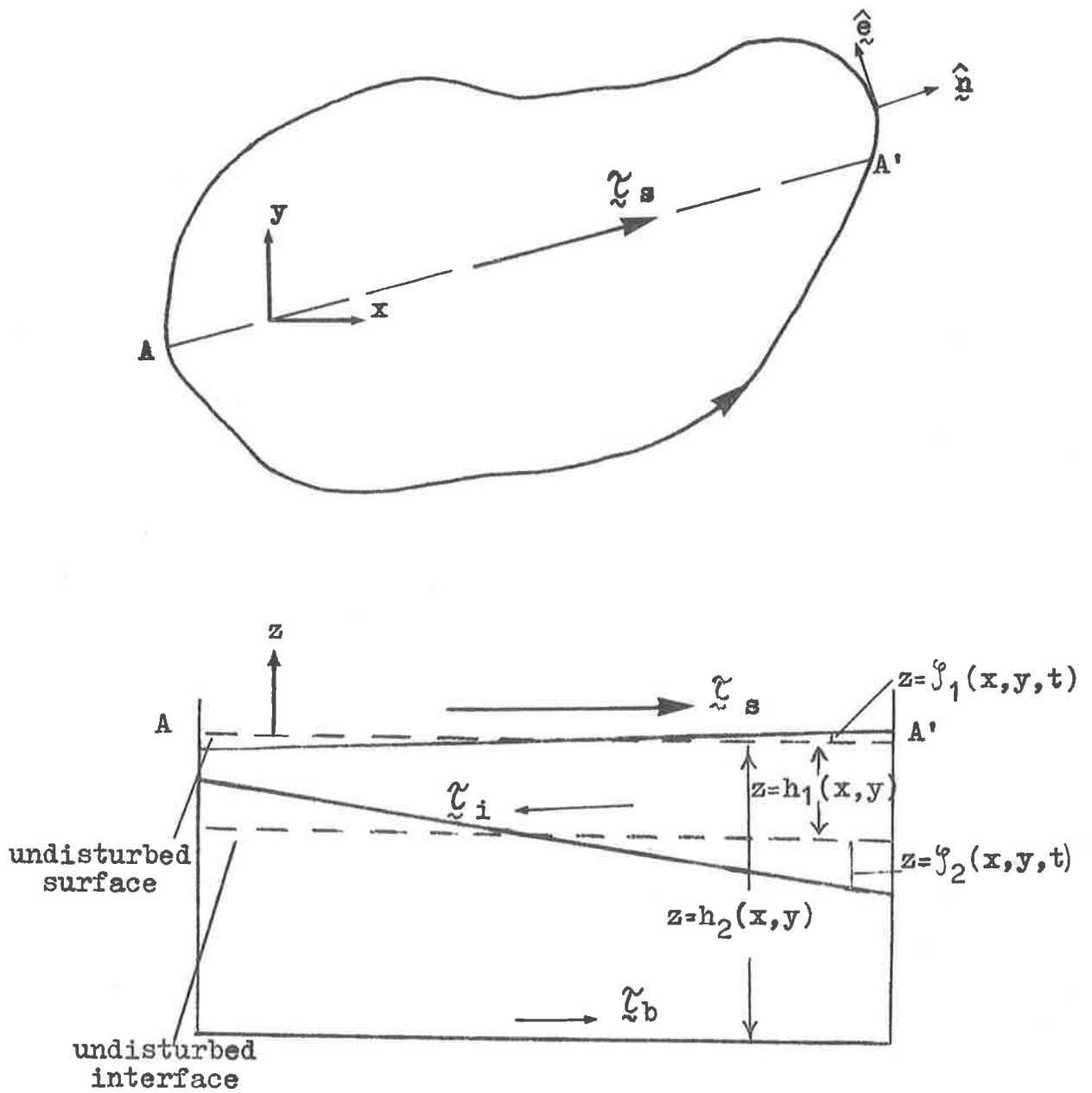
FIGURE 6.1 : PLAN AND SECTION OF CONSTANT DEPTH, TWO-LAYERED
LAKE ACTED ON BY WIND STRESS VECTOR $\underset{\sim}{\tau}_s$.

FIGURE 6.2 : (a) RESPONSE FUNCTIONS FOR SURFACE DISPLACEMENT OF LAKE
WINDERMERE AT STATION 0.75L WITH (i)α=0 sec^{-1}, (ii)α=
10^{-4} sec^{-1} . GAINS HAVE BEEN NORMALIZED WITH RESPECT TO
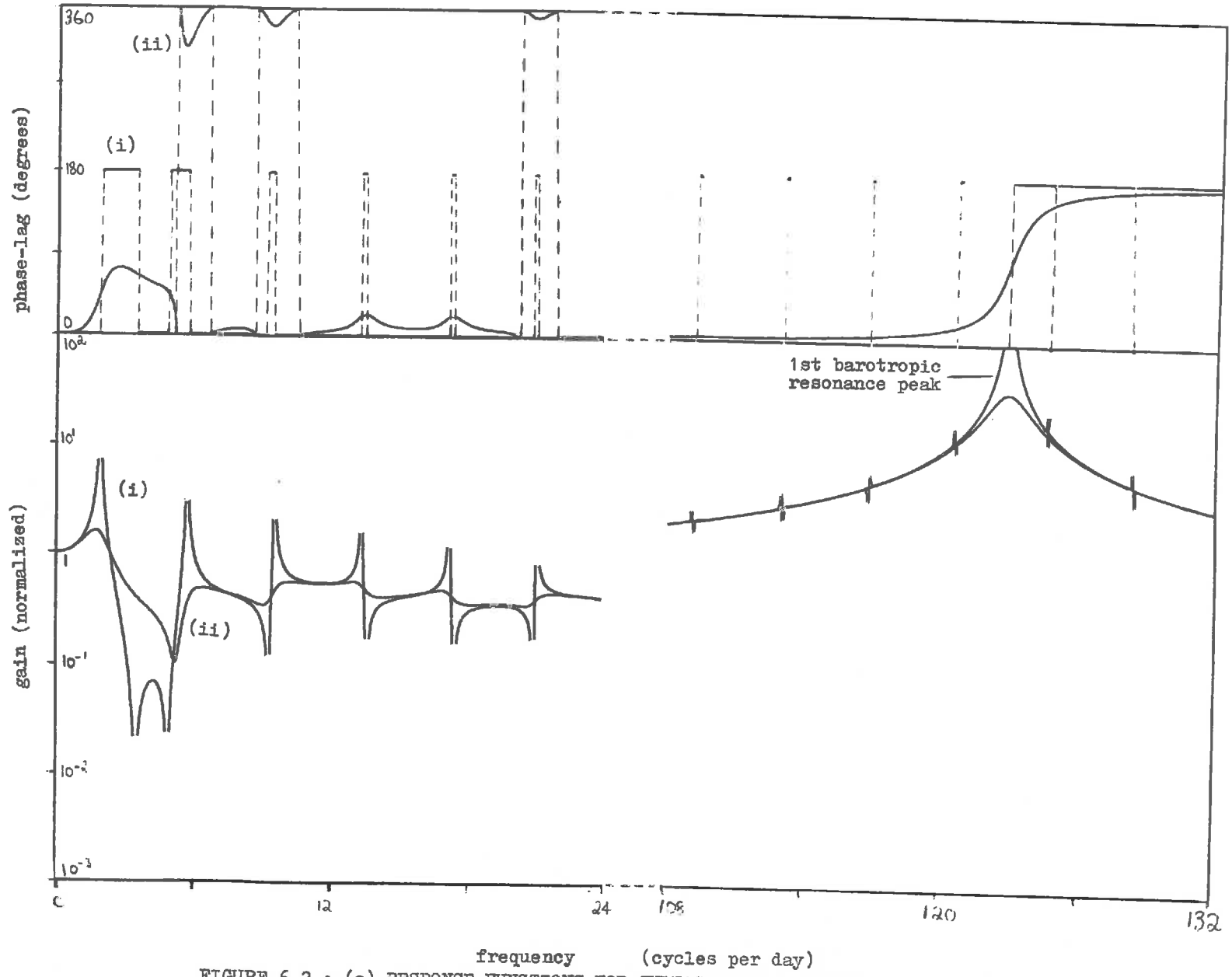THE EQUILIBRIUM RESPONSE, VIZ. 0 0112 m .
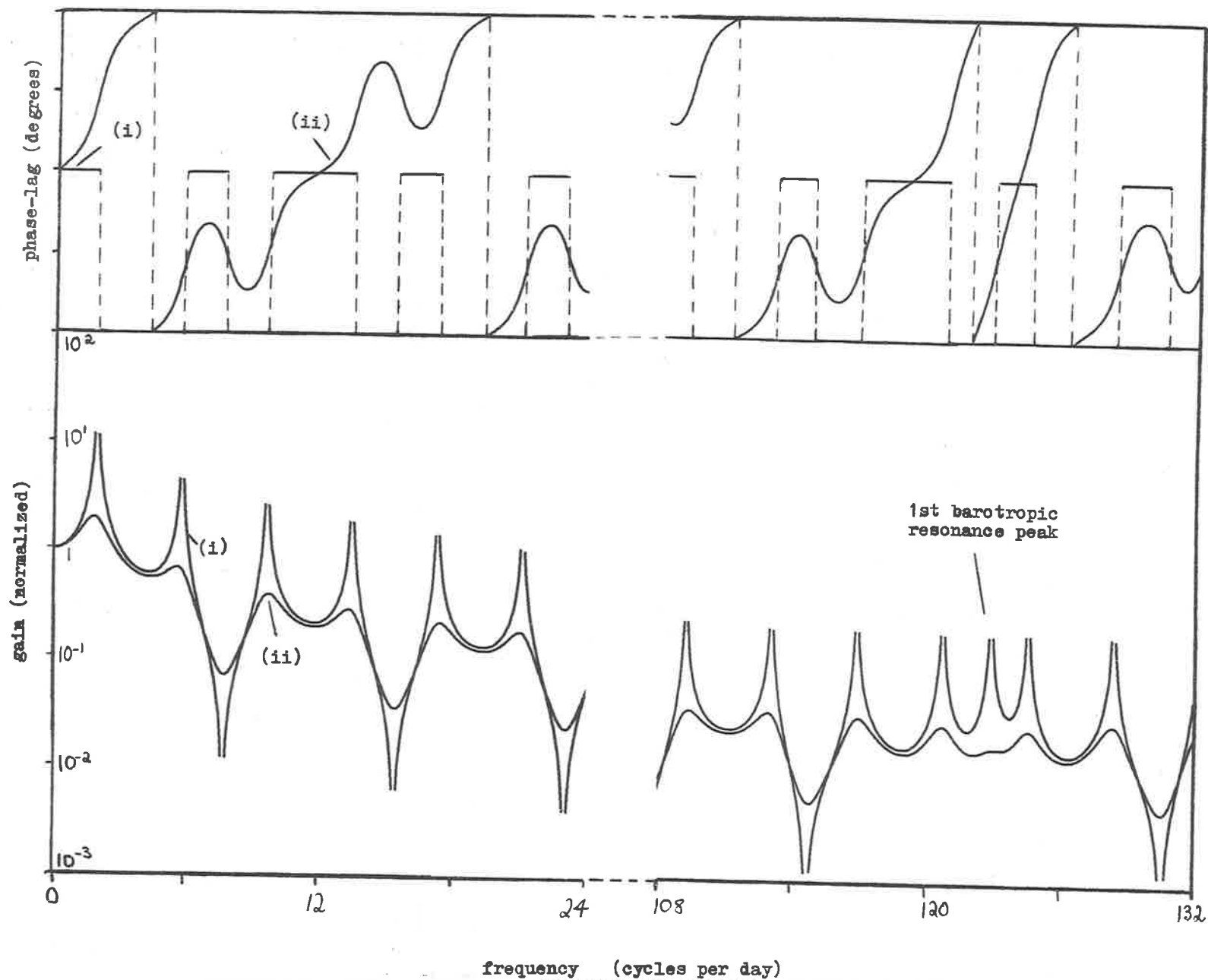
FIGURE 6.2 : (b) RESPONSE FUNCTIONS FOR INTERFACE DISPLACEMENT OF LAKE
WINDERMERE AT STATION 0.75L WITH (i) $\alpha=0$ sec^{-1}, (ii) $\alpha=$
10^{-4} sec-1 . GAINS HAVE BEEN NORMALIZED WITH RESPECT TO
THE EQUILIBRIUM RESPONSE, VIZ. 11.2 m .

CHAPTER 7

WIND EFFECTS ON CONNECTED LAKE SYSTEMS

7.1 Introduction

In Chapter 5 we examined, by means of numerical modelling, wind-induced flow exchange between Lakes Albert and Alexandrina through the Narrung channel. It was shown that channel velocities were always much larger than velocities in the separate lakes, regardless of the direction of the surface wind stress acting on the system. The narrow opening known as Hell's Gate which connects the North and South Coorong lagoons is similarly characterized by high velocities. Measurements taken by Noye (1970) led him to conclude, however, that any efflux of water through Hell's Gate has only slight effects on the mean level in the two separate lagoons.

In this chapter we examine, from an analytic point of view, the question of the degree to which two lakes, joined by an opening or channel, act independently of each other in their reaction to wind stress forcing.

Consider, for example, the two rectangular lakes shown in Fig. 7.1, divided by a partition at $x = L_1$, with an opening of width ϵ' (not necessarily 'small'). The two lakes have the same constant depth, H, and are acted on by a wind stress $\tau_s(t)$ blowing always parallel to the x-axis. We shall ignore the effect of the Coriolis force.

It was shown in Chapter 4 that for a closed basin of constant depth the form of the boundary contour does not affect the equilibrium surface slope, provided some damping forces act within the lake. Applying this

result to the total system of Fig. 7.1 we thus have, remarkably, that the width of the opening does not influence the equilibrium response, provided ε' is non-zero.

Given that the wind stress has the form $\tau_s(t) = \tau_o e^{j\omega t}$, we may consider at what frequencies the two parts of the total system begin to exhibit independent behaviour. A variety of analytical techniques are at our disposal in the solution of this problem, and we may draw on analogies with other problems, both in hydrodynamics and related fields.

As an example, the phenomenon of harbour resonance has, over the past decade, received considerable attention since the paper of Miles and Munk (1961). Here, a bay or harbour is connected, through an opening, to an infinite ocean, and responds to incoming waves at the opening in much the same way as the two basins in Fig. 7.1 respond to surface wind stress. The main mechanism of energy loss in the harbour resonance problem occurs through radiation away from the mouth, and a major theoretical difficulty is that of determining how best to account for this energy loss. Problems of water wave transmission through openings such as breakwaters (Tuck (1971)) may also be seen as related to the present problem. Analogies may also be drawn with problems in acoustics - the coupling of rectangular cavities has been treated by Morse and Ingard (1970), §10.4 - as well as with waveguide problems in electromagnetics.

Let us attempt a direct solution to the problem of Fig. 7.1 where the wind stress is of the form $\tau_s = \tau_o e^{j\omega t}$ with τ_o constant. We shall consider firstly the left-hand basin alone. We kow that the steady state surface

response has the form

$$\zeta_1(x,y,t) = Z_1(x,y,\omega)e^{j\omega t}$$

where $Z_1(x,y,\omega)$ satisfies the Helmholtz equation

$$(\nabla^2 + k^2)Z_1 = 0 \qquad (7.1.1)$$

with $k^2 = (\omega^2 - 2j\alpha\omega)/c^2$; note that $k(\omega)$ in (7.1.1) is equivalent to $k_c(\omega)$ of (4.1.12a). Along the closed boundaries the relevant conditions are, from (4.1.9c), given by

$$\frac{\partial}{\partial y} Z_1(x,0) = \frac{\partial}{\partial y} Z_1(x,B_1) = 0, \quad x\epsilon[0,L_1] \qquad (7.1.2a)$$

$$\frac{\partial}{\partial x} Z_1(0,y) = T \qquad , y\epsilon[0,B_1] \qquad (7.1.2b)$$

$$\frac{\partial}{\partial x} Z_1(L_1,y) = T, y\epsilon[0,d] \text{ and } y\epsilon(d+\epsilon',B_1]. \qquad (7.1.2c)$$

with $T = K\tau_0/c^2$, $K = (1+m)/\rho$. Denoting by $P^*(y,\omega)$ the amplitude of the x-component of volume transport through the opening, then from (4.1.4a) with $f = 0$ we have, further, that

$$\frac{\partial}{\partial x} Z_1(L_1,y) = T - \frac{jk^2 P^*}{\omega}, \quad y\epsilon[d,d+\epsilon']. \qquad (7.1.2d)$$

Note that the possibility of a velocity discontinuity at the edges of the opening has not been excluded by these boundary conditions.

We make an initial simplification by means of the transformation

$$Z_1^* = Z_1 - T\frac{\sin\{k(x-L_1/2)\}}{k\cos(kL_1/2)} \qquad (7.1.3)$$

If $\epsilon' = 0$ then (from (4.3.3)) $Z_1 = T\sin\{k(x-L_1/2)\}/\{k\cos(kL_1/2)\}$ so $Z_1^*(x,y,\omega)$ represents the contribution to the surface response of the basin

which results from the opening itself.

Combining (7.1.1), (7.1.2), (7.1.3) gives

$$(\nabla^2+k^2)Z_1^* = 0 \qquad\qquad (7.1.4)$$

subject to

$$\frac{\partial}{\partial y} Z_1^*(x,0) = \frac{\partial}{\partial y} Z_1^*(x,B_1) = 0, x\epsilon[0,L_1] \qquad (7.1.5a)$$

$$\frac{\partial}{\partial y} Z_1^*(0,y) = 0, \; y\epsilon[0,B_1] \qquad\qquad (7.1.5b)$$

$$\frac{\partial}{\partial x} Z_1^*(L_1,y)= 0, \; y\epsilon[0,d] \text{ and } y\epsilon(d+\epsilon',B_1] \qquad (7.1.5c)$$

$$\frac{\partial}{\partial x} Z_1^*(L_1,y)= - \frac{jk^2 P^*}{\omega} , \; y\epsilon[d,d+\epsilon']. \qquad (7.1.5d)$$

A solution to (7.1.4) satisfying (7.1.5) is not difficult to find by separation of variables. It is

$$Z_1^* = \frac{jk}{B_1\omega} \; \{Q_1^* \; \frac{\cos(kx)}{\sin(kL_1)} \; -2k \sum_{n=1}^{\infty} Q_{1n}^* \; A_{1n} \; \cosh(\gamma_{1n}x)\cos(\theta_{1n}y)\} $$

$$(7.1.6)$$

where

$$\theta_{1n} = n\pi/B_1$$

$$\gamma_{1n}(\omega) = (\theta_{1n}^2-k^2)^{1/2}$$

$$A_{1n}(\omega) = 1/\{\gamma_{1n}\sinh(\gamma_{1n}L_1)\}, \; n = 1,2, \dots$$

and where the coefficients $Q_1^*(\omega)$, $Q_{1n}^*(\omega)$ are defined by

$$Q_1^*(\omega) = \int_d^{d+\epsilon'} P^* \; dy \qquad\qquad (7.1.7a)$$

$$Q_{1n}^*(\omega) = \int_d^{d+\epsilon'} P^* \cos(\theta_{1n}y)dy, \; n = 1,2, \dots \qquad . \qquad (7.1.7b)$$

$Q_1^*(\omega)$ is the total discharge through the opening and is an important physical parameter of the total system.

The solution to (7.1.1) subject to (7.1.2) is then simply

$$Z_1(x,y,\omega) = \frac{T\sin\{k(x-L_1/2)\}}{k\cos(kL_1/2)}$$

$$+ \frac{jk}{B_1\omega}\{Q_1^* \frac{\cos(kx)}{\sin(kL_1)} -2k \sum_{n=1}^{\infty} A_{1n}Q_{1n}^* \cosh(\gamma_{1n}x)\cos(\theta_{1n}y)\}.$$

(7.1.8a)

Similarly in the right-hand basin the solution is

$$Z_2(\overline{x},\overline{y},\omega) = \frac{T\sin\{k(\overline{x}-L_2/2)\}}{k\cos(kL_2/2)}$$

$$+ \frac{jk}{B_2\omega}\{Q_2^* \frac{\cos(k\overline{x})}{\sin(kL_2)} -2k \sum_{n=1}^{\infty} A_{2n}Q_{2n}^* \cosh(\gamma_{2n}\overline{x})\cos(\gamma_{2n}\overline{y})\}$$

(7.1.8b)

(with $\overline{x} = -x + L_1 + L_2$, $\overline{y} = y + s$), where θ_{2n}, γ_{2n}, A_{2n} are defined in a similar manner to θ_{1n}, γ_{1n}, A_{1n} and where

$$Q_2^*(\omega) = -\int_d^{d+\epsilon'} P^* \, dy = - Q_1^*(\omega) \equiv -Q^*(\omega) \qquad (7.1.9a)$$

$$Q_{2n}^*(\omega) = -\int_d^{d+\epsilon'} P^* \cos(\theta_{2n}y)dy, \quad n = 1,2, \ldots \qquad (7.1.9b)$$

Neither (7.1.8a) nor (7.1.8b) explicitly satisfies the respective boundary conditions at $x = \ell_1 (\overline{x} = \ell_2)$, i.e. the coefficients $Q_1^*(\omega)$ and $Q_{1n}^*(\omega)$ are unknown. A determination of the coefficients requires that these conditions be satisfied. In particular the two solutions must be matched across the opening. The matching condition, quite clearly, is that the amplitude of surface displacement should be continuous across the

opening, i.e.

$$Z_1(L_1,y,\omega) = Z_2(L_2,y+s,\omega), y\epsilon[d,d+\epsilon'].$$ (7.1.10)

In order to simplify this determination let us suppose that the two basins are identical (Fig. 7.2), so that $Q_{1n}^* = Q_{2n}^*$ $(\equiv Q_n^*)$. Further, we place a new set of horizontal co-ordinate axes as shown. Then (7.1.8a), (7.1.8b) may be written in terms of these coordinates as

$$Z_1(x,y,\omega) = \frac{T\sin\{k(x+L/2)\}}{k\cos(kL/2)}$$

$$+ \frac{jk}{B\omega}\{Q^*\frac{\cos(k(x+L))}{\sin(kL)} -2k\sum_{n=1}^{\infty} A_nQ_n^* \cosh(\gamma_n(x+L))\cos(\theta_ny)\}$$ (7.1.11a)

$$Z_2(x,y,\omega) = \frac{-T\sin\{k(-x+L/2)\}}{k\cos(kL/2)}$$

$$- \frac{jk}{B\omega}\{Q^*\frac{\cos(k(-x+L))}{\sin(kL)} -2k\sum_{n=1}^{\infty} A_nQ_n^* \cosh(\gamma_n(-x+L))\cos(\theta_ny)\}$$ (7.1.11b)

where $A_{1n} = A_{2n}$ $(\equiv A_n)$, $\gamma_{1n} = \gamma_{2n}$ $(\equiv \gamma_n)$. Clearly the problem is now reduced to a determination of the coefficients Q^* and Q_n^* for $n = 1,2, \ldots$. Further, it is clear that the amplitude of surface displacement is an odd function about $x = 0$, i.e. $Z_1(-x,y,\omega) = -Z_2(x,y,\omega)$. Hence the matching condition (7.1.10) reduces to

$$Z_1(0,y,\omega) = Z_2(0,y,\omega) = 0, y\epsilon[d,d+\epsilon'].$$ (7.1.12)

Thus in this simplified case we may obtain a solution for the total system by considering only the behaviour in the left-hand basin.

7.2 An Approximate Solution

Ippen and Raichlen (1961) in an early approach to the harbour resonance problem, considered the coupling of a small, highly reflective rectangular basin (modelling the harbour) to a large rectangular basin (the ocean) through an opening. They produced separate solutions in each basin which were then matched across the opening by assuming constant surface slope <u>across</u> the harbour entrance and equating the 'average' of each solution evaluated at the entrance.

In this section we use a similar method in considering the wind forced coupling of two identical rectangular basins. Specifically, we assume that $P^*(y,\omega)$ is constant across the opening between the two lakes. If $\varepsilon' = B$, i.e. the two basins are fully connected, then this approximation is exact. In fact, we know that in this case

$$P^* = K\tau_o - c^2 \left(\frac{\partial Z_1}{\partial x} \right)_{x=0}$$

$$= \frac{j\omega T \tan(kL/2)}{k^2 \cot(kL)} \quad . \tag{7.2.1}$$

More generally, when $\varepsilon' \neq B$ and P^* is a constant, P_o, it is clear that

$$Q^* = Q_o = \varepsilon' P_o \tag{7.2.2a}$$

$$Q_n^* = \frac{P_o \delta_n}{\theta_n} = \frac{Q_o \delta_n}{\varepsilon' \theta_n} \tag{7.2.2b}$$

where $\delta_n = \sin\{\theta_n(d+\varepsilon')\} - \sin\{\theta_n d\}$. Thus (7.1.11a) gives

$$Z_1(0,y,\omega) = \frac{T}{k} \tan(kL/2) + \frac{jkQ_o}{B\omega} \{\cot(kL) - \frac{2k}{\varepsilon'} \sum_{n=1}^{\infty} C_n \cos(\theta_n y)\}$$

$$\tag{7.2.3}$$

where $C_n(\omega) = A_n \delta_n \cosh(\gamma_n L)/\theta_n$. Now an approximation to the condition $Z_1(0,y,\omega) = 0, y\epsilon[d,d+\epsilon']$ is

$$\frac{1}{\epsilon'} \int_d^{d+\epsilon'} Z_1(0,y,\omega)dy = 0, \qquad (7.2.4)$$

i.e. the <u>average</u> displacement across the opening is zero. Combining (7.2.3), (7.2.4) gives

$$Q_o = \frac{j\omega BT\tan(kL/2)}{k^2(\cot(kL) - \frac{2k}{(\epsilon')^2} \sum_{n=1}^{\infty} D_n)} \qquad (7.2.5)$$

where $D_n(\omega) = C_n \delta_n/\theta_n$.

The infinite series in the denominator of (7.2.5) is convergent if $\epsilon' \neq 0$. When $\epsilon' = B$, for example, $D_n = 0$ so

$$P_o \left(= \frac{Q_o}{B}\right) = \frac{j\omega T\tan(kL/2)}{k^2\cot(kL)} \quad ,$$

equivalent to (7.2.1).

Finally, (7.1.11a) becomes

$$Z_1(x,y,\omega) = \frac{T\sin\{k(x+L/2)\}}{k\cos(kL/2)}$$

$$+ \frac{jkQ_o}{B\omega} \left\{ \frac{\cos(k(x+L))}{\sin(kL)} - \frac{2k}{\epsilon'} \sum_{n=1}^{\infty} E_n \cosh(\gamma_n(x+L))\cos(\theta_n y) \right\} \qquad (7.2.6)$$

where $E_n(\omega) = A_n \delta_n/\theta_n$.

Let us model the combined North Coorong - South Coorong system as two identical lakes, each with length 50km, breadth 2.5km and depth 1.25m, connected by an opening of width 100m which models the Hell's Gate channel. The length d is set to zero. The left hand basin may be said to act

independently of the right hand basin at a given frequency when the surface response function (gain and phase-lag) at each point along the axis of the left hand basin (except close to the opening) is almost equivalent to the surface response function at the identical point in the case when the two basins are unconnected.

In Fig. 7.3 we present the surface response function as determined from (7.2.6) for the Seven Mile Point station, equivalent in this instance to the point $(-L/4, B/2)$. For comparison, the response function for the Seven Mile Point station assuming the lakes are unconnected, is also presented here. In Fig. 7.4 the surface response function at the position $(-L/2, B/2)$ for the connected system is shown; for the unconnected system, the response is always zero at this position. Finally in Fig. 7.5, the gain and phase-lag of the discharge $Q_o(\omega)$ are presented.

Regardless of the value of the damping parameter α, it is clear that at sufficiently low frequencies the two lakes act as a single unit, exhibiting the familiar wind set-up along the axis of the combined system. Further, at higher frequencies and with $\alpha = 0$, there is a marked difference between the response of the connected and unconnected systems. The effect of an opening of non-zero width between two basins is to increase the possible number of normal modes and hence resonant frequencies within the component parts of the total system (Mei and Ünlüata (1973)). However, as $\omega \rightarrow \infty$, the magnitude of the discharge $Q_o(\omega) \rightarrow 0$, so that even with $\alpha = 0$ the influence of these 'connected' modes becomes minimal at sufficiently high frequencies and the two basins act independently of each other.

An increase in the damping parameter α in general causes a decrease in the discharge $Q_0(\omega)$ at each frequency, so the basins begin to respond independently of each other at lower frequencies. For sufficiently high α, they act essentially independently at almost all frequencies.

We have previously indicated that if the North Coorong is considered closed at Hell's Gate, the damping parameter α assumes a value of $0(2.5 \times 10^{-4} \; \sec^{-1})$. For such values our analysis indicates that the North and South Coorong basins behave largely independently at frequencies greater than 1 cpd. For example, at Seven Mile Point there is an equivalence between gains, the errors being at most 15%, while phase-lags also correspond closely. At the station $(-L/2, B/2)$, the gain of the connected system is low frequency dominated, the response at frequencies above about 2 cpd being very small. For diurnal frequencies there is a good first order agreement at Seven Mile Point between the gains of the connected and unconnected systems. However there is a phase difference magnitude of about 90° for this frequency. At frequencies much smaller than the diurnal (e.g. wind stresses involved in large scale storm cycles), it is clear that the separate basins act very much as one.

A brief mention should be made of alternative methods of solution to the problem presented in this chapter. One alternative involves deriving integral equations(in the case d=0) for $P^*(y,\omega)$, $y \epsilon [0, \epsilon']$ and $Z_1(0, y, \omega)$, $y \epsilon [\epsilon', B]$. Approximate solutions to these equations enable upper and lower bounds to be placed on the quantity $Q_0(\omega)$. Similar methods are used in electromagnetics (refer Jones (1964), §5.12)) and have recently been most successfully employed in water wave problems (Evans and Morris (1972)).

The method was applied to the present problem, though solutions were only possible for the restricted case $\alpha = 0$. The results confirmed that even when the width of the opening between the lakes is very small the degree of interaction between them may be considerable at certain frequencies.

Another alternative involves use of a 'small-hole' theory similar to that of Mei and Ünlüata (1973) used to study the harbour resonance problem. The general theory has recently been formalized by Tuck (1974). It was not attempted in the present instance, but may prove to be of great relevance in studying the related and more complicated problem of wind effects on basins connected by a straight channel.

We conclude at this stage our simplified analysis of wind effects on connected lakes. Results have shown that the conclusions of Noye (1970) regarding the effect of flows through Hell's Gate on water levels in the Coorong lagoons are generally correct, but this is only so because of the heavily damped nature of the system.
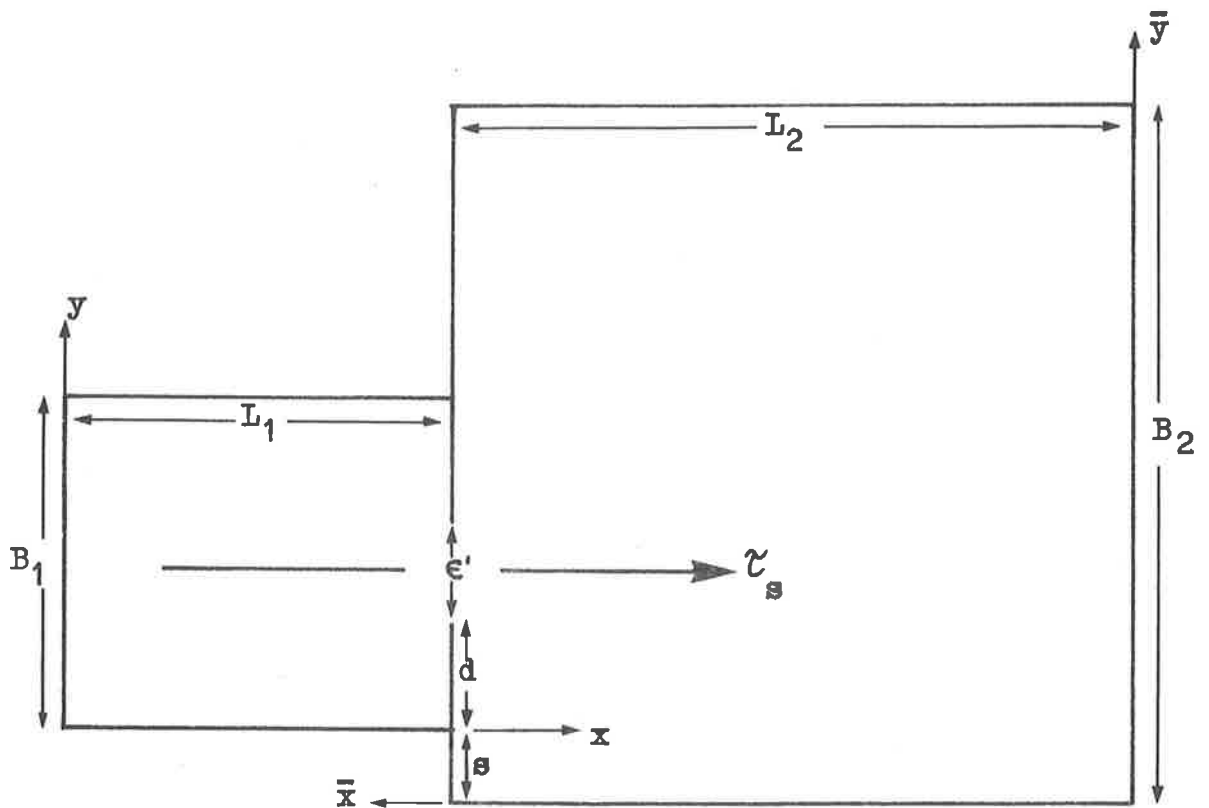
FIGURE 7.1 : ARBITRARY RECTANGULAR BASINS JOINED BY AN OPENING
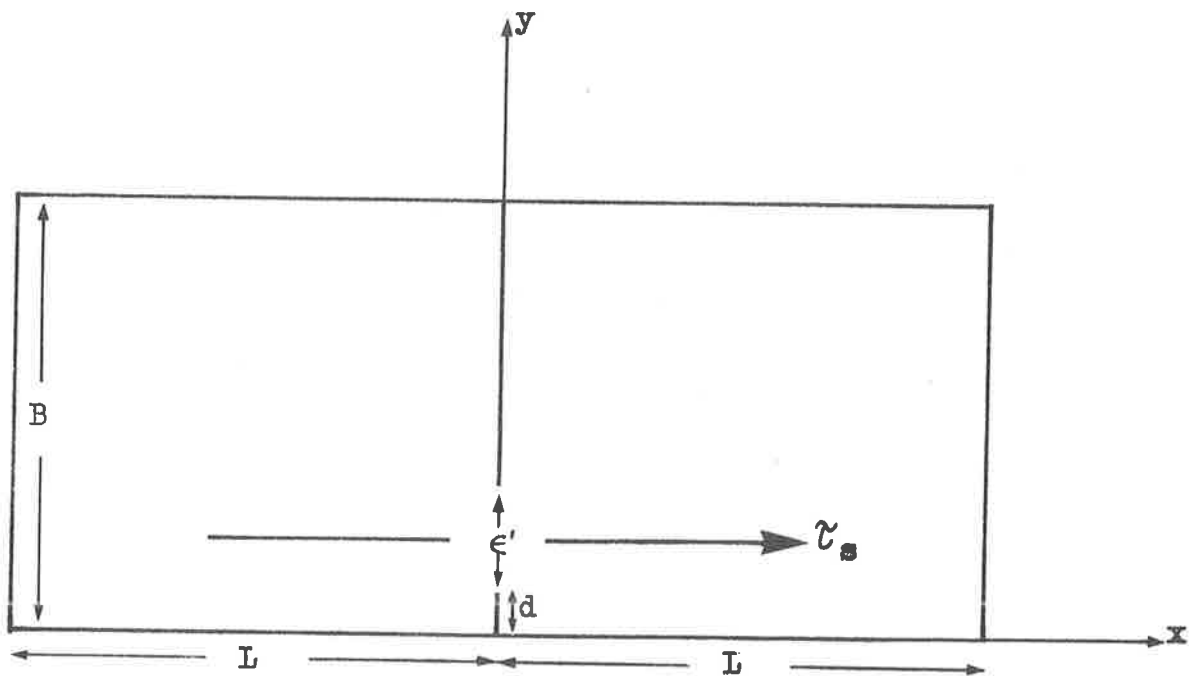OF WIDTH ϵ', ACTED ON BY WIND STRESS τ_s .

FIGURE 7.2 : IDENTICAL RECTANGULAR BASINS JOINED BY AN OPENING
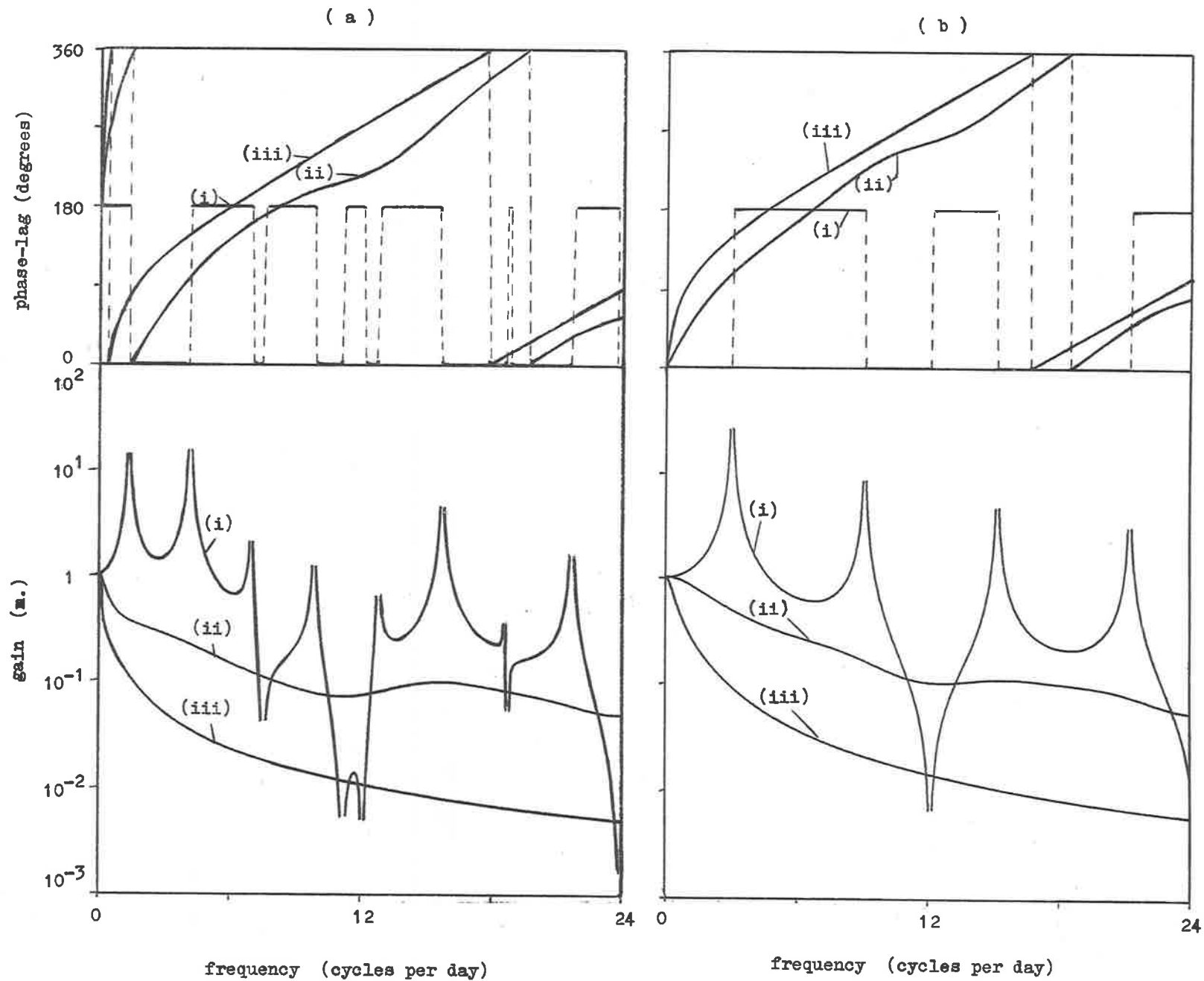OF WIDTH ϵ', ACTED ON BY WIND STRESS τ_s .

FIGURE 7.3 : RESPONSE FUNCTIONS FOR SURFACE DISPLACEMENT AT SEVEN MILE
POINT STATION FOR (a) CONNECTED SYSTEM, (b) UNCONNECTED
SYSTEM, WITH (i) 0 sec^{-1}, (ii) 2.5 x 10^{-4} sec^{-1},
(iii) 10^{-3} sec^{-1} .

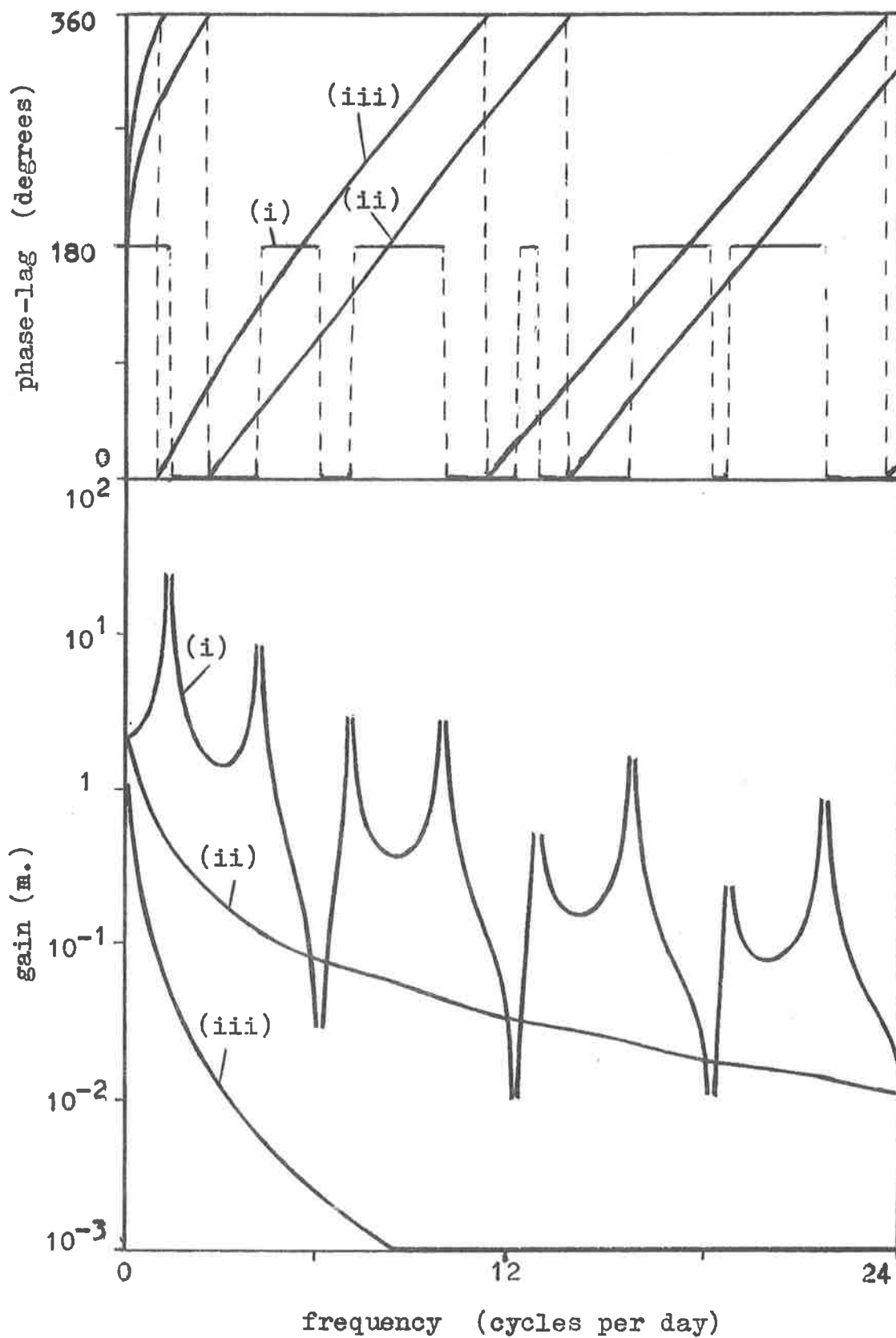FIGURE 7.4 : RESPONSE FUNCTIONS FOR SURFACE DISPLACEMENT AT STATION (-L/2,B/2) FOR THE CONNECTED COORONG SYSTEM, WITH (i)α= 0 sec-1, (ii)α= 2.5 x 10-4 sec-1, (iii)α= 10-3 sec-1 .
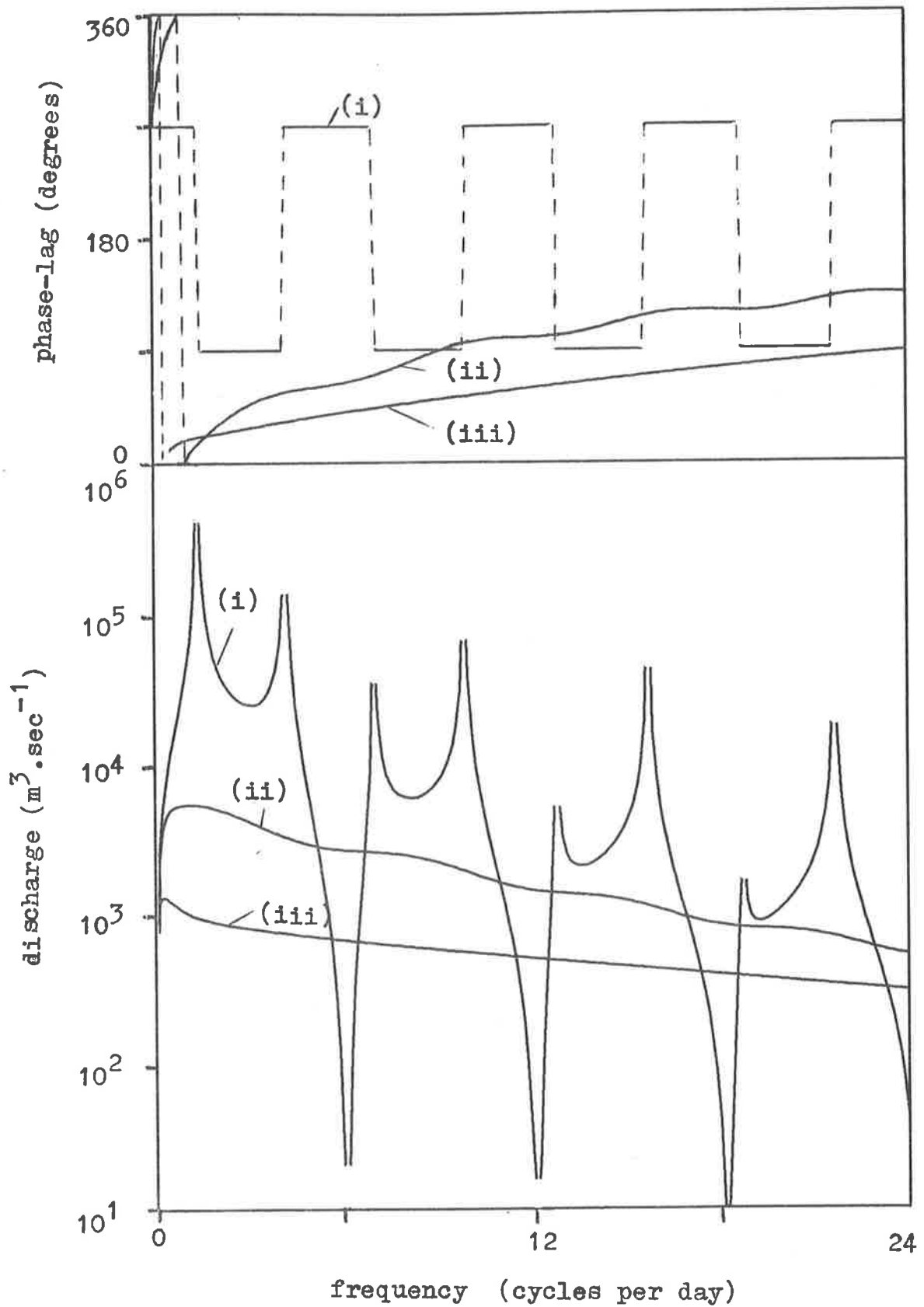
FIGURE 7.5 : GAIN AND PHASE-LAG OF DISCHARGE THROUGH THE OPENING
BETWEEN THE TWO COORONG LAGOONS, FOR (i)α= 0 sec^{-1},
(ii)α= 2.5 x 10^{-4} sec^{-1}, (iii)α= 10^{-3} sec^{-1} .

CHAPTER 8

A COMPARISON OF THEORY AND EXPERIMENT

8.1 Experimental Estimate of Response Function

The Coorong lagoons obey the 'narrow lake' approximation, i.e. only
the component of wind stress parallel to the lake axis is important in
determining wind effects in the lagoons. As such, only a single response
function is needed to characterize the system.

Experimental estimates of this function for the North and South Coorong
have been made by time series analysis of wind velocities recorded at
Mundoo Island and water levels recorded at Seven Mile Point and Noye's
Island respectively. We assume that wind velocities at Mundoo Island are
equivalent to those at other points along the lagoon axes, i.e. the wind
stress is homogeneous; also that the flows through Hell's Gate have minimal
effect on the surface responses of the separate basins. Thus, by a com-
parison of these experimentally determined response functions with the
theoretical response functions determined by the analytical methods of
Sections 3.2, 3.3 and the numerical methods of Section 5.2, estimates may
be made of the values of the various damping parameters used to character-
ize the system.

The data used to estimate the response function for the North Coorong
is shown in Fig. 8.1a; that used for the South Coorong is shown in Fig.
8.1b. In each case, the wind velocities were obtained from the chart
record of a Dynes anemometer, its sensor being 10m above ground level. The
corresponding surface stress is calculable from (1.1.1), and thus the

component of wind stress along the axis of each lagoon may be calculated. The axes of the North and South lagoons are regarded as positive in the south-east and north-west directions respectively; this follows the notation of the analytical model of the North Coorong (Section 3.2) and the numerical model of the South Coorong (Section 5.2). The method of recording water levels is reported elsewhere by Noye (1970).

The longitudinal component of surface wind stress and corresponding surface displacement at a given station may be regarded as the input and output functions respectively of a linear system. The gain and phase of the linear system may be estimated directly by cross-spectral analysis of the input-output data. Often the gain function $G(\omega)$ at a given angular frequency ω has been found from

$$P_L(\omega) = G^2(\omega) P_W(\omega) \qquad (8.1.1)$$

where $P_W(\omega)$ is the power spectrum of the wind-stress input and $P_L(\omega)$ is the spectrum of the water-level output. Thus,

$$G(\omega) = \left(\frac{P_L(\omega)}{P_W(\omega)}\right)^{1/2} . \qquad (8.1.2)$$

However such a procedure does not take account of any noise which might be generated within the system. If there is an independent noise contained in the output record, then

$$P_L(\omega) = G^2(\omega) P_W(\omega) + P_N(\omega) \qquad (8.1.3)$$

which differs from (8.1.1) only by the inclusion of $P_N(\omega)$ (the power spectrum of the noise) with the contribution from the input. The effects of this extra term can be accounted for in the following way. Jenkins and

Watts (1968), p.352 have shown that

$$P_N(\omega) = P_L(\omega) \{1 - R^2_{WL}(\omega)\} \tag{8.1.4}$$

where $R^2_{WL}(\omega)$ is the squared coherence between the input and output at angular frequency ω. This equation shows that, when the whole of the output spectrum consists of noise, the squared coherence is zero; when there is no noise, the squared coherence is unity. From (8.1.3) and (8.1.4) it follows that

$$G(\omega) = |R_{WL}(\omega)| \left(\frac{P_L(\omega)}{P_W(\omega)}\right)^{1/2} . \tag{8.1.5}$$

This formula was used in the analysis of the wind and water-level data of Fig. 8.1 to determine the gain of each wind-water level system. The power spectra $P_W(\omega)$ and $P_L(\omega)$, the coherence $R_{WL}(\omega)$ and the phase difference $\theta(\omega)$ were found and the gain calculated using (8.1.5).

Fig. 8.2 shows the gain $G(\omega)$ and phase-lag $\{-\theta(\omega)\}$ of the wind-water level system for the North Coorong and South Coorong systems. It can be seen that for both there is a steady fall in the gain while water level lags the wind stress by increasing amounts as the frequency increases.

In Fig. 8.3 curve-fitting of the analytical gain and phase-lag at Seven Mile Point as determined from (3.2.9) and (3.3.13), (assuming the North Coorong is a rectangular lake of constant depth), suggests that $\alpha = 2.5 \times 10^{-4} \text{ sec}^{-1}$ and $N = 4.0 \times 10^{-4} \text{ sec}^{-1}$. Similar curve-fitting of the gain and phase-lag at Noye's Island determined numerically in the manner of Section 5.2 indicates that for the South Coorong $r = 7.5 \times 10^{-4} \text{ m.sec}^{-1}$. These values should be regarded as estimates only. The theoretical curves

drawn in Fig. 8.3 approximate the upper and lower bounds of the 95% confidence limits of the experimentally determined gains. The corresponding phase-lag curves do not match so well with experimentally determined phase-lag values. Nevertheless these estimates confirm our previously-held suspicion that the response of both Coorong lagoons to variable wind stresses is heavily damped. In particular, the appearance of the fundamental longitudinal seiche in either lagoon is unlikely.

Wind-water level systems without a 'preferred direction" must be specified by two response functions, as indicated in Section 2.2. Lakes Alexandrina and Albert clearly come within this category. The task of extracting two response functions from a given record of wind velocities and corresponding water levels is more complicated than for the case outlined above, and has not been attempted here.

8.2 Water Level Predictions

The ultimate test of any scientific theory is provided by the degree to which its predictions match reality. In the case of wind effects on closed lakes we may, using recorded surface wind stress as input to the theoretical system, compare water levels predicted by the linear theory of previous sections with recorded water levels. Using the approximate Fourier analysis technique sketched in Section 2.2, several such comparisons are made here between predicted and recorded water levels for the lakes of the Murray Mouth.

For a 'narrow lake' the input record consists of the longitudinal wind

stress $\tau_s(t)$ recorded at station x_o. The record is of finite length T, extending from t = 0 to t = T. It is a continuous record, but for practical purposes it must be sampled at intervals Δt over the range [0,T] to produce a discrete (digitized) record consisting of 2L ($\equiv T/\Delta t$) sample values $(\tau_s)_r$, r = 0,1, ... , 2L-1 such that

$$(\tau_s)r = \tau_s(r\Delta t).$$

Then, as shown by Jenkins and Watts (1968), p.19, the finite Fourier series

$$A_o + 2 \sum_{m=1}^{L-1} \{A_m \cos(\omega_m t) + B_m \sin(\omega_m t)\} + A_L \cos(\omega_L t)$$

with

$$\omega_m = \frac{2\pi m}{T}, \quad m = 1,2, \ldots , L \tag{8.2.1a}$$

$$A_m = \frac{1}{2L} \sum_{r=0}^{2L-1} (\tau_s)_r \cos\left(\frac{\pi m r}{L}\right), \quad m = 0,1, \ldots , L \tag{8.2.1b}$$

$$B_m = \frac{1}{2L} \sum_{r=0}^{2L-1} (\tau_s)_r \sin\left(\frac{\pi m r}{L}\right), \quad m = 1,2, \ldots , (L-1) \tag{8.2.1c}$$

provides an approximation $\tilde{\tau}_s(t)$ to the continuous record $\tau_s(t)$ over the range [0,T] in the sense that

$$(\tau_s)_r \equiv \tilde{\tau}_s(r\Delta t), \quad r = 0,1, \ldots , 2L-1 .$$

The highest frequency component present in the approximation $\tilde{\tau}_s(t)$ is L/T = $1/2\Delta t$, corresponding to a period of 2 sampling intervals. The approximation $\tilde{\tau}_s(t)$ to $\tau_s(t)$ over the range [0,T] is defined for all t and is a periodic function with period T.

If $\tilde{\tau}_s(t)$ is taken as the input to the wind-water level system at station x_o, then the form

$$A_o Z(x_o,0) + 2 \sum_{m=1}^{L-1} [A_m \text{Re}\{Z(x_o,\omega_m)e^{j\omega_m t}\}$$

$$+ B_m \text{Im}\{Z(x_o,\omega_m)e^{j\omega_m t}\}] + A_L \text{Re}\{Z(x_o,\omega_L)e^{j\omega_L t}\}$$

where $Z(x_o,\omega)$ is the response function for the system, is the resultant steady state output, $\tilde{\zeta}(x_o,t)$. It is periodic, with period T, and approximates the true system response, $\zeta(x_o,t)$, to the input $\tau_s(t)$ over the range [0,T]. However, the approximation would be expected to break down at the ends of this range; it is therefore desirable that the record length, T, be as large as possible, so confining such distortions to relatively small regions.

The block diagram of Fig. 8.4a summarizes the procedures involved in water level predictions for 'narrow lakes' using response functions.

Such methods are equally applicable to lakes without a preferred direction. Here, however, the wind stress vector $\underset{\sim}{\tau}_s(t)$ measured at station (x_o,y_o) over the range [0,T] is resolved into components $\tau_{sx}(t)$, $\tau_{sy}(t)$ which may both be approximated by finite Fourier series $\tilde{\tau}_{sx}(t)$, $\tilde{\tau}_{sy}(t)$ of the above form. These separately produce system responses $\tilde{\zeta}_1(x_o,y_o,t)$, $\tilde{\zeta}_2(x_o,y_o,t)$ which may be added to produce an approximation to the true total response, $\zeta(x_o,y_o,t)$, of the basin. A block diagram of this procedure is given in Fig. 8.4b.

Both the methods outlined in Fig. 8.4 have been used in water level predictions for the Murray Mouth lakes. The method of Goertzel (1962) was

programmed for an efficient calculation of the series (8.2.1b), (8.2.1c).
Wind speeds have been converted into stresses using the form (1.1.1).

Fig. 8.5 shows a prediction of water level at Seven Mile Point for the
11 day period depicted in Fig. 8.1b. The response function values used in
the prediction are determined from (3.2.9) (assuming the North Coorong as a
rectangular, constant depth basin) with $\alpha = 2.5 \times 10^{-4} \sec^{-1}$. Fig. 8.6 shows
a water level prediction at Noye's Island over the 11 day period depicted in
Fig. 8.1a. The response function values are determined from the numerical
method of Section 5.2 with $r = 7.5 \times 10^{-4} m.\sec^{-1}$. Fig. 8.7 shows a water
level prediction at Tauwitchere barrage for a 19 day period in December,
1971. Response function values for elevation point 184 of the model of
Section 5.4 with $r_\ell = 5 \times 10^{-4} m.\sec^{-1}$ and $r_c = 10^{-3} m.\sec^{-1}$ have been used
here, the wind velocities being resolved into south-north and west-east
components.

In each of these three cases, the input record was digitized to half
hourly readings; the highest frequency component present in the Fourier
series approximation to the wind stress input is thus 24 cpd. This makes it
impossible to reproduce, through the prediction process, any high frequency
(> 24 cpd) fluctuations in the observed water level. This is not a serious
problem for the Coorong lagoons where such effects are a minor part of the
surface response. Indeed, it is clear that very satisfactory comparison
between observed and predicted water level has been achieved for both the
Coorong predictions. From the results of the North Coorong prediction we
conclude that the rectangular, constant depth model is a realistic representa-
tion of the actual basin.

For Lake Alexandrina, the observed and predicted water levels at Tauwitchere barrage do not compare as well. (Variation of r_ℓ and r_c showed that values of 5×10^{-4} m.sec^{-1} and 10^{-3} m.sec^{-1} respectively gave the best fit). There are several possible causes for these discrepancies.

Firstly, from the response function for Tauwitchere barrage shown in Fig. 5.15, it may be concluded that high frequency components are an important part of the water level response and should not be omitted. It would be preferable, therefore, for the sampling interval to be somewhat less than 1/2 hr. Secondly, the numerical model of Section 5.4 fails to give a very accurate representation of the lake contour in the region of Tauwitchere barrage. Unfortunately, the only records suitable for analysis were from this region. In all probability, more satisfactory comparisons would be achieved at places like Milang and Wellington. Thirdly, the flow through the barrages is variable and has an effect on the water level at Tauwitchere barrage that cannot be incorporated into our model.

In summary, the satisfactory comparison obtained between observed and predicted water levels, particularly for the Coorong lagoons, justifies the use of response functions for purposes of predicting water levels on closed lakes. Further work on refinement of the numerical model of Section 5.4 and the collection of water level data at points other than Tauwitchere barrage needs to be undertaken to improve comparisons in the 'non-narrow' Lakes Alexandrina and Albert.

FIGURE 8.1 : (b) WIND VELOCITIES (MUNDOO ISLAND) AND WATER LEVELS
(NOYE'S ISLAND) FOR THE PERIOD 9 - 19 DECEMBER 1971,
USED TO ESTIMATE A RESPONSE FUNCTION FOR THE SOUTH
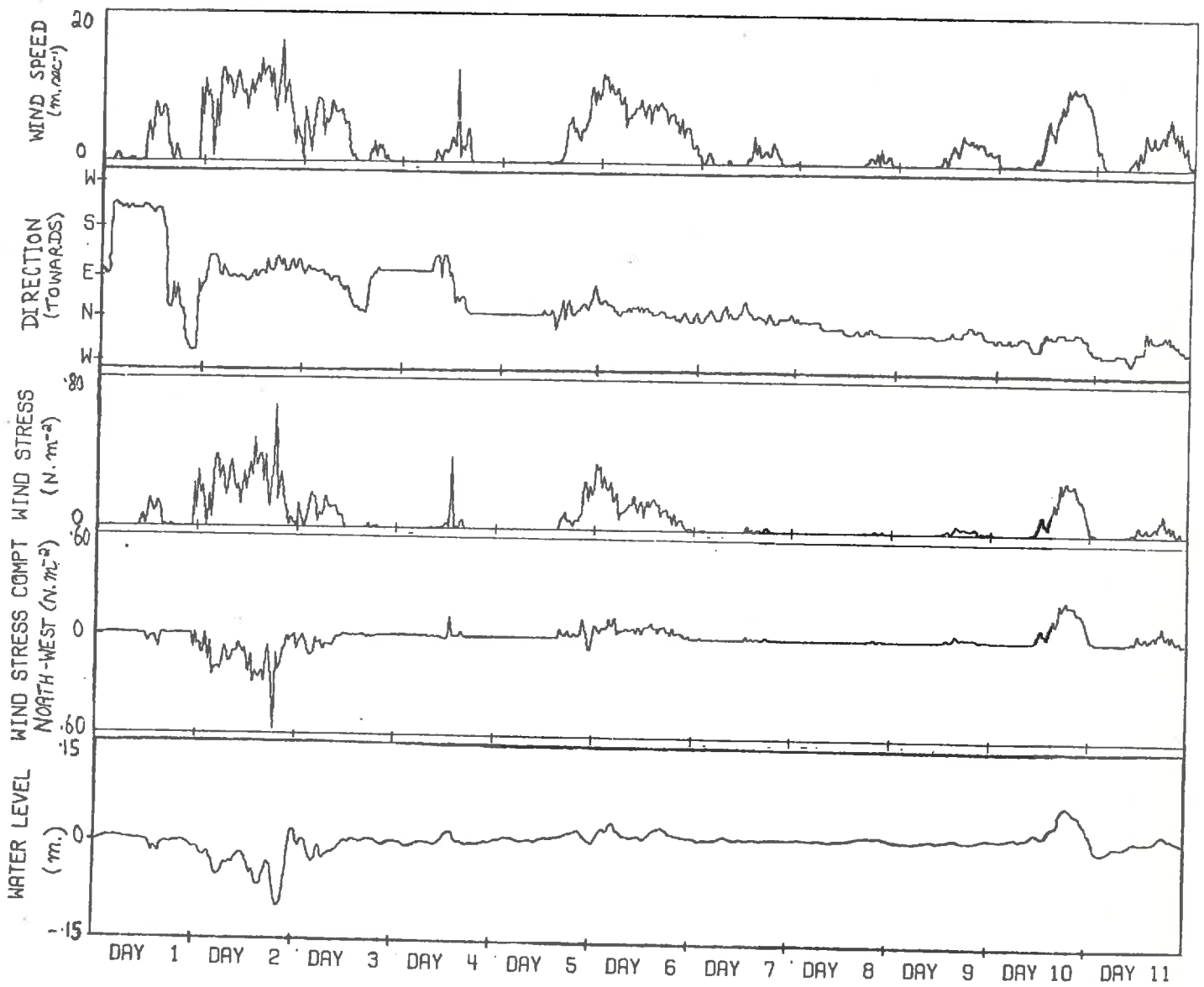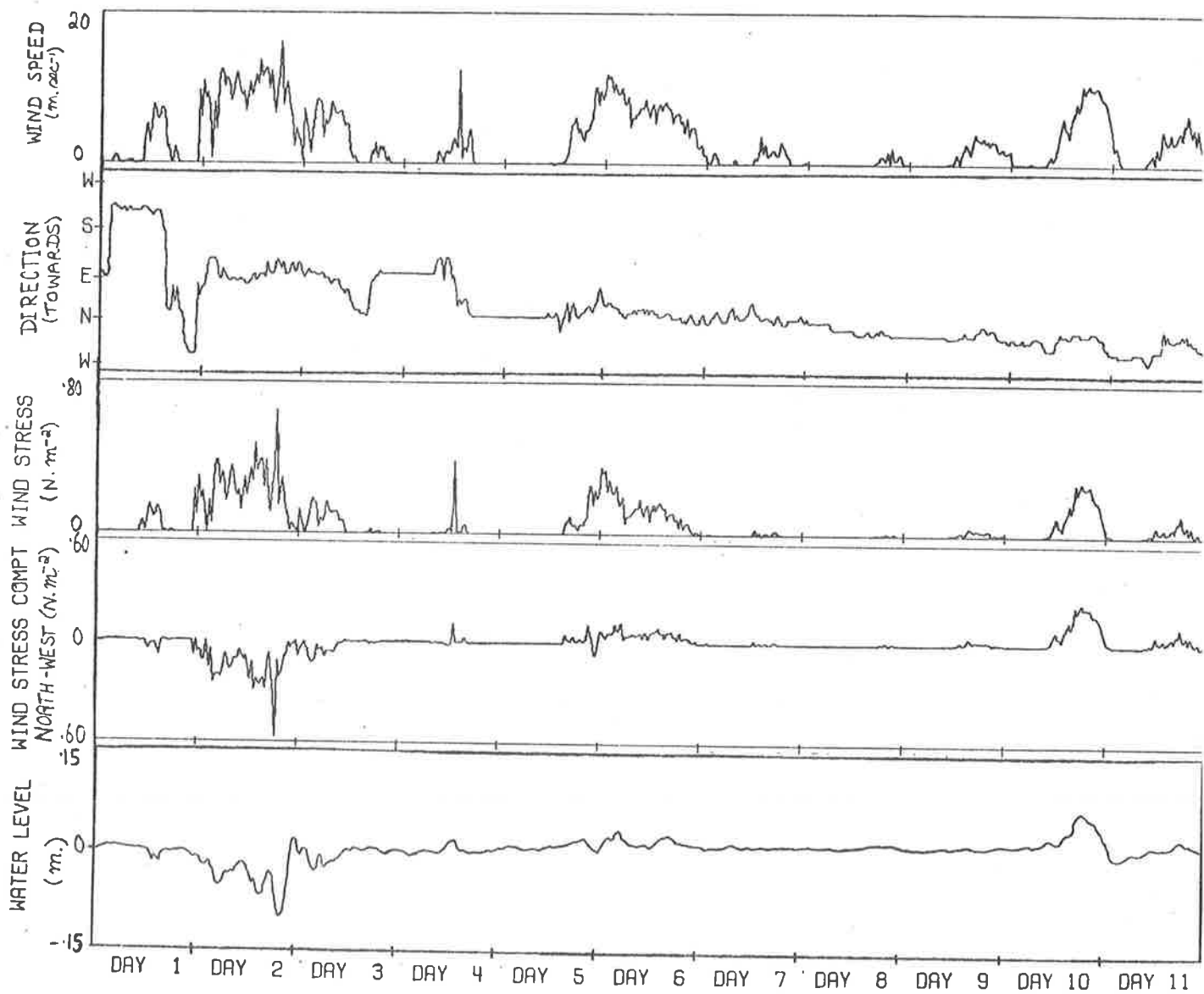COORONG .

FIGURE 8.1 : (b) WIND VELOCITIES (MUNDOO ISLAND) AND WATER LEVELS (NOYE'S ISLAND) FOR THE PERIOD 9 - 19 DECEMBER 1971, USED TO ESTIMATE A RESPONSE FUNCTION FOR THE SOUTH COORONG .
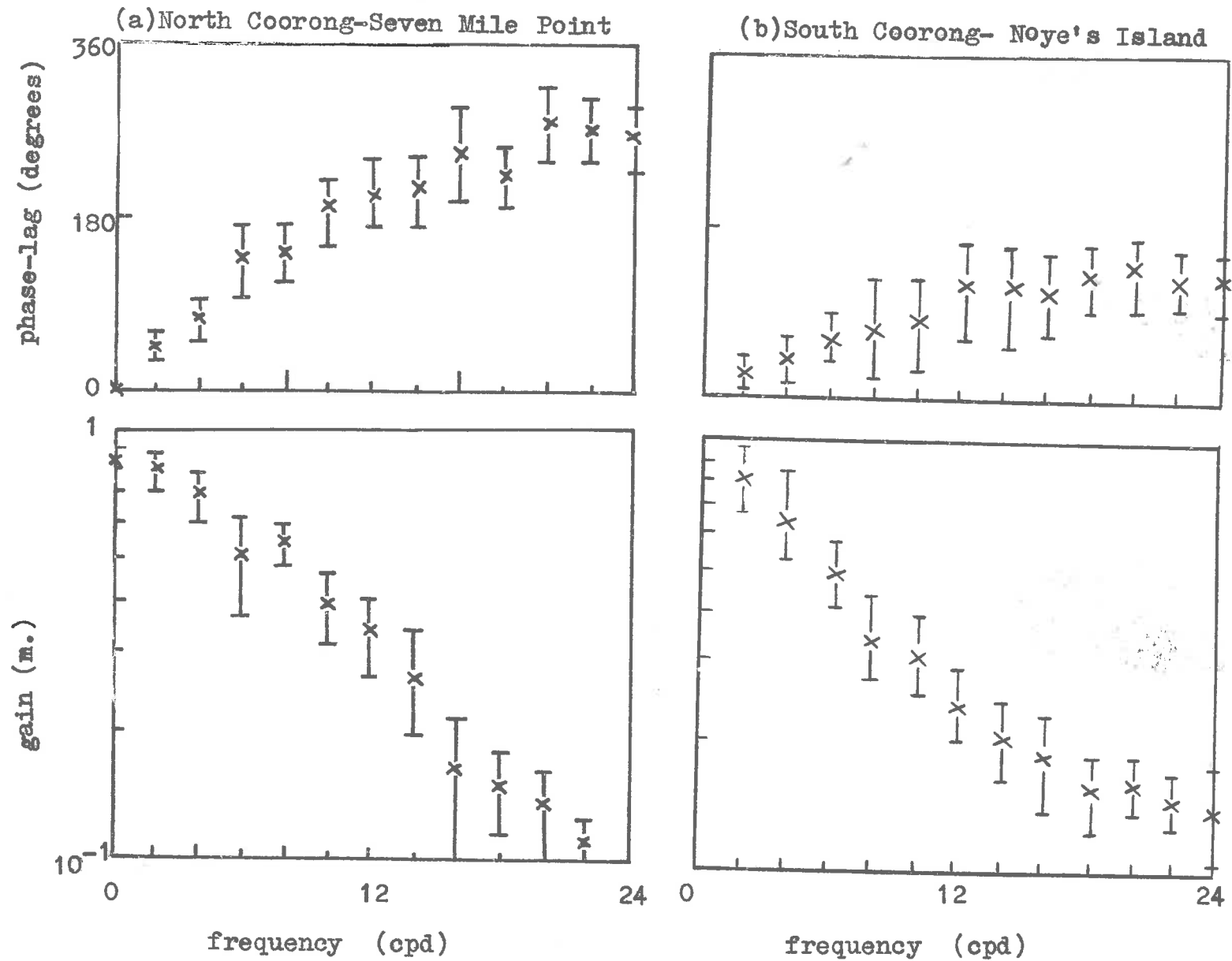
FIGURE 8.2 : EXPERIMENTAL ESTIMATES OF RESPONSE FUNCTIONS FOR COORONG
LAGOONS. THE CROSSES ARE ESTIMATES OF GAIN AND PHASE-LAG;
THE VERTICAL LINES INDICATE THE 95% CONFIDENCE LIMITS ON
THESE ESTIMATES .
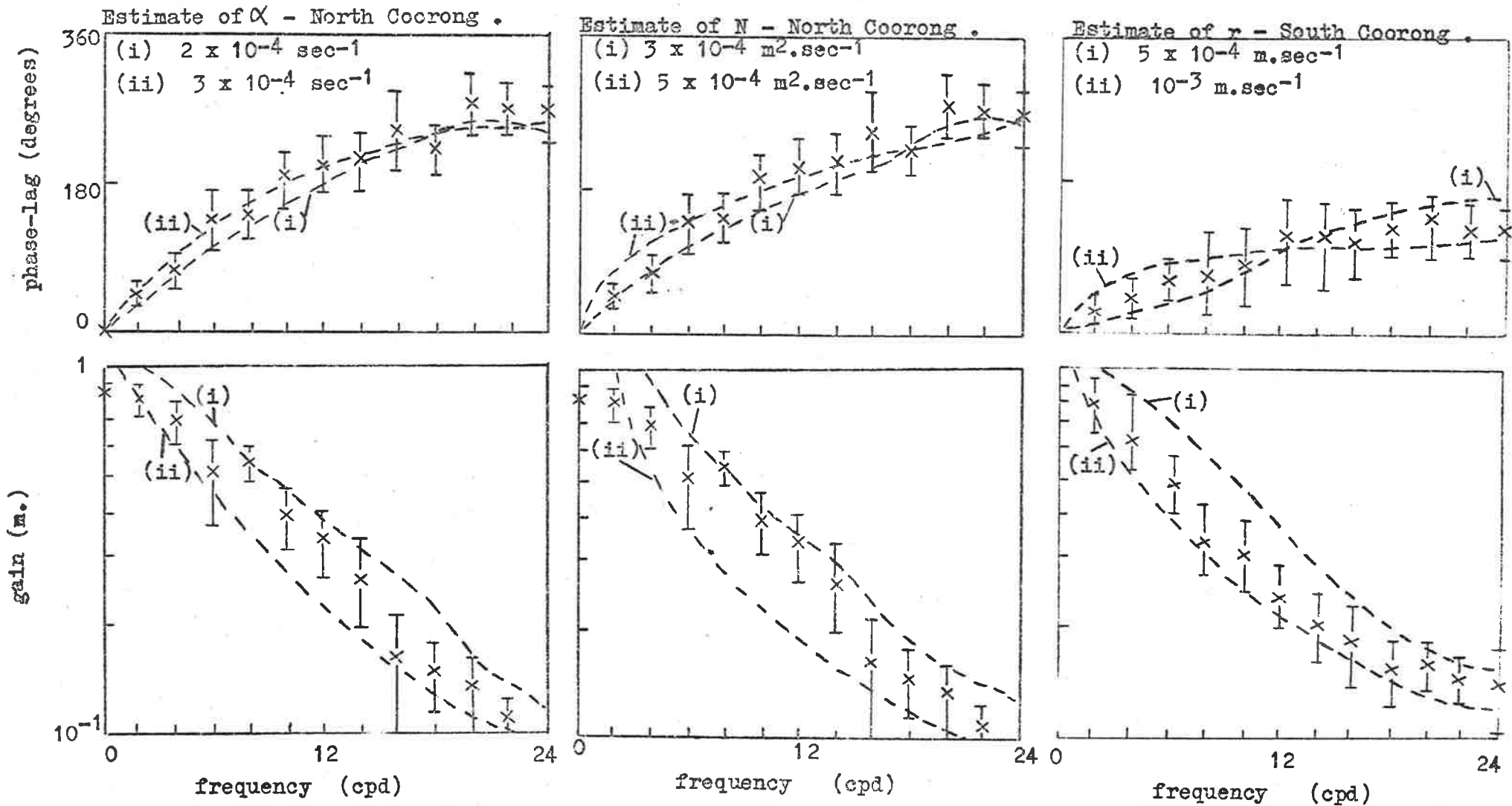
FIGURE 8.3 : COMPARISONS OF THEORETICAL AND EXPERIMENTAL RESPONSE
FUNCTIONS TO PRODUCE ESTIMATES FOR THE VARIOUS DAMPING
PARAMETERS FOR THE COORONG LAGOONS .
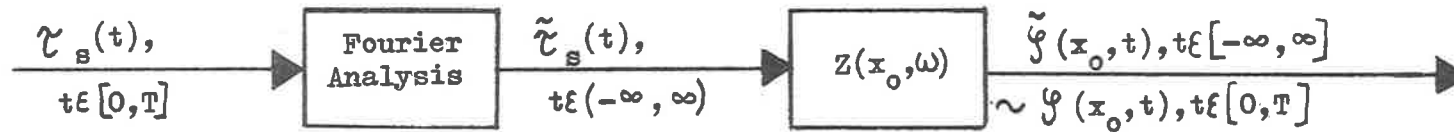
FIGURE 8.4 : (a) PREDICTION PROCEDURE FOR 'NARROW' LAKE .
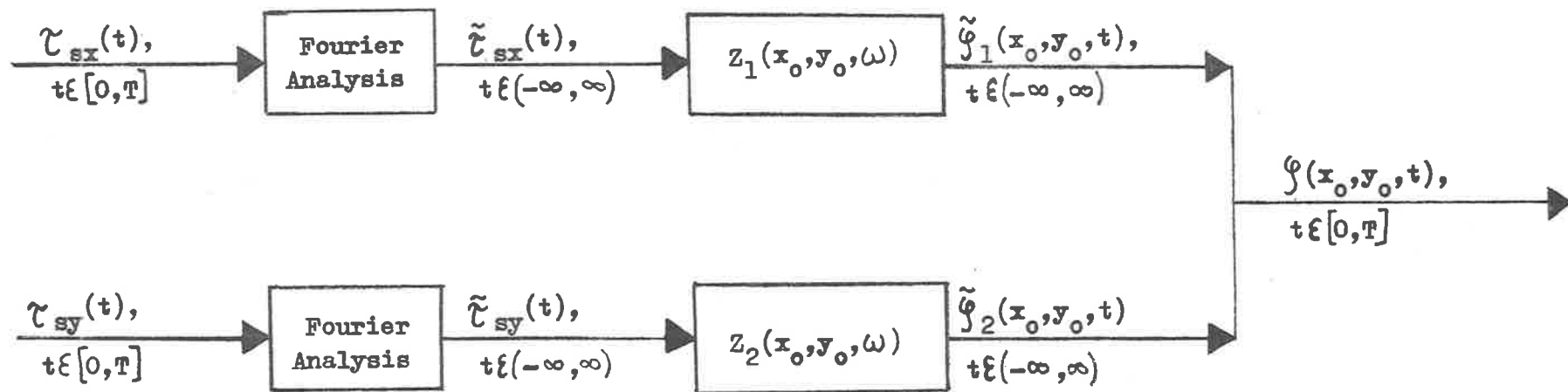
FIGURE 8.4 : (b) PREDICTION PROCEDURE FOR 'NON-NARROW' LAKE .

WATER LEVEL PREDICTED FROM WIND VELOCITY, SEVEN-MILE POINT, NORTH COORONG.DEC 71

———— EXPECTED WATER LEVEL

----- RECORDED WATER LEVEL
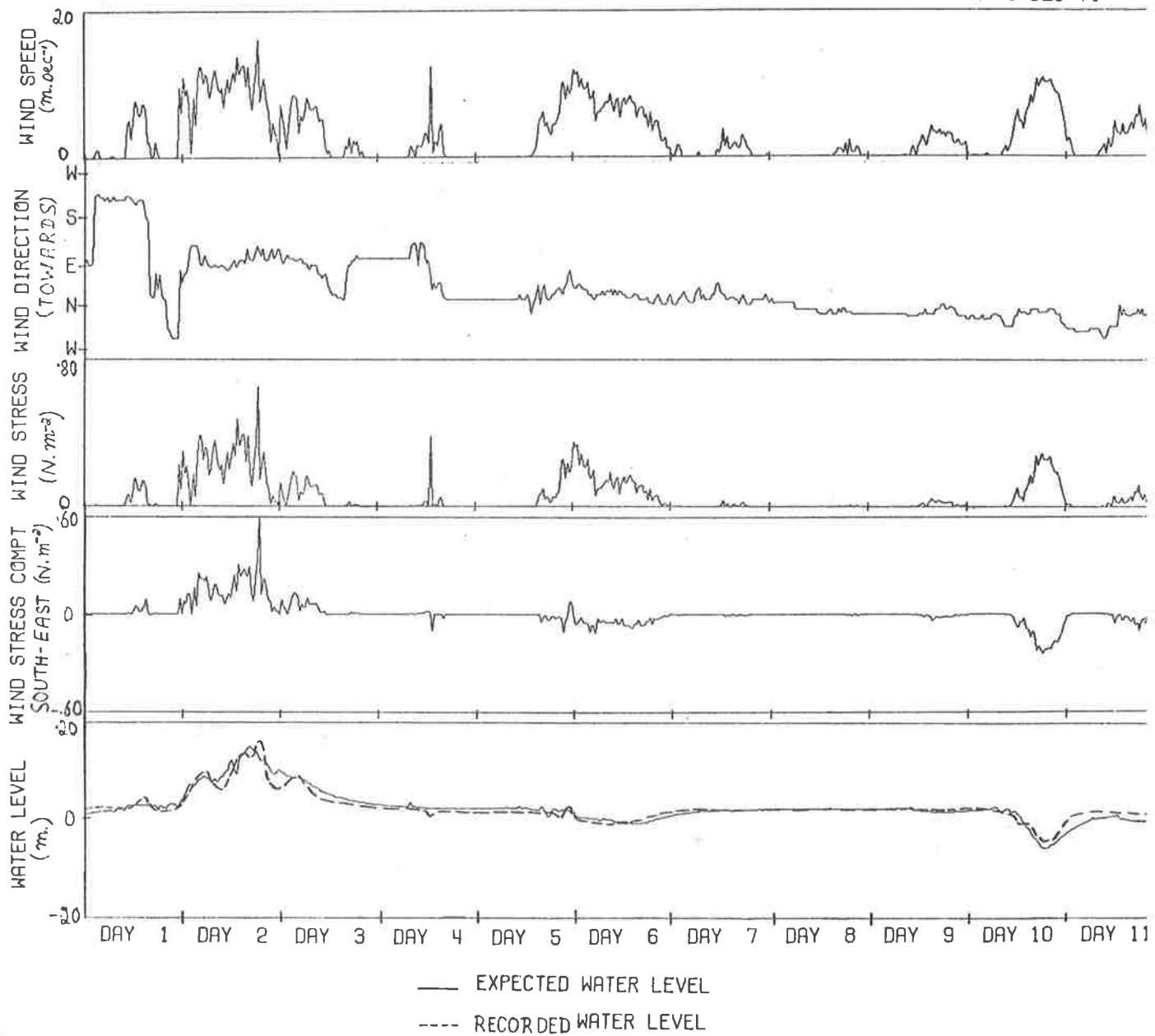
FIGURE 8.5 : WIND VELOCITIES AT MUNDOO ISLAND USED TO PREDICT
WATER LEVEL VARIATIONS FOR SEVEN MILE POINT, FOR
THE PERIOD 9 - 19 DECEMBER, 1971 .

WATER LEVEL PREDICTED FROM WIND VELOCITY, NOYES ISLAND, SOUTH COORONG, NOV 1967
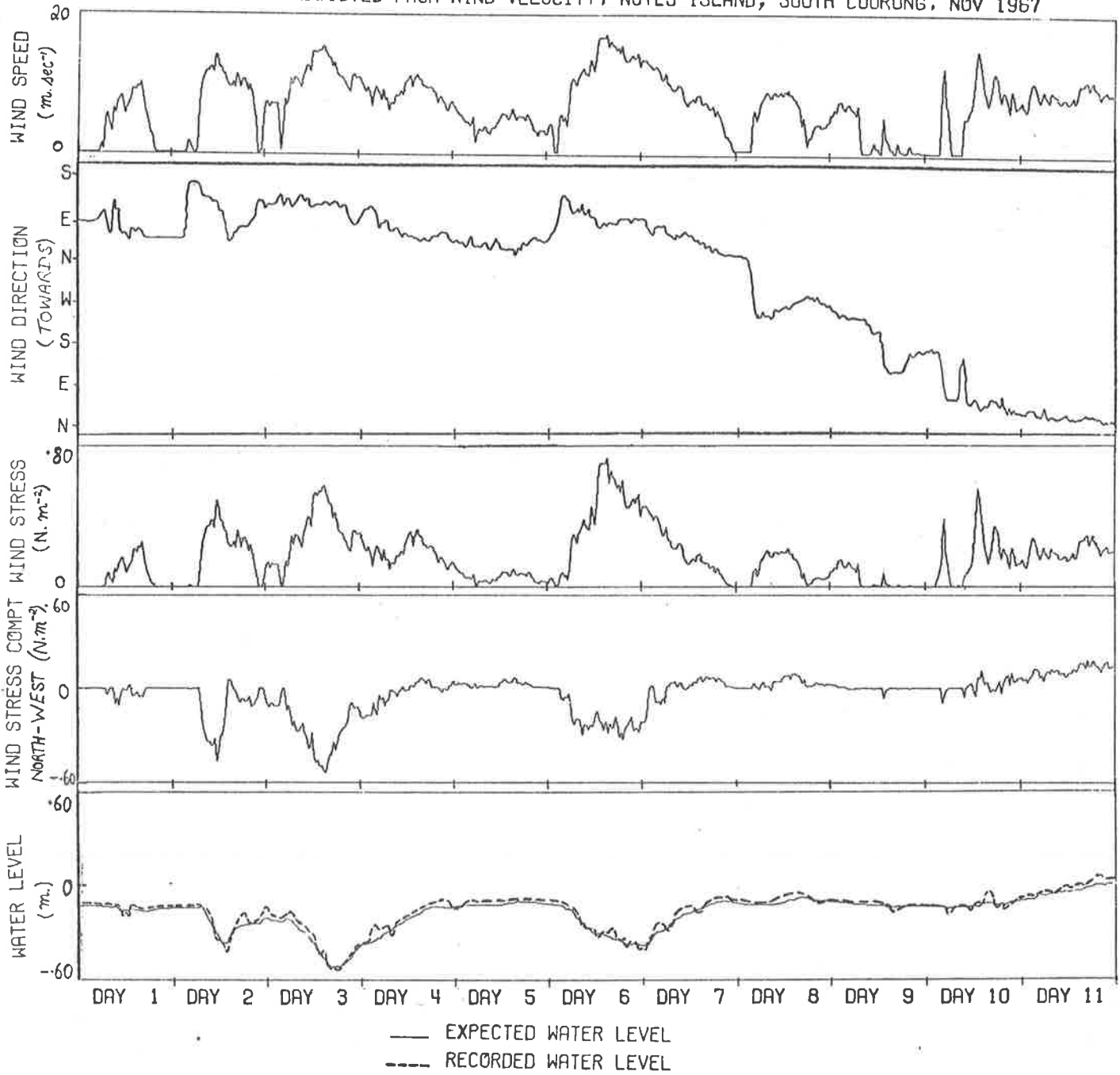
FIGURE 8.6 : WIND VELOCITIES AT MUNDOO ISLAND USED TO PREDICT
WATER LEVEL VARIATIONS FOR NOYE'S ISLAND, FOR THE
PERIOD 20 - 30 NOVEMBER, 1967 .

WATER LEVEL PREDICTED AT TAUWITCHERE BARRAGE - 1/12/71 TO 19/12/71

FIGURE 8.7 : WIND VELOCITIES AT MUNDOO ISLAND USED TO PREDICT
WATER LEVEL VARIATIONS FOR TAUWITCHERE BARRAGE,
FOR THE PERIOD 1-19 DECEMBER 1971 . WATER LEVELS
DUE TO EASTERLY WIND COMPONENT (i) AND NORTHERLY
COMPONENT (ii) ADD TO GIVE THE TOTAL WATER LEVEL
(iii) .

CONCLUSIONS

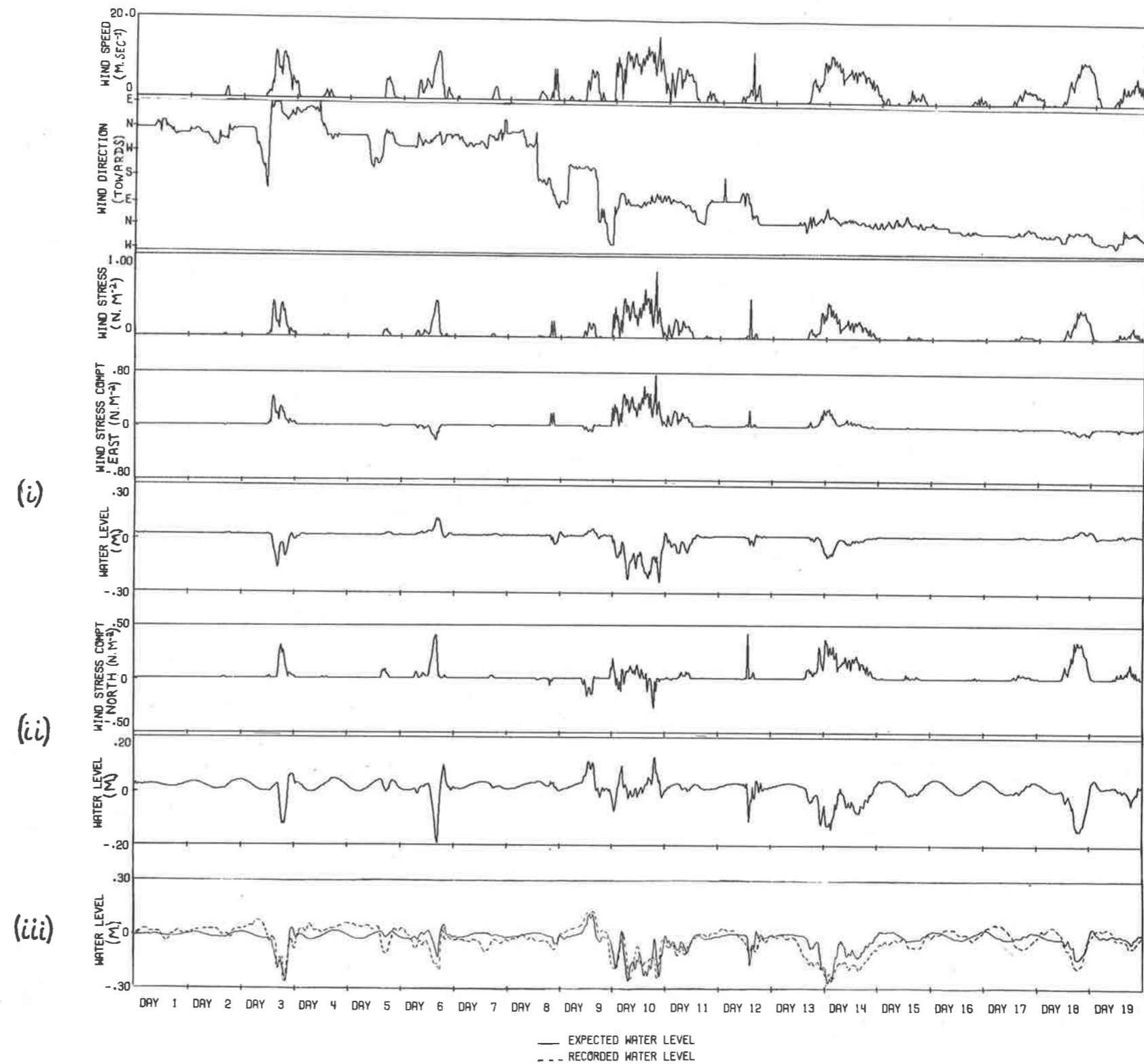The analytical and numerical results of this thesis indicate that use of response functions provides a simple means of characterizing the wind induced response of a given lake. A wide class of wind effect problems may be treated in this manner and a systematic derivation provided to many results otherwise obtainable only by more lengthy procedures.

A comparison of theoretical and experimentally determined response functions suggests that damping processes dominate the wind induced response of the Coorong lagoons. Such heavily damped behaviour is due to the extreme shallowness of the basins. It is concluded that the fundamental longitudinal seiche resulting from a suddenly imposed wind is overdamped in both North and South Coorong, a result in agreement with the experimental conclusions of Noye (1970).

The characteristic diurnal oscillation in the Coorong water levels is simply explained as a _forced_ response to periodic wind stresses. Water level displacements at least of O(10cm) may be induced by such prevailing winds. It is, therefore, likely that non-linear responses will become important, particularly in the shallow end regions of the Coorong where surface displacements are greatest. Elucidation of the theoretical non-linear response of a closed basin to variable wind stresses is required before further progress can be made in this area.

From the simplified analysis of Chapter 7, it seems that damping processes are also important in determining the largely separate behaviour of the Coorong lagoons. Future work, particularly concerning wind effects on

lakes coupled by a narrow channel, should extend and strengthen this
conclusion.

The theoretical results of Chapter 4 suggest that the earth's rotation
plays an unimportant role in the response of Lakes Alexandrina and Albert to
surface wind stress. This is due to a combination of the rather small hori-
zontal dimensions of the lakes, the much larger value of the Rossby radius
of deformation and to significant damping influences.

Numerical experiments of Section 5.4 highlight the importance of Narrung
channel flow in determining the response of Lakes Alexandrina and Albert.
Generally, the magnitudes of characteristic water level displacements due to
prevailing winds are of $0(1 - 10cm)$. Mean current speeds within the separ-
ate lakes are generally small $(0(0.1-1cm.sec^{-1}))$ but are amplified many times
with the narrow confines of the Narrung channel. Such a conclusion agrees
with local observations.

The numerical modelling of Lakes Alexandrina and Albert reported here
is the first theoretical study of the motions of the waters of these lakes
to be undertaken. Though reasonable agreement between observed and computed
water levels has been obtained, there is need for improvement, particularly
in the sophistication of the numerical models used in the prediction and in
the gathering of accurate and more reliable wind and water level data. In
addition, far too little is known of the depth contours in either of the
lakes, of conditions within the Narrung channel and of the effect that open-
ing and closing of the barrages has on water levels within the lakes. Until
such knowledge has been accumulated, continued theoretical advances will be
of little direct benefit.

BIBLIOGRAPHY

BIRCHFIELD, G.E.
1969.   Response of a circular model Great Lake to a suddenly imposed wind
        stress.   J. Geophys. Res., 74(23), 5547-5554.

BOWDEN, K.F.
1956.   The flow of water through the Straits of Dover related to wind and
        differences in sea level.   Phil. Trans. Roy. Soc., A248, 517-551.

CAHN, A.
1945.   An investigation of the free oscillations in a simple current
        system.   J. Meteorol., 2(2), 113-119.

CHARNEY, J.G.
1955.   The generation of oceanic currents by wind.   J. Mar. Res., 14(4),
        477-498.

CHENG, R.T.
1972.   Numerical investigation of lake circulation around islands by the
        finite element method.   Int. J. Numerical Methods in Eng., 5,
        103-112.

CHENG, R.T. and C. TUNG.
1970.   Wind driven circulation by the finite element method.   Proc. 13th
        Conf. Great Lakes Res., 891-903.

CHENG WAN-LI.
1972.   Personal communication, Institute of Atmospheric and Marine Sciences,
        Flinders Univ. of S. Aust.

CHESTER, C.R.
1971.   Techniques in partial differential equations, McGraw-Hill, 440pp.

CLARKE, D.J.
1966.   Seiches in inland lakes and harbours.   M.Sc. Thesis (Mathematics),
        Univ. of Adelaide, 170pp.

CSANADY, G.T.
1967.   Large-scale motion in the Great Lakes.   J. Geophys. Res., 72(16),
        4151-4162.

CSANADY, G.T.
1968a. Wind driven summer circulation in the Great Lakes.   J. Geophys. Res.,
        73(8), 2579-2589.

CSANADY, G.T.
1968b. Motions in a model Great Lake due to a suddenly imposed wind.   J.
        Geophys. Res., 73(20), 6435-6447.

CSANADY, G.T.
1972. Response of large, stratified lakes to wind. J. Phys. Oceanog. 2(1), 3-13.

DEACON, E.L. and E.K. WEBB.
1962. Interchange of properties between sea and air: small scale interactions, from Vol. 1 of "The Sea: ideas and observations on progress in the study of the seas", ed. M.N. Hill, Interscience, (N.Y.), 43-87.

DEFANT, A.
1961. Physical Oceanography, Vol. 1, Pergamon Press, (N.Y.), 729pp.

EMERY, K.O. and G.T. CSANADY.
1973. Surface circulation of lakes and nearly land-locked seas. Proc. Nat. Acad. Sci., U.S.A. 70(1), 93-97.

ENGINEERING and WATER SUPPLY DEPARTMENT OF SOUTH AUSTRALIA.
1973. The River Murray in South Australia - Water Pollution Control, Report, 10pp.

EVANS, D.V. and C.A.N. MORRIS.
1972. The effect of a fixed vertical barrier on obliquely incident surface waves in deep water. J. Inst. Maths Applics, 9, 198-204.

FELSENBAUM, A.I.
1956. Relation of the wind to the level and established currents of a shallow sea. Proc. (Doklady). Acad. Sci., U.S.S.R., 109(1), 93-98.

FORTAK, H.G.
1962. Concerning the vertically averaged hydrodynamic equations with respect to basic storm surge equations. U.S. Dept. of Commerce, Nat. hurricane res. project, Rep. No. 51, 70pp.

FRANCIS, J.R.D.
1954. A note on the velocity distribution and bottom stress in a wind driven water current system. J. Mar. Res., 12(1), 93-98.

FREEMAN, N.G., A.M. HALE and M.B. DANARD.
1971. A modified sigma equations approach to the numerical modelling of Great Lakes hydrodynamics. Internal Rep., Univ. of Waterloo, Ontario.

GALLAGHER, R.H., J.A. LIGGETT and S.T.K. CHAN.
1973. Finite element lake circulation analysis. J. Hyd. Div., Proc. A.S.C.E., 99(HY7), 1083-1096.

GOERTZEL, G.
1962. Fourier analysis, from "Mathematical methods for digital computers", ed. A. Ralston and H.S. Wilf, Wiley & Sons Inc. (N.Y.), 258-262.

GREENSPAN, H.P.
1968. The theory of rotating fluids, Monographs on Mechanics and Applied Mathematics, Cambridge U. P., 327pp.

GROEN, P. and G.W. GROVES.
1962. Surges, from Vol. 1 of "The Sea: ideas and observations on progress in the study of the seas", ed. M.N. Hill, Interscience (N.Y.), 611-646.

HARLEMAN, D.R., E. HOLLEY, J. HOOPES and R. RUMER.
1962. The feasibility of a dynamic model of Lake Michigan, Publ. No. 9, Great Lakes Res. Div., Univ. of Michigan, 51-67.

HARRIS, D.L.
1954. Wind tide and seiches in the Great Lakes. Proc. 4th Conf. on Coastal Eng., Council on Wave Res., 25-51.

HAURWITZ, B.
1951. The slope of lake surfaces under variable wind stresses. U.S. Army Beach Erosion Board, Tech. Mem. No. 25., 23pp.

HEAPS, N.S.
1969. A two-dimensional numerical sea model. Phil. Trans. Roy. Soc., A265, 93-137.

HEAPS, N.S. and A.E. RAMSBOTTOM.
1966. Wind effects on the water in a narrow, two-layered lake. Phil. Trans. Roy. Soc., A259, 391-430.

HELLSTROM, B.
1941. Wind effects on lakes and rivers. Ingen. Vetensk. Akad. Handl., No. 158, 191pp.

HUTCHINSON, G.E.
1957. A treatise on limnology, Vol. 1, Wiley & Sons Inc. (N.Y.), 1015pp.

IPPEN, A.T. and F. RAICHLEN.
1962. Wave induced oscillations in harbours: the problem of coupling of highly reflective basins. R.M. Parsons Lab. for Water Res. and Hydrodyn., Rep. No. 49.

JENKINS, G.M. and D.G. WATTS.
1968. Spectral analysis and its applications. Holden-Day (San Francisco), 525pp.

JONES, D.S.
1964. The theory of electro-magnetism, Oxford, Pergamon, 807pp.

KEULEGAN, G.H.
1951. Wind tides in small closed channels. J. Res. Nat. Bur. Stand., 46, 358-381.

LAMB, H.
1932. Hydrodynamics, 6th edition, Cambridge U. P., 738pp.

LIGGETT, J.A.
1969.   Unsteady circulation in shallow homogeneous lakes.   J. Hyd. Div.,
        Proc. A.S.C.E., 95 (HY4), 1273-1288.

LIGGETT, J.A. and C. HADJITHEODOROU.
1969.   Circulation in shallow homogeneous lakes.   J. Hyd. Div. Proc.
        A.S.C.E., 95 (HY2), 609-620.

LINDH, G. and L. BENGTSSON.
1971.   Wind induced circulation in a lake.   Proc. 1st Int. Conf. on Port
        and Ocean Eng. under Arctic Conditions, Tech. Univ. of Norway 2,
        893-908.

MEI, C.C. and U. ÜNLÜATA.
1973.   Long wave excitation in harbours - an analytical study.   R.M.
        Parsons Lab. for Water Res. and Hydrodyn., Rep. No. 171, 284pp.

MILES, J. and W. MUNK,
1961.   Harbour Paradox.   J. Waterways and Harbours Div., Proc. A.S.C.E.,
        87 (WW3), 111-130.

MORSE, P.H. and K.U. INGARD.
1970.   Theoretical acoustics, McGraw-Hill (N.Y.), 927pp.

MURTY, T.S., A. TADEPALLI and D.B. RAO.
1970.   Wind generated circulations in Lakes Erie, Huron, Michigan and
        Superior.   Proc. 13th Conf. Great Lakes Res., 927-941.

NOYE, B.J.
1970.   On the physical limnology of shallow lakes and the theory of tide
        wells.   Ph.D. Thesis (Mathematics), Univ. of Adelaide, 121pp.

NOYE, B.J.
1973.   The response of lake levels to an unsteady wind stress.   Bull.
        Austral. Math. Soc., 8(3), 423-433.

NOYE, B.J.
1974.   The Coorong, Publ. No. 39, Dept. of Adult Ed., Univ. of Adelaide,
        118pp.

PAPOULIS, A.P.
1962.   The Fourier integral and its applications, McGraw-Hill, 318pp.

PHILLIPS, O.M.
1969.   The dynamics of the upper ocean, Monographs on Mechanics and Applied
        Mathematics, Cambridge U. P., 261pp.

PLATZMAN, G.W.
1958.   A numerical calculation of the surge of June 26, 1954 on Lake
        Michigan.   Geophysica, 6, 407-438.

PLATZMAN, G.W.
1963.   The dynamical prediction of wind tides on Lake Erie.   American
        Met. Soc., Mon., 4,(26), 44pp.

PLATZMAN, G.W.
1965.   The prediction of surges in the southern basin of Lake Michigan.
        Monthly Weather Review, 93, 275-281.

PLATZMAN, G.W.
1966.   The daily variation of water level on Lake Erie.   J. Geophys. Res.,
        71(10), 2471-2483.

PLATZMAN, G.W. and D.B. RAO.
1964.   The free oscillations of Lake Erie, from "Studies in Oceanography"
        (Hidaka Anniversary Volume), ed. K. Yoshida, Univ. of Tokyo Press,
        359-382.

PROUDMAN, J.
1924.   On a class of expansions, Proc. Lond. Math. Soc., (2), 24, 131-139.

PROUDMAN, J.
1953.   Dynamical Oceanography, Methuen (London), 409pp.

PROUDMAN, J.
1954.   Note on the dynamical theory of storm surges.   Arch. Meteorol.
        Geophys. Bioklim. A7, 344-351.

PROUDMAN, J. and A.T. DODDSON.
1924.   Time-relations in meteorological effects on the sea.   Proc. Lond.
        Math. Soc., (2), 24, 140-149.

RAO, D.B.
1966.   Free gravitational oscillations in rotating rectangular basins.
        J. Fl. Mech., 25(3), 523-555.

REID, R.O.
1956.   Modification of the qudratic bottom stress law for turbulent channel
        flow in the presence of surface wind stress.   A. & M. Coll. of
        Texas, Dept. Oceanography, Tech. Rep. 2, Ref. 56-27T. 32pp.

REPORT OF THE COMMITTEE ON ENVIRONMENT.
1972.   The Environment in South Australia, S. Aust. Govt. Printer.

ROSSBY, C.G.
1938   On the mutual adjustments of pressure and velocity distributions in
        certain simple current systems, II, J. Mar. Res., 1(3), 239-263.

SAITO, Y.
1949.   A solution to the oscillation of lake water generated by wind.   J.
        Met. Soc. Japan, (2), 27, 20-25.

SAVILLE, T.
1952. Wind set-up and waves in shallow water. U.S. Army Beach Erosion
       Board, Tech. Mem. No. 27, 19pp.

SIMONS, T.J.
1972. Development of numerical models of Lake Ontario, Part II. Paper
       presented at 15th Conf. Great Lakes Res.

SMITH, E.B.
1973. Wind driven and seiche forced water motion in Grand Traverse Bay,
       Michigan. Ph.D. dissertation (Engineering Mechanics), Univ. of
       Michigan, 130pp.

SOUTH AUSTRALIAN STATE PLANNING AUTHORITY.
1973a. Outer metropolitan planning area - development plan, draft.

SOUTH AUSTRALIAN STATE PLANNING AUTHORITY.
1973b. Monarto - new town, Report on proposed designated site under Murray
       New Town (Land Acquisition) Act 1972, 22pp.

STOKER, J.J.
1957. Water Waves, Interscience (N.Y.), 560pp.

TAREYEV, B.A.
1958. Stationary wind set-up and circulation in a shallow rectangular
       basin. Izv., Geophys. Ser. (transl.), 661-663.

TICKNER, E.G.
1957. Effects of bottom roughness on wind tides in shallow water. U.S.
       Army Beach Erosion Board, Tech. Mem. No. 95, 25pp.

TICKNER, E.G.
1961. Transient wind tides in shallow water, U.S. Army Beach Erosion
       Board, Tech. Mem. No. 123., 48pp.

TRANTER, C.J.
1971. Integral transforms in mathematical physics, Chapman and Hall
       (Science Paperback), 139pp.

TRONSON, K.T.
1973. Personal communication, Dept. of Applied Maths, Univ. of Adelaide.

TUCK, E.O.
1971. Transmission of water waves through small apertures. J. Fl. Mech.,
       49(1), 65-73.

TUCK, E.O.
1974. Matching problems involving flow through small holes, (to be
       published in Advances in Applied Mechanics, 15).

VERONIS, G.
1956. Partition of energy between geostrophic and non-geostrophic oceanic motions. Deep Sea Res., 3, 157-177.

WALSH, P.J. and B.J. NOYE.
1974. Modelling long-wave wind effects on the lakes of the Murray Mouth. Proc. 2nd S. Aust. Reg. Conf. on Physical Oceanography, Univ. of Adelaide, 187-215.

WEENINK, M.P.
1958. A theory and method of calculation of wind effects on sea levels in a partly enclosed sea, with special application to the southern coast of the North Sea. Konninkl. Ned. Met. Inst., Med. Verhandel., No. 73, 111pp.

WELANDER, P.
1957. Wind action on a shallow sea: some generalizations of Ekman's theory. Tellus, 9, 45-52.

WELANDER, P.
1961. Numerical prediction of storm surges. Advances in Geophysics, 8, 316-379.

WILSON, B.W.
1960. Note on surface wind stress over water at low and high wind speeds. J. Geophys. Res., 65(10), 3377-3382.

WILSON, B.W.
1972. Seiches. Advances in Hydro-science, 8, 1-94.

WUNSCH, C.
1973. On the mean drift in large lakes. Limnology and Oceanography, 18, 793-795.

WYLIE, C.R.
1966. Advanced engineering mathematics, 3rd edition, McGraw-Hill, 813pp.

APPENDIX A

THE MURRAY MOUTH LAKES

1.   Introduction

The River Murray, 2500km long, forms at its mouth a most peculiar and fascinating system of lakes (Fig. A1).

It drains into Lake Alexandrina (450km^2) which in turn is connected to the smaller Lake Albert (100km^2) through the narrow, 8km long Narrung channel, and to the Southern Ocean through an extremely small opening, only a few hundred metres wide, which is the real mouth of the River Murray.

Stretching south-east from the Murray Mouth for a distance of about 80km is the Coorong, an elongated coastal lagoon of average width about 2km, separated from the Southern Ocean by the narrow ridge of sandhills called Younghusband Peninsula. In reality the Coorong consists of two lagoons, the North Coorong and the South Coorong, joined by the opening known as Hell's Gate only a hundred metres wide.

Few detailed studies of any kind have been carried out on any part of this system of lakes. It would be true to say that very little is known about any of the lakes of the Murray Mouth.

For example, the only recorded depth measurements of Lake Alexandrina are at present held by the Engineering and Water Supply Department of South Australia. They were made in 1912 and consist of data from several traverses made approximately north-south across the lake and through the

Narrung channel into Lake Albert. One can estimate an average summer depth of between 3 and 3.5m for Lake Alexandrina. More recently, measurements of Lake Albert depths made by Cheng Wan-Li (1972) show the average depth of this basin to be about 2m. Approximate summer contours drawn from these sets of data are shown in Fig. A2. Noye (1974) estimates the average summer depths of the two Coorong lagoons to be between 1 and 2m.

The Coorong is geologically the most interesting and environmentally the most finely balanced of the lakes of the Murray Mouth. For this reason it has received the most attention from scientists, though even for the Coorong our knowledge is very limited. A most comprehensive summary of the important aspects of the Coorong region has recently been published by Noye (1974). It contains in detail much of the information reported only briefly in this Appendix concerning the environmental decay of the Coorong lagoons.

It is believed that the inner shoreline of the Coorong represents the stranded beach of a past geological age. It is thus slowly undergoing a natural geological death, a process being hastened by the influence of man (refer Section 2 of this Appendix).

Much of the Coorong area is under State protection as a national park, game reserve or sanctuary. The area has, in the past, supported great numbers of bird life, especially pelicans and wild duck, and contains many unique specimens of marine life in the form of crabs, sea-grasses, etc. Prior to World War II many fishermen earned a profitable living from the waters of the Coorong.

2. The Impact of Man on the Murray Mouth Lakes

(i) The Barrages

The Coorong water is basically sea water. However, in the South Coorong its salinity during summer may be as much as three times that of normal sea-water.

On the other hand, the water of Lake Alexandrina and Lake Albert is relatively fresh and is quite suitable for irrigation of surrounding pastures. It has been so, however, only since the completion in 1940 of a series of barrages across the south-western end of Lake Alexandrina (Fig. A1), constructed in order to prevent the upstream flow of water from the Southern Ocean during the summer months when the River Murray ceases to flow.

The barrages are normally closed during the summer months and open during the winter months, though extraordinary seasons may alter this pattern. During very dry seasons it is possible to wade across the Murray Mouth at low spring tide.

The opening of the barrages in winter causes a large influx of fresh water into the Coorong, with a consequent rise in water level and drop in salinity. Conversely, the closure of the barrages during summer leads to an abnormal increase in salinity and decrease in water level.

It is thought that sudden changes in salinity may adversely affect certain species of sea-grass and fish. It is certain that unseasonal variations in water level can upset the nesting habitats and routines of water birds such as pelicans. The reduced flow of fresh water into the Coorong

during the summer months is also believed partly responsible for the almost stagnant nature of the South Coorong water over the past few years.

From a comparison of the two sets of data mentioned in Section 1 of this Appendix for Lake Albert depths, one taken in 1912 and the other in 1972, it seems that the construction of the barrages has led to an approximate increase in the average depth of Lakes Alexandrina and Albert of 1m. Noye (1974) has documented the fact that winter depths in the Coorong lagoons are approximately twice the summer depths due both to man-made influences and to natural effects.

(ii)   The South-East Drainage Scheme

Prior to World War II Salt Creek was an important source of fresh water for the South Coorong. However the South-East drainage scheme, completed in 1946, diverted these waters and as a result Salt Creek has not flowed since 1948. The effect of cutting off this fresh-water source seems to have been a slow increase in the salinity of the South Coorong over the past twenty-five years, which in turn has adversely affected the ecology of the lagoon.

As an example, fish numbers in the South Coorong seem to have dropped considerably in this time. In addition, sea-grasses are believed to have been adversely affected and it is thought that the decrease in the abundance of these sea-grasses may be responsible for the obvious and alarming drop in bird numbers. The sight of foam lining the South Coorong shores is now quite common, even in winter.

Thus, due in part to the summer closure of the barrages and also to the now negligible flow of Salt Creek, the South Coorong is rapidly decaying into a stagnant environment.

(iii) Shore Pollutants

The Report of the Committee on Environment in South Australia (1972) lists the two main pollution problems associated with the River Murray as saline pollution and effluent discharge from towns, industrial plants and river-craft. Periodic salinity increase is considered to be the bigger problem of the two.

It would be reasonable to suppose that a large amount of upstream pollution finds its way into the lakes of the Murray Mouth. These lakes might therefore be considered as a partial indicator of the state of environmental decay of the River Murray itself.

So far there has been little evidence produced to show that the Murray Mouth lakes are being threatened by upstream pollutants. A greater threat to the lakes is presently being posed by farms and towns situated on its shores. Signs of eutrophication, possibly a result of superphosphate being washed into the lakes from surrounding farmland or of other nitrogeneous effluents, have begun to appear.

A recent report on water pollution control of the River Murray by the E. & W.S. Department (1973) comments (p.3):-

"Judged by the level of pollution which exists in many of the major river systems of the United States of America and Europe, the River Murray in South Australia is a clean river. However,

there is no room for complacency as there is already growing evidence of unbalanced aquatic biological activity in the River Murray in South Australia - particularly in the back-waters, the lower reaches of the River itself, Lake Alexandrina and the Goolwa channel."

3. Future Uses of the Lakes

The decision of the South Australian Government to site a new city, Monarto, near the present town of Murray Bridge (Fig. 1) as part of its decentralization policy has raised considerable speculation as to the future uses of the lakes of the Murray Mouth.

At present the lakes provide life-giving fresh water to surrounding farmland. It seems that within a decade this use as a water resource will have greatly increased in scope. One recent proposal, for example, was to place a barrage across the Narrung channel and to use the water of Lake Albert as a source of fresh water for both Monarto and Adelaide.

A more certain forecast is that the lakes will become an important recreational source, a quiet retreat for the future inhabitants of Monarto. Care must be taken to ensure not only that the system of lakes is kept in a fit state for recreational usage but also that such usage does not itself destroy the system.

The recreational potential of the lakes is already under investigation by the South Australian State Planning Authority (1973a). Reporting on proposals for the land adjoining the Lower Murray River and Lake Alexandrina,

it comments (p.116):-

> "The coasts, riversides and lakefronts are unique water land
> boundaries. Being fixed and finite they are a community asset
> for which no substitute is available. .... Along the shorelines
> fronting Lake Alexandrina and the Lower Murray River, sites
> should be allocated for tourist accommodation areas and recrea-
> tional facilities which have as little effect as possible on
> the natural and scenic qualities of the area."

It is likely, too, that unless great care is taken, Monarto will
greatly increase the load of upstream pollutants presently entering the
system. The South Australian State Planning Authority (1973b) in its
report on the site selection of Monarto, says (p.19):-

> "Sewage disposal will require detailed planning. The possi-
> bility of eutrophication in the River, and salinity build-up
> in irrigated areas will require careful consideration. Piping
> the effluent to Lake Alexandrina and/or nutrient stripping
> may have to be provided in the long term."

In summary then, it seems that the lake waters will, in future years,
be used in many more diverse and possibly conflicting ways. Conflict is
unavoidable - it can be minimized only by the application of carefully
planned policies and guidelines for development.

Clearly the greatest barrier to efforts at preserving the lakes of the
Murray Mouth is our overall lack of knowledge of the system itself.

For example, much attention has recently been focussed on the decay
of the ecologically fragile Coorong. It has been proposed that a channel
be cut to connect Lake Albert to the North Coorong or the Southern Ocean to
the South Coorong near Salt Creek. In this way it ought to be possible to

satisfactorily flush out the Coorong waters and thus maintain salinities at a more stable level.

Such a proposal, however, will remain as mere speculation rather than a definitely committed plan until a large-scale, multi-disciplinary study has been undertaken to determine the effectiveness and, indeed, possible side effects of the scheme. It was with the intention of contributing to our knowledge of the lakes of the Murray Mouth that the studies reported in this thesis were undertaken.
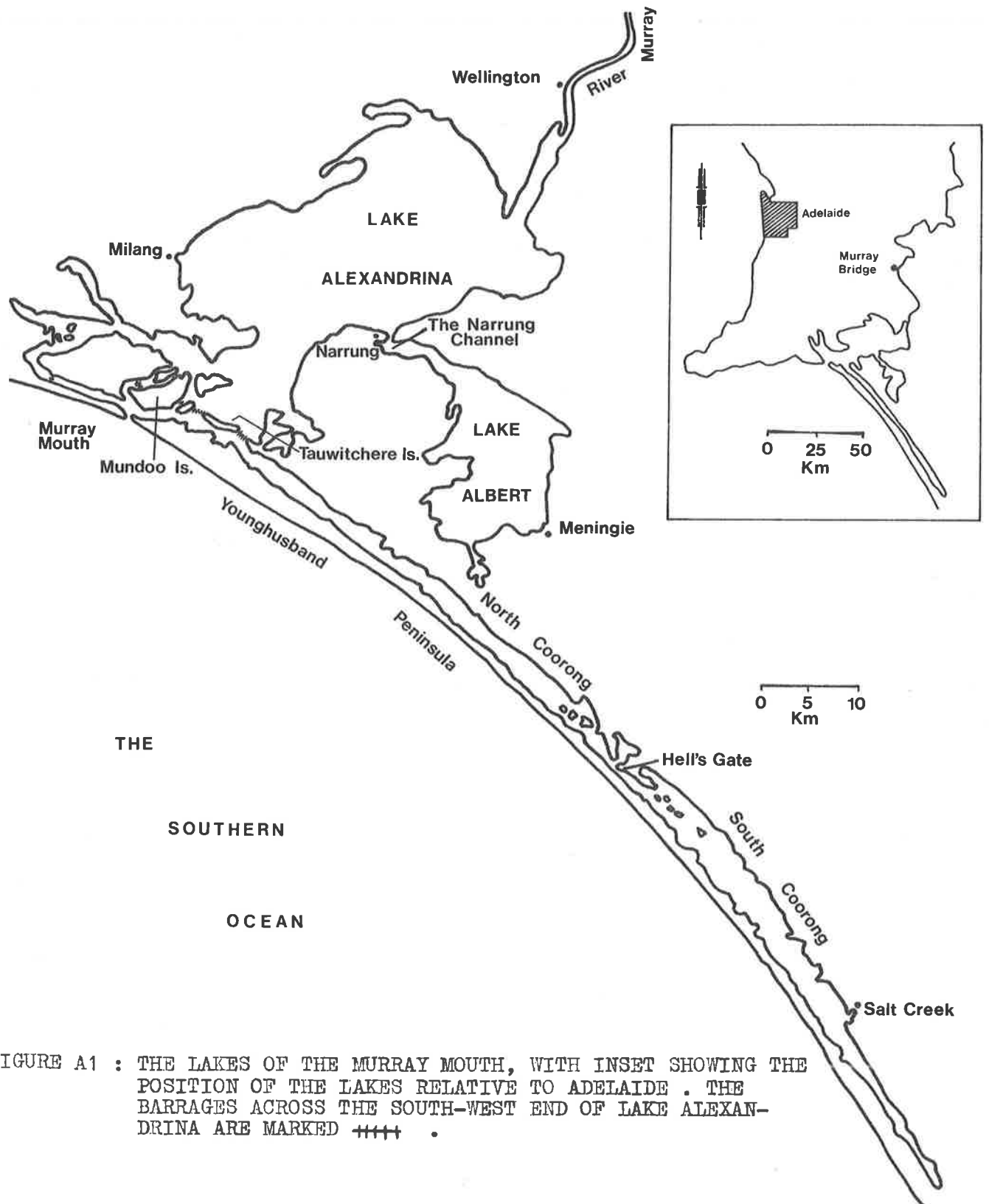
FIGURE A1 : THE LAKES OF THE MURRAY MOUTH, WITH INSET SHOWING THE
POSITION OF THE LAKES RELATIVE TO ADELAIDE . THE
BARRAGES ACROSS THE SOUTH-WEST END OF LAKE ALEXAN-
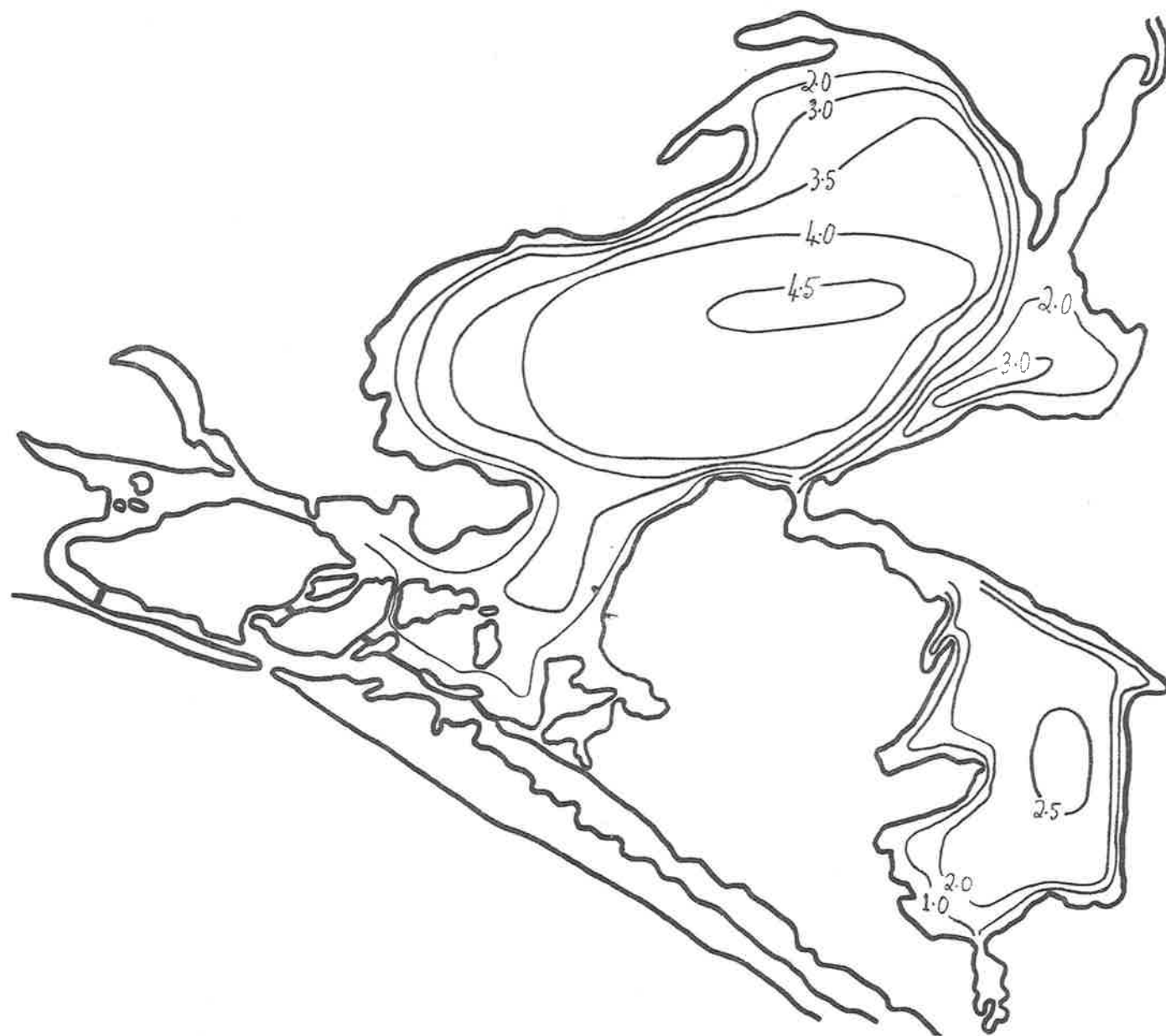DRINA ARE MARKED ┼┼┼┼ .

FIGURE A2 : APPROXIMATE DEPTH CONTOURS FOR LAKES ALEXANDRINA AND
ALBERT AS DETERMINED FROM RECORDS OF THE E. & W.S.
DEPT. AND MEASUREMENTS TAKEN BY CHENG WAN-LI (1972).

APPENDIX B

SOME PROPERTIES OF RESPONSE FUNCTIONS FOR CAUSAL, LINEAR SYSTEMS

The response function, $J(\omega)$, of a linear system may be <u>defined</u> as the Fourier transform of the impulse response $h(t)$, (i.e. the response to a unit impulse $\delta(t)$ of the system), viz.

$$J(\omega) = \int_{-\infty}^{\infty} h(t)e^{-j\omega t}dt \qquad (B.1a)$$

with inversion

$$h(t) = \frac{1}{2\pi}\int_{-\infty}^{\infty} J(\omega)e^{j\omega t}d\omega. \qquad (B.1b)$$

Papoulis (1962), p.86 shows this definition to be equivalent to that given in Section 2.2 of this thesis.

Now, the impulse response is a real-time function so that writing $J(\omega) = R(\omega) + jX(\omega)$ where $R(\omega)$ and $X(\omega)$ are real, we have from (B.1) that

$$R(\omega) = \int_{-\infty}^{\infty} h(t)\cos(\omega t)dt \qquad (B.2a)$$

$$X(\omega) = -\int_{-\infty}^{\infty} h(t)\sin(\omega t)dt \qquad (B.2b)$$

i.e. the real and imaginary parts of the response function of a linear system are even and odd functions respectively of the angular frequency ω. Further, $X(0) = 0$ so that

$$J(0) = R(0) . \qquad (B.3)$$

The step response and impulse response are related by the form

$$a(t) = \int_0^t h(\tau)\, d\tau$$

which follows from (2.2.4) with $f_i(t-\tau) \equiv \delta(t-\tau)$. Also, for a causal system (B.1a) becomes

$$J(\omega) = \int_0^\infty h(t)e^{-j\omega t}\, dt$$

so that

$$J(0) = \int_0^\infty h(t)\, dt.$$

Thus we have finally that

$$\lim_{t \to \infty} \{a(t)\} = J(0) = R(0) \tag{B.4}$$

provided the limit exists, i.e. the equilibrium response of a causal linear system is equal to the system gain at zero frequency. If the limit does not exist we may speak of $J(0)$ only as a quasi-equilibrium (or quasi-static equilibrium) response. Such is the case in wind-effect problems when no damping forces are acting within the fluid.

APPENDIX C

UNIQUENESS PROPERTIES FOR THE BOUNDARY VALUE PROBLEMS (4.2.11), (4.2.14)

To prove that any solution to (4.2.14) is unique, it suffices to con-sider the following generalized boundary value problem in three-dimensional space:-

$$(\nabla^2 - \lambda^2)\Psi = f(x,y,z) \qquad (C.1a)$$

within a closed volume $\overline{V}$, subject to the boundary condition

$$\Psi = g(x,y,z) \qquad (C.1b)$$

on the surface $\overline{S}$ of the volume $\overline{V}$. In (C.1a), λ is a _real_ constant. We shall prove that any solution $\Psi(x,y,z)$ to the boundary value problem (C.1a) is unique.

To this end, suppose there are two separate solutions to the problem, viz. $\Psi_1(x,y,z)$ and $\Psi_2(x,y,z)$. Then the difference $\Psi_1 - \Psi_2 = \Psi_3$ satisfies

$$(\nabla^2 - \lambda^2)\Psi_3 = 0 \text{ within } \overline{V}, \qquad (C.2a)$$

$$\Psi_3 = 0 \text{ on } \overline{S}. \qquad (C.2.b)$$

Further, the function $\Psi_3(x,y,z)$, subject to the conditions of continuity of all first derivatives within $\overline{V}$ and continuity on $\overline{S}$, satisfies the following corollary of the divergence theorem (Chester (1971) p.69):-

$$\iiint_{\overline{V}} (\nabla\Psi_3)^2 d\overline{V} = \iint_{\overline{S}} \Psi_3 \frac{\partial\Psi_3}{\partial n} d\overline{S} - \iiint_{\overline{V}} \Psi_3 \nabla^2\Psi_3 d\overline{V} \qquad (C.3)$$

where $\hat{n}$ is the outwardly directed normal to the surface $\overline{S}$. Combining (C.2a), (C2.b) and (C.3) gives

$$\iiint\limits_{\overline{V}} \{ (\nabla \Psi_3)^2 + (\lambda \Psi_3)^2 \} d\overline{v} = 0 \tag{C.4}$$

from which, since the integral of the left hand side of (C.4) is never negative, we conclude that $\Psi_3 \equiv 0$ within $\overline{V}$.

Thus, it follows that if a solution to (4.2.14) exists then that solution is unique. A similar analysis applied to (4.2.11) shows that uniqueness is guaranteed to within an additive constant. (Of course, this also follows from (4.2.12) and the uniqueness of (4.2.14)).

APPENDIX   D

FINITE DIFFERENCE SPECIFICATION OF THE BOUNDARY CONDITIONS

FOR THE NUMERICAL MODEL OF SECTION 5.3

Here we consider in detail the relevant form of the boundary condition (4.1.9a) applying to each type of boundary stream point, and derive the "degenerate" form of the difference equations (5.3.3) satisfied at each. The form of the boundary condition at 270° corner points is a point of dispute. Clearly, it cannot be defined explicitly using (4.1.9a). We choose the simple, though unnatural condition of zero flow at such points.

Group 3

$$0 \underset{i+n}{\xleftarrow{}} \; 2d \xrightarrow{} 0_{i+n+1}$$
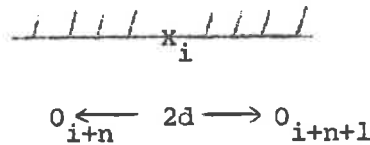
Values for Z_{i+n}, Z_{i+n+1} are starting values. Here (4.1.9a) gives

$$Q_i = 0 \qquad\qquad\qquad\qquad (D.1a)$$

so that $P_i + Q_i = P_i - Q_i$, i.e.

$$S_i - D_i = 0 . \qquad\qquad\qquad\qquad (D.1b)$$

The appropriate difference equation to determine S_i (and hence D_i) is determined from (5.3.1a). Using a "one-sided" difference approximation for $\left(\frac{\partial Z}{\partial x}\right)_i$, viz.

$$\left(\frac{\partial Z}{\partial x}\right)_i \sim \frac{1}{2d} \; (Z_{i+n+1} - Z_{i+n})$$
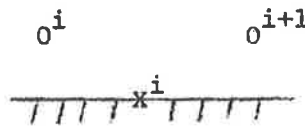
then (5.3.1a) gives

$$\beta_i P_i = - \gamma_i (Z_{i+n+1} - Z_{i+n}) + K\tau_{ox}$$

or

$$S_i = \frac{1}{\beta_i} \{- \gamma_i (Z_{i+n+1} - Z_{i+n}) + K\tau_{ox}\} \qquad \text{(D.1c)}$$

while D_i may be determined from (D.1b).
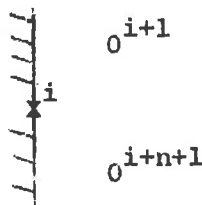
Group 4

$$0^i \qquad\qquad 0^{i+1}$$

Values for Z_i, Z_{i+1} have been calculated as part of the iterative scheme. Again we have that $S_i - D_i = 0$. Now a value for D_i may be determined from (5.3.3b). Further, taking a similar one-sided difference approximation for $\left(\frac{\partial Z}{\partial x}\right)_i$, then (5.3.1a) gives

$$S_i = \frac{1}{\beta_i} \{- \gamma_i (Z_{i+1} - Z_i) + K\tau_{ox}\} . \qquad \text{(D.2a)}$$

Defining at this point the 'end-value" $e = S_i - D_i$, then if $e = 0$, the boundary condition (D.1b) is satisfied.

Group 5

$$0^{i+1}$$
$$i$$
$$0^{i+n+1}$$

Values for Z_{i+1}, Z_{i+n+1} are starting values. Here (4.1.9a) gives

$$P_i = 0 \qquad\qquad \text{(D.3a)}$$

so $(P_i + Q_i) = -(P_i - Q_i)$, i.e.

$$S_i + D_i = 0. \qquad\qquad \text{(D.3b)}$$

Using a one-sided difference approximation for $\left(\frac{\partial Z}{\partial y}\right)_i$, viz.
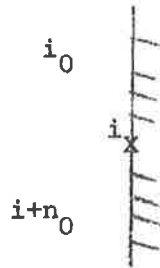
$$\left(\frac{\partial Z}{\partial y}\right)_i \sim \frac{1}{2d} (Z_{i+1} - Z_{i+n+1})$$

then (5.3.1b) gives

$$S_i = \frac{1}{\beta_i} \{- \gamma_i (Z_{i+1} - Z_{i+n+1}) + K\tau_{oy}\} \qquad (D.3c)$$
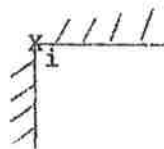
while D_i may be determined from (D.3b).

Group 6

Values for Z_i, Z_{i+n} have been previously calculated. Again $S_i + D_i = 0$.
Now (5.3.1b) gives

$$S_i = \frac{1}{\beta_i} \{- \gamma_i (Z_i - Z_{i+n}) + K\tau_{oy}\} \qquad (D.4)$$

while a value for D_i may be determined from (5.3.3b). The end value is
defined by $e = S_i + D_i$.

Group 7

Here we have simply that $P_i = Q_i = 0$, i.e.

$$S_i = D_i = 0. \qquad (D.5)$$

The condition (D.5) is also satisfied at stream points belonging to groups
8, 9 and 13. For stream points belonging to groups 10, 11, 12 and 14 it is
required that (D.5) be satisfied. In each of these cases a value for D_i is
calculable from (5.3.3c); we may thus define the end value $e = D_i$ for such
points.

APPENDIX E

THE COMBINED LAKE ALEXANDRINA - LAKE ALBERT MODEL

1. Details of the Narrung Channel Array

Equations (5.2.7a), (5.2.7b) are used in the calculation of elevations and transports for the array points of Fig. 5.14b. (Knowledge of the channel transport at grid point 1 and elevation at grid point 2 is necessary to initiate the process; this is obtained from the matching conditions with the two-dimensional model).

For simplicity, transports at grid points 1, 3 have a north-south alignment, i.e. parallel to the verticals of the two-dimensional array; at grid point 5, the alignment is south-east; for grid points 7, 9,11, 13 it is west-east (parallel to the horizontals of the two-dimensional array); while for the remaining grid points of the one-dimensional array, transports again have a south-east alignment.

Only the component of wind stress amplitude parallel to the alignment of ξ_{i+2}, i = 1, 23, (2) is used in the calculation of Z_{i+3} from (5.2.7b). Thus the one-dimensional scheme of Section 5.2 is modified here to the extent that wind stress inhomogeneities are incorporated into the difference equations. We, therefore, have accounted for the channel curvature in a simple yet physically realistic manner.

2. Matching Conditions

We are required to match the two-dimensional flows in the separate lakes onto the one-dimensional channel flow.

Part of the matching condition requires continuity of flow at the junctions between the separate lakes and the channel. The first and last channel points are assumed to coincide with stream points 129 and 162 respectively of the two-dimensional array. At grid point 129, a value for the quantity D_i is calculated from (5.3.5b) and then $S_i = -D_i$ gives the direction of the computed flow as parallel to the verticals of the two-dimensional array. The computed transport amplitude at this point then becomes equivalent to the channel flow amplitude ξ_1, when multiplied by the width of the channel at this point.
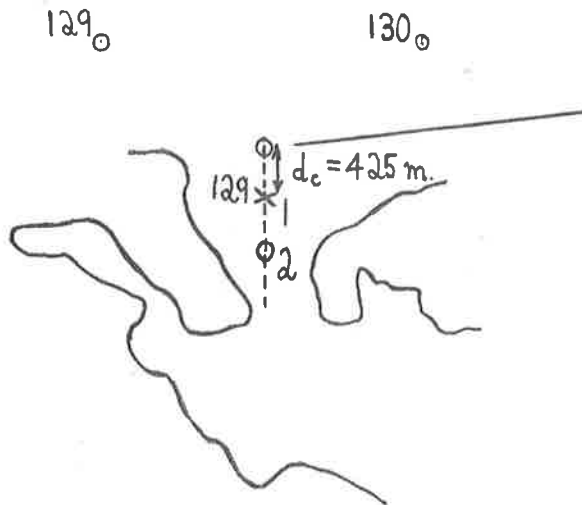
Elevation amplitudes must also be matched across the junction. At the Lake Alexandrina junction, this has been done by supposing that the mean of elevation amplitude values for grid points 129, 130 of the two-dimensional array is equivalent to the elevation amplitude at a distance d_c ($d_c \equiv$ channel grid length) <u>north</u> of channel point 1. This value is then used, in conjunction with the known value for ξ_1 to calculate a value for Z_2 using (5.2.7b).

Matching procedures at the Lake Albert end of the channel are similar. Knowledge of the channel flow at grid point 25 enables a calculation to be made of the quantities S_i, D_i at grid point 162 of the two-dimensional array. The flow at this point always has a south-east alignment. An elevation amplitude value for grid point 178 is calculated on the assumption of its equivalence with the elevation at a distance d_c south-east of channel grid point 25 as calculated from (5.2.7b). Fig. E1 illustrates the main features of these matching conditions. Though the matching of elevations is only approximate it has been shown to give quite satisfactory results.

Essentially, the iterative scheme for the combined model operates as for the two-dimensional scheme of Section 5.2. However, the fact that the lakes are connected means that at stream point 129 and elevation point 178 we no longer need to specify end and starting values respectively.

In order to consider the <u>unconnected</u> behaviour of the model Lakes Alexandrina and Albert, we may simply close off the channel ends. Thus stream point 129 of the two-dimensional array becomes a group 4 point, elevation point 178 becomes a group 16 point and stream points 162, 163 both become group 3 points. (In the connected model, velocities at the latter point are set to zero). We then proceed through the iterative scheme of Section 5.3 for each basin separately.
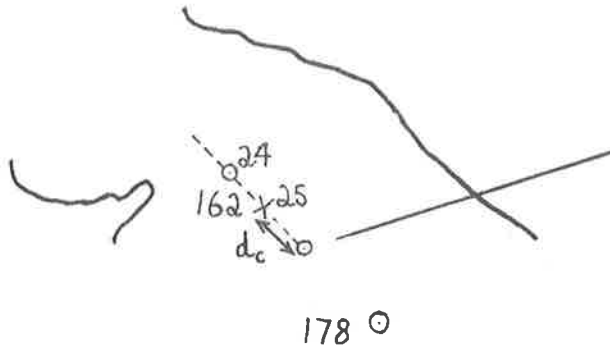
LAKE ALEXANDRINA END

$129_\odot$ $130_\odot$

fictitious
elevation pt.

$d_c = 425\,m.$

$$Z_f = \tfrac{1}{2}\left(Z_{129} + Z_{130}\right)$$

129

ϕ_1

ϕ_2

LAKE ALBERT END

fictitious
elevation pt.

24

162   25

d_c

$178 \odot$

$$Z_{178} = Z_f$$

FIGURE E1 : MATCHING CONDITIONS AT THE TWO ENDS
OF THE NARRUNG CHANNEL .